

University of Mississippi

eGrove

Electronic Theses and Dissertations

Graduate School

2019

The Synthesis of New Donor-sigma-Acceptor Compounds as Potential Current Rectifiers

Trey Gautier Vaughan
University of Mississippi

Follow this and additional works at: <https://egrove.olemiss.edu/etd>

 Part of the [Chemistry Commons](#)

Recommended Citation

Vaughan, Trey Gautier, "The Synthesis of New Donor-sigma-Acceptor Compounds as Potential Current Rectifiers" (2019). *Electronic Theses and Dissertations*. 1706.
<https://egrove.olemiss.edu/etd/1706>

This Dissertation is brought to you for free and open access by the Graduate School at eGrove. It has been accepted for inclusion in Electronic Theses and Dissertations by an authorized administrator of eGrove. For more information, please contact egrove@olemiss.edu.

The Synthesis of New Donor-sigma-Acceptor Compounds as Potential Current Rectifiers

A Dissertation

presented in partial fulfillment of requirements for the degree of

Doctor of Philosophy

in the Department of Chemistry and Biochemistry

The University of Mississippi

By Hal Gautier Vaughan III

May 2019

Copyright © 2018 by Trey G. Vaughan

All rights reserved.

Abstract

Five novel donor-sigma-acceptor (D- σ -A) compounds were synthesized and spectroscopically characterized. A successful synthesis of a model zwitterionic pyridinium-triethylborate D- σ -A was used to validate the initial proof-of-concept of a zwitterionic D- σ -A based on an anionic borate donor. An analogous D- σ -A based on a trifluoroborate donor was then successfully synthesized. Next, three perylene diimide (PDI) D- σ -A's were synthesized. As a result, this research is divided into two parts: 1. Zwitterionic D- σ -A's. 2. Neutral D- σ -A's.

The zwitterionic D- σ -A's are characterized by having an anionic donor, a cationic acceptor, an intervening sigma-bond bridge, and an aliphatic tail. The aliphatic tail is of such length as to impart greater solubility in organic solvents since the formal charges on the donor and acceptor lead to poor solubility. Additionally, the aliphatic tail is required for Pockels-Langmuir deposition to facilitate the favorable van der Waal's packing when combined to form dense monolayer registries. These monolayers may then be suitable for measuring the bulk electrical properties.

The neutral D- σ -A's are all based on perylene diimide (PDI) acceptors. The three PDIs in this study vary in the type of donor. The respective donors used are a pyrene with a saturated 3-carbon tether, a pyrene with an unsaturated 3-carbon tether, and a ferrocene with an unsaturated 3-carbon tether. An aliphatic swallow-tail is tethered onto the perylene diimide.

List of Abbreviations and Symbols

Ac	acetyl
aq.	aqueous
Ar	aryl
B ₂ NPG ₂	bis(neopentyl glycolato)diboron
B ₂ Pin ₂	bis(pinacolato)diboron
Bn	benzyl
Bp	boiling point
Bu (ⁿ Bu)	butyl
Bz	benzoyl
°C	degree Celsius
ca	circa (approximately)
CAM	ceric ammonium molybdate (Hanesian's Stain)
cat.	catalytic
CDCl ₃	deuterated chloroform
Δ	heat

d	days (length of reaction time)
D- σ -A	donor- σ -acceptor
DCC	dicyclohexylcarbodiimide
DCM	dichloromethane
DCU	<i>N,N'</i> -dicyclohexylurea
DMF	<i>N,N</i> -dimethylformamide
DMS	dimethylsulfide
DMSO	dimethylsulfoxide
DPA	diisopropylamine
DMSO	dimethyl sulfoxide
EDC	1-ethyl-3-(3-dimethylaminopropyl)carbodiimide
ESI-MS	electrospray ionization-mass spectrometry
EtOAc	ethyl acetate
eq. (equiv.)	equivalent
Fc	ferrocenyl
Fmoc	9-fluorenylmethoxycarbonyl

g	gram(s)
h or hr(s)	hour(s)
HCl	hydrochloric acid
HOBt	1-hydroxybenzotriazole
HWE	Horner-Wadsworth-Emmons
Hz	Herz
Imid (Im)	imidazole
IPA	isopropyl alcohol
IR	infrared spectroscopy
LAH	lithium aluminum hydride
<i>m</i>	meta
M	molarity
Me	methyl
MeOH	methanol
min	minute
mL	milliliter

mp	melting point
MOM	methoxymethyl acetal
MS	mass spectrometry
MS	molecular sieves
<i>n</i>	normal (i.e. normal branched alkane chain)
NMR	nuclear magnetic resonance
NPC	normal phase chromatography
NR	no reaction
Nu	nucleophile
<i>o</i>	ortho
<i>p</i>	para
%	percent
Ph	phenyl
PDI	perylene diimide
PMA	perylene monoanhydride
PTCDA	perylene-3,4,9,10-tetracarboxylic dianhydride

Py	pyridine
quant.	quantitative
↑ ↓	reflux condition
r.t.	room temperature
R _f	retention factor
Red-Al	sodium <i>bis</i> (2-methoxyethoxy) aluminum hydride
s	seconds
satd.	saturated
<i>sec</i>	secondary
SET	single electron transfer
SiO ₂	silica
TEA	triethylamine
temp	temperature
TFAA	trifluoroacetic anhydride
THF	tetrahydrofuran
TLC	thin layer chromatography

TME	trimethylolethane
TMSCl	trimethylsilyl chloride
Tol	toluene
UV	ultraviolet
vol	volume

Acknowledgements

I would like to acknowledge my advisor, Dr. Daniell Mattern, unfailing in his patience and decency, and ever the optimist. No better measure of the positivity of a person's outlook could be expressed than through one's family, who showed great hospitality to me during many holidays. So, I would also like to include Dr. Mattern's family in my acknowledgment.

Second, my committee: Dr. Steven Davis, Dr. Jared Delcamp, Dr. Nathan Hammer, and Dr. Corina L. Petrescu for their time and effort. It is greatly appreciated. They all helped me learn a language, foreign at first, but familiar over time.

Dr. Davis is a rare combination of humility and brilliance. Dr. Delcamp, being the youngest of my committee, is well-liked by his students and known especially for his good sense of humor, which was described in one student-review as "wicked funny." Dr. Hammer runs his research team like a well-oiled machine but never neglects being helpful and supportive. I was privileged to sit in on a group meeting and was especially impressed by the level of contribution of his students as well as his encouragement to his students.

My outside committee member, Dr. Corina L. Petrescu, has been supportive since I first took her German course as an undergraduate years ago. She has always been unfaltering in encouraging the highest standards. She kept an open door and an open ear.

Dr. Takashi Tomioka deserves a special acknowledgement. His lab was my first research group as an undergraduate. Dr. Tomioka took the time to personally train me on every conceivable synthetic organic technique. Dr. Tomioka was a thoughtful man of few words. But his words

were always substantive. I will forever be indebted to him for taking such an active role in teaching me useful chemistry techniques.

To the Dass Research Group many thanks for their timely ESI-MS work; Milan Rambukwella, Vigneshraja Ganeshraj, Naga Arjun Sakthivel, Chanaka Kumara. Thank you.

Finally, my friends and colleagues: Mike Cunningham from Dr. Rimaldi's research group was an invaluable sounding board for new ideas. Asantha Dharmaratne was a good friend and always lent his time no matter the lateness of the hour. Rambabu Sankranti and Yusuke Takahashi both started in the research group of Dr. Takashi Tomioka and finished in the Mattern Research Group with me. We had a lot of adventures that were never dull.

Table of Contents

ABSTRACT.....	ii
LIST OF ABBREVIATIONS AND SYMBOLS.....	iii
ACKNOWLEDGEMENTS.....	viii
LIST OF FIGURES.....	xviii
LIST OF SCHEMES.....	xx
CHAPTER 1:INTRODUCTION.....	1
1.1 Historical.....	2
1.2 Monolayer Organic Films.....	3
1.3 Measurements of Surface Pressure (Isotherm).....	5
1.4 Monolayer Deposition Considerations.....	7
1.5 Rectification Ratio and Molecular Design Rule Constraints.....	9
1.6 Rectification Mechanism.....	11
1.7 Properties of Good Electron Donors.....	16
1.8 Properties of Good Electron Acceptors.....	19

1.9 Perylene Diimides, a Robust Platform for Accessing D- σ -A's.....	22
CHAPTER 2: RESULTS AND DISCUSSION: ZWITTERIONIC DONOR-σ-ACCEPTOR (D-σ-A) COMPOUNDS.....	33
2.1 The Synthesis of Zwitterionic Donor- σ -Acceptors.....	33
2.1.1 Preparation of the Zwitterionic Model Compound Containing an Anionic Borate Donor and a Pyridinium Acceptor.....	34
2.2 Attempted Preparation of Amino-Naphthylboronic Acids.....	37
2.2.1 Attempted Preparation of 1-aminonaphthalene-4-boronic acid 6.3	37
2.2.2 Attempted preparation of 1-amino-5-naphthylboronic acid 173	48
2.2.2.1 Synthesis of 1-bromo-5-nitronaphthalene 144	48
2.2.2.2 Synthesis of 1-amino-5-bromonaphthalene 149	48
2.2.2.3 Attempted Synthesis of 5-(5,5-Dimethyl-[1,3,2]dioxaboronan-2-yl)-naphthalen-1-yl]-amine 155.1	49
2.2.2.4 Attempted Preparation of 1-Amino-5-naphthylboronic Acid 173	52
2.3 Retrosynthetic Analysis for AQuANaB Compounds.....	57
2.4 Amides, A-Fragments, Syntheses of.....	59
2.4.1 Model Compound Amides 167	60
2.4.2 Model Compound Amides 171	61
2.4.3 <i>N</i> -(4-bromonaphthalen-1-yl)quinoline-6-carboxamide 202	62

2.4.4 <i>N</i> -(4-Bromonaphthalen-1-yl)- <i>N</i> -methylquinoline-6-carboxamide 254	64
2.4.5 <i>N</i> -(5-Bromonaphthalen-1-yl)quinoline-6-carboxamide 272	66
2.4.6 Attempted synthesis of <i>N</i> -(5-bromonaphthalen-1-yl)- <i>N</i> -methylquinoline-6-carboxamide 247	66
2.5 Syntheses of B-Fragments.....	69
2.5.1.1 Model, 2-(((tert-Butyldimethylsilyl)oxy)methyl)-2-methylpropane-1,3-diol, 222	69
2.5.1.2 Model, Synthesis of tert-butyldimethyl((5-methyl-1,3,2-dioxaborinan-5-yl)methoxy)silane, 221	69
2.5.1.3 Model, Synthesis of methyl 4-(5-(((tert-butyldimethylsilyl)oxy)methyl)-5-methyl-1,3,2-dioxaborinan-2-yl)benzoate, 225	70
2.5.1.4 Model, tert-Butyldimethyl((5-methyl-2-(<i>o</i> -tolyl)-1,3,2-dioxaborinan-5-yl)methoxy)silane, 224	71
2.5.1.5 Model, methyl 4-(5,5-dimethyl-1,3,2-dioxaborinan-2-yl)benzoate, 229	72
2.5.1.6 Model, <i>N</i> -(4-(5-(((tert-Butyldimethylsilyl)oxy)methyl)-5-methyl-1,3,2-dioxaborinan-2-yl)naphthalen-1-yl)benzamide, 231	73
2.5.1.7 Model, <i>N</i> -(4-(5,5-dimethyl-1,3,2-dioxaborinan-2-yl)naphthalen-1-yl)benzamide, 232	74
2.5.2 <i>N</i> -(4-(5-(((tert-butyldimethylsilyl)oxy)methyl)-5-methyl-1,3,2-dioxaborinan-2-yl)naphthalen-1-yl)quinoline-6-carboxamide, 227	75

2.5.3 <i>N</i> -(4-(4,4,5,5-Tetramethyl-1,3,2-dioxaborolan-2-yl)naphthalen-1-yl)quinoline-6-carboxamide, 214	76
2.5.4 <i>N</i> -Methyl- <i>N</i> -(4-(4,4,5,5-tetramethyl-1,3,2-dioxaborolan-2-yl)naphthalen-1-yl)quinoline-6-carboxamide, 259	77
2.5.5 <i>N</i> -(5-(4,4,5,5-Tetramethyl-1,3,2-dioxaborolan-2-yl)naphthalen-1-yl)quinoline-6-carboxamide, 308	79
2.6 Syntheses of <i>N</i> -Alkyl Quinoliniums, C and D-Fragments.....	81
2.6.1 Syntheses of Alkylhalides and Alkylpseudohalides.....	81
2.6.1.1 Hexadecyl 4-Methylbenzenesulfonate 194	81
2.6.1.2 1-Iodotetradecane 195	82
2.6.1.3 Hexadecyl Trifluoromethanesulfonate 355	83
2.6.1.4 2-octyldodecyl trifluoromethanesulfonate 354	83
2.6.2 Syntheses of C-Fragments.....	84
2.6.2.1 6-((4-Bromonaphthalen-1-yl)carbamoyl)-1-tetradecylquinolin-1-ium iodide, 201	89
2.6.2.2 6-((4-Bromonaphthalen-1-yl)carbamoyl)-1-tetradecylquinolin-1-ium 4-methylbenzenesulfonate, 207	90
2.6.3 Synthesis of D-Fragments.....	93
2.6.3.1 Attempted Synthesis of 215 from C-Fragment 201	93

2.6.3.2 Synthesis of 1-Tetradecyl-6-((4-(4,4,5,5-tetramethyl-1,3,2-dioxaborolane-2-yl)naphthalen-1-yl)carbamoyl)quinolin-1-ium iodide, 215	94
2.6.3.3 6-(Methyl(4-(4,4,5,5-tetramethyl-1,3,2-dioxaborolan-2-yl)naphthalen-1-yl)carbamoyl)-1-tetradecylquinolin-1-ium iodide, 261	96
2.7 Synthesis of AQuANaB Compounds.....	97
2.7.1 Attempted Synthesis of 4-Methyl-1-(4-(1-tetradecylquinolin-1-ium-6-carboxamido)naphthalen-1-yl)-2,6,7-trioxa-1-borabicyclo[2.2.2]octan-1-uide, 213	98
2.7.2 4-Methyl-1-(4-(1-Tetradecylquinolin-1-ium-6-carboxamido)naphthalen-1-yl)-2,6,7-trioxa-1-borabicyclo[2.2.2]octan-1-uide, 262	99
2.7.3 Model, Trifluoro(1-methylpyridin-1-ium-3-yl)borate, 216	100
2.7.4 Synthesis of Trifluoro(4-(1-tetradecylquinolin-1-ium-6-carboxamido)naphthalen-1-yl)borate, 217	100
2.8 Synthesis of Triol, E-Fragment.....	104
2.8.1 Synthesis of 2-(Hydroxymethyl)-2-octylpropane-1,3-diol 116	105
2.9 Other Zwitterionic Donor- σ -Acceptors (D- σ -As)	105
2.9.1 Aryl Oxide Donors.....	106

2.9.2 Aryl Carboxylate Donors.....	110
2.9.3 Aryl Sulfonate Donor.....	115
2.9.4 Aryl Thiolate Donor.....	117
2.10 Conclusion.....	125
CHAPTER 3: RESULTS AND DISCUSSION: NEW PERYLENE DIIMIDE DONOR-σ-ACCEPTOR COMPOUNDS.....	127
3.1 The Synthesis of Perylene Diimide Donor- σ -Acceptors (D- σ -A's).....	127
3.2 General Retrosynthetic Scheme for Synthesis of Perylene diimides (PDI)s.....	128
3.3 Synthesis of the Swallowtail Fragment.....	129
3.3.1 Synthesis of 10-Nonadecanone Oxime via 10-Nonadecanone.....	129
3.3.2 Synthesis of 10-Nonadecanamine via 10-Nonadecanone Oxime.....	130
3.4 Synthesis of the Perylene Monoanhydride (PMA) Fragment.....	130
3.4.1 Synthesis of PDI-(bisalkyl)	130
3.4.2 Synthesis of PMA.....	131
3.5 Synthesis of the Donor Fragments.....	132
3.5.1 Synthesis of 1-Pyrenepropylamine 313	132

3.5.2 Synthesis of (<i>E</i>)-3-(pyren-1-yl)prop-2-en-1-amine 295	133
3.5.2.1 Conversion of 1-Pyrenecarboxaldehyde to (<i>E</i>)-3-(Pyren-1-yl)acrylonitrile 291	134
3.5.2.2 Conversion of (<i>E</i>)-3-(Pyren-1-yl)acrylonitrile to (<i>E</i>)-3-(Pyren-1-yl)prop-2-en-1-amine 295	137
3.5.3 Synthesis of (<i>E</i>)-3-Ferrocenylprop-2-en-1-amine 352	139
3.5.3.1 Conversion of Ferrocenecarboxaldehyde to (<i>E</i>)-3-Ferrocenylacrylonitrile 346	140
3.5.3.2 Conversion of (<i>E</i>)-3-Ferrocenylacrylonitrile to (<i>E</i>)-3-Ferrocenylprop-2-en-1-amine 352	141
3.6 Syntheses of PDIs 317, 319, 353	141
3.6.1 The Synthesis of PDI 317	142
3.6.2 The Synthesis of PDI 319	143
3.6.3 The Synthesis of PDI 353	144
3.7 Conclusion.....	146
CHAPTER 4: EXPERIMENTAL.....	147
BIBLIOGRAPHY.....	186

VITA.....199

LIST OF FIGURES

Figure 1.1 Original Aviram-Ratner Donor- σ -Acceptor.....	2
Figure 1.2.1 Irving Langmuir’s surface film balance.....	4
Figure 1.3.1 Monolayer (a) expanded, (b) semi-compressed, (c) compressed.....	6
Figure 1.3.2 Rayleigh’s isotherm.....	7
Figure 1.5.1 Nijhuis and coworkers’ molecular rectifier.....	11
Figure 1.5.2 Asymmetric anchoring proposal by Van Dyck and Ratner.....	11
Figure 1.6.1 Aviram Ratner rectification (left), no bias and no rectification (center), Anti Aviram Ratner Rectification (right).....	12
Figure 1.6.2 Band compression of HOMO-LUMO gap upon electrode attachment.....	13
Figure 1.6.3 When frontier HOMO-LUMO levels are in alignment with metal electrode transmission window (Fermi levels), probability of electron transmission is high.....	13
Figure 1.6.4 At negative bias (left) coulomb interactions at Fc-metal result in greater contact optimization.....	14
Figure 1.6.5 Asymmetric rectification.....	15
Figure 1.6.6 Molecular orbitals in asymmetric rectification “Janus Rectifiers”. From left to right (a) at positive bias, (b) zero bias, and (c) at negative bias.....	15

Figure 1.7.1 Good donors.....	16
Figure 1.7.2 Various D- σ -A's synthesized in this lab with pyrene and ferrocene donors.....	17
Figure 1.7.3 Various D- σ -A's synthesized in this lab with ferrocene and TMPD donors.....	18
Figure 1.8.1 Good acceptors' electron affinity.....	19
Figure 1.8.2 Benzoquinone radical aromatic stabilization.....	19
Figure 1.8.3 Ashwell's cationic acceptors.....	21
Figure 1.9.1 Chart on left shows solubility of PDIs in heptane as a function of swallowtail length (n). ⁷ Solid arrow on chart correlates to indicated structure on the right.....	22
Figure 1.9.2 Bay substituent effect on HOMO/LUMO levels.....	26
Figure 1.9.3 HOMO/LUMO levels of compounds with various EDG-substituents in bay positions.....	27
Figure 2.2.2.4 Preparative Scale TLC isolation attempt of 173	56
Figure 2.4.3.1 <i>O</i> -acylurea intermediate is obtained in the absence of HOBt.....	62
Figure 2.7.1 General form for AQuANaB type compounds.....	98
Figure 3.1.1 Three new PDI-type D- σ -A's.....	127

LIST OF SCHEMES

Scheme 1.1 Perylene diimide synthetic route from 1 to 2 requires aggressive conditions due to PDI persistence. The conversion of labile 2 to persistent 3 is facile.....	24
Scheme 1.2 Halogenation of perylene tetracarboxylic dianhydride (PTCDA) occur at the bay positions.....	25
Scheme 1.3 Bay substitution of PDI.....	26
Scheme 1.4 Direct trifluoromethylation of PTCDA in solvent free conditions. ³	29
Scheme 1.5 A schematic view of regioselective 2,5,8,11-tetrasubstitutions of PDIs.....	31
Scheme 2.1 Initial scheme for anionic borate D- σ -A.....	35
Scheme 2.2 Hydrolysis of 27 to 7.4 proves problematic.....	36
Scheme 2.3 <i>N</i> -alkylation of 37 proved problematic.....	35
Scheme 2.4 Successful model compound synthetic scheme.....	36
Scheme 2.5 Amino naphthalene to amino boronic acid.....	38
Scheme 2.6 Comparison of results of reaction performed on Substrate A vs. Substrate B.....	39
Scheme 2.7 Acid catalyzed protodeborylation (possible routes)	40
Scheme 2.8 Lithiation fails but Miyaura coupling success.....	42
Scheme 2.9 Attempted paths to the synthesis of 1-amino-4-bromonaphthalene.....	43

Scheme 2.10 Ni(II) catalyzed borylation.....	46
Scheme 2.11 Catalysts screened for a Miyaura Reaction (Method E)	47
Scheme 2.12 3-step synthetic sequence to the boronate ester 155.1	49
Scheme 2.13 Simplified scheme for degradation.....	52
Scheme 2.14: Conversion of boronate to boronic acid by alternate methods.....	54
Scheme 2.15 Revised retrosynthetic approach to so-called AQuANaB compounds.....	59
Scheme 2.16 Amidation of 1-amino-4-bromonaphthalene via TFAA.....	61
Scheme 2.17 Amidation of 1-amino-4-bromonaphthalene via benzoyl chloride.....	62
Scheme 2.18 Amidation of 1-amino-4-bromonaphthalene with 6-quinoline-carboxylic acid via DCC/HOBt protocol.....	63
Scheme 2.19 Synthesis of 4-bromo- <i>N</i> -methylnaphthalen-1-amine as alternative amine substrate for amidation.....	65
Scheme 2.20 <i>N</i> -alkylation of amide.....	66
Scheme 2.21 Synthesis of 272 through DCC coupling.....	66
Scheme 2.22 Attempted synthesis of <i>N</i> -(5-bromonaphthalen-1-yl)- <i>N</i> -methylquinoline-6- carboxamide 247	68
Scheme 2.23 Monosilylation of triol.....	69
Scheme 2.24 Borylation of 222	70

Scheme 2.25 Ni(II) catalyzed borylation of an aryl bromide.....	71
Scheme 2.26 Ni(II) catalyzed borylation of o-iodotoluene.....	72
Scheme 2.27 Ni(II) catalyzed borylation of methyl-4-bromobenzoate via BH(NPG).....	73
Scheme 2.28 Ni(II) catalyzed borylation of 171 via 221	74
Scheme 2.29 Ni(II) catalyzed borylation of 171 via BH(NPG).....	75
Scheme 2.30 Ni(II) catalyzed borylation of 202 via BH(NPG).....	75
Scheme 2.31 Miyaura Reaction of 202 to give 214	76
Scheme 2.32 Miyaura reaction of 254 to give 259 through two separate methods.....	78
Scheme 2.33 Miyaura Reaction of 272 to give 308	80
Scheme 2.34 The synthesis of hexadecyl 4-methylbenzenesulfonate 194 from hexadecanol.....	82
Scheme 2.35 Finkelstein Reaction synthesis of 1-iodotetradecane 195	82
Scheme 2.36 Synthesis of hexadecyl trifluoromethanesulfonate, 355	83
Scheme 2.37 Synthesis of 2-octadodecyl trifluoromethanesulfonate 354	83
Scheme 2.38 Direct attempts at the <i>N</i> -alkylation of 6-quinolinecarboxylic acid.....	85
Scheme 2.39 The <i>N</i> -alkylation of 202 to form quinolinium 201	90
Scheme 2.40 The <i>N</i> -alkylation of 202 to form quinolinium 207	91

Scheme 2.41 The <i>N</i> -alkylation of 272 to form quinolinium 284	92
Scheme 2.42 Attempted Pd(0)-catalyzed synthesis of 215 from B-Fragment 201	94
Scheme 2.43 Synthesis of 215 from C-Fragment 214	95
Scheme 2.44 Synthesis of 261 from C-Fragment 259	97
Scheme 2.45 Failed transesterification of 212 resulted in polymerization.....	99
Scheme 2.46 Failed transesterification of 261	99
Scheme 2.47 Conversion of model substrate 00 to trifluoroborate zwitterion 216	100
Scheme 2.48 Synthesis of trifluoroborate 217 via boronate ester 215	101
Scheme 2.49 ¹ H NMR tube reaction to convert trifluoroborate 217 to boronic acid 218	102
Scheme 2.50 Tollens condensation of decanal onto formaldehyde to give triol 116	105
Scheme 2.51 All routes using 1-amino-4-naphthol gave crude reaction mixtures which could not be purified.....	107
Scheme 2.52 Copper catalyzed hydroxylation failed to give targets.....	108
Scheme 2.53 Successful amidation to obtain 322 and subsequent <i>N</i> -alkylation to give 323	109
Scheme 2.54 Multistep, multi-route synthetic attempts to obtain D-σ-As with a carboxylate donor.....	111
Scheme 2.55 Synthesis of sulfonate-donor containing 374	116

Scheme 2.56 Attempted <i>N</i> -alkylation of zwitterionic 374 to zwitterion 396	117
Scheme 2.57 Amidation of 4-aminophenyl disulfide to give 378 with <i>N</i> -alkylation attempts....	119
Scheme 2.58 Amidation of 4-aminophenyl disulfide to give 389 followed by <i>N</i> -alkylation to give 391 and then attempted disulfide cleavage.....	121
Scheme 15 General retrosynthetic analysis for PDI.....	129
Scheme 16 Synthesis of 10-nonadecanone oxime.....	129
Scheme 17 Oxime reduction to amine via Red-Al.....	130
Scheme 18 Synthesis of PDI-(bisalkyl).....	131
Scheme 19 Formation of PMA via base-hydrolysis.....	132
Scheme 20 1-pyrenepropylamine synthesis via 1-pyrenebutyric acid.....	133
Scheme 21 1-pyrenepropylamine synthesis via 1-pyrenebutyric acid with intermediates.....	133
Scheme 22 Synthesis of (<i>E</i>)-3-(pyren-1-yl)acrylonitrile 291	134
Scheme 23 Competing reductions of acrylonitriles.....	137
Scheme 24 Attempted 1,2-reduction of 291 was <i>unsuccessful</i>	138
Scheme 25 Successful 1,2-reduction of 291	139
Scheme 26 Wittig-Horner conversion of ferrocenecarboxaldehyde to (<i>E</i>)-3-ferrocenylacrylonitrile.....	140

Scheme 27 Reduction of 346 to allylic amines.....	142
Scheme 28 Synthetic scheme of 317	143
Scheme 29 Synthetic scheme of 319	144
Scheme 30 Synthetic scheme of 353	145

CHAPTER 1: INTRODUCTION

1.1 Historical

Unimolecular electronics (UE) is the field that studies the electrical processes of molecules on either the molecular scale or assembled into thin monolayers.² As first envisaged in 1974 by Mark A. Ratner and Avieh Aviram (Figure 1.1), the aim was to study the current-voltage relationship of a molecule which would contain an electron-rich pi-donor (D) insulated from an electron-poor pi-acceptor (A) via a methylene linked sigma-bridge (σ).¹² Separation of the donor (D) from the acceptor (A) via a non-conjugated sigma (σ) bridge was required to prevent direct overlap of the (D) and the (A) orbitals.^{13,14} These D- σ -A systems were to be tethered to electrodes and then upon application of voltage biased current, the system would display an electrical bias when positive-voltage current was taken as a ratio against negative-voltage current. In short, the molecule would act as a small diode. While the concept of current-rectification was not new in 1974, the idea of using a single molecule to effect this phenomenon was. This marked the beginning of the field of unimolecular electronics.

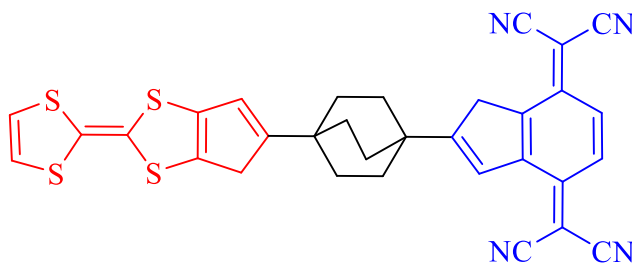


Figure 1.1: Original proposed Aviram-Ratner Donor- σ -Acceptor

Although the original proposal for a unimolecular rectifier was based on the donor being decoupled from the acceptor via sigma-bridge, variations on this concept have been developed.⁸ ¹⁵⁻²¹ Donor- π -acceptors (**D- π -As**) are now routinely employed as molecular rectifiers and an example molecule is given below (Figure 1.1.2). The general route by which a **D- π -A**'s donor is decoupled from the acceptor is by a dihedral twist of the donor against the acceptor. This is so that orbital overlap is minimized. The net effect is a decoupling of the donor from the acceptor.

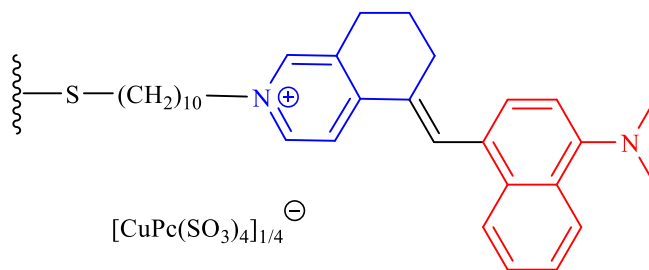


Figure 1.1.2: Cationic Donor- π -Acceptor (**D- π -A**).⁸

1.2 Monolayer Organic Films

A digression from the topic of unimolecular rectifiers to the topic of monolayer organic films must now be made. The investigation of whether a molecule possesses the capacity to rectify has necessitated various preparation methods from which reliable electrical measurements might be made. One such method is the monolayer organic film.

The science of thin organic films has its origins in the observation of how oil behaves when it comes into contact with water. Although preceded by other accounts of the phenomenon, Benjamin Franklin was the first person to approach the matter scientifically and report his findings.²² Franklin poured oil onto the surface of multiple ponds and noted how quickly the oil dispersed until it became so thin as to appear transparent. Franklin's report on the subject helped to renew interest in the physical phenomena behind oil films on water.

Agnes Pockels added her contribution to the science of thin organic films when she developed an apparatus to measure the surface tension effects of various monolayers on water. With dimensions of 70 cm x 5 cm x 2 cm, this tin bath would be filled to the brim with water. A flat strip of tin would then be raked across the surface to first clean the water surface from contamination. Next, oil could be dispersed across the water surface and its effect on the surface tension could be measured by the force required to lift the float (a button).^{11, 23-25} This apparatus accurately measured pressure per area at the monolayer interface and formed the basis of the first pressure area isotherms. Agnes Pockel's instrument and technique was further developed by the work of Irving Langmuir who ultimately received the Nobel Prize.⁴

The surface film balance, as developed by Langmuir and now referred to as the Langmuir trough (Figure 1.2.1), was used in many studies to analyze monolayer films with much of the bench-work being carried out by Catherine Blodgett.²⁶

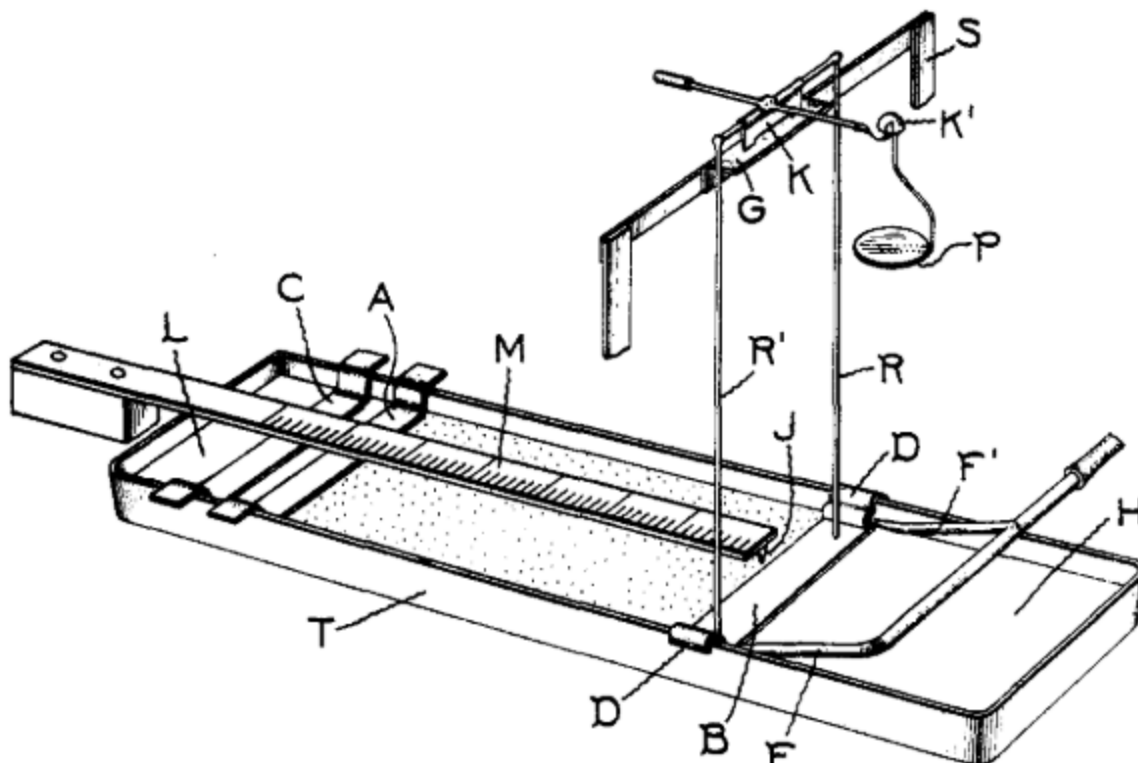


Figure 1.2.1: Irving Langmuir's surface film balance.⁴

Substances which form good monolayers are those which contain a hydrophilic head and a hydrophobic tail. The sample of interest is dissolved in an organic solvent such as chloroform, then poured onto the water bath. The hydrophilic head orients towards the polar water surface with the hydrophobic tail orienting away from the water bath. The sample disperses onto the water surface. A mechanical arm or other suitable device is used to delicately skim the surface, bringing the molecules into closer proximity. Ultimately the molecules form into a tightly packed monolayer registry. A monolayer formed by this process is referred to as a Langmuir monolayer while a Langmuir-Blodgett film is formed from multiple monolayers.²⁷ Since Langmuir's device was in fact based largely on that developed by Agnes Pockels, a more apt description is the Pockels-Langmuir film.

1.3 Measurements of Surface Pressure (Isotherm)

When a sample is on the water-bath surface in an expanded state (i.e. when the distance between molecules is large), then the intermolecular interactions are small. However, as the mechanical arm slowly forces the molecules together into a tightly packed monolayer, the intermolecular interactions become stronger. The resulting changes in surface pressure can be plotted as a function of surface area. This is known as an isotherm.²⁸

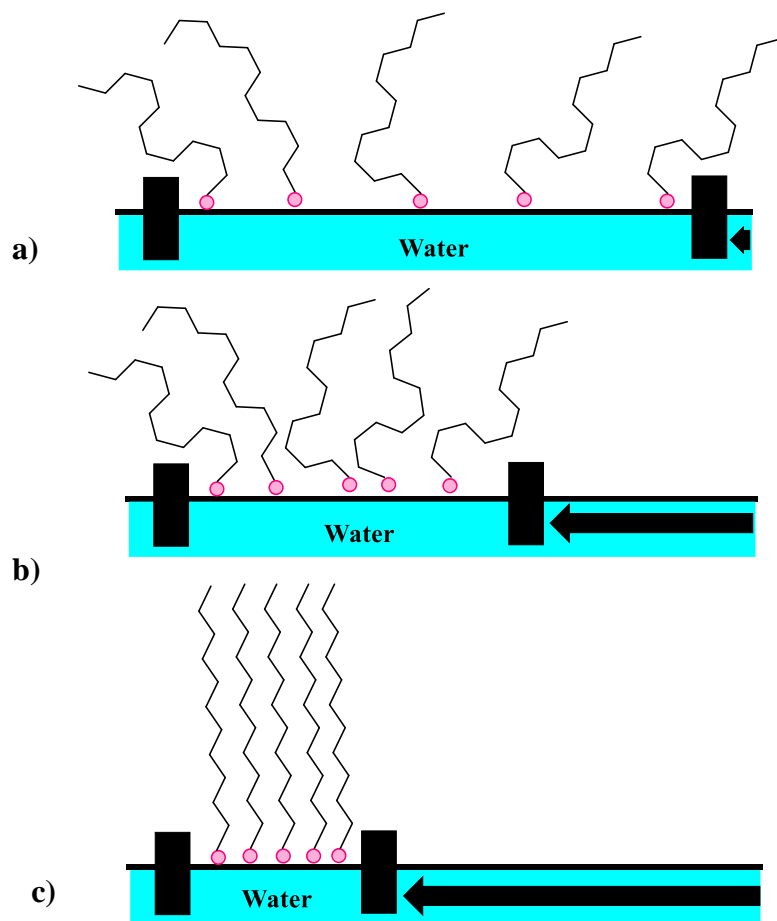


Figure 1.3.1: Monolayer (a) expanded, (b) semi-compressed, (c) compressed.

The isotherm measurements can provide useful physical information, such as surface pressure, in addition to information on phase-change and intermolecular packing. Furthermore, it will be appreciated that when molecules are similarly oriented and tightly packed in a monolayer (condensed phase) and surface pressure is examined, then surface pressure data is reflective of the intermolecular forces at work. Lord Rayleigh first intuited the correlation of intermolecular forces, and therefore monolayer thickness, with rising surface tension. Rayleigh's isotherm data¹¹ was derived from instrumentation reproduced from Agnes Pockel's work.²⁴ He accurately predicted that S (Figure 1.3.2) was the point in which the layer was one molecule thick.

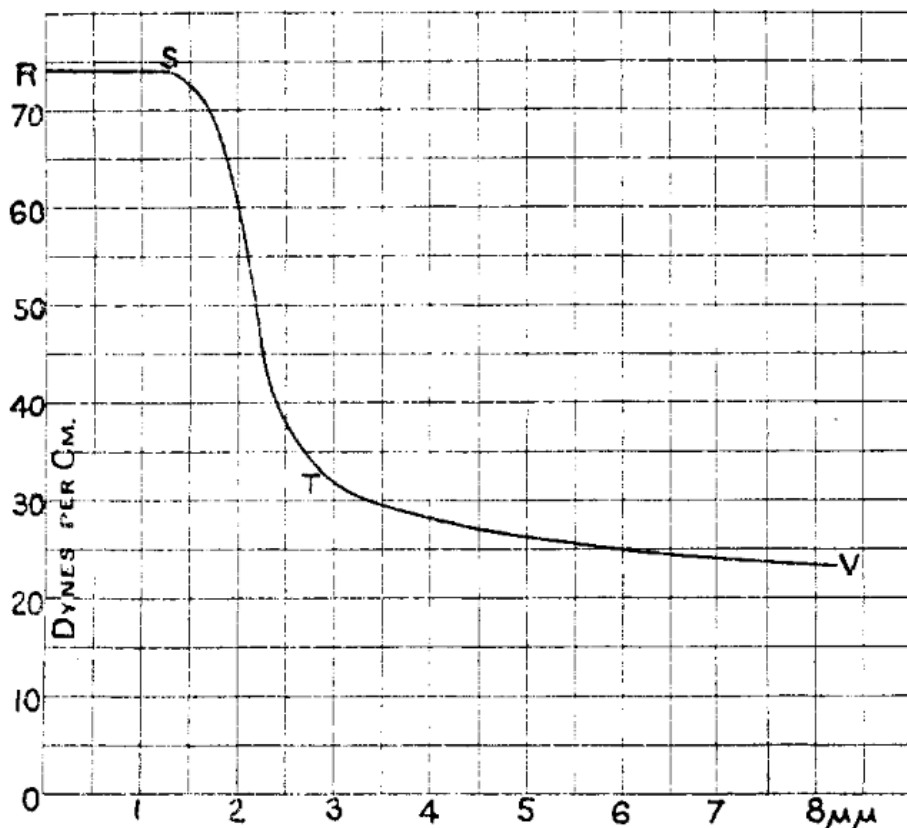


Figure 1.3.2. Rayleigh's isotherm.¹¹

Having studied and understood Raleigh's methods, Irving Langmuir developed a more precise and accurate instrument. He published the first comprehensive and systematic

examination of a large body of various compounds.⁴ While the scope of the study was impressive, it was the deductions discerned from the data which really added to the understanding of how molecules were interacting with their environment and with each other. Langmuir was able to extrapolate molecular size, orientation, which functional groups were in contact with the water, and the general shape of the carbon skeletons of the aliphatic chains.

1.4 Monolayer Deposition Considerations

There are various measurements used to analyze the electrical properties of a molecule. These measurements are preceded by the requirement that the substrate must first be attached to a suitable electrode. The two major methods used to attach substrates to electrodes are chemisorption and physisorption.

Chemisorption is the formation of a chemical bond with the electrode. Self Assembled Monolayers (SAMs) are molecules which have been chemisorbed to a surface. The most common chemisorption seen in SAMs is that of the covalent bond between thiols and gold. This covalent bond is comparatively strong and can displace impurities on the metal surface during the bonding process. However, monolayers derived from chemisorbed processes lack the long range order which occurs in Pockels-Langmuir monolayers.²

Physisorption is a weaker attachment method. In the Pockels-Langmuir deposition process, the monolayer is physisorbed onto the metal surface. The advantage of this procedure is the ability to retain the inherent order of the monolayer registry. One disadvantage is the requirement of stringent cleaning and polishing protocols to prepare a flat, defect free metal surface. Whereas chemisorption can displace a metal defect, physisorption will only cover the defect.² Furthermore, during repeated cycling voltage measurements, the physisorbed

monolayers can shift orientation and/or become desorbed completely,²⁹ whereas chemisorbed monolayers are more stable.

There are two popular methods for transferring a Pockels-Langmuir monolayer to a solid surface. The first method is known as Langmuir-Blodgett (LB). The second method is known as Langmuir-Schaefer (LS).³⁰ The Langmuir-Blodgett technique is the transfer of a monolayer to a solid substrate by vertical dipping. The Langmuir-Schaefer (LS) technique is the transfer of a monolayer to a solid substrate by horizontal attachment.

There has been an effort to combine the tight ordered packing of a Pockels-Langmuir film with the inherent stability of a chemisorbed Self Assembled Monolayer (SAM).^{8, 15, 19, 31-35} The idea is to first generate a monolayer via the Pockels-Langmuir technique. Next, the monolayer is transferred to a reactive metal surface and then chemisorbed onto the surface while the monolayer is still in its tightly packed monolayer. This concept was tested using thioacetate (RSC(O)CH_3) tethers which were cleaved with base to give thiolate. This method was found to be partially successful. There are still some technical hurdles to improve upon the process, but it seems this hybrid technique is a logical extension of how to combine Pockels-Langmuir with a chemisorption deposition.

There are many reasons for the interest in utilizing monolayer films developed on Langmuir troughs. The technique is useful to make a uniform and tightly packed assembly. In Pockels-Langmuir monolayers, controlling the orientation of molecules is relatively easy to achieve. Additionally, since the process is done at reasonable temperatures, problems associated with more energetic processes like those of evaporation, sputtering, or growth from a plasma can be avoided.²⁸

1.5 Rectification Ratio and Molecular Design Rule Constraints

At the heart of the study of unimolecular electronics is the property known as rectification ratio. Upon attachment of a substrate to electrodes, the rectification ratio may be obtained when positive current at one voltage is taken as a ratio against negative current at the reverse voltage. In terms of robustness and performance, organic single molecule rectifiers still fall short of the benchmarks held by inorganic rectifiers.⁶ A better understanding of how to make good molecular rectifiers is slowly being developed.

Since the original Aviram-Ratner proposal that certain molecules should be able to rectify, unimolecular rectification in organic molecules has indeed been confirmed.^{29, 36} Unfortunately, inorganic diodes continue to display much higher rectification ratios than single molecule rectifiers. When comparing single molecule organic rectifiers against inorganic diodes, the difference is a rectification ratio of one order of magnitude for typical organic rectifiers versus five orders of magnitude for inorganic diodes.³⁷⁻⁴⁰ Rectification ratios for bulk monolayers (Langmuir Blodgett, Langmuir Schaeffer, and SAMs) have been reported and can be much higher.

In one case by Ashwell and coworkers, a **D- π -A** with a cationic acceptor chemisorbed onto a gold surface gave impressive rectification ratios (RR) as high as three orders of magnitude.⁸ In another example, here in the lab of Mattern and coworkers, a TMPD donor on a perylene diimide (PDI) gave a surprisingly high RR, which was also three orders of magnitude.⁴¹ The PDI-TMPD rectifier is, to this author's knowledge, the highest RR ever recorded for a **D- σ -A**.

Nijhuis and coworkers' recent report on an asymmetrically placed **D- π -D** rectifier (Figure 1.5.1), which gave an RR of five orders a magnitude, is a major milestone!¹⁰ Finally, organic rectifiers are reaching parity with the inorganic rectifiers. Nijhuis and coworkers' rectifier will certainly contribute to a better understanding of design strategies but more importantly, how to best harness the design to achieve impressive benchmarks like the high rectification ratios.

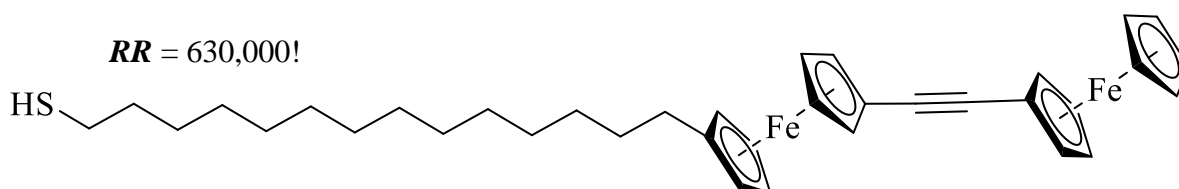


Figure 1.5.1: Nijhuis and coworkers' molecular rectifier

Colin Van Dyck and Mark A. Ratner have developed new design rules for new organic rectifiers.⁶ In the new proposal, the molecules are pinned to the electrodes with asymmetric functional groups (Figure 1.5.2) to effect a Fermi pinning phenomenon. The two functional groups are connected by a conjugated alkene which is decoupled with a saturated sigma bridge.

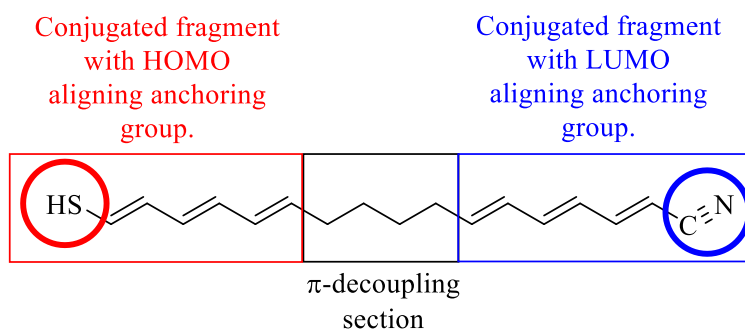


Figure 1.5.2: Asymmetric anchoring proposal by Van Dyck and Ratner.⁶

The choice of functional groups should correspond with the donor HOMO and the acceptor LUMO, respectively. When an electrical bias is introduced in one direction, the Fermi

pinning phenomenon results in transmission. When the bias is reversed, the HOMO and LUMO effectively become separated, breaking the transmission of electrons. Based on this understanding, they propose that low rectification ratios may benefit from greater alignment control by taking advantage of Fermi pinning phenomena at the metal-molecule interface.

1.6 Rectification Mechanism

The early molecular orbital proposal of rectification in organic rectifiers is based on the transmission of an electron from the electrode through the LUMO of the acceptor into the HOMO of the donor and to the opposite electrode.¹² This is known as Aviram-Ratner (AR) rectification (Figure 1.6.1, on left). A great deal of work has been done in order to understand the mechanism of electron transport. However, current theory and experimental evidence seem to favor the anti-AR model for many of the rectifiers studied to date.⁴²⁻⁴⁴

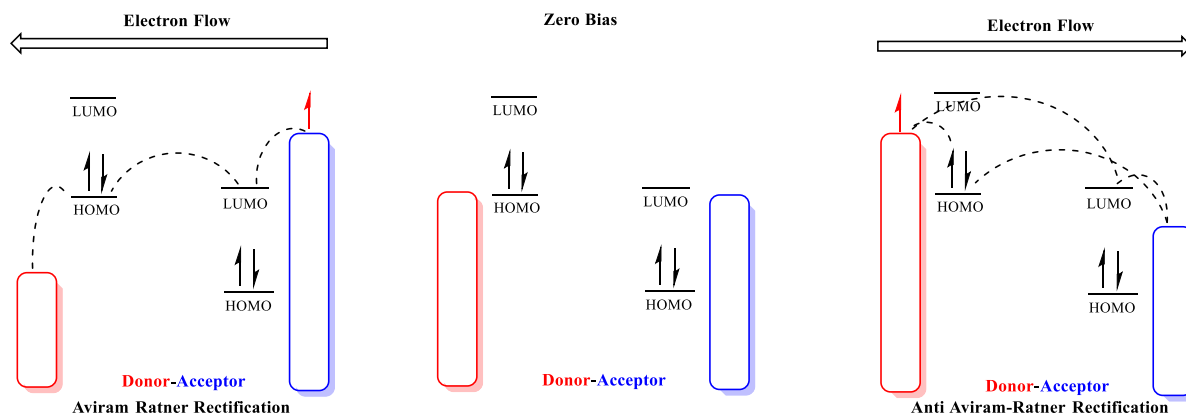


Figure 1.6.1: Aviram Ratner (left), no bias and no electron flow (center), Anti Aviram Ratner

Although we can easily compare rectification mechanisms as shown above, to more accurately model electron rectification, one must also consider the method of attachment to the electrode, how this affects HOMO-LUMO energy levels, and how this can affect electron transport. In Figure 1.6.2, there exists a D- σ -A which has not yet been attached to the metal

electrode surface (left). Once attached to the metal (right), the **D- σ -A**'s HOMO and LUMO are now coming into respective alignment with the Fermi level of the metal. The result is that the HOMO-LUMO gap of the *attached* molecule is different than that of the *unattached* molecule.

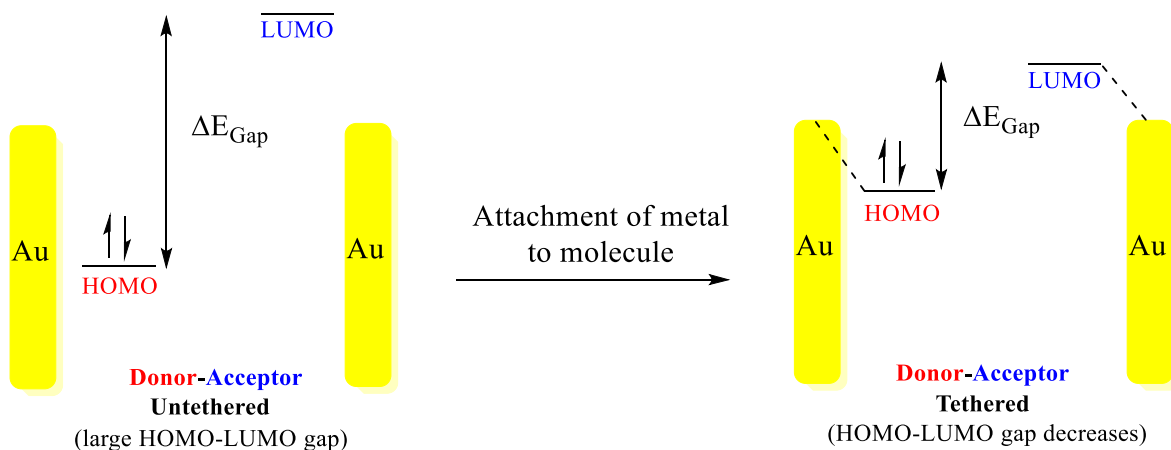


Figure 1.6.2: Band compression of HOMO-LUMO gap upon electrode attachment⁶

In Figure 1.6.3, the tethered **D- σ -A** is shown at positive Aviram-Ratner bias (left) compared against the **D- σ -A** at negative bias (right). When a positive (Aviram-Ratner) bias is applied, the HOMO-LUMO gap increases and the orbitals fall outside of the transmission window (denoted by the grey dashed line). The probability of electron transmission is small. When a negative (anti-Aviram-Ratner) bias is applied, the HOMO-LUMO gap aligns the orbitals within the transmission window (Fermi levels) of the metal electrode. The probability of electron transmission is high.

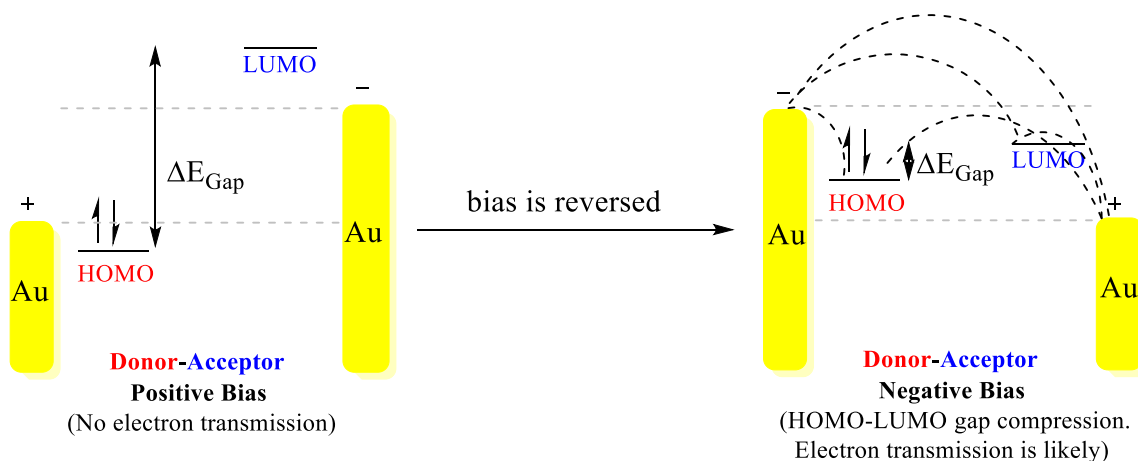


Figure 1.6.3: When frontier HOMO-LUMO levels are in alignment with metal electrode transmission window (Fermi levels), probability of electron transmission is high.⁶

Christian A. Nijhuis and coworkers have recently proposed a new rectification mechanism to account for their extremely high rectification ratios¹⁰ (5 orders of magnitude!). Acknowledging that the Landauer equation predicts a theoretical maximum RR of only up to 1000, the mechanism, they argue, must be operating under an alternative means of charge transport.⁴⁵ In Figure 1.6.4, they show sequential tunneling under negative bias (left). In the sequential tunneling electron transport mechanism, more molecules become involved in electron transport due to electrostatic interactions between the electrode and the HOMO of the ferrocene donors.

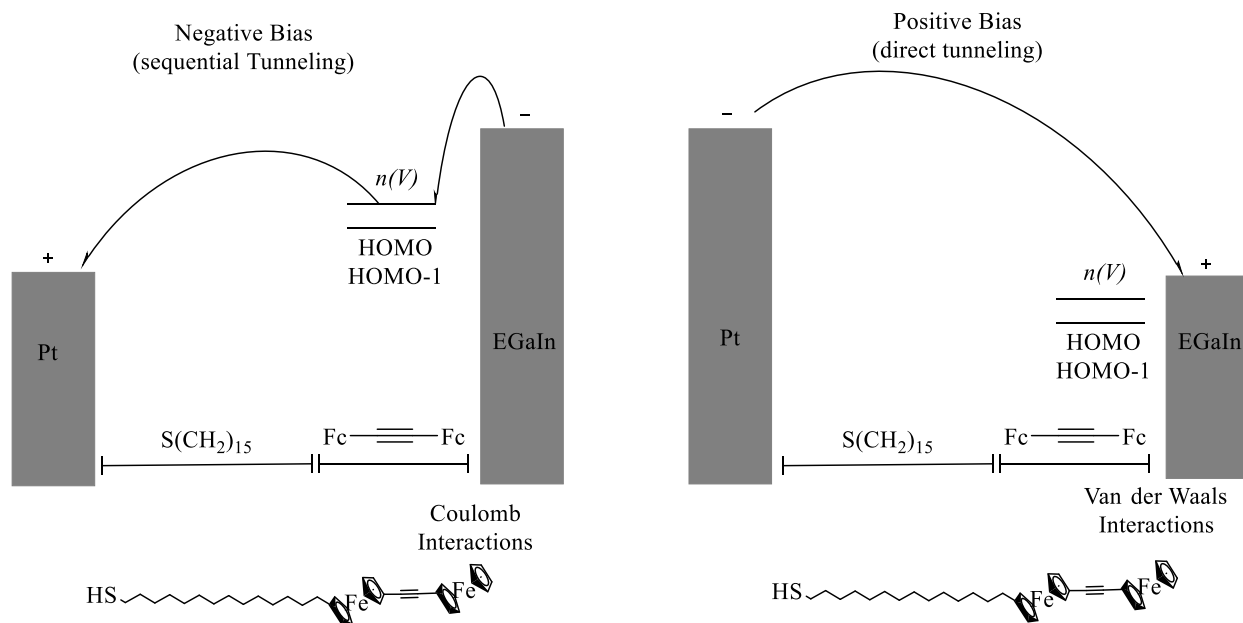


Figure 1.6.4: At negative bias (left) coulomb interactions at Fc-metal result in greater contact

Of interest in the above figure is the absence of participation of the LUMO orbital. Absence of the LUMO orbital is attributed to two factors. When platinum is the electrode, there exists a high bond dipole between metal and molecule. The high bond dipole ensures the LUMO does not align well with the transmission window¹⁰ and transmission probability is low, resulting in a lack of significant current transmission. Also, the LUMO is really high in energy because there is no acceptor group.

Recently some surprising experimental results^{32, 41, 46} have challenged conventional thinking on the rectification behavior of molecules. Conventional data for unimolecular rectifiers has shown rectification to be unidirectional. That is to say, unimolecular rectifiers rectify in one direction. Recently however, good rectification ratios were found in opposing directions when voltages were changed. As seen in Figure 1.6.5, asymmetric rectification ratios were documented. Coined “Janus Rectifiers”, this complex behavior might open new niche

applications for which to employ unimolecular rectifiers.

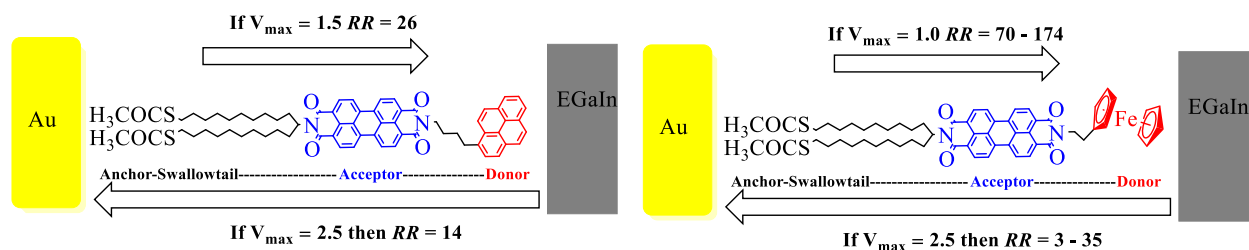
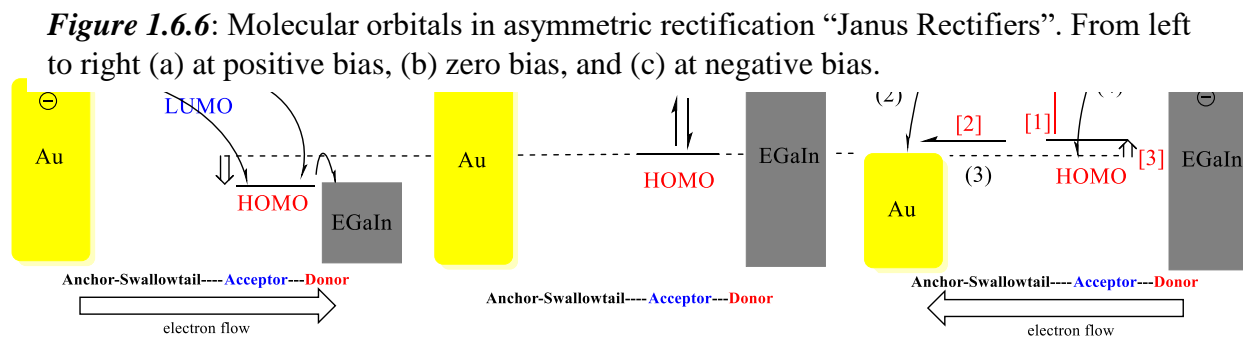


Figure 1.6.5: Asymmetric rectification.

Although the majority of rectifiers have followed an anti-Aviram-Ratner rectification - model (overall flow of electron from donor to acceptor), a few rectifiers have followed the Aviram-Ratner rectification model. In Figure 1.6.6, in (b) there is zero bias. However, when a positive bias (a) or a negative bias (c) is applied, the acceptor LUMO affinity level and donor HOMO level shift (indicated by the open arrow) by raising (a) or lowering (c) to come into alignment with the Fermi energy levels of the electrodes.^{32, 41}



In (a) the shifted acceptor LUMO is outside of the transmission window and is therefore not involved in electron transmission. It is hypothesized that the shifted donor HOMO donates an electron to the right electrode via resonant tunneling. The shifted HOMO then receives an

electron from the left electrode. In (c) there are several possibilities which are denoted by either parenthesis or brackets. In the scenario involving the numbered parenthesis only, an electron is donated from the right electrode to the shifted acceptor LUMO (1) then the electrons tunnel to the left electrode (2). The shifted donor HOMO electron tunnels to the left electrode (3). Lastly the EGaIn-electrode electron tunnels to the donor HOMO (4).^{32, 41}

In the alternate scenario involving the numbered square brackets only, the shifted donor HOMO electron is pre-excited by the applied field at negative bias. The shifted HOMO electron donates [1] into the empty shifted LUMO acceptor orbital. Next, resonant tunneling from the shifted LUMO acceptor orbital to the left electrode occurs. This scenario could be simply referred to as the Anti-Aviram Ratner like model.⁴⁷ Lastly, an electron can be alternately be donated from the right electrode to the shifted donor HOMO and then to the left electrode.⁴⁸

1.7 Properties of Good Electron Donors

A good donor can be qualitatively described as a molecule which is able to be a single electron donor. In terms of a quantitative description, the favorable ability to donate an electron is measured in terms of ionization energy (IE) of a molecule in the gas phase. IE can be measured by photoelectron spectroscopy, which requires vaporizing solid molecules into the gas phase. For organic donors that are not amenable to gas phase ionization, the IE values can be extrapolated by electrochemical redox data.⁴⁹ Some good donors are shown below.¹⁻²

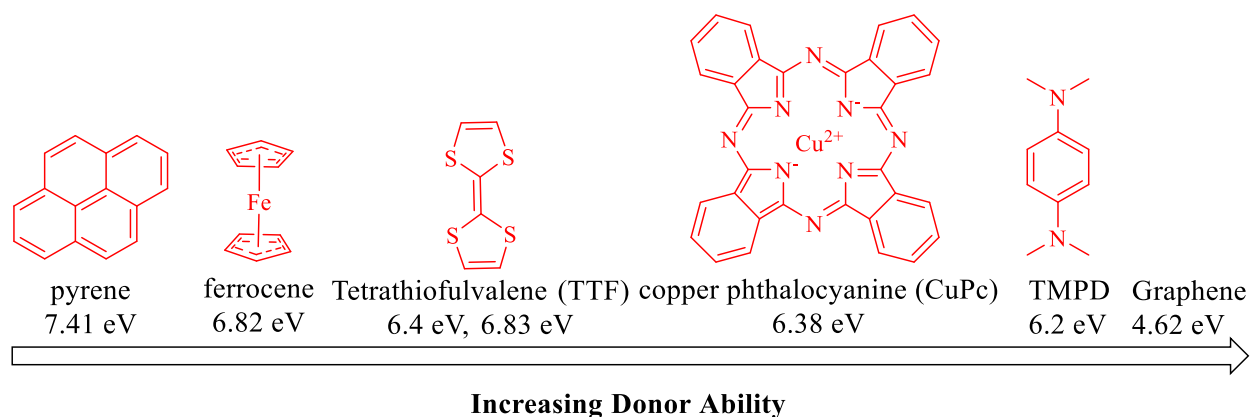


Figure 1.7.1: Good donors with ionization energies shown. ¹⁻²

In this lab^{32, 48} various **D-σ-A**'s containing pyrene and ferrocene donors appended to perylene diimide cores have been synthesized. Some of the results can be seen in Figure 1.7.2. Despite the similarity of compounds **2** and **3**, **2** forms a defect-ridden monolayer and rectifies poorly at best. Whereas **2**'s alkyl swallowtails terminate with methyls, **3**'s alkyl swallowtails are terminated with thioacetates. Compounds **1-3** contain pyrene donors whereas **4** contains a ferrocene donor. With an ionization potential ~1.4 eV smaller than pyrene, ferrocene is a better donor. Unsurprisingly, the perylene diimide with the ferrocene donor gives the best rectification ratio in this set. When the donor is allowed to remain the same (ferrocene) but the aliphatic swallowtail is terminated with a thioacetate anchor (Figure 1.7.3), the rectification ratio jumps an order of magnitude.

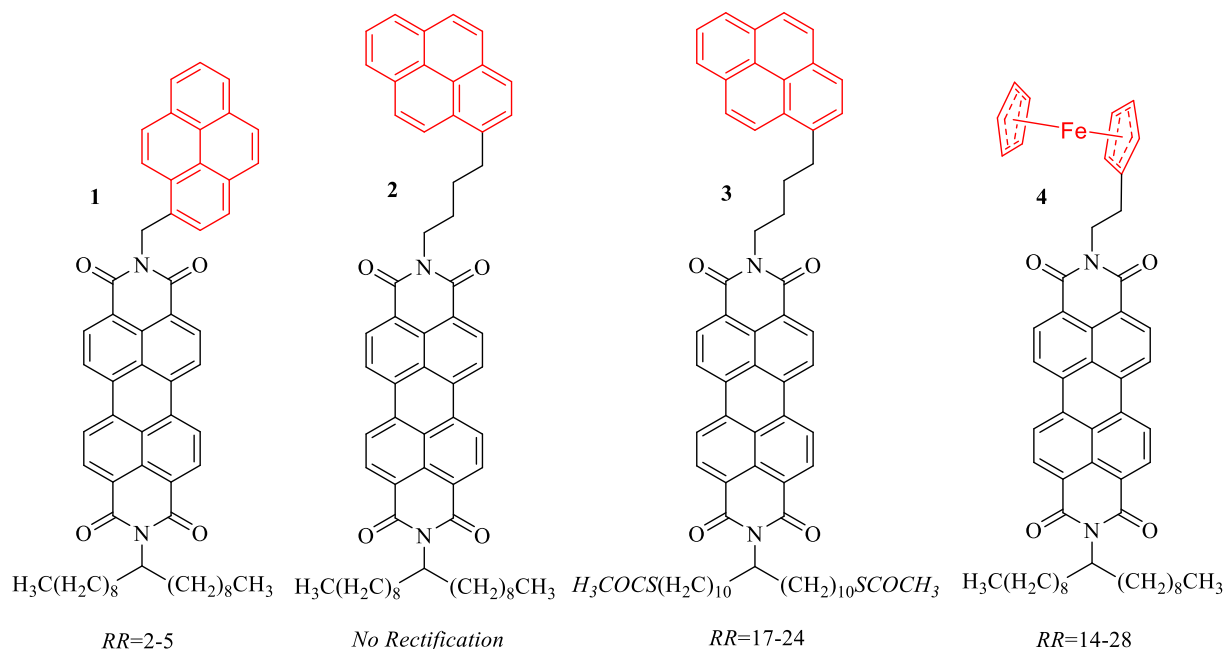


Figure 1.7.2: Various $D-\sigma-A$'s synthesized in this lab with pyrene and ferrocene donors.

The trend of increasing donor strength is more clearly revealed in a more recent study⁴¹ based on molecules synthesized in this lab.⁵⁰ The TMPD donor, as characterized by very low ionization energies (see Figure 1.7.1), is a stronger donor than ferrocene. In fact, compound **6** which has the strong TMPD donor, is reported to have one of the highest RR's known for $D-\sigma-A$. Clearly, with an RR one order of magnitude higher than ferrocene and two orders of magnitude higher than pyrene, the TMPD stands in a category of its own.

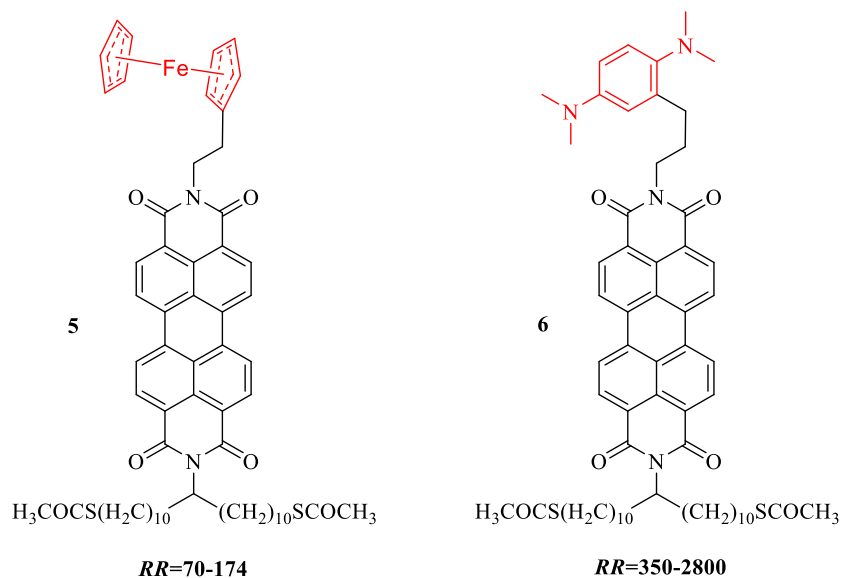


Figure. 1.7.3: Various D- σ -A's synthesized in this lab with ferrocene and TMPD donors.

1.8 Properties of Good Electron Acceptors

The characteristic which makes an organic molecule a good acceptor is the ability to accept a single electron. This property can be measured in terms of the electron affinity (EA) or in terms of the half-wave reduction potential ($E_{1/2}$). Good acceptors have a high affinity for electrons and therefore have high EAs and high reduction potentials.

The electron affinity (EA) is the amount of energy that is released when a molecule in the gas phase accepts one electron to form the respective anion. Obtaining the EAs in practice can be difficult. This difficulty stems from the expensive equipment and complex conditions required to make good measurements.⁵¹ Often it can be more practical to obtain half wave reduction potentials as an analogous means to derive a molecule's capability to accept electrons. An example of some electron acceptors is shown below.^{49, 52}

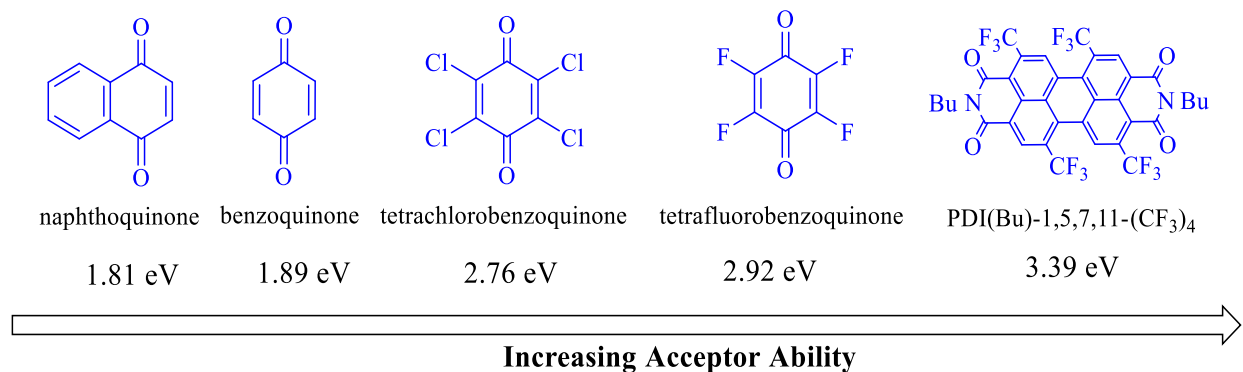


Figure 1.8.1: Good acceptors' electron affinities

In Figure 1.8.1, there are essentially two traits which contribute to the high electron affinity of benzoquinone (BQ) type compounds. First, when a BQ type compound accepts an electron to form the radical anion, the resulting radical is stabilized by the increased delocalization energy of the aromatic radical (Figure 1.8.2). Thus, aromaticity is a driving force for the high EA of benzoquinone type moieties.

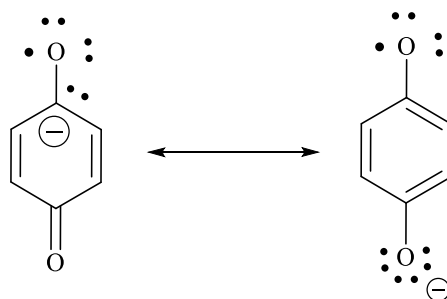


Figure 1.8.2: Radical stabilization by aromaticity.

The other trait is an electronic effect. When BQ is substituted with electron withdrawing groups such as BQCl₄ and BQF₄, the electron affinity increases dramatically. Furthermore, as the electron affinity of the acceptor increases, the energy of the LUMO is lowered. The ultimate result is the general ability to manufacture better D-σ-A's.

The excellent D-σ-A's synthesized in this lab and briefly mentioned in section 1.6 relied on the perylene diimide core which is a good one-electron acceptor ($E_{1/2}$ -0.50 V vs. SCE), similar in acceptor ability to that of benzoquinone.⁵³ PDIs are also both a photochemically and

thermostable class of compounds which were originally developed for their characteristics of being good dyes.⁵⁴ When subjected to a one electron reduction, PDI gives a stable, highly delocalized radical. The stability of the reduced species is no doubt a strong driving force for the high electron affinity of PDIs.

Another acceptor now in use is quinolinium. Unlike PDI, which is a neutral molecule, quinolinium is cationic. When compared against quinoline, the quinolinium LUMO is very low in energy. Furthermore, the formal positive charge of quinolinium results in a very high electron affinity. In short, quinolinium is an excellent acceptor.

As an example of how acceptor strength is being used in molecular rectifiers, Ashwell and coworkers achieved high rectification ratios with Self Assembled Monolayers (SAMs) based on cationic quinolinium acceptors.^{8, 16-18, 20} In the Figure **1.8.3** examples, alkanethiols were chemisorbed onto gold electrodes. When all other things were equal, rectification ratios were good but varied strongly with respect to the choice of counter anion.

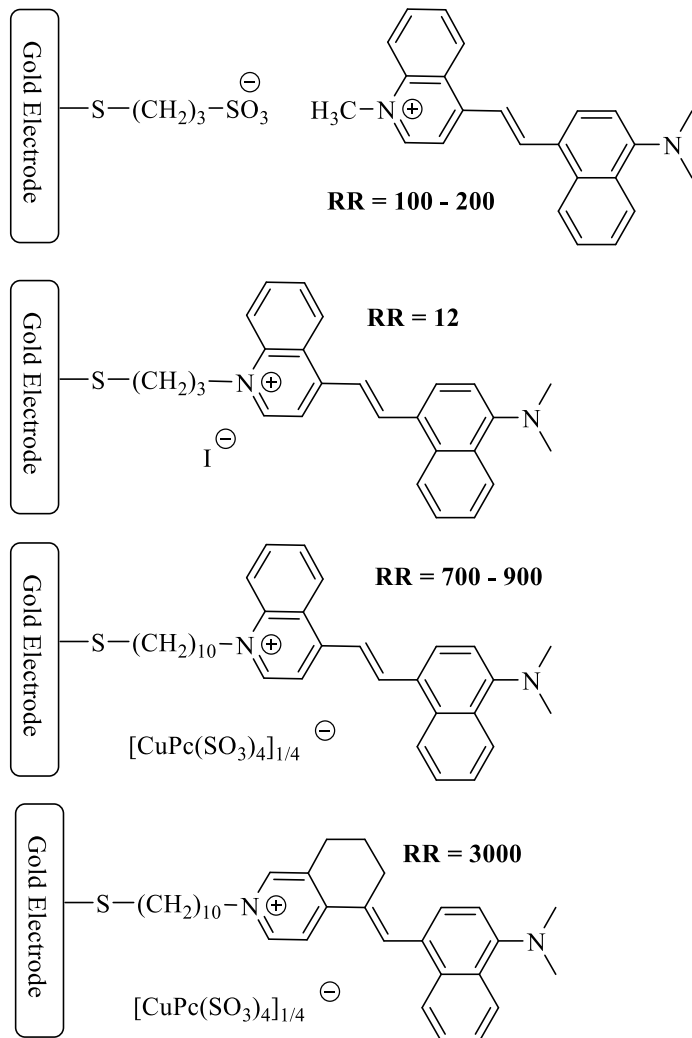


Figure 1.8.3: Ashwell's cationic acceptors

1.9 Perylene Diimides, a Robust Platform for Accessing **D- σ -A**'s

One of the initial technical difficulties with the PDI dyes was the very poor solubility. The work of Heinz Langhals and colleagues approached the problem by appending *t*Bu-aryl groups to improve solubility.⁵⁵⁻⁵⁶ In another case, secondary alkyl groups (so called swallowtails) were used to enhance solubility.^{7, 57} In one of these latter two studies, Langhals and colleagues quantitatively describe an optimum swallowtail length.

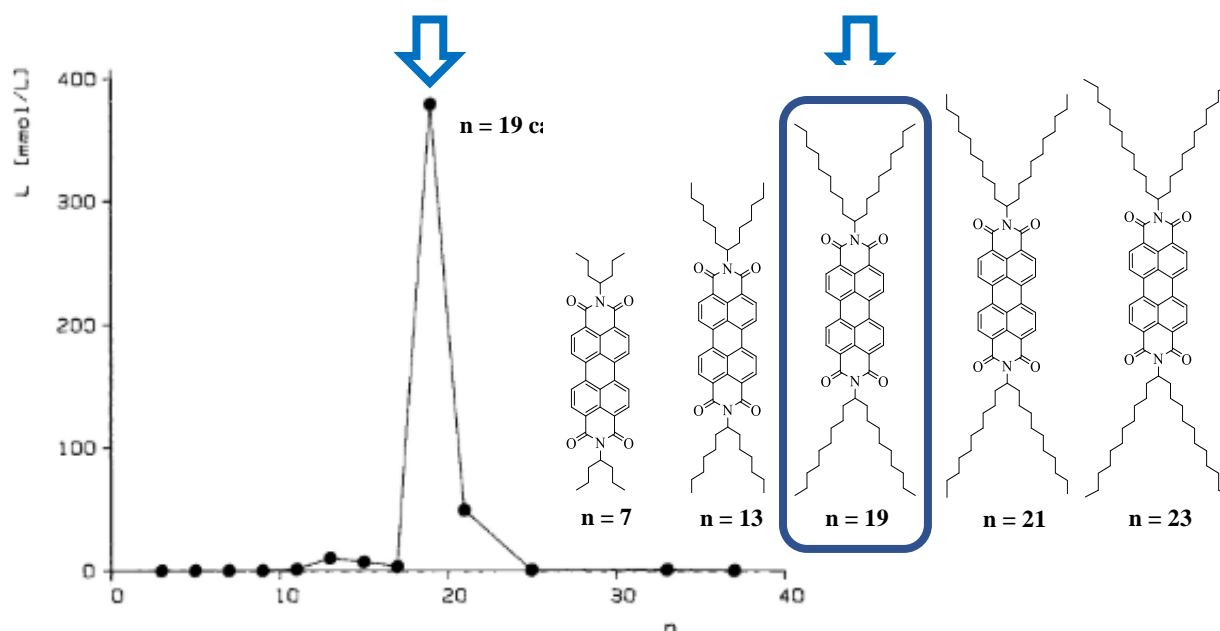
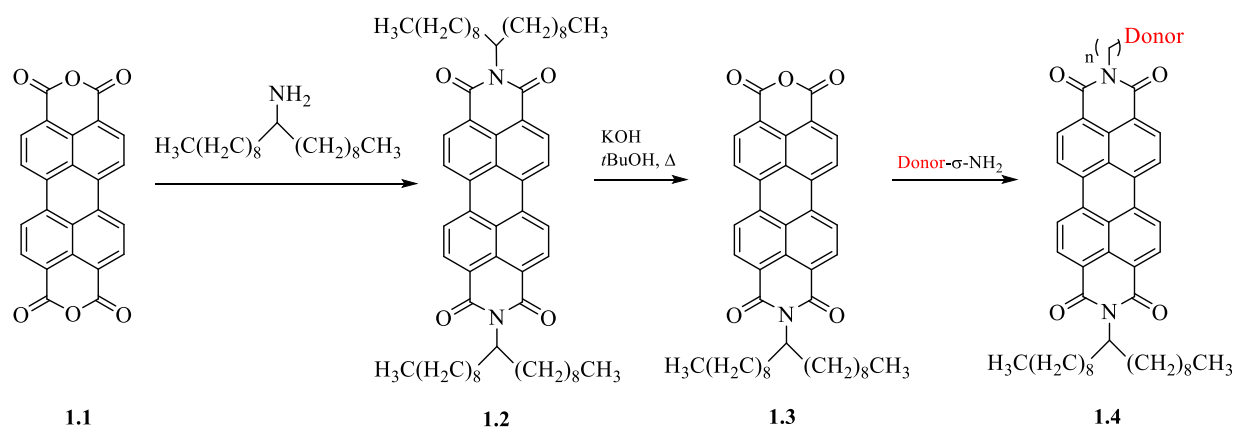


Figure 1.9.1: Chart on left shows solubility of PDIs in heptane as a function of swallowtail length (n).⁷ Solid arrow on chart correlates to indicated structure on the right.

The solubility of PDIs containing aliphatic swallowtails of varying lengths was initially determined in chloroform. When PDIs of increasing swallowtail length were dissolved in chloroform the solubility increase was exponential. The extremely high solubility made measurements difficult. Langhals and coworkers then switched to heptanes and it was found that solubility initially increased slowly with increasing chain length then reached a flat maximum at $n = 13$ ($n =$ number of carbons). Surprisingly, solubility dropped off slightly from $n = 13$ to $n = 17$ whereupon at $n = 19$ the solubility reached a maximum. Beyond $n = 19$, solubility decreased.

Although initially conceived as dyes, PDIs are now being used for many applications. Their synthesis and behavior trends with respect to structure modifications have been studied.⁵⁸⁻
⁵⁹ Some of the applications for which PDIs are now being used include dye lasers⁶⁰, light emitting diodes⁶¹, field-effect transistors⁶², thin film transistors⁶³, and photovoltaic cells. The subject has been thoroughly reviewed in the literature.⁶⁴

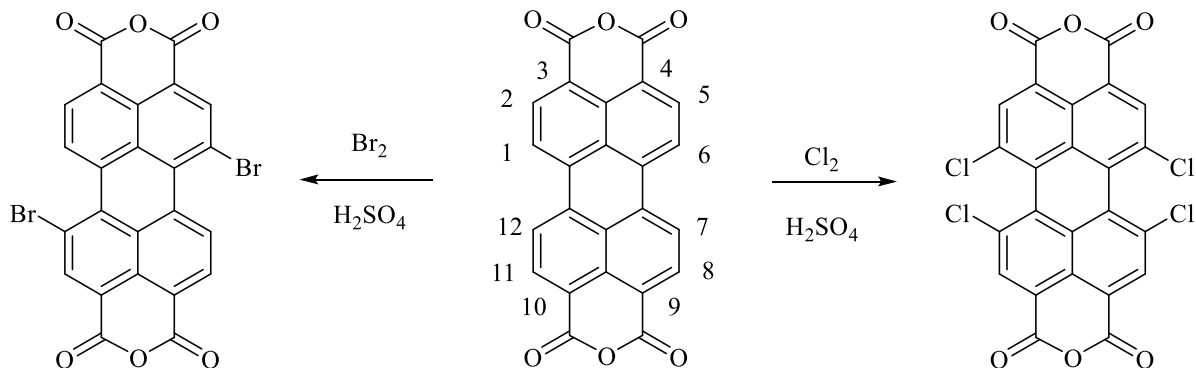
PDI s are planar, photostable compounds. They are highly persistent and resist all but the most aggressive reagents.⁵⁸ The planarity of the perylene backbone is one of the reasons PDI s form well ordered monolayers on Pockels-Langmuir troughs. Synthetically speaking, converting the accessible starting material perylenetetracarboxylic dianhydride (PTCDA) **1.1** to PDI **1.2** is facile, but **1.2** to monoanhydride **1.3** (shown in Scheme 1) requires carefully controlled conditions. Fortunately, the monoanhydride **1.3** is labile. Various donors with amine handles are easily condensed onto **1.3**. The robust synthetic protocol is facile and is one reason the PDI platform is favored.



Scheme 1.1: Perylene diimide synthetic route from **1** to **2** requires conditions that avoid hydrolysis of both imides. The conversion of labile **1.3** to persistent **1.4** is facile

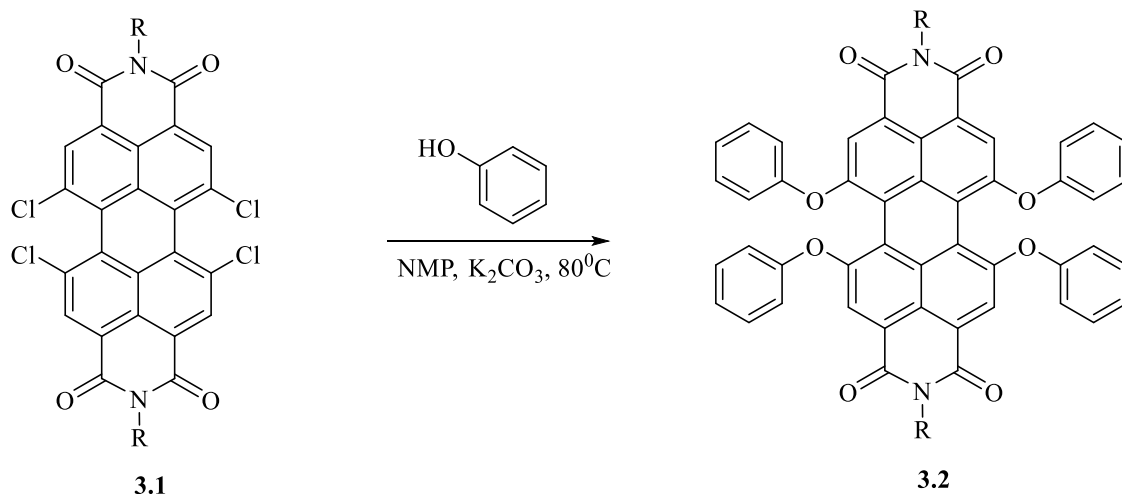
This modularity allows one to focus on variations of both donor type as well as sigma-bridge length while retaining the PDI core. However, in some instances one may wish to alter the PDI core as opposed to merely functionalizing the monoanhydride with various donors. In Scheme 1.2, PTCDA may be either brominated or chlorinated. PTCDA's carbons have been numbered for the sake of furthering subsequent synthetic explanations. Halogenations with a sulfuric acid/chlorine protocol can result in tetrasubstitution at the 1,6,7,12 (bay) positions. Halogenations with a sulfuric acid/bromine protocol result in disubstitution at the 1 and 7

positions. The procedure for conversion of PTCDA to the tetrachloro analogue via $\text{Cl}_2/\text{H}_2\text{SO}_4$ is reputed to have originated in 1988.⁶⁵



Scheme 1.2: Halogenations of perylene tetracarboxylic dianhydride (PTCDA) occur at the bay positions.

In the late 1980's BASF was interested in a way to help improve upon the solubility of some of their existing PDI dyes. However, unlike Langhals and coworkers, their early approach did not involve condensation of swallowtails onto PTCDA. Their synthetic scheme⁶⁶ (Scheme 1.3) begins with a PDI where R = methyl (but could presumably be any alkyl variation). An aryl hydroxy – in this scheme phenol is shown – is substituted for the chloro groups. Interestingly the steric strain at the bay positions causes the molecule to twist significantly (42°). The subsequent twist from planarity results in a dramatic increase in solubility in organic solvents. Additionally, in this same publication, they report that exchange reactions have been performed in dipolar aprotic solvents with KF, CuCN, mercaptans, sulphinic acids, alcohols, phenols and amines.



Scheme 1.3: Bay substitution of PDI.

Since the PDI core's role in **D- σ -A** chemistry is that of acceptor, the ability to functionalize the acceptor can be extremely useful. Based on previous work in this lab, some of the PDI based **D- σ -A**'s occasionally showed a tendency to agglomerate into insoluble supramolecular structures. This drop in solubility is driven by formation of supramolecular aggregates due to concerted π - π interactions as well as hydrogen-bonding.⁶⁷ To a certain extent, PDI s with swallowtails can interrupt the full extent of π - π interactions due to one half of the aliphatic swallowtail's tendency to protrude above the plane of the perylene while the other half of the swallowtail is oriented below the plane of the perylene. While this can help interrupt the PDI's tendency to form insoluble supramolecular aggregates it is not always sufficient. In these cases, substitution at the bay positions with bulky substituents can help disrupt the supramolecular forces.

It must then be considered how bay substitutions on the perylene core might affect the PDI's ability to function as an acceptor. One of the driving reasons for favorable electron affinity of PDI, and hence utility as an acceptor, is the ability of the large planar surface of the PDI to

delocalize radical formation through the large conjugated π -system. Electron withdrawing substituents should lower the energy of the acceptor's LUMO making it a better acceptor by increasing its electron affinity (EA). However, if an electron withdrawing substituent disrupts the conjugated π -system by forcing a dihedral twist of the PDI chromophore, then EA might suffer due to the twisting of the PDI chromophore.

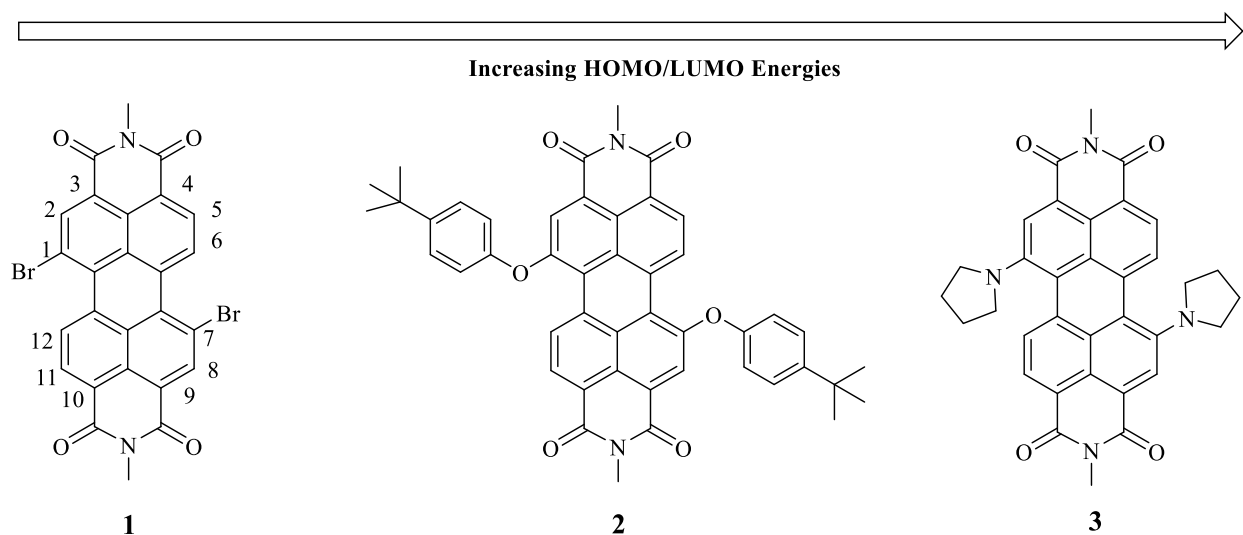


Figure 1.9.2: Bay substituent effect on HOMO/LUMO levels.

As noted in Figure 1.9.2 and Figure 1.9.3, when electron donating ability of substituents in the bay position increases, both HOMO and LUMO levels increase.⁶⁸ The change in LUMO levels is a key consideration of designing $D-\sigma-A$'s with the goal of containing acceptors with low LUMOs. Interestingly, the same publication reported the dihedral angles measured at C6 – CC – C7 and C1 – CC – C12 to be greatest for the dibromo analogue. The overall dihedral angles for the three molecules were 22.1°, 12.8°, and 20.8°. Thus, in this case, the extent of dihedral twist in planarity of the PDI seems to play less of a role in LUMO level than does the ability of substituent to donate electrons.

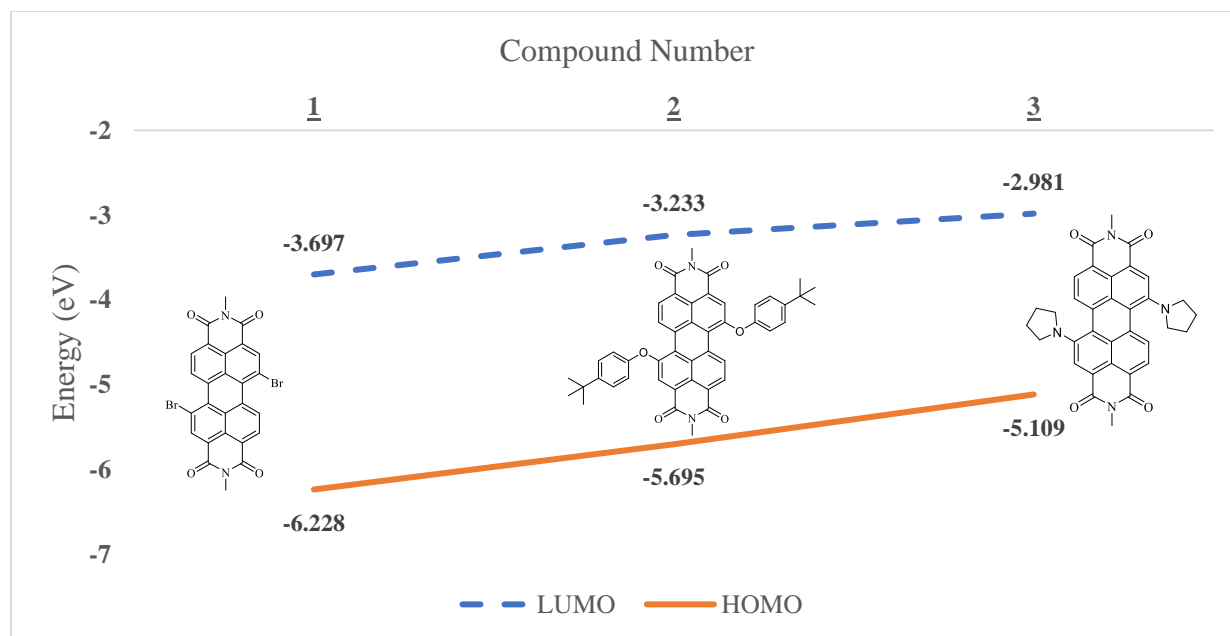
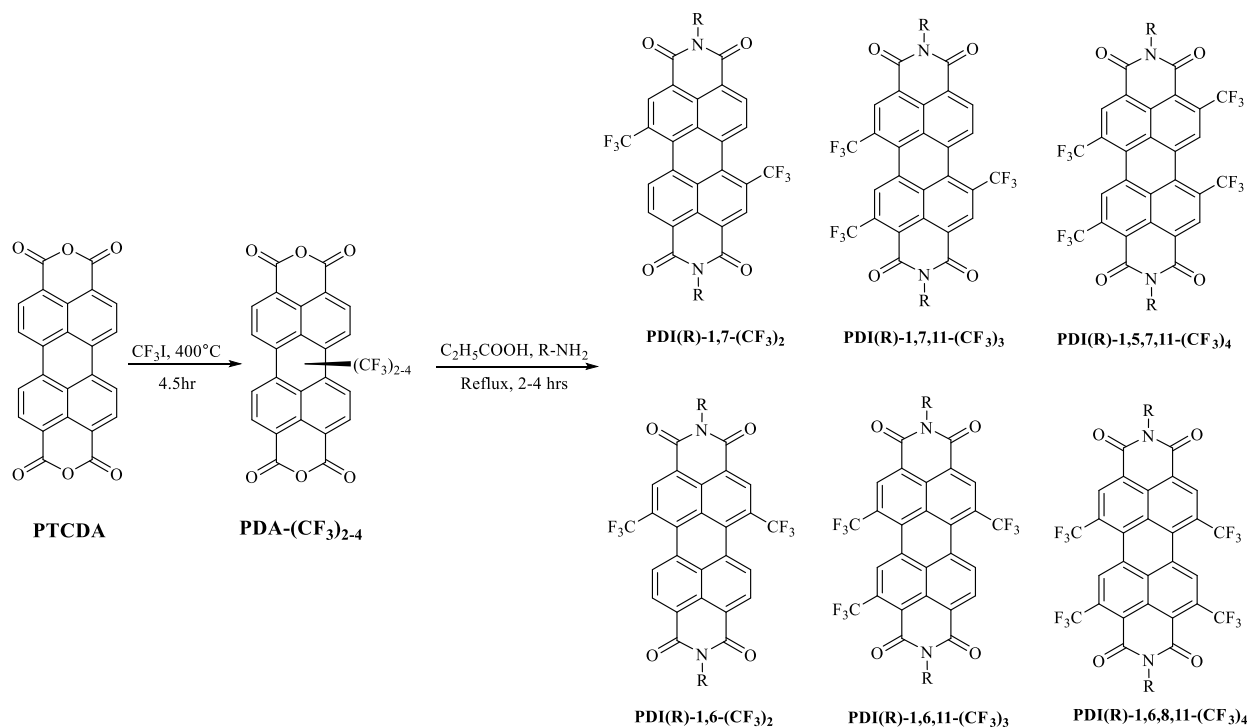


Figure 1.9.3: HOMO/LUMO levels of compounds with various EDG-substituents in bay positions computed at the B3LYP/def2-SVP level

Recently, a simple and direct trifluoromethylation of PTCDA in solvent free conditions was achieved.³ This elegant synthesis, shown in Scheme 1.4, is capable of simultaneous substitution in the bay *and* ortho positions. The successful introduction of two to four trifluoromethyl groups was achieved. The subsequent isomers were all efficiently separable via chromatography. Additionally, these polytrifluorinated PDIs were found to be soluble in organic solvents and thermally stable. Most importantly, electron affinities (EAs) rivaling that of the dibromo compound (Fig. 1.9.3) were experimentally determined. EAs of 3.00 eV, 3.20 eV, and 3.38 eV were determined for PDI(Bu)-1,7-(CF₃)₂, PDI(Bu)-1,7,11-(CF₃)₃, and PDI(Bu)-1,5,7,11-(CF₃)₄ respectively. These excellent EA values could likely make these PDIs excellent candidates for a new set of D-σ-A's based on the functionalization of the PDI acceptor as opposed to a mere change of donors.

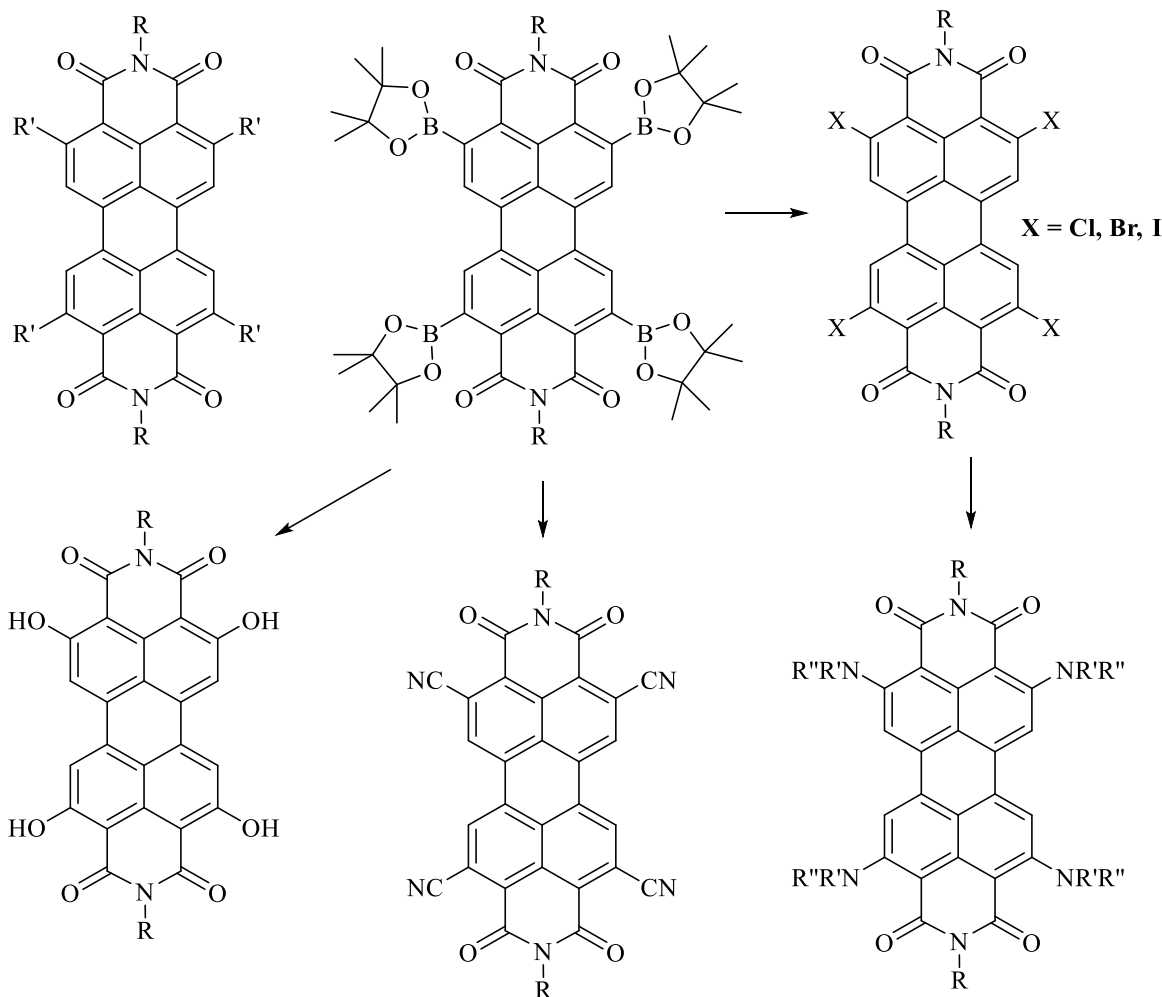


Scheme 1.4: Direct trifluoromethylation of PTCDA in solvent free conditions.³

Although the aforementioned polytrifluoromethylation³ gives PDIs with desirable stability and electron affinity (EA) characteristics, it is difficult to say to what type of monolayers could be formed. The bay substitution will undoubtedly result in some degree of dihedral shift of the bay-substituted PDI core away from the planarity of the unsubstituted PDI. It is possible that a less dense and less uniform monolayer registry results. While it seems desirable to be able to control the electronic properties of the PDI acceptor core, one of the limitations of much of the previously referenced work is the absence of regioselective schemes, which could give primarily ortho-substituted PDIs. Fortunately, such regioselective synthetic protocols now exist.⁶⁹⁻⁷⁰

In 2009, an exciting new synthetic breakthrough occurred. Satomi Nakazono and colleagues established a regioselective ruthenium-catalyzed direct alkylation of PDIs.⁷⁰ That

study was quickly followed up with a procedure for the regioselective ortho-arylation of PDIs.⁶⁹ Another group then reported a regioselective ruthenium-catalyzed reaction of PDIs which gives 2,5,8,11-tetraboronate derivatives.⁷¹ Once the ability to functionalize the PDIs outside the bay position was established, the same authors quickly realized a means to convert the boronate ester to the iodinated compound. The iodinated compound was then found to be easily aminated. Takuro Teraoka and coworkers used an iridium catalyst to access the 2,5,8,11-tetraboronate derivative. This was subsequently oxidized with hydroxylamine hydrochloride to give the 2,5,8,11-tetrahydroxy derivative in an excellent yield. The tetra-substituted cyano derivatives were obtained by Battagliarin and coworkers by using a copper mediated cyanation of the boronate.⁷² These are of interest because they would be the best acceptors of this series. Scheme 1.5 shows in greater detail various analogues which are now synthetically accessible.⁷³



Scheme 1.5: A schematic view of regioselective 2,5,8,11-tetrasubstitutions of PDIs

To sum up the evolution of the perylene diimide (PDI) platform as laid out in this chapter, PDIs can be synthetically manipulated in essentially three positions which are most relative to the type of $D-\sigma-A$'s which have been synthesized in this lab. Langhals and colleagues manipulated swallowtail type and length at the imide nitrogen to improve solubility. At the bay position, halogenations were developed and shortly followed by substitutions which allowed the chemist to manipulate HOMO and LUMO levels through various electron withdrawing and releasing functional groups. Additionally, steric repulsion of bay substituents resulted in torsion of the perylene core and subsequent improvement upon solubility by lowering the π -stacking

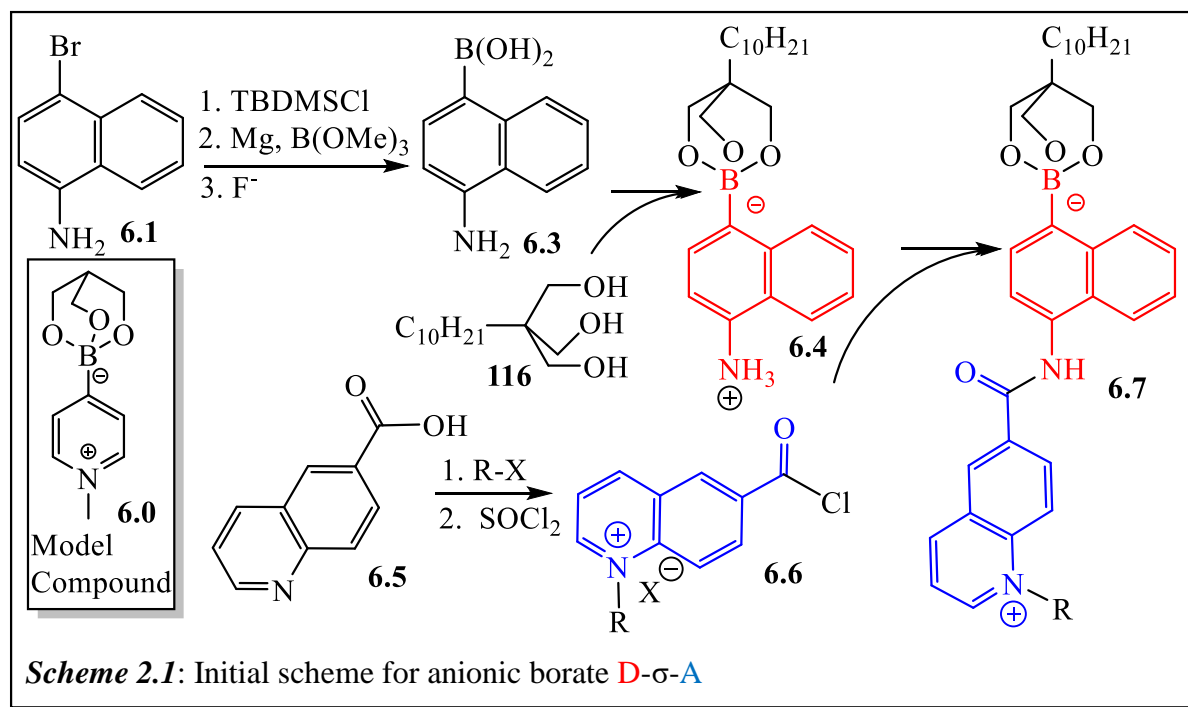
interactions. Most recent has been the development of regioselective additions at the ortho position. This latest of contributions will help to establish PDIs as robust platforms for thoughtful design towards the next generation of $D-\sigma-A$'s.

CHAPTER 2: ZWITTERIONIC DONOR- σ -ACCEPTOR (D- σ -A) COMPOUNDS

2.1 The Synthesis of Zwitterionic Donor- σ -Acceptors (D- σ -A's)

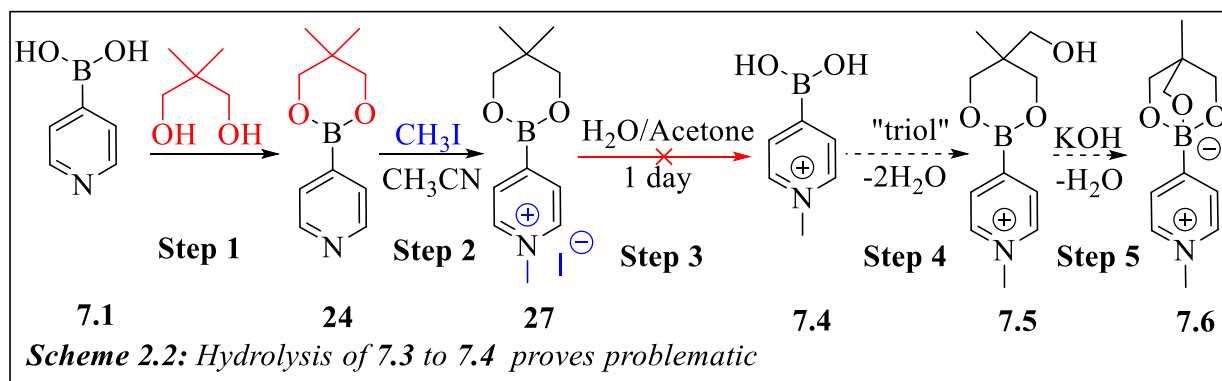
As a general principle in materials chemistry, the form of a molecule should always be based on the material's intended function. In the case of unimolecular rectifiers, the function is rectification of DC current. The measure of a unimolecular rectifier's performance, and therefore inherent value as a material, is in having a high rectification ratio (RR). The design of D- σ -As is based on principles covered in the introduction. The rationale for proposing the targets is that an anionic donor should have a high-energy HOMO while a cationic acceptor should have a low-energy LUMO. For the first project of this dissertation, the target molecule **6.7** contains an anionic borate donor (high HOMO) and a cationic acceptor quinolinium (low LUMO). The feasibility of the concept was investigated by synthesizing a similar model compound **6.0** (Scheme 2.2).

The zwitterionic model-compound synthesis target based on an anionic borate donor was successfully achieved, as will be discussed in 2.1.1. Encouraged by our results, we then directed our efforts towards synthesis of target **6.7** (Scheme 2.1). However, the planned synthetic route was problematic and required alterations which will be discussed.

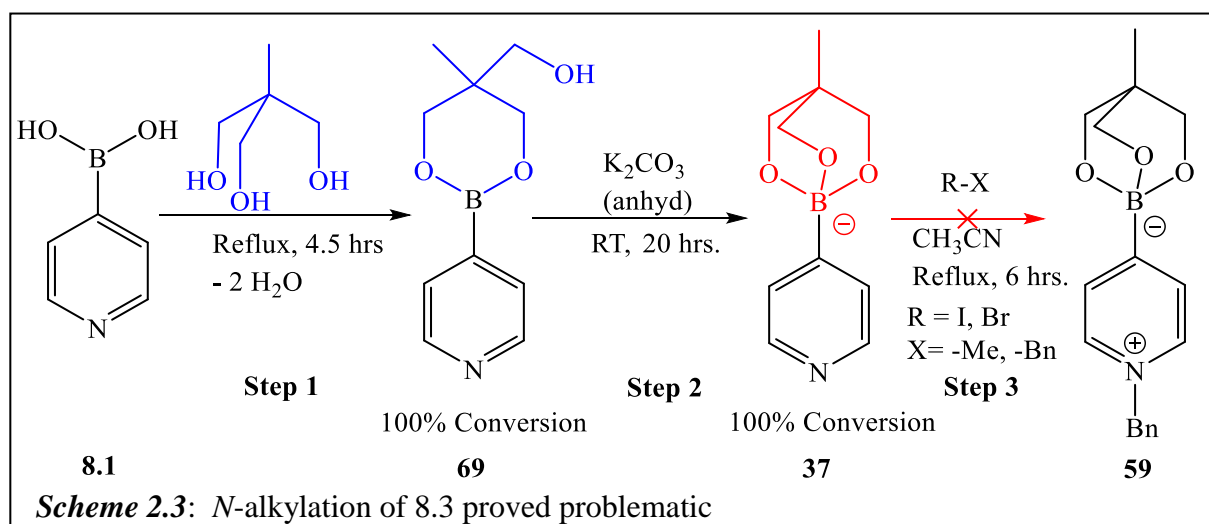


2.1.1 Preparation of the Zwitterionic Model Compound Containing an Anionic Borate Donor and a Pyridinium Acceptor.

The synthesis of model compound **7.6** (Scheme 2.2) began by condensation of diol (neopentyl glycol) onto boronic acid **7.1** to give boronate ester **24** in 91% yield. *N*-Alkylation of **24** with iodomethane gave the methyl pyridinium **27** in 92% yield. The boronate ester **27** was deprotected in acetone/water to give **7.4**. Purification of **7.4** proved problematic.⁷⁴ Despite multiple triturations with diethyl ether, the diol byproduct could not be completely removed. As a result, an alternate (and shorter) scheme was envisioned which would eliminate the protection/deprotection protocol (steps 1 and 3, respectively, from Scheme 2.2).

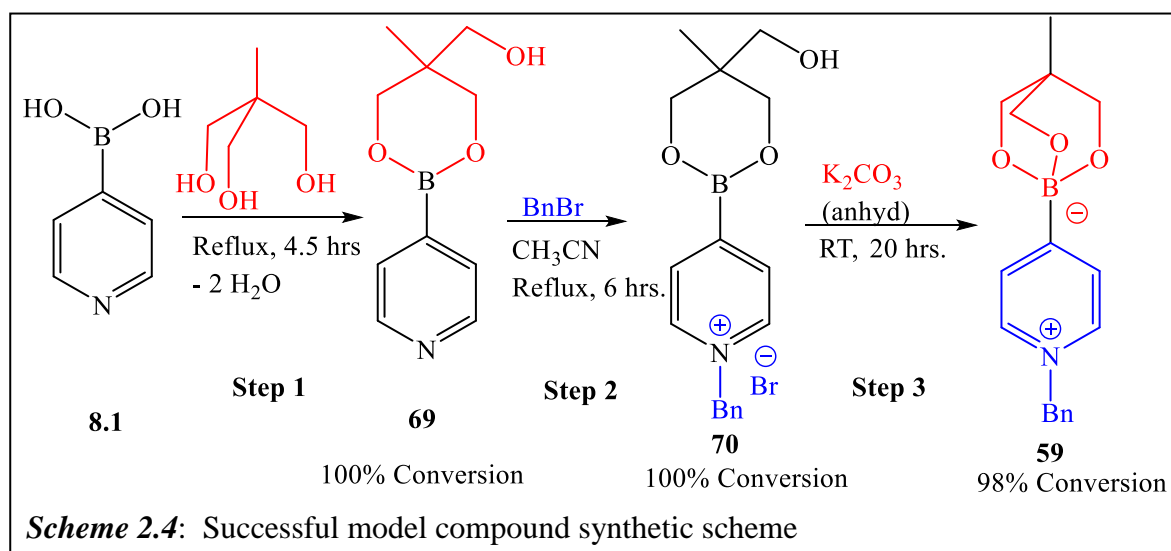


In Scheme 2.3, condensation of the triol trimethylolthane (TME) onto boronic acid **8.1** gave boronate ester **69** quantitatively. Deprotonation of **69**'s pendant alcohol and subsequent cyclization gave the anionic borate **37** quantitatively.⁷⁵ *N*-Alkylation of triolborate **37** was initially attempted with iodomethane and then later with benzyl bromide. Iodomethane is a logical first-choice *N*-alkylation reagent because post-reaction, excess iodomethane can be easily stripped via rotary evaporation. However, the inability to optimize the *N*-alkylation step when iodomethane was the reagent led to the use of another alkylating reagent. Both attempts were unsuccessful (complex mixture of products as determined by ¹H NMR).



There was always a thermochromic effect observed when *N*-alkylation (using either iodomethane or benzyl bromide) was attempted from the triolborate **37**. Upon reaching approximately 65°C, both methylation and benzylation reaction mixtures became inky violet. With cooling, the color disappeared, but reappeared upon heating. Exposure of the flask to ambient air would result in an abrupt quenching of the violet color. The color change was presumably due to the presence of a radical species.⁷⁶⁻⁷⁷ ¹H NMR analysis was conducted at various times when either iodomethane or benzyl bromide was used as the reagent. In all cases, evidence of a triplet proton in the aromatic region was observed, which implies the likelihood of a deborylation event. The spectra were consistent with the formation of multiple products.

Due to the problems associated with having the *N*-alkylation as the last step in Scheme 2.3, the reaction order was changed so that *N*-alkylation would precede ring closure (Scheme 2.4). It was determined that the key step for the synthesis of the model zwitterionic compound is that *N*-alkylation must precede ring closure. In fact, this solved the deborylation problem. Furthermore, the final product **59** was obtained in 98% conversion over three steps.



Stability studies of **59** were obtained in neutral, acid, and basic conditions in various NMR solvents (DMSO-d₆ and D₂O) over 11 days. Basic conditions resulted in sample degradation while acidic and neutral conditions showed no decomposition. Encouraged by the ability to synthesize the model compound, the attempted synthesis of the target (Scheme 2.1, **6.7**) was started.

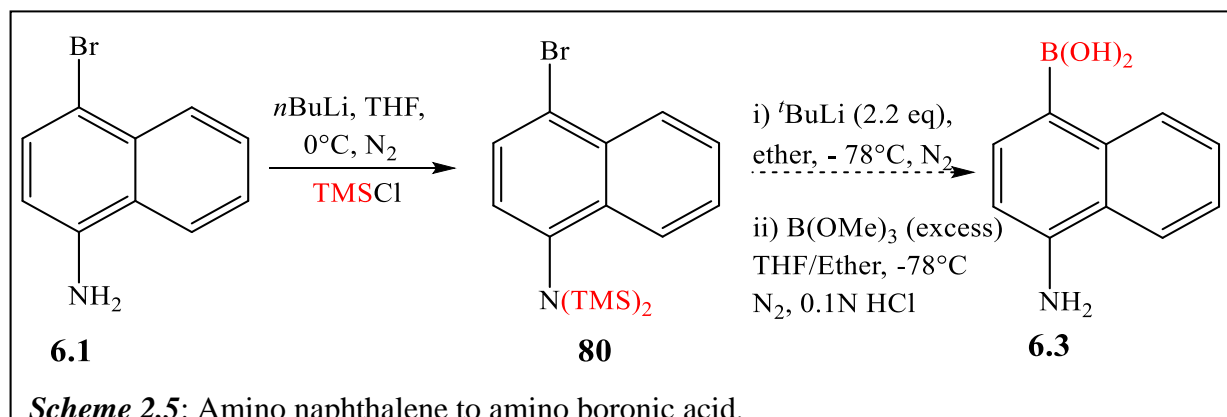
2.2 Attempted Preparation of Amino-naphthylboronic Acids

In the following sections, the synthesis of amino-naphthyl boronic acids was attempted many times. Most of these efforts failed. The most likely reason for the difficulty in synthesizing amino-naphthyl boronic acids can be summarized as follows: a nucleophilic amine group in the presence of an aryl-boronic acid leads to a host of potential problems. These problems will be covered in subsequent subsections.

2.2.1 Attempted Preparation of 1-Aminonaphthalene-4-boronic Acid **6.3**

As previously laid out in the convergent synthesis depicted in the general Scheme 2.1, the goal was conversion of 1-amino-4-bromonaphthalene **6.1** to 1-aminonaphthalene-4-boronic acid **6.3**. Surprisingly, a SciFinder[®] search of 1-aminonaphthalene-4-boronic acid turned up *no* results for the compound or any substructures. As a result, a literature protocol⁷⁸ based on the synthesis of 4-amino-3-fluorophenylboronic acid from the starting material 4-bromo-2-fluoro aniline was used.

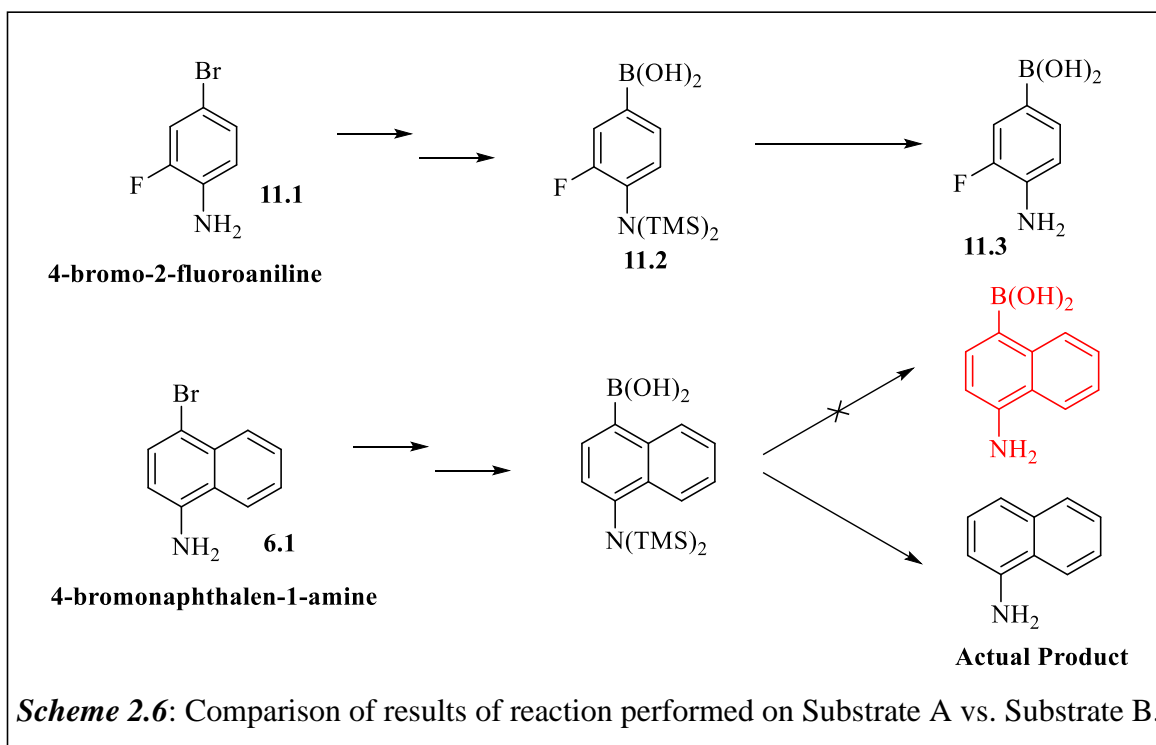
In Scheme 2.5, the bistrimethylsilylation protection of 1-amino-4-bromonaphthalene's amine is brought about by deprotonation of the amine followed by addition of TMSCl. The crude bistrimethylsilylated product's ¹H NMR is characterized by disappearance of amine hydrogens at 4.2 ppm and a doublet around 6.6 ppm, and subsequent appearance of a doublet at 6.9 ppm. The product was purified via NPC to give **80** at 61% yield.



The next step of the Scheme 2.5 reaction sequence was lithium/halogen exchange followed by borylation. This reaction repeatedly failed to produce the target boronic acid. The main product isolated from these attempts was 1-aminonaphthalene. This was confirmed by $^1\text{H}/^{13}\text{C}$ NMR against known spectra. Thus, a model substrate of bromobenzene was chosen as a positive control for which to assess the lithium/halogen exchange – borylation protocol. After workup, the NMR spectral data were assessed and found to match that of phenyl boronic acid. Thus the method works, but does not work to convert **80** to the target 1-amino-4-naphthaleneboronic acid. In short, it is most likely that during the acidic workup, protodeborylation occurred.

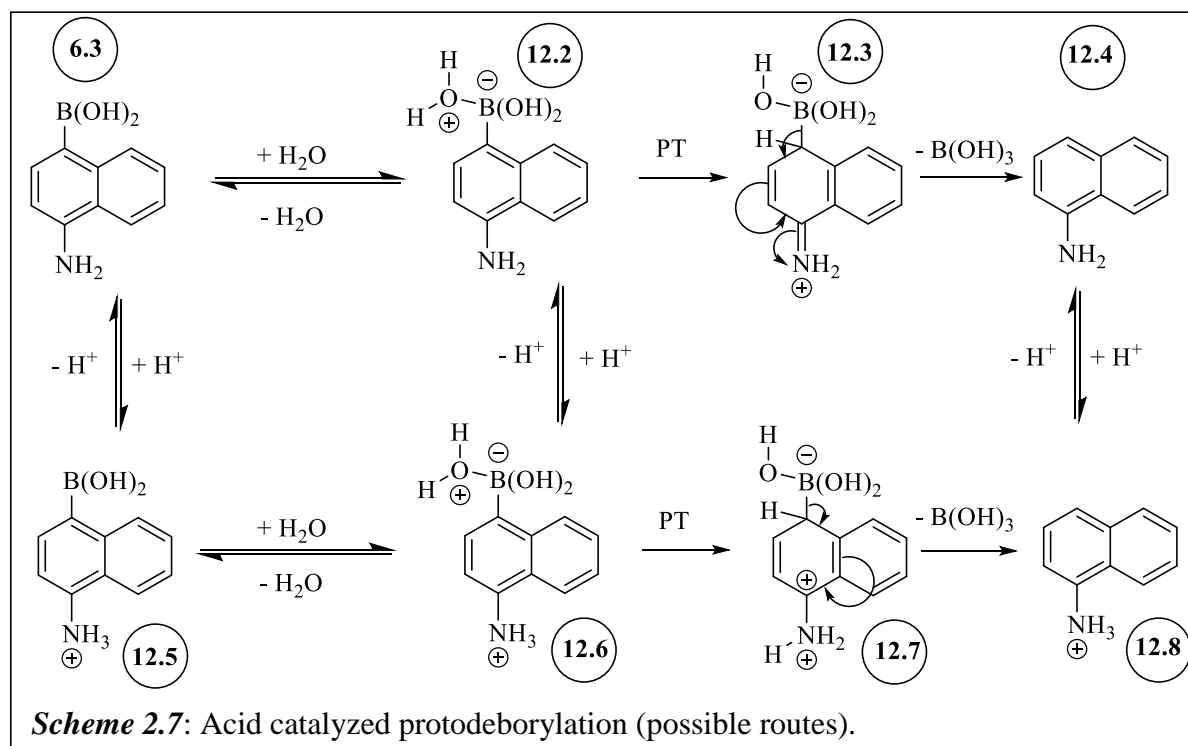
There has been a great amount of research attempting to understand the mechanistic trends of protodeborylation.⁷⁹⁻⁸³ One of the most well-reasoned and easily understood explanations can be found in the systematic study⁸⁴ performed by the group of David M. Perrin and coworkers at the University of British Columbia. Concerning the stability of aryl boronic acids in acidic solutions he states, “EWG-groups [sic] are known to retard acid-catalyzed protodeborylation, along with the fact that in our hands all EWG arylboronic acids were stable in 0.1 M HCl over a period of days.” Thus, there is the distinct possibility that the converse is true: electron donating groups destabilize aryl boronic acids against protodeborylation.

In the procedure upon which Scheme 2.5 is based⁷⁸, the substrate is 4-bromo-2-fluoroaniline **11.1** (substrate A) and the product is (4-amino-3-fluorophenyl)boronic acid **11.3**. A comparison of substrates is shown in Scheme 2.6. Substrate A's ring contains a fluoro group which is ortho to the amine. This fluoro group should pull electron density from the ring, which should stabilize the boronic acid against acid catalyzed protodeboronation. On the other hand, Substrate B (**6.1**) does *not* contain the EWG-fluoro. However, since substrate B is a naphthyl ring system it has greater delocalization energy, an effect which *should* help stabilize the boronic acid.



In order to explain the deboronation results, the mechanism for an acid-catalyzed protodeboronation is shown in Scheme 2.7. Since (4-aminonaphthalen-1-yl)boronic acid is amphoteric, there are two likely – but competing – mechanisms under aqueous acidic conditions. Either water coordinates with the boric acid first *or* the amine nitrogen becomes protonated first.

If the amine nitrogen is protonated then **12.5** becomes more Lewis acidic at the boronic acid empty p-orbital. This should accelerate water coordination onto the boronic acid to give the tetrahedral “-ate” complex **12.6**. On the other hand, if water coordinates to boron’s empty p-orbital first, the resulting anionic borate complex **12.2** should increase basicity at the amine-nitrogen’s lone pair resulting in protonation of amine to give **12.6**.



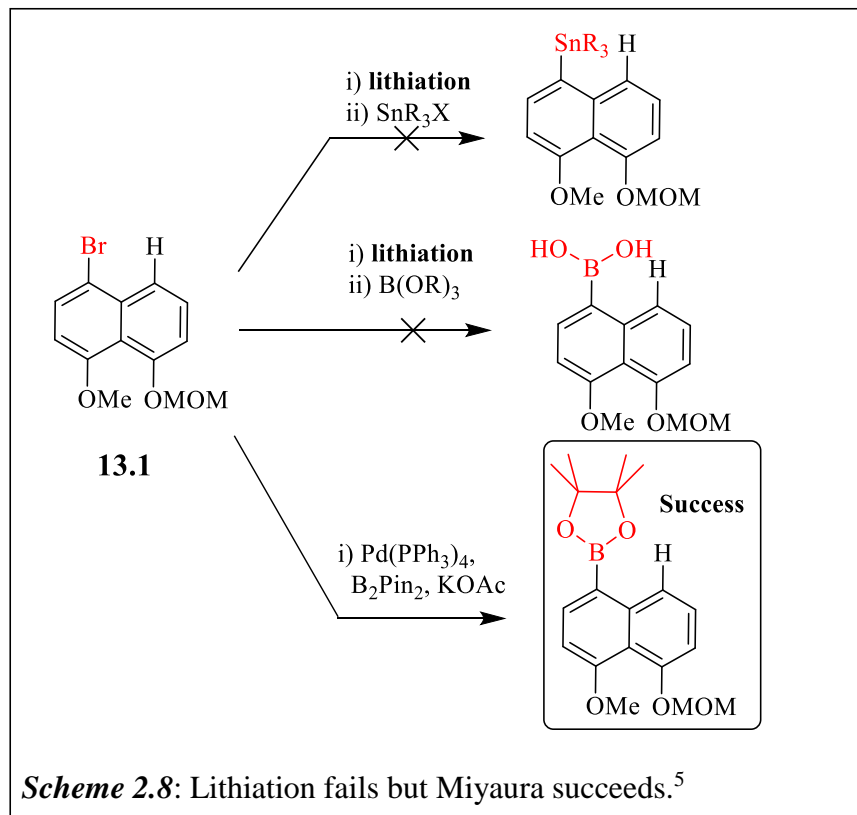
It seems likely that protonation of the amine should be kinetically faster than coordination of water on the boronic acid. Thus, it seems likely that the equilibrium should favor the path of **12.1** to **12.5**. The protonation of the amine nitrogen should result in a more electron deficient ring. This, in turn should lead to a more Lewis acidic boronic acid so that coordination by water gives **12.6**. Protonation at the boron-ipso position would result in a seemingly high-energy structure **12.7** with multiple formal positive charges. Comparatively speaking, **12.3** has less charge buildup and seems to be a better intermediate. Therefore, based on the above considerations it

seems likely the following sequence occurred; **12.1** → **12.5** → **12.6** → **12.2** → **12.3** → **12.4** → **12.8**.

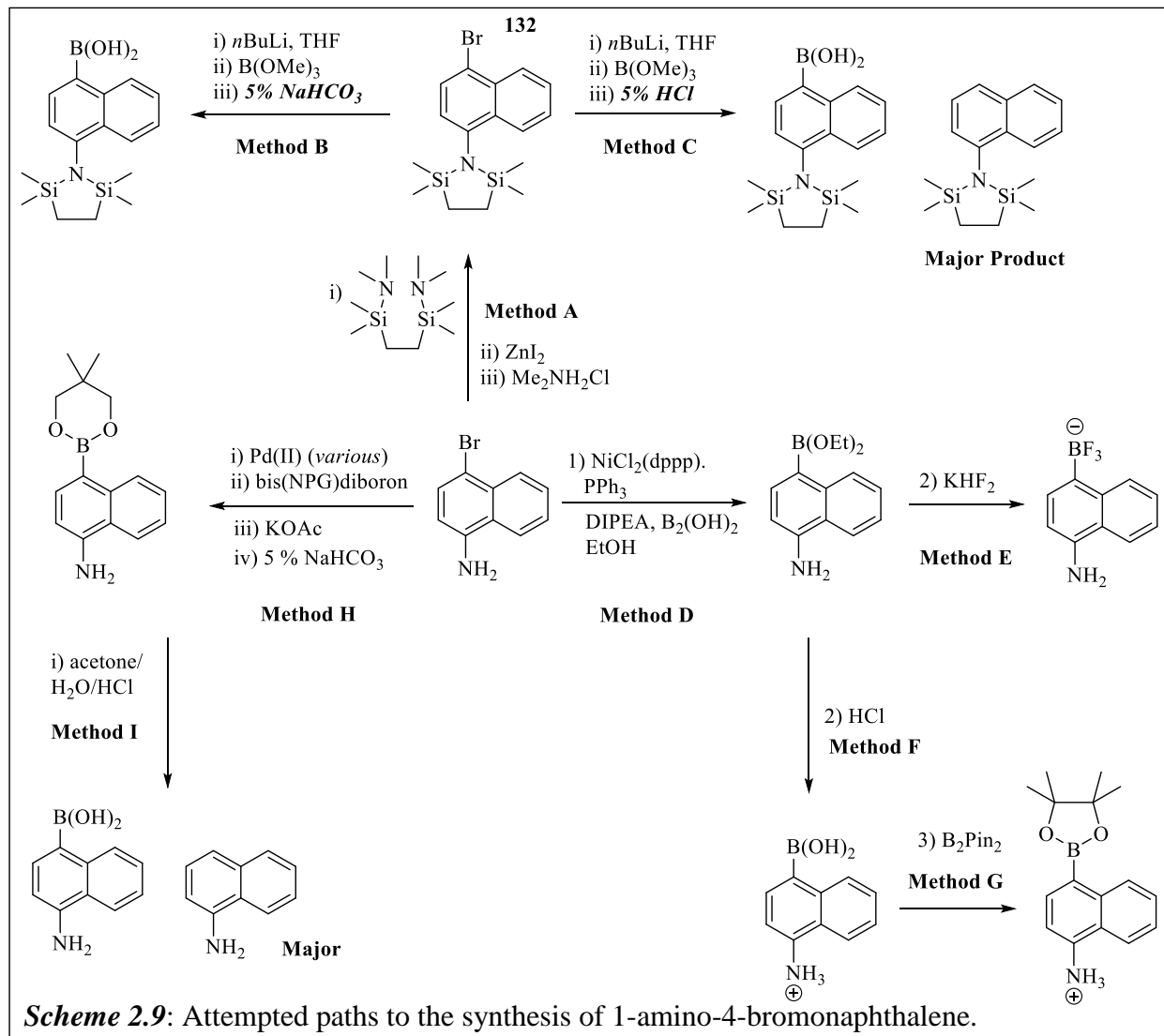
The remaining question is why the disparity between two substrates (substrate A vs. substrate B in Scheme 2.6) should give such different results when – presumably – substrate A is electronically similar to substrate B. One possibility is that a steric difference from the peri hydrogen of the naphthyl group is somehow assisting the C-B bond-breaking event. In fact, when electronic effects between substrate A and substrate B are so close, the most likely logical argument left to be made is that the notable steric strain of the peri hydrogen could be contributing to the final deboronation step.

These hypotheses are predicated on the assumption that boronation has followed lithiation. Admittedly however, this assumption could be erroneous. It is possible the reaction failed *after* lithiation but *prior to borylation*.

In the total synthesis of (±)-Spiroxin C, Miyashita and coworkers reported⁵ an interesting and yet possibly related failure. All attempts to functionalize **13.1** (Scheme 2.8) by preparing organotin or boronic acid *via lithiation* result in failure. They attribute the failed efforts to the hydrogen in the peri position. Interestingly, when they use the Miyaura reaction (no lithiation involved) for functionalizing **13.1**, the boronate ester product is successfully obtained in high yields. Considering that **13.1** is similar to **12.1** (our target) because it *also* contains an EDG para to the boronate (in our target case, boronic acid), we believed that investigation of a milder route (such as the Miyaura Reaction) merited closer examination.



We attempted various synthetic routes (Scheme 2.9) in our efforts to make 1-aminonaphthalene-4-boronic acid **6.3**. In some cases, deborylation was clearly the dominant reaction and we would isolate mostly 1-aminonaphthalene. In other cases, the NMR spectra were indecipherable. Attempts to purify the multiple products were unsuccessful and again gave NMR spectra which were indecipherable. We will discuss each method in more detail below.



We decided to change our protecting group to the so-called STABASE⁸⁵⁻⁸⁶ (Method A), which is less labile than the TMS protecting group. The protection of an aryl amine with STABASE is convenient because, unlike bis-TMS protection, it does not require $n\text{BuLi}$. The reagent ZnI_2 activates the pendant bis-dimethylamine groups towards nucleophilic attack by the aryl amine, resulting in a STABASE protected aryl amine.

The crude ^1H NMR showed complete disappearance of substrate 1-bromo-4-naphthylamine. The material was purified by normal phase silica to give 95% yield. A ^1H NMR of the pure STABASE protected **132** was obtained. The key spectral feature which indicates formation of **132** is a singlet (4H) at 1.02 ppm, which represents the two methylenes of the STABASE protecting group.

Since our previous efforts to synthesize the target 1-aminonaphthalene-4-boronic acid **6.3** through the use of lithium-halogen exchange with tert-butyllithium had failed, we wondered if perhaps a *different* lithiating reagent might succeed. We used *n*BuLi as the lithiating reagent in Method B and Method C.⁸⁷ Method C used an aqueous acidic quench whereas Method B⁸⁷ used mild aqueous base conditions.

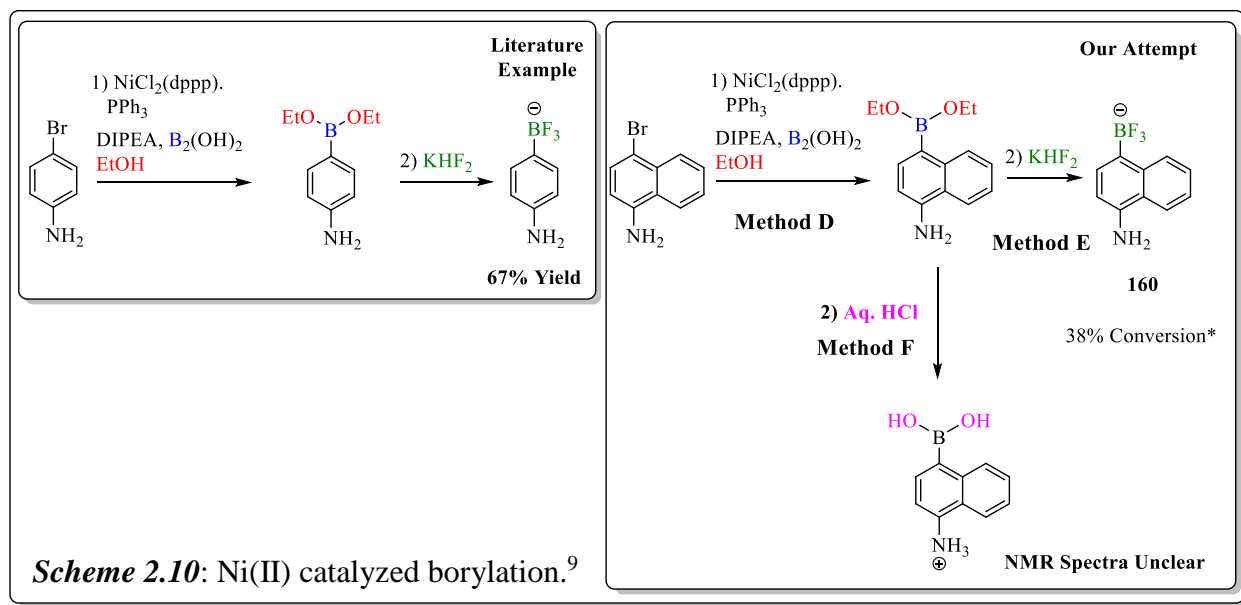
The acidic-quench-reaction's ^1H NMR showed complete consumption of substrate as evidenced by the disappearance of a doublet (8.2 ppm, 1H). When isolated, 48% of the protodeboronated material was recovered while the remaining isolated material gave indecipherable spectra. Conversion to the *unwanted* protodeboronated material was the *dominant* spectral feature of the crude ^1H NMR spectrum. Based on the extensive protodeboronation by using Method C (acidic quench), this method was abandoned.

Method B⁸⁷ used 5% sodium bicarbonate to quench. When the reaction was run, the crude ^1H NMR spectrum showed complete consumption of substrate as evidenced by the disappearance of a doublet (6.8 ppm, 1H). The formation of a new doublet (9.37 ppm, 1H) indicated significant aromatic deshielding over that of the starting material. Purification was attempted but resulted in the formation of many new aromatic peaks, which could not be identified.

We thought that if we couldn't purify the product mixture by chromatography, then perhaps we could resolve the boronic acid from the mixture (assuming there was enough present) as the boronate ester. By treating the mixture with a triol, the subsequent boronate ester should be more stable on a column. This was attempted but ultimately gave 1-naphthylamine, which is the unwanted protodeboronation product *minus* the STABASE protecting group. As a result, we abandoned any further attempts with Method B.

We attempted a Ni(II) catalyzed borylation with tetrahydroxydiboron (Scheme 2.9, Method D),⁹ following a literature model for bromoaniline (Scheme 2.10). In the literature's proposed mechanism for the catalytic cycle, tetrahydroxydiboron is in equilibrium with ethanol to form tetraethoxydiboronate ester. DIPEA coordinates to the ester thereby activating it towards transmetallation. Transmetallation is followed by reductive elimination to give the diethyl arylboronate (Method D, Scheme 2.10).

From the diethyl arylboronate, acidic hydrolysis under aqueous conditions (Method F, Scheme 2.10) *should* give the aryl boronic acid. Alternatively, if the diethyl arylboronate is treated with a methanolic solution of KHF_2 (Method E, Schemes 2.9 and 2.10), the aryltrifluoroborate should be the result.

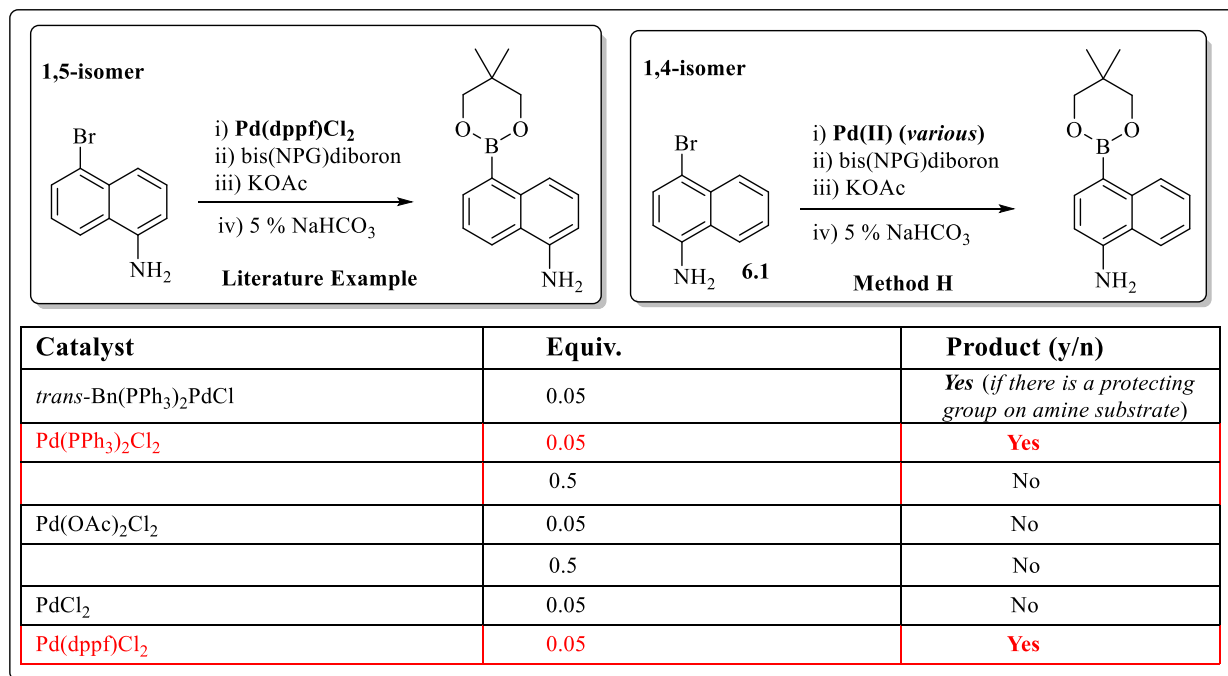


Trifluoroborate salts are generally bench stable and can be purified using acetone with a Soxhlet extraction device.⁹ Method E was attempted with the diethyl trifluoroboronate and the crude mixture was analyzed by ¹H/¹³CNMR. It was clear that either a new product was being formed or we were seeing some complex of the catalyst mixture. Nonetheless, the NMR was too complex to decipher without greater ability to purify the material. We attempted Soxhlet extraction, recrystallization, and ion-exchange. We were not able to resolve a pure material. We abandoned this Method.

Next we tried Method F and Method G (Scheme 2.9). The TLC obtained from Method F showed mostly unreacted starting material. Despite *apparent* lack of conversion to boronic acid in Method F, we decided to attempt Method G. The ¹H NMR seemed to support the fact that little or no conversion had occurred. Both of these methods were abandoned.

For the last portion of Scheme 2.9, we attempted a Miyaura Reaction (Method H). Multiple catalysts were screened. In instances where the reaction gave the target boronate ester, we attempted deprotection to the boronic acid (Method I).⁸⁸

We screened five different Pd(II) catalysts (Method H, Scheme 2.11). We found that Pd(dppf)Cl₂ and Pd(PPh₃)₂Cl₂ gave the target when used at 0.05 equivalents. Interestingly, when Pd(PPh₃)₂Cl₂ was run at a tenfold excess of catalyst (0.5 eq), no target was detected. Meanwhile, *trans*-Bn(PPh₃)₂PdCl did not give the target, but when the STABASE protected amine was used as the substrate (and not 1-amino-4-bromonaphthalene) the target was obtained. This suggests a negative correlation between presence of free aryl amine and conversion to target.



Scheme 2.11: Catalysts screened for a Miyaura Reaction (Method E).

We ultimately decided to use Pd(dppf)Cl₂ following an established literature procedure.⁸⁸ The reaction was scaled up from the initial successful screening. Lastly, the crude product was purified by normal phase chromatography to give a semi-pure material clean enough for the final hydrolysis step (Method I, Scheme 2.9).

The literature procedure⁸⁸ for the conversion of the 1,5-boronate ester to the boronic acid was followed (Method I, Scheme 2.9). However, the target 1,4-boronic acid was not achieved. Both ¹H/¹³C NMR confirm, quite unambiguously, that the product is 1-naphthylamine. This trend agrees with our previous findings that upon exposure to aqueous acidic conditions the resulting product is the protodeborylated material (and not the boronic acid). We were therefore curious if we could even replicate the literature procedure in which the 1,5-boronic acid isomer is successfully synthesized via aqueous acidic deprotection conditions of the 1,5-boronate ester (Scheme 2.11, Literature example). Although we were doubtful as to its success, we wanted to exhaust all reasonable possibilities.

2.2.2 Attempted Preparation of 1-Amino-5-naphthylboronic Acid 173

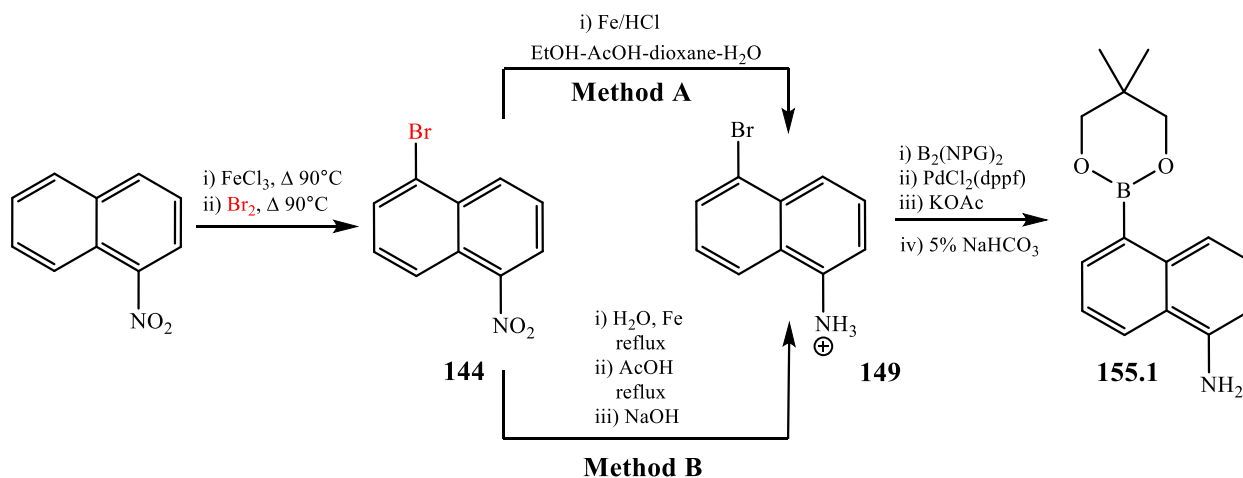
2.2.2.1 Synthesis of 1-Bromo-5-nitronaphthalene 144

1-Nitronaphthalene was successfully brominated to give 1-bromo-5-nitronaphthalene **144** (Scheme 2.12) The material was purified by recrystallization from ethanol to give yellow, needle-shaped crystals. Yield 37%, mp = 120-121°C (literature mp 119–120°C).⁸⁷ The ¹H/¹³C NMR and FTIR were in good agreement with the literature values.

2.2.2.2 Synthesis of 1-Amino-5-bromonaphthalene 149

1-Bromo-5-nitronaphthalene **144** was successfully reduced to 1-amino-5-bromonaphthalene **149** (Scheme 2.12). Two slightly different methods employing iron with different solvents and acids were used to achieve the target. The first method, Method A,⁸⁷ was followed by purification using normal phase chromatography. While the literature reports 97% yield, in our hands (using Method A), we obtained 21% yield. Material was characterized by ¹H NMR, which matched the literature. Additionally, mp = 62-66°C (lit. mp = 64-69°C)

Unsatisfied with the high disparity in the yield percentages of our results compared against that of the literature,⁸⁷ we turned to a different literature procedure⁸⁹ (Scheme 2.12, Method B). After having run Method B, we chose to attempt purification by recrystallization of the HCl salt. The salt was recrystallized from dilute HCl to give a yield of 39%. A melting point was attempted and it was found that mp ~ 242 (dec), (lit.⁹⁰ m.p. > 225° (dec.)). A ¹H NMR of the HCl salt obtained shows six aromatic peaks containing 4 doublets and 2 triplets, all downfield shifted due to the amine salt. This was consistent with our expectations. The HCl salt was converted back to the free amine and the ¹H NMR spectrum matched that of the literature. We found this purification method superior to normal phase chromatography. Additionally, the HCl salt seems to be a better way to store the amine, only converting to the free amine directly prior to usage.



Scheme 2.12: 3-Step synthetic sequence to the boronate ester **155.1**

2.2.2.3 Attempted Synthesis of 5-(5,5-Dimethyl-[1,3,2]dioxaboronan-2-yl)-naphthalen-1-yl]-amine **155.1**

We attempted, somewhat successfully, to synthesize 5-(5,5-dimethyl-[1,3,2]dioxaboronan-2-yl)-naphthalen-1-yl]-amine **155.1** from 1-amino-5-bromonaphthalene **149** (Scheme 2.12) using the established literature procedure.⁸⁸ At best, we obtained 85% conversion to **155.1** (as determined by ¹H NMR integrated values of product doublet ~ 8.19 ppm against **149**'s doublet ~ 6.77 ppm).

Despite numerous attempts at normal phase chromatographic purification, a pure **155.1** could never be obtained. There was always contamination by (what was assumed to be) the starting material bis(neopentyl glycolato)diboron ($B_2(NPG)_2$). We thought a good strategy would be to effect a precipitation of **155.1** from an organic solvent while simultaneously leaving behind $B_2(NPG)_2$. The target **155.1** has an amine which is able to be protonated while $B_2(NPG)_2$ is not under similar conditions. Therefore, we treated **155.1** with anhydrous HCl (as a 1M HCl preparation in diethyl ether). Addition of the HCl caused an immediate color change of the solution to a dark brown. Although difficult to clearly see (due to the dark color of the solution), a finely textured and extremely small, almost colloidal dispersion of particles appeared. These *could not* be made to grow larger despite cooling. This solution (suspension?) was filtered with a fine porosity filter-paper but no solid was collected.

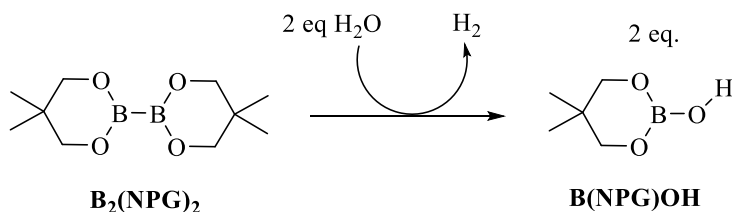
To our disappointment, we found that the $B_2(NPG)_2$ reagent was not very bench stable. This added to some of the difficulty in optimizing the reaction conditions. The general procedure uses a stoichiometry of compound **149** to $B_2(NPG)_2$ of 1:2. Over time, our crude ¹H NMR spectra began showing a serious change in the ratio of $B_2(NPG)_2$'s methylene singlets (at 3.59 ppm) versus the target **151.1**'s boronate methylene singlets (at 3.88 ppm). To assess the cause of the problem, the purity of all reagents and solvents were rechecked. However, our instinct was that $B_2(NPG)_2$ was the likely culprit as its texture had changed to more sticky (versus a drier

powder when the reagent had been initially opened). An extremely wide melting point range prompted a $^1\text{H}/^{13}\text{C}$ NMR analysis, which revealed decomposition to some unknown compound.

It would seem the most likely process causing reagent degradation would be water. If the water coordinates to the empty p-orbital of either of the two $\text{B}_2(\text{NPG})_2$'s boron atoms, then presumably the anionic “-ate” complex (i.e. $(\text{B}_2(\text{NPG})_2\cdot\text{H}_2\text{O})$) would be the initial result. However, if this *had* occurred, then one should notice a pretty significant upfield chemical shift on the $\text{B}_2(\text{NPG})_2$'s methylenes and – to a lesser extent – the terminal methyl singlets. Instead, ^1H NMR indicates the opposite. A very slight downfield shift (+ 0.075 ppm) at the methylenes while a lesser downfield shift (+0.021 ppm) at the terminal methyl groups had occurred. Furthermore, if the material *had* formed some anionic complex it would most likely be insoluble in the CDCl_3 NMR solvent, which is what was used.

The result of a $\text{B}_2(\text{NPG})_2$ hydrolysis – as a reasonable possibility – is dissociation of the neopentyl glycol (NPG). If this *had* occurred, then tetrahydroxydiboron $\text{B}_2(\text{OH})_2$ and NPG would have been present. While $\text{B}_2(\text{OH})_2$ is problematic to analyze with $^1\text{H}/^{13}\text{C}$ NMR, fortunately NPG is *not*. Based on $^1\text{H}/^{13}\text{C}$ NMR comparison against the known compound NPG, we were able to rule out – without question – the presence of NPG.

The reason we wanted to understand how the $\text{B}_2(\text{NPG})_2$ reagent was degrading was so that we might possibly take advantage of this property as a means of removing the excess reagent, which consistently plagued our attempts to synthesize **155.1** (Scheme 2.12). Since $^1\text{H}/^{13}\text{C}$ NMR was insufficient in telling us to what compound the reagent had been degrading, we turned to ATR-FTIR. We discovered a strong broad peak around 3200 cm^{-1} which we attribute to an -OH as is consistently seen in -BO-H stretching. Thus, we believe the diboron product had somehow degraded to the compound $\text{B}(\text{NPG})\text{OH}$ in scheme 2.13.



Scheme 2.13: Simplified scheme for degradation

Despite taking all reasonable precautions with latter bottles of the $\text{B}_2(\text{NPG})_2$ reagent, we continued to have our reagent degrade. As previously noted, the literature procedure⁸⁸ calls for a two-fold excess of $\text{B}_2(\text{NPG})_2$ to substrate **149**. We believed this was likely due to others having a similar problem with this reagent and likely compensating by using excess reagent. Using a new bottle of the $\text{B}_2(\text{NPG})_2$ reagent, the purity of which was measured prior to the reaction at 91% by ^1H NMR, we tried increasing the $\text{B}_2(\text{NPG})_2$ ratio from 2:1 to 10:1. This gave us the highest percentage conversion to **155.1** we obtained (85%), but only 6% higher than simply using a 2:1 ratio (of reagent:substate) of the same purity reagent.

If the degraded 31% purity $\text{B}_2(\text{NPG})_2$ was used at a ratio of 2:1, then percent conversion to **155.1** dropped to only 20%. This suggests that when the reagent reaches a high level of impurity, compensating by using excess reagent is simply not enough to prevent low percentage conversion to the target. In other words, there is a negative correlation between high reagent impurity ratios with respect to the percent conversion to **155.1**.

Lastly, it seems sensible that if one of the problems with this reaction is the post-reaction removal of the excess $\text{B}_2(\text{NPG})_2$, then using less reagent *should* make purification easier. We believe that is a reasonable step to take *if the reagent is of high purity*. We ultimately decided, however, to move on to a better (less labile) reagent for use as our Miyaura borylating reagent.

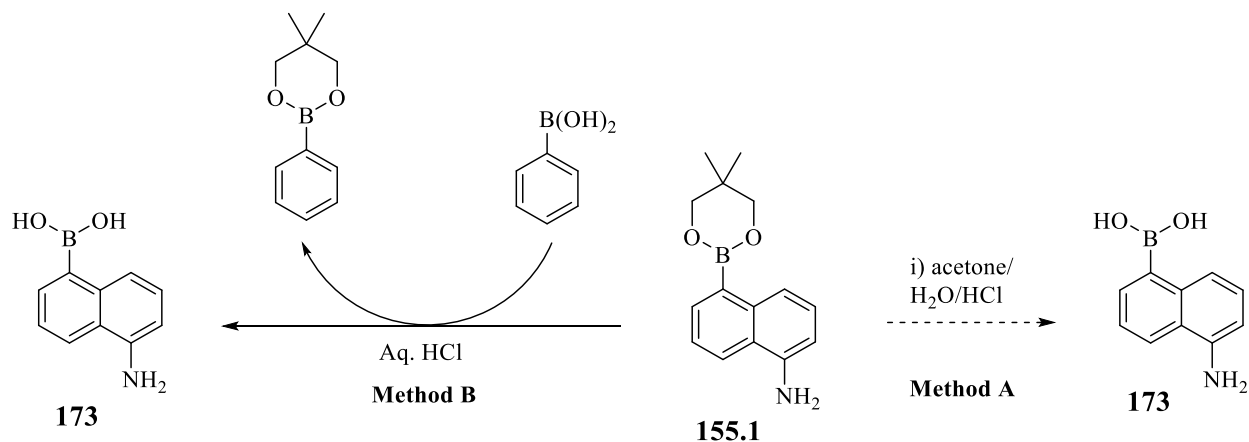
2.2.2.4 Attempted Preparation of 1-Amino-5-naphthylboronic Acid **173**

As previously mentioned, aryl boronate esters can be deprotected to the aryl boronic acids using a solution of aq. acetone with a catalytic amount of acid. Previously when we attempted this with the 1,4-isomer (Scheme 2.9, Method F), the unambiguous result was protodeboronation to give 1-naphthylamine. In Scheme 2.14 (Method A), the exact same conditions were used on the 1,5-isomer, but only a small amount of the unwanted 1-naphthylamine was detected. More importantly, despite our substrate **155.1** being identical to that used in the literature procedure,⁸⁸ in our hands, we were unable to obtain the target boronic acid **173** as stated in the procedure.

Previously, when we had run the Miyaura reaction on 1-amino-4-bromonaphthalene to get the target boronate ester, the unreacted $B_2(NPG)_2$ reagent could never be completely removed. This trend continued when performing the Miyaura reaction on 1-amino-5-bromonaphthalene to get the boronate ester **155.1**. In the former example, when hydrolysis would lead to the protodeboronated product 1-naphthylamine, there would be a *complete absence of the previously un-removable $B_2(NPG)_2$* . Yet when the same conditions were employed on boronate ester **155.1**, the $B_2(NPG)_2$ remained.

In Method A, when the standard 4-hour-reaction time was insufficient to give the target, the time was increased to 21 hours. Although there was no conversion to the target **173**, the ratio of $B_2(NPG)_2$ (previously un-removable post Miyaura reaction) to boronate ester **155.1** went from 3:1 to 2:1. At this point, we began to have indication of protodeboronation and subsequent 1-naphthylamine formation as evidenced by a multiplet at 7.8 ppm (2H). We resumed the reaction time for 22 hours and the 1-naphthylamine peak was now dominant over the unreacted boronate ester **155.1**. The $B_2(NPG)_2$ to boronate ester **155.1** ratio had not changed much and was slightly less than 2:1. We can conclude from these reactions that aqueous-acid catalyzed

protodeboronation (Method A) is much slower with boronate ester **155.1** than it is with the 1,4-analogue but that it remains the dominant reaction. We decided to abandon Method A.



Scheme 2.14: Conversion of boronate to boronic acid by alternate methods.

In Method B, we applied a literature method⁹¹, which uses phenylboronic acid in the deprotection of **155.1**. This method takes advantage of solubility differences of phenylboronic acid (which is water soluble) and the phenylboronate ester (which is insoluble in water). In order to ensure our substrate **155.1** was in the aqueous layer, we used slightly acidic aqueous conditions to ensure the amine would be protonated. One equivalent of the water-soluble phenylboronic acid was added to the aqueous acidic solution containing **155.1**. Addition of diethyl ether was followed by stirring then decanting off the ether and replacing with fresh ether. This was repeated several times over one day. We found that within the first two hours, we had recovered 63% of our total expected mass (based on molecular weight of the phenylboronate ester). By the end of a day we had recovered 93% of our total expected mass.

If phenylboronic had successfully been esterified to the phenylboronate ester this would be indirect evidence that **155.1** had been hydrolyzed to **173**. Furthermore, an idea of the extent of deprotection could be determined by dividing the mass against the molecular weight of the

phenylboronic ester. Thus, the decanted ethereal layers were combined and analyzed by ^1H NMR. By comparing our spectra against literature ^1H NMR values, we were able to determine that the phenylboronate ester had indeed been successfully formed! A second compound was identified as phenylboronic acid. The ratio of the ester:acid was 74:26.

The aqueous acidic mixture was quenched with 5% sodium bicarbonate and chromatographed but could not be *completely* purified. Interestingly, the two spots on TLC were both highly fluorescent. This fluorescence property is consistent with the publication by Zhang and colleagues which examines the use of boronic acids (including **173**) as ratiometric saccharide sensing devices.⁹²

Because there was never evidence of our ability to resolve these two spots by column chromatography (they always eluted together), we decided to simply use a preparative-scale TLC plate. A preparative-scale TLC plate can be advantageous compared to running a column. Unlike a column, separation can be visibly confirmed as it occurs. A diluted sample is loaded onto the plate along a tight line that spans the bottom of the plate horizontally. Whereas a TLC plate is loaded as a small “spot” (touching of the capillary tube to the silica), a preparative scale plate is essentially the result of multiple “spots” loaded (usually at higher concentration) along a tight horizontal line. Thus, a TLC will elute as a collection of spots while a preparative-scale TLC plate will elute as a collection of bands.

Based on the hydrogen bond interaction differences of the various compounds in the sample to the silanols (of the silica), different bands will travel to different heights of the plate. Once separation is verified (by UV lamp in our case), the band at the desired R_f can be removed by scratching away the silica (with a knife). Then, the silica (which contains the adsorbate) can

be dissolved in a solvent (we used DCM), and analyzed by TLC. We decided to use this method. This way, we could be *certain* we had only *one* of the two bands.

As can be seen in Figure 2.2.2.4, we attempted this method. To our surprise, upon back-dissolution of the silica-adsorbed-sample "A" into DCM (from the preparative-scale TLC plate) we found that what was previously only *one* fluorescent band would revert to *two* fluorescent bands. Curiously, the retention factors of the two spots on the TLC plate matched the retention factors originally seen. We believe one possible reason for the two spots of might simply have been the complexing of **173** with the methanol from our eluting solvent mixture forming an equilibrium mixture of complexed and uncomplexed **173**. At the time we did not re-attempt TLC analysis with a different solvent system as the original literature procedure⁸⁸ also used methanol. Another possibility could be that the boronate is in a slow equilibrium on the TLC plate and we can effect separation. But when redissolved into a solvent, the equilibrium leads to the two distinct compounds (as evidenced by the two spots).

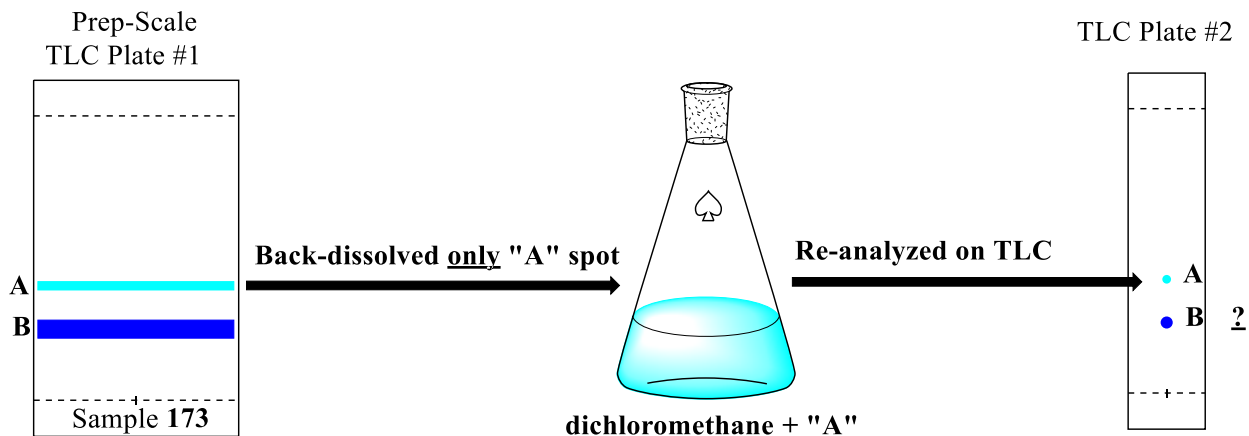


Figure 2.2.2.4: Preparative Scale TLC isolation attempt of **173**

Satisfied there could be no further purification with this method, we concentrated the DCM solution (containing “A”) and we obtained the ^1H NMR in CD_3OD . Although unrealized at the time, we now believe the authors of the original publication⁸⁸ mistakenly reported the ^1H NMR values as being in CD_3OD when in fact their spectrum was very likely obtained in CDCl_3 . We believe this because after our first isolation attempt, we obtained our spectrum in CDCl_3 and the peaks matched the peaks that they reported as being in CD_3OD (their ^{13}C NMR was obtained in CDCl_3) This might be of importance if in fact methanol/methanol- d_4 forms a complex with the Lewis acidic boronic acid which complicates the ^1H NMR spectrum.

Nevertheless, we *were* able to verify the almost complete disappearance of the methylenes of boronate ester **155.1**. Thus, we believe the strategy of using boric acid to deprotect boronate ester **155.1** is synthetically sound. When combined with the fact that the phenylboronate ester had been recovered (which indirectly suggests deprotection of **155.1** to boronic acid **173**), we believe we obtained the target **173**.

Nevertheless, after *multiple* chromatographic purifications, and an extremely low yield of still-impure boronic acid, we decided to make some serious changes to our synthetic approach. We believe the free amine on the naphthyl ring was likely causing many problems. After all, amines *are* borophiles. Furthermore, we believe we exhausted all reasonable efforts at accessing boronic acids from substrates containing free amines, by using either the 1-amino-4-bromonaphthalene or 1-amino-5-bromonaphthalene.

2.3 Retrosynthetic Analysis for AQuANaB Compounds

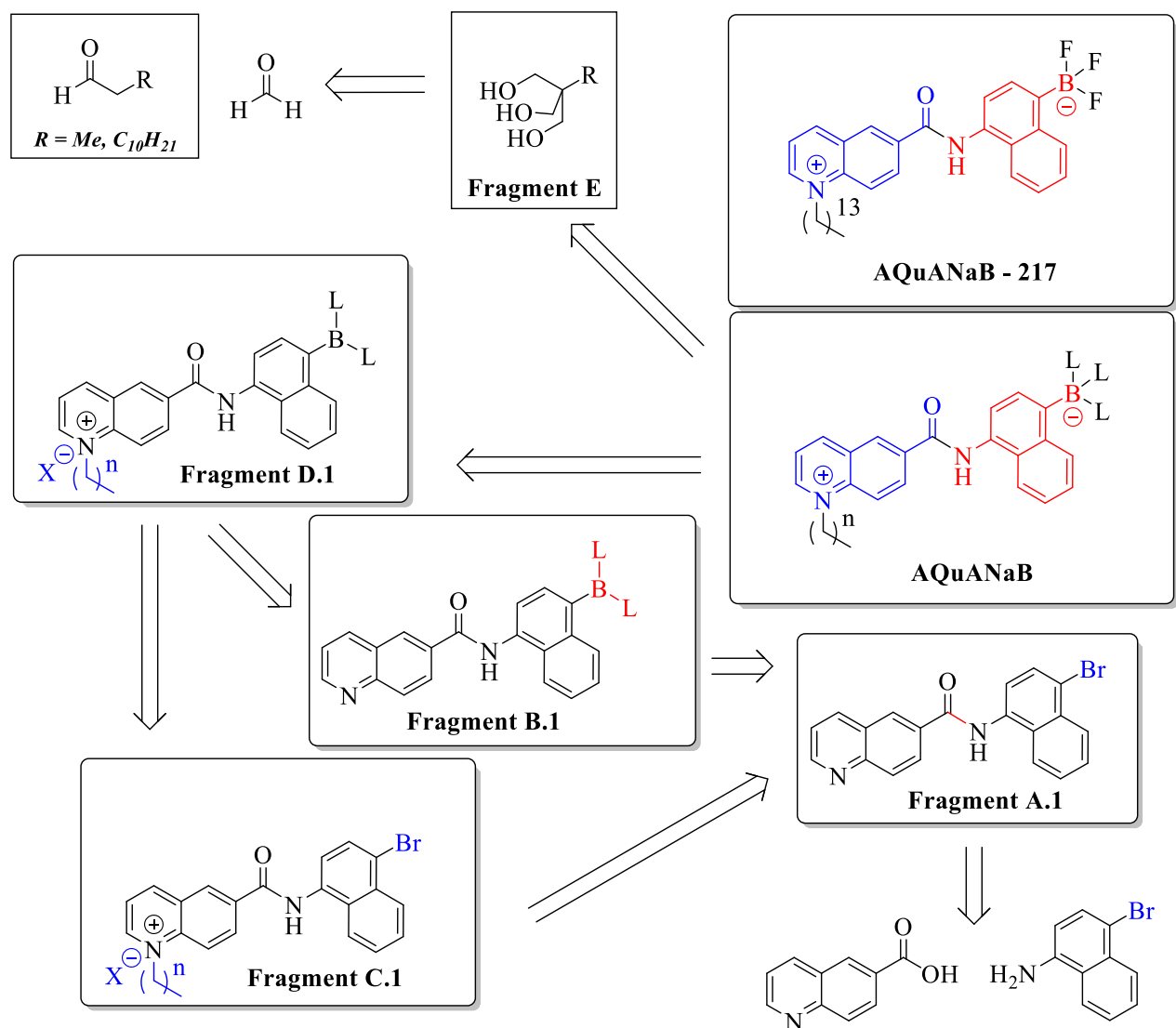
To facilitate ease in the discussion of compounds like our target zwitterionic D- σ -A **6.7** (Scheme 2.1), we will now use the more general term “AQuANaB.” AQuANaB (Scheme 2.15)

shall serve as a general acronym for compounds containing alkyl-quinolinium-amide-naphthylborate. When discussing a specific AQuANaB variant, we will use a modifier such as the successfully synthesized AQuANaB – **217**.

In the Scheme 2.15 retrosynthetic analysis, we have taken into account the previously encountered problems and modified our synthetic strategy accordingly. It became obvious to us that the best synthetic strategy to access AQuANaBs would begin by an amide bond formation. We alternately coupled several different amines to 6-quinoline carboxylic acid.

In general, we will call the amide formed by coupling of either 1-amino-4-bromonaphthalene or 1-amino-5-bromonaphthalene to 6-quinoline carboxylic acid as Fragment A. The amide from specific coupling of 1-amino-4-bromonaphthalene to 6-quinoline carboxylic acid will be referred to as “Fragment A.1”.

Fragment B will represent either a boronic acid or a boronate ester. Fragment C is the result of the *N*-alkylation of Fragment A (to give quinolinium). The condensation of a triol (Fragment E) onto Fragment D would lead to an AQuANaB type compound. Ultimately, formation of the triolborate version of AQuANaB was not successful. Fortunately, we *were* able to synthesize AQuANaB – 217! This shows that indeed our retrosynthetic strategy was a sound one. We will discuss the synthesis of all fragments (and model compounds of the fragments), in the following sections.



Scheme 2.15: Revised retrosynthetic approach to so-called AQuANaB compounds.

2.4 Amides, A-Fragments, Syntheses of

Amide bond forming reactions are now the most common bond-forming reaction in the entirety of synthetic chemistry.⁹³ In this research project, we successfully formed amides from a variety of methods. The chemistry was straightforward.

In the first method, a carboxylic acid can be converted to the *highly reactive* acid chloride using reagents such as thionyl chloride or oxalyl chloride. In an addition-elimination ($\text{Ad}_{\text{N}}\text{E}$)

mechanism, the nucleophilic amine-nitrogen attacks the electrophilic carbonyl-carbon of the acid chloride to give a tetrahedral intermediate, which then readily collapses, eliminating the chloride. A bit of base is used to trap the HCl generated in the formation of an amide bond from this route.

In the second method, a carboxylic acid can be activated by a carbodiimide type reagent (we used DCC). Upon activation, an *O*-acylurea intermediate is formed. The amine then attacks the activated carboxylic acid intermediate, which should result in elimination of a urea by-product as well as the target amide.⁹⁴

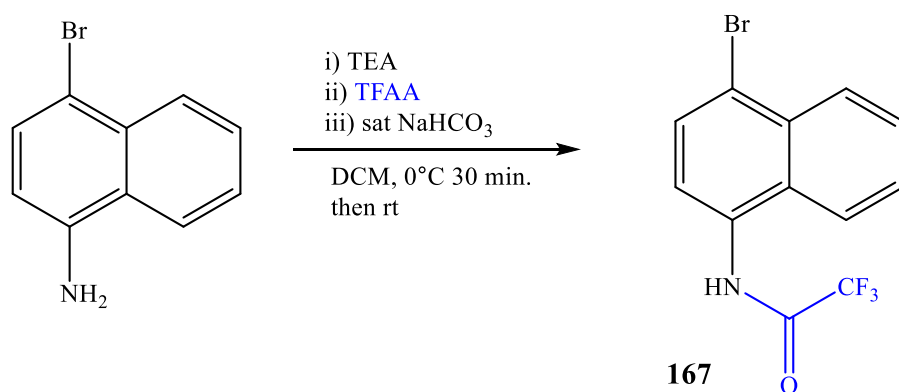
One of the well-known disadvantages of the DCC coupling protocol is the difficult-to-remove by-product *N,N*-dicyclohexylurea (DCU). Another disadvantage can occur when the amine is sterically bulky (our substrate amine is). A bulky amine's approach to the *O*-acylurea is made much more difficult due to steric hindrance. The reactivity can become ponderously slow (or not react at all).

We initially encountered this problem. Although we will speak in greater detail about the cause of this problem in later sections, we were able to quickly work out a solution. The remedy to these sluggish reactions was to use a benzotriazole additive (we used HOBt).

When using the DCC reagents, we generally obtained high yields of amide (up to 85%). Although the DCU can be slightly troublesome to remove, we found efficient means to remove it. Often, we found several filtrations sufficient to remove most of the DCU but this depended on the substrate. In cases where the DCU would persist, we found it most efficient to move on to the borylation step and that the DCU would come out during the subsequent purification of the boronate ester.

2.4.1 Model Compound Amide 167

We wanted to first synthesize several model compound amides. The purpose of synthesizing model amides was to gauge the likelihood of successfully borylating using various conditions. We anticipated that borylation would be the problematic step as we had still not found an efficient means to get pure either boronic acids or boronate esters.

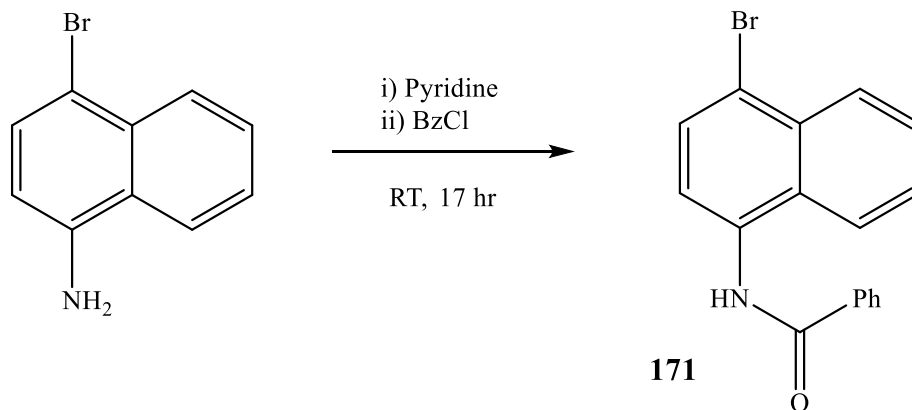


Scheme 2.16: Amidation of 1-amino-4-bromonaphthalene via TFAA

The substrate 1-amino-4-bromonaphthalene was converted to amide **167** through reaction with trifluoroacetic anhydride (TFAA) following a patent procedure.⁹⁵ Material was chromatographed on normal-phase chromatography and recovered in 93% yield. ¹H/¹³C NMR revealed a very small amount of aliphatics (grease). The sample was recrystallized from EtOH to give granular textured crystals with a melting point of 141 – 141.5 °C.

2.4.2 Model Compound Amides 171

The substrate 1-amino-4-bromonaphthalene was converted to amide **171** through reaction with benzoyl chloride (BzCl) following a literature procedure.⁹⁶ Material was purified by recrystallization from EtOH. The bone-white colored crystals had a melting point of 235 – 237°C (lit. 237.5-238°C). Sample purity was confirmed through ¹H/¹³C NMR. Furthermore, FT-IR analysis showed an N-H stretch at 3262 cm⁻¹.



Scheme 2.17: Amidation of 1-amino-4-bromonaphthalene via benzoyl chloride

2.4.3 *N*-(4-Bromonaphthalen-1-yl)quinoline-6-carboxamide **202**

We initially attempted the synthesis of **202** *without* the HOBt additive. As previously mentioned, the reaction can be much slower (or not react at all) if the substrate is bulky. In our case, a post reaction TLC indicated mostly unreacted starting amine. We were able to establish that the reaction had stopped at the *O*-acylurea intermediate (Figure 2.4.3.1), which was obtained in 12% yield after a recrystallization from benzene. ¹H NMR was sufficient to identify the *O*-acylurea. Thus, we decided to try the reaction using HOBt.

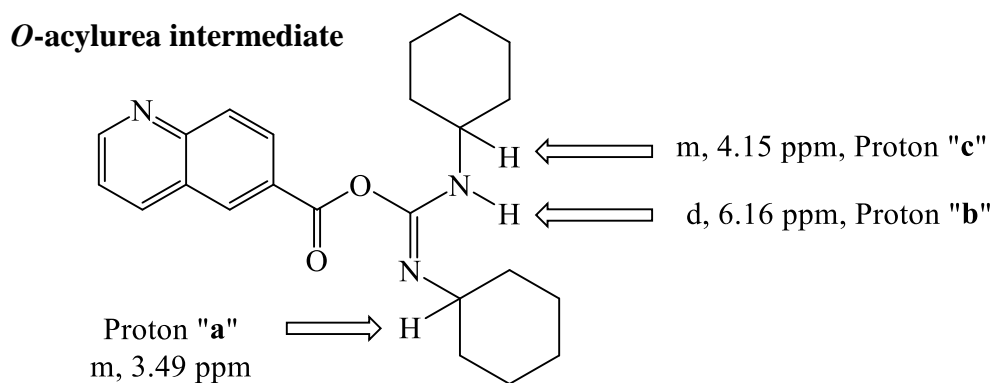
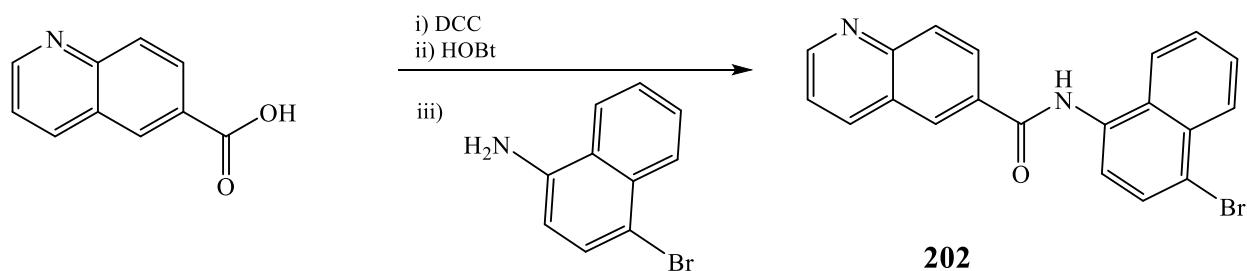


Figure 2.4.3.1: *O*-Acylurea intermediate is obtained in the absence of HOBt.

We synthesized **202** by use of an established DCC coupling protocol including HOBt.⁹⁷ The reaction was purified by normal phase chromatography to give a bone-white solid, which gave a yield of 85%. The material was recrystallized from EtOH. The melting point was 217 - 220°C. This compound was thoroughly characterized by multiple NMR experiments (¹H/¹³CNMR, COSY, and HMQC). We were able to successfully assign *all* protons.



Scheme 2.18: Amidation of 1-amino-4-bromonaphthalene with 6-quinoline-carboxylic acid via DCC/HOBt protocol

Although our yield of **202** was good, we were curious whether other methods might give equally good (or better) yields without the problematic DCU by-product formation. We attempted one reaction following a literature procedure.⁹⁸ The procedure uses isobutylchloroformate, which presumably activates the carboxylic acid. As determined by ¹H NMR, our percent conversion was around 25%. We abandoned the isobutylchloroformate route.

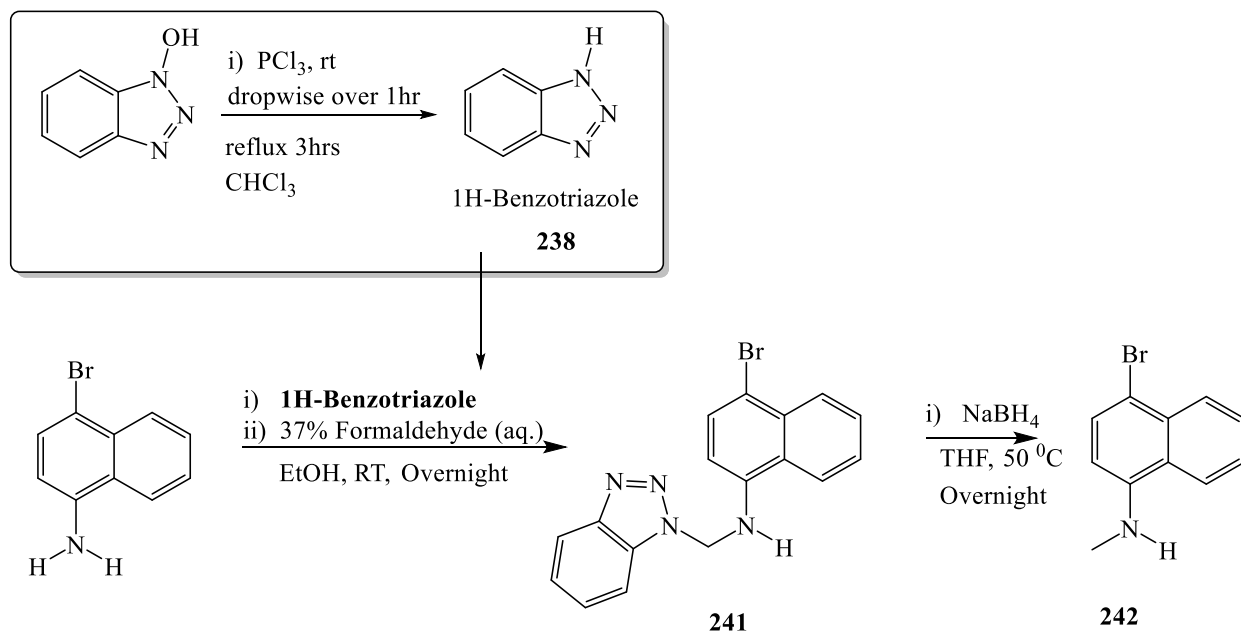
We decided to attempt a different procedure. This time, we used another carbodiimide reagent, 1-ethyl-3-(3-dimethylaminopropyl)carbodiimide (EDC). One of the advantages of EDC is its solubility in water and organic solvents. The urea by-product can be removed by a water wash. When we ran this reaction, a ¹H NMR of the crude product indicated 11% percent conversion. We abandoned this route.

2.4.4 *N*-(4-Bromonaphthalen-1-yl)-*N*-methylquinoline-6-carboxamide **254**

The purpose in our synthesis of compound **254** (see Scheme 2.20) was multifaceted. We believed that the *N*-methylation of the amide nitrogen would improve solubility and purification of any products obtained from the substrate. Another reason was to preempt the possibility of the amide nitrogen coordinating to the palladium or nickel catalyst and possibly hindering borylation. We weren't sure that the amide nitrogen *was* having a negative effect on the catalyst but we wanted to eliminate it as a possibility. We focused on two routes for the synthesis of **254**. In the first route (Scheme 2.19) we reduced 1*H*-benzo[d][1,2,3]triazol-1-ol to **238**. The sample was purified by recrystallization from benzene to give a yield of 50%. The melting point was 91 - 95°C (lit. 90 - 92°C).⁹⁹

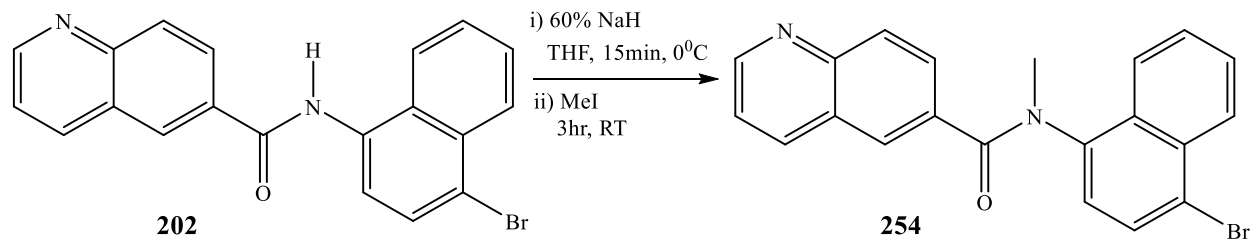
Next, we used **238** and formaldehyde to successfully *N*-alkylate 1-amino-4-bromonaphthalene to **241**.⁸⁸ The material was purified by recrystallization from EtOH to give violet-tinted needle-like crystals. The melting point was 140-142°C. The yield was 65%. The sample was used without further characterization.

Lastly, **241** was reduced to give the *N*-methylated amine **242**.⁸⁸ ¹H NMR of the crude material was used to confirm appearance of methyl singlet at 3.0 ppm with subsequent absence of benzotriazole. This indicated the successful reduction of **241**. Only a crude yield was obtained, which gave values greater than the theoretical maximum. However, the crude ¹H NMR seemed reasonably pure, the main contaminant being residual THF. Although we envisioned using **242** by reacting with the acid chloride of 6-quinoline carboxylic acid (prepared by its reaction with SOCl₂) to give **254**, we made it as far as **242** and during the course of this process found a better alternative. Thus, we abandoned this route.



Scheme 2.19: Synthesis of 4-bromo-*N*-methylnaphthalen-1-amine as alternative amine substrate for amidation.

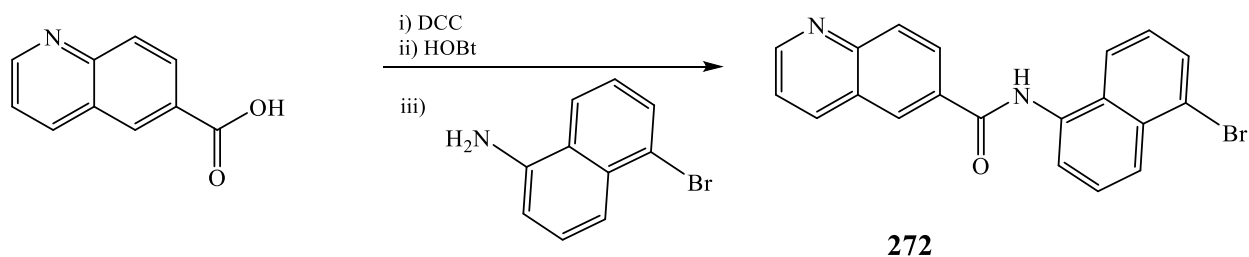
The second route (Scheme 2.20) was the better of the two routes (one step vs. 3). In the second route, we simply *N*-methylated the amide nitrogen of **202**. In a literature procedure, the amide N-H is deprotonated with sodium hydride. The deprotonated amide is then quenched with iodomethane to give the target amide.¹⁰⁰ In our case, a small amount of optimization was required to find the best ratio of NaH to use. Ultimately, **254** was successfully synthesized. The material was purified by recrystallization from benzene and the yield was 66%. A melting point was obtained, mp = 172 - 174°C. The mixture was analyzed by FT-IR to confirm disappearance of the N-H stretching at 3262 cm^{-1} , while ^1H NMR was used to confirm presence of methyl singlet at 3.58 ppm.



Scheme 2.20: N-alkylation of amide

2.4.5 N-(5-Bromonaphthalen-1-yl)quinoline-6-carboxamide 272

The synthesis of **272** (Scheme 2.21) followed the same procedure as that shown in Scheme 2.18.⁹⁷ The yield was unexpectedly poor when compared against the 1,4-isomer (29% vs 85%). The low solubility in most organic solvents precluded normal phase chromatography. The material was recrystallized from EtOH to give a melting point of 216-218°C. FT-IR revealed the characteristic N-H stretch at 3276 cm^{-1} and amide carbonyl stretch at 1642 cm^{-1} . Material was characterized with $^1\text{H}/^{13}\text{C}$ NMR.

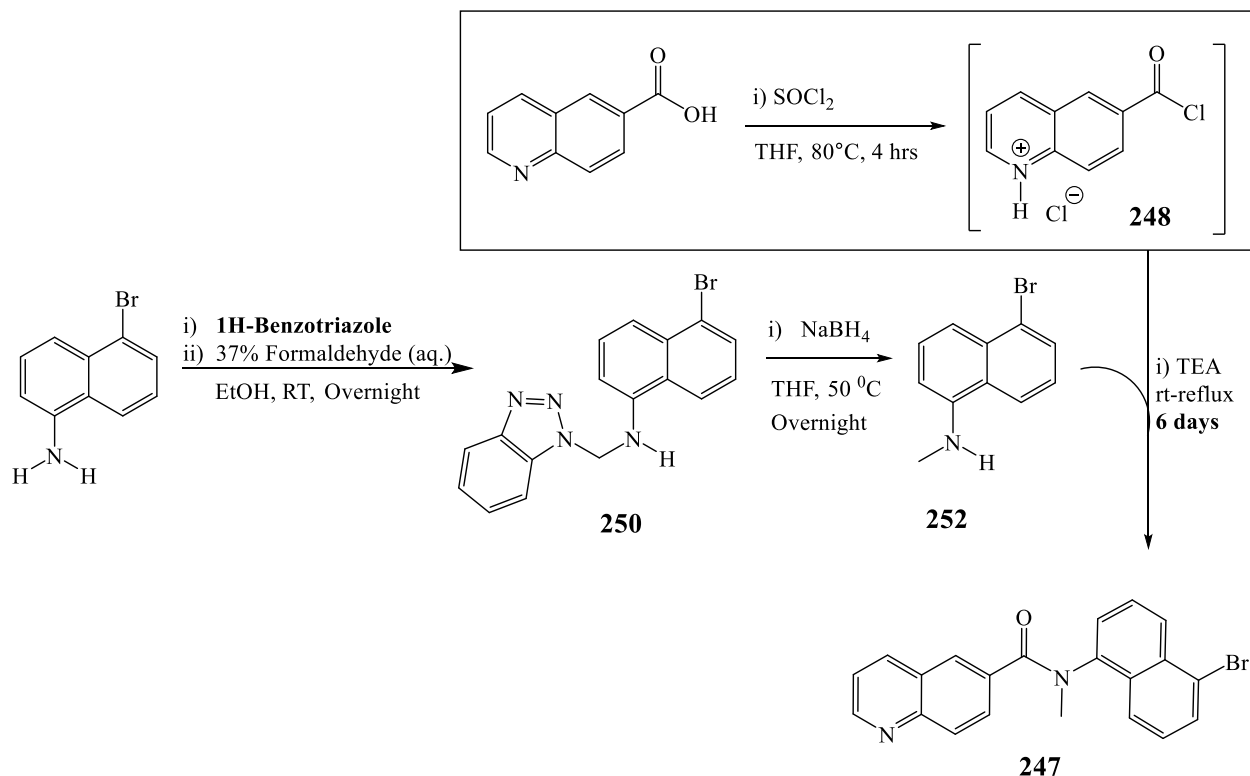


Scheme 2.21: Synthesis of **272** through DCC coupling.

2.4.6 Attempted Synthesis of N-(5-Bromonaphthalen-1-yl)-N-methylquinoline-6-carboxamide 247

We attempted to synthesize amide **247** (Scheme 2.22) by first *N*-alkylating 1-amino-5-bromonaphthalene in a manner analogous to that previously mentioned in Scheme 2.19. In this instance however, we purchased the 1H-benzotriazole to avoid an unnecessary step. In the first step (synthesis of **250**), the crude product was purified via recrystallization from EtOH to give an off-white colored solid at a yield of 69% and a melting point of 191-193°C. The key observable spectral features via ¹H NMR distinguishing product formation are the appearance of a doublet at 6.28 ppm (attributed to the methylene) and a broad singlet at 5.5 ppm (attributed to the N-H hydrogen). The ¹³C NMR spectra gave a peak at 58.6 ppm (attributed to the methylene).

Next, the pendant benzotriazole was cleaved by NaBH₄ to give the *N*-methylated amine **252**.⁸⁸ The product was characterized by ¹H/¹³C NMR. The most notable spectral features in the ¹H NMR were the disappearance of **250**'s methylene with subsequent appearance of a new singlet at 2.99 ppm, attributed to the N-Me hydrogens. Additionally, the broad singlet at 5.5 ppm (attributed to the N-H hydrogen) shifted upfield to 4.4 ppm. The ¹³C NMR showed complete disappearance of starting material methylene (which was at 58.6 ppm) and subsequent appearance of a peak at 31.2 ppm (attributed to the N-Me carbon). No further purification was necessary. Yield was 95%.



Scheme 2.22: Attempted synthesis of *N*-(5-bromonaphthalen-1-yl)-*N*-methylquinoline-6-carboxamide **247**

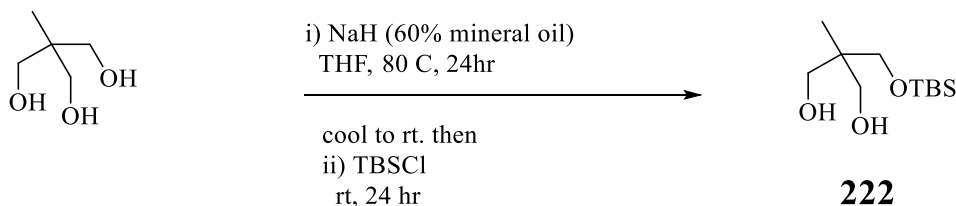
The substrate 6-quinoline carboxylic acid was converted to the acid chloride **248** by using thionyl chloride in an established procedure.¹⁰¹ After four hours, the thionyl chloride was stripped via rotary evaporation and **248** was used directly. Using a literature procedure for a similar substrate,⁹⁶ we found this reaction to be extremely sluggish at the literature conditions of room temperature for 4 hours. Our initial efforts using the literature protocol (of 4 h at room temperature) gave only a 9% conversion to target (as determined by ^1H NMR ratio of the N-Me methyl singlet of **252** against that of **247**). We increased reaction time and then heat. After 6 days, our percentage conversion reached a maximum of 47% where it was static. By TLC, we could see that the remaining acid chloride had hydrolyzed back to the carboxylic acid. We decided to abandon any further efforts at this route.

2.5 Syntheses of B-Fragments

The synthesis of the B-Fragment was one of the key steps of this total synthesis. Previously we had attempted borylation of 1-amino-4-bromonaphthalene and 1-amino-5-bromonaphthalene and had been unable to purify the products as either boronate esters or boronic acids. In the synthesis of the B-Fragment, amidation has preceded borylation. We attempted many model reactions to determine the best route of borylation. Ultimately, the Miyaura reaction (to give the boronate ester) using B_2Pin_2 would prove to be the best route.

2.5.1.1 Model, 2-(((tert-Butyldimethylsilyloxy)methyl)-2-methylpropane-1,3-diol, **222**

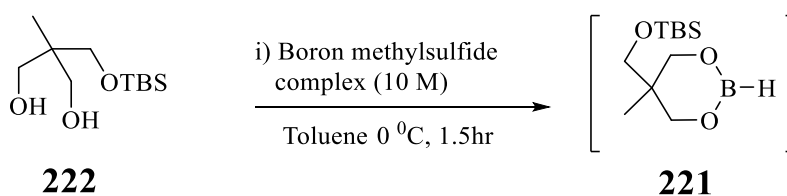
The triol tris(hydroxymethyl)ethane was monosilylated with TBSCl to give **222** following a literature procedure (Scheme 2.23).¹⁰² Material was purified using normal phase chromatography to give a yield of 44%. A 1H NMR spectrum was used to confirm disappearance of the triol's methylene doublet at 3.67 ppm (6H) and subsequent appearance of two new doublets (3.71 ppm, 2H, and 3.57, 2H) and a singlet at 3.60 ppm (2H). The singlet is consistent with a methylene *not* being split by protons on an adjacent heteroatom (-OH). Two additional singlets at 0.71 ppm (6H) and 0.90 ppm (9H) are consistent with the TBS group. A ^{13}C NMR was used to confirm 7 carbons. The values agreed with the literature.



Scheme 2.23: Monosilylation of triol.

2.5.1.2 Model, tert-Butyldimethyl((5-methyl-1,3,2-dioxaborinan-5-yl)methoxy)silane, **221**

The main purpose of the following reaction was to confirm the reaction's viability by observing the consumption of the starting material **222**. We did not expect this compound to be isolable as the literature procedure we had followed¹⁰² had attempted isolation of **221** but had always been unsuccessful. Since **222** is used with a stoichiometric amount of the borane methyl sulfide complex (BMS), our spectroscopic strategy was to run a negative control. We ran two reactions containing BMS, one with **222** and the other without **222**. We compared the ¹H NMR spectra of the negative control against the actual reaction.

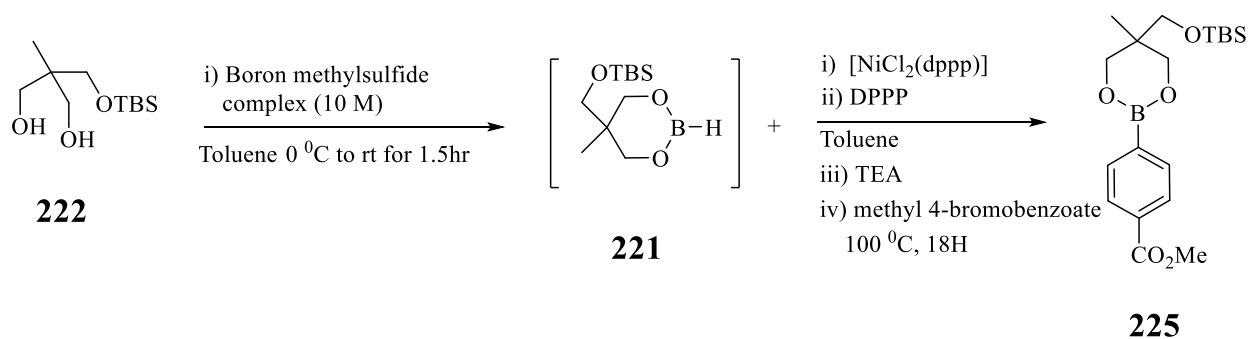


Scheme 2.24: Borylation of **222**

Since **221** is likely volatile, rotary evaporation was not a viable option. Thus, an aliquot from both reactions was obtained. The ¹H NMR spectra were anticipated to contain large toluene peaks but these should not interfere in the chemical shift regions of interest. We were able to confirm several things. First, there was the expected consumption of the BMS reagent in the main reaction. Second, the negative control did not show consumption of the BMS, which was also expected. Third, there was a definite change in the chemical shift and multiplicity of **222**'s methylenes, though the latter was somewhat convoluted. Based on the consumption of the BMS and **222** we hypothesized that the reaction was viable and decided to use it in the subsequent step.

2.5.1.3 Model, Synthesis of Methyl 4-(5-(((tert-Butyldimethylsilyl)oxy)methyl)-5-methyl-1,3,2-dioxaborinan-2-yl)benzoate, **225**

We had previously synthesized **222** and then the *in situ* active borane species **221** for the purpose of borylating aryl bromides through a nickel catalyzed borylation.¹⁰² When we ran the entire reaction, a TLC of the crude product indicated mostly unreacted methyl 4-bromobenzoate starting material. The reaction conditions called for 2 equivalents of **222** and we recovered 85% (1.7 eq.) of **222** by isolation. If the reaction had gone to 100% conversion, we would have collected – at most – 1 eq. of **222**. This means that (at maximum) our yield could be no greater than 30%. We isolated a small amount (< 0.1 eq.) of what appeared to be evidence of a homocoupled (biphenyl) product. In the same sample was what appeared to be a small amount of the target (< 0.1 eq.). However, as this was only a model reaction, no further purification was attempted.

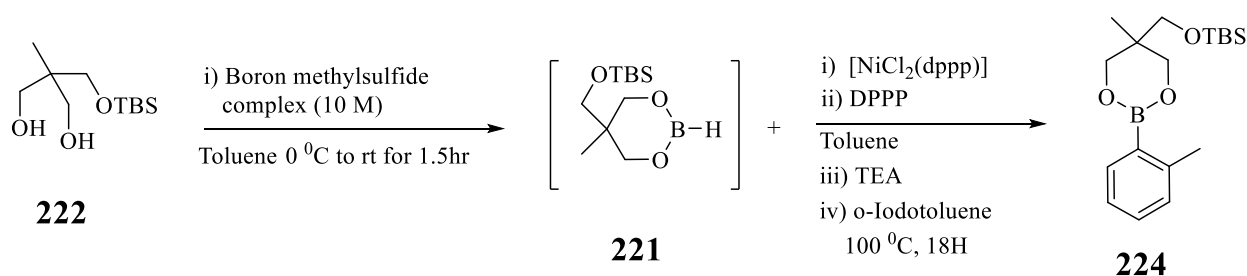


Scheme 2.25: Ni(II) catalyzed borylation of an aryl bromide

2.5.1.4 Model, *tert*-Butyldimethyl((5-methyl-2-(*o*-tolyl)-1,3,2-dioxaborinan-5-yl)methoxy)silane, **224**

We attempted this model reaction to synthesize **224** using the same reaction scheme as was used previously, but with an aryl iodide instead of an aryl bromide.¹⁰² We wanted to attempt this reaction because we believed the ¹H NMR of **224** would be much more easily interpreted than **225** (Scheme 2.25). Furthermore, we believed the ortho-methyl would be a better model for

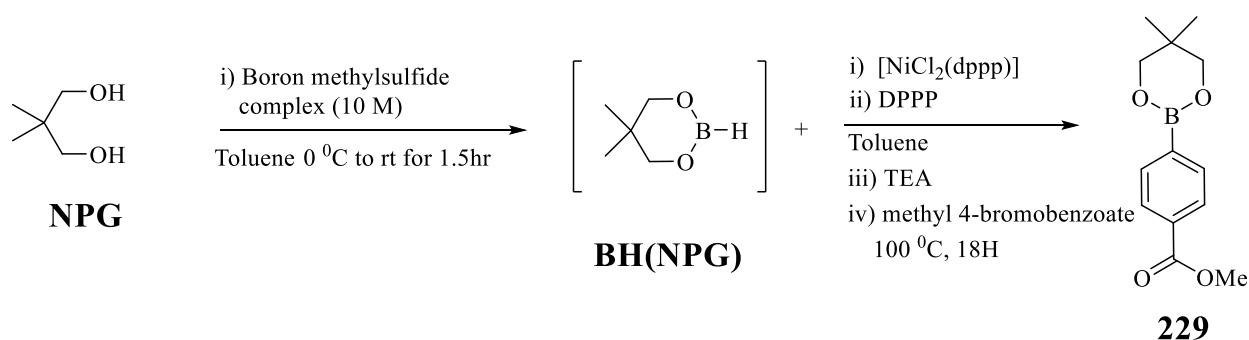
a naphthyl substrate (B-Fragment). Unfortunately, when this reaction was run, the crude ^1H NMR did not *clearly* indicate presence of target (although target peaks might have been buried). In order to follow the literature procedure *exactly*, we purified the crude mixture by Kugelrohr distillation. However, the collected fractions were clearly absent of *any* target. In this case, we attributed the cause of failure to the *o*-iodotoluene reagent which was a deep blue in color. We hypothesized the reagent had partially decomposed to molecular iodine and that this had in turn poisoned the catalyst. Rather than purify the reagent, we moved on to several other models.



Scheme 2.26: Ni(II) catalyzed borylation of *o*-iodotoluene

2.5.1.5 Model, Methyl 4-(5,5-Dimethyl-1,3,2-dioxaborinan-2-yl)benzoate, 229

This model reaction is simpler than the previous two examples in that neopentyl glycol (NPG) is the starting substrate (rather than **222**). We used a slightly modified version of the previous procedure (Scheme 2.27).¹⁰²⁻¹⁰³ In this version, the work-up involved an acidic quench (of the excess borane) with saturated NH_4Cl . We ran this reaction and purified the crude product using normal phase chromatography to obtain a white solid. The yield was 90%. For characterization of this known compound we compared our $^1\text{H}/^{13}\text{C}$ NMR spectral values against literature.¹⁰⁴

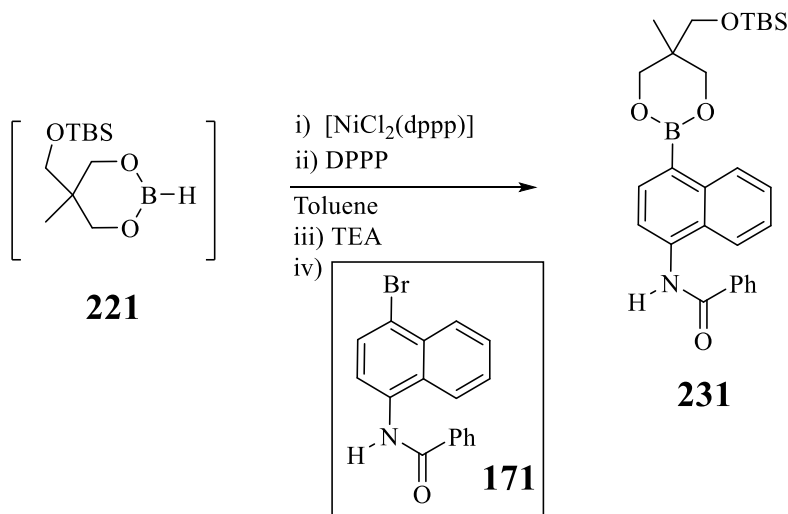


Scheme 2.27: Ni(II) catalyzed borylation of methyl-4-bromobenzoate via **BH(NPG)**

2.5.1.6 Model, *N*-(4-(5-(((*tert*-Butyldimethylsilyl)oxy)methyl)-5-methyl-1,3,2-dioxaborinan-2-yl)naphthalen-1-yl)benzamide, **231**

Having established that we could successfully use the nickel (II) catalyzed borylation protocol from an *in situ* prepared borane **BH(NPG)** (Scheme 2.27, *vide supra*), we wanted to expand the complexity of the model system. By following the previously described procedure,¹⁰²⁻¹⁰³ and applying it to substrate **171**, we hoped to synthesize model **231**. We ran the reaction (Scheme 2.28) as before and analyzed the crude sample by ^1H NMR. We could detect a downfield shift of the two β -boron methylenes (3.7 ppm to 3.9 ppm and 3.57 ppm to 3.64 ppm) and a downfield shift of the boronate methyl group singlet (0.79 ppm to 0.90 ppm). Surprisingly, there was an *upfield* shift of the α -OTBS methylene. The presence of new aromatic peaks, when taken with evidence of methylene shifts (attributed to the boronate), indicate formation of the target.

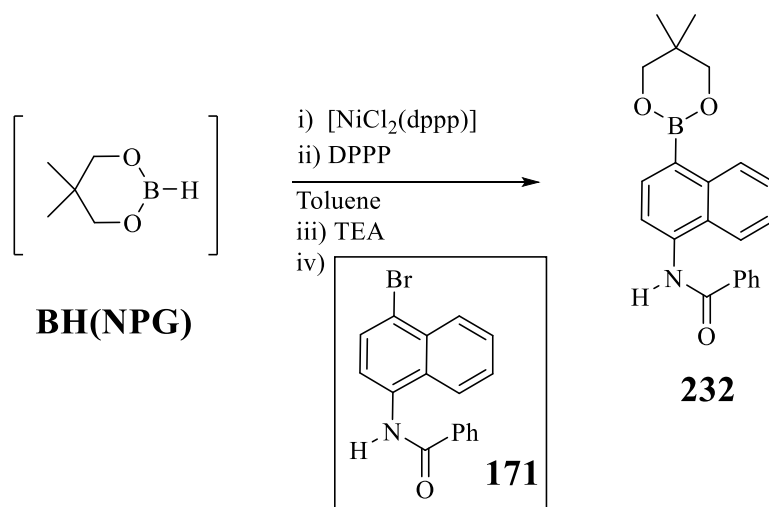
Purification using normal phase chromatography was attempted. This was unsuccessful. The boronate ester peaks disappeared which seems to indicate attempted purification on the column resulted in removal of the boronate. However, the aromatic region remained too complex to decipher. Thus, we believe we synthesized the target **231**, but somehow failed to purify it (maybe the boronate ester hydrolyzes on the column to **222** or deboronation occurs).



Scheme 2.28: Ni(II) catalyzed borylation of **171** via **221**

2.5.1.7 Model, *N*-(4-(5,5-Dimethyl-1,3,2-dioxaborinan-2-yl)naphthalen-1-yl)benzamide, **232**

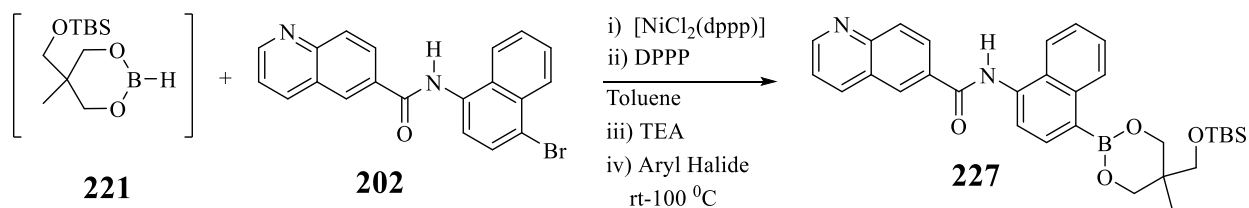
Again, we attempted a simpler model using the NPG boronate **BH(NPG)** (Scheme 2.29). Using ^1H NMR, we confirmed the formation of the boronate ester **232** (methylene singlet at 3.9 ppm) before attempting purification by normal phase chromatography. Despite two isolations on the column, the ^1H NMR remained very convoluted and could not be deciphered. It seems strange that **229** (Scheme 2.27) was easily purified but that boronates on the 1-position of naphthyl rings have always proven impossible for us to isolate. One possible explanation (in this case) is the presence of differing proportions of amide rotamers due to the double-bond character of the amide C-N bond. It is known that benzanilides can have different conformations.¹⁰⁰ However, in cases where we directly borylated 1-amino-4-bromo-naphthalenes (which should not have different conformations like benzanilides), those could never be sufficiently purified either. In those cases, we believed the free amine might have been forming complexes with the Lewis-acidic boron p-orbital.



Scheme 2.29: Ni(II) catalyzed borylation of **171** via **BH(NPG)**.

2.5.2 *N*-(4-(5-(((*tert*-Butyldimethylsilyl)oxy)methyl)-5-methyl-1,3,2-dioxaborinan-2-yl)naphthalen-1-yl)quinoline-6-carboxamide, **227**

We ran the borylation reaction in Scheme 2.30, multiple times.¹⁰²⁻¹⁰³ There was either little or no conversion. In one case where it seemed there might have been conversion to target, we isolated the crude mixture on normal phase chromatography to obtain nearly a 100% recovery of **221**'s precursor, the monosilylated triol **222** (determined by ^1H NMR). This mirrored the problems which had plagued the model reaction in Scheme 2.25 (we recovered 85% of **222**).



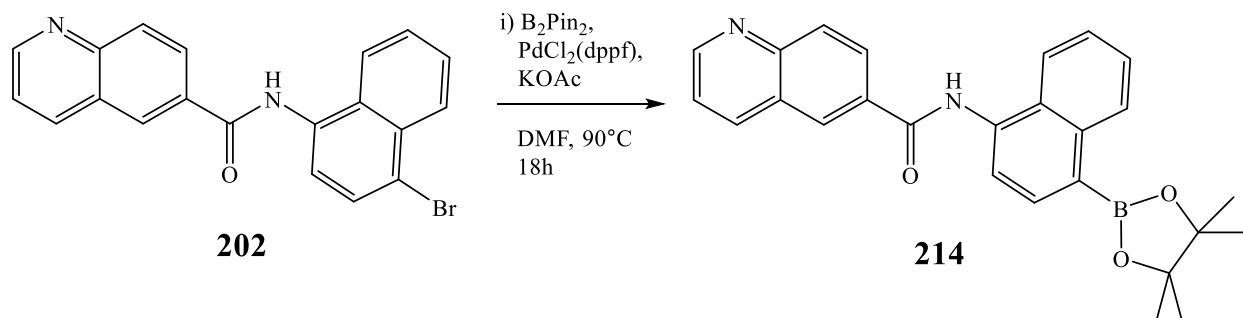
Scheme 2.30: Ni(II) catalyzed borylation of **202** via **BH(NPG)**.

Although in one instance (Scheme 2.27) when we had begun from the *in situ* **BH(NPG)** species, we were able to purify and successfully characterize the boronate ester **229**, this success

could not be expanded in scope to apply to naphthyl bromide substrates. Additionally, the reaction also failed if the monosilylated triol **222** was used to form the *in situ* species **221**. We abandoned further attempts at Ni(II) catalyzed borylations and turned to Pd-catalyzed B₂Pin₂ borylations.

2.5.3 *N*-(4-(4,4,5,5-Tetramethyl-1,3,2-dioxaborolan-2-yl)naphthalen-1-yl)quinoline-6-carboxamide, **214**

We successfully synthesized **214** (Scheme 2.31) from substrate **202** using a literature procedure.¹⁰⁵ The key spectral features of the ¹H NMR (in the aromatic region) were the disappearance of doublets at 7.8 ppm (1H) and 7.9 ppm (1H) and subsequent appearance of an overlapping doublet and broad singlet at 8.83 ppm (1H) and 8.87 ppm (1H). The appearance of a large singlet at 1.4 ppm (12H) is attributed to the four methyls of the pinacol group of the boronate ester **214**.



Scheme 2.31: Miyaura Reaction of **202** to give **214**

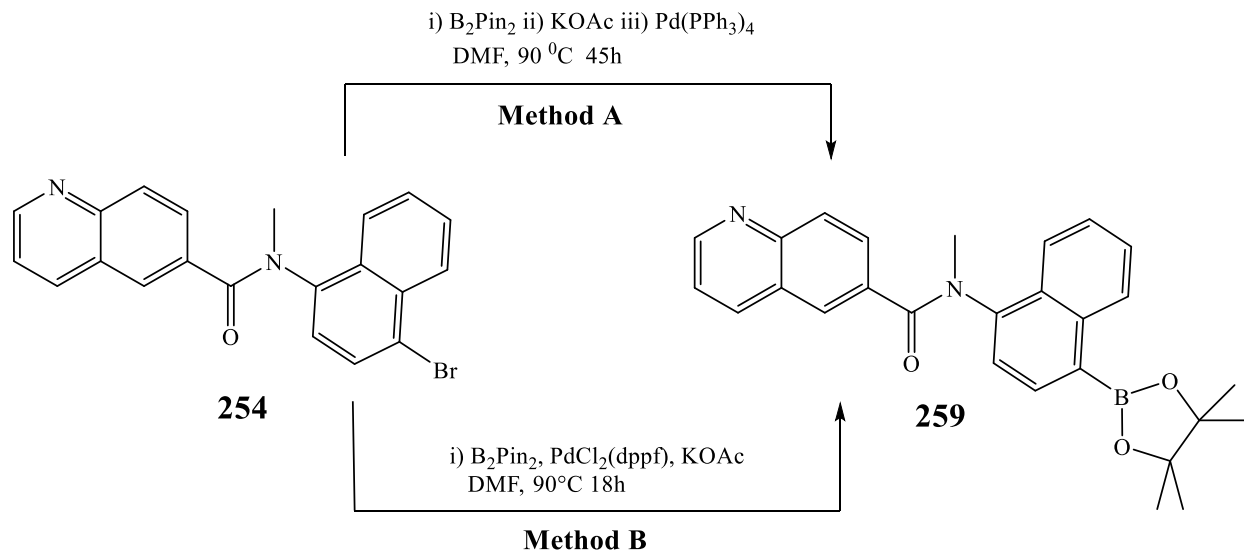
As was previously the case for the analogous reaction (Scheme 2.12) when the reagent B₂(NPG)₂ was used and post-isolation always contained excess B₂(NPG)₂, in these reactions some B₂Pin₂ always remained. Furthermore, in one instance when the material spent a significant amount of time on the column, there seemed to be hydrolysis of the pinacol from the boronate

ester of **214**. As a result, we were *extremely* hesitant to attempt further purification, and assumed the crude product was pure enough for the following step. Since the following step was an *N*-alkylation of the quinoline nitrogen (to give the D-Fragment), we believed that once **214** was *N*-alkylated, the subsequent product would represent a *significant* shift in either the solubility characteristics, the retention factor characteristics (chromatography), or both. As a result, we believed a more efficient strategy was to forgo purification of **214** until formation of the D-Fragment.

A conversion yield could be *approximated* from integrated ¹H NMR values of **202** and **214** (88-95% conversion). The ¹H NMR integrated ratio of methyl singlets of **214** taken against B₂Pin₂ told us there was 1 equivalent of **214** to every 0.03 equivalents of B₂Pin₂. In this manner, we were able to know what percentage of the product mass represented our target **214**.

2.5.4 N-Methyl-N-(4-(4,4,5,5-tetramethyl-1,3,2-dioxaborolan-2-yl)naphthalen-1-yl)quinoline-6-carboxamide, 259

Two methods were used for the borylation of **254** to give **259**. Method “A” used a Pd(0) catalyst.¹⁰⁰ Method “B” used a Pd(II) pre-catalyst.¹⁰⁵ The ¹H NMR spectra of the crude reactions from Method “A” and Method “B” both indicated near quantitative conversion of **254** as evidenced by disappearance of a doublet at 8.26 ppm (1H). Since Method “A” and Method “B” differed in the amount of B₂Pin₂ that the procedure called for (1.1 eq vs 1.5 eq, respectively), we could not make any further estimations based on the ratio of **254** boronate methyl singlets compared against B₂Pin₂. However, we prefer Method “B” because the Pd(II) catalyst is more bench stable than the Pd(0) catalyst used in Method “A”. Furthermore, Method A takes 2.5 times longer to react.



Scheme 2.32: Miyaura reaction of **254** to give **259** through two separate methods

Of the two methods, we only attempted to isolate **259** obtained from Method “B” (we used the Method “A” product directly). Our reasoning behind this has already been explained in the previous section (Section 2.5.3). Unlike our previous Miyaura reactions’ purification (Scheme 2.31, compound **214**, and Scheme 2.12, compound **155.1**), this was the *first* reaction in which we were able to remove the excess borylating reagent!

We had previously proposed that a free amine **155.1** should complex with boron’s empty p-orbital so (in that case) perhaps we could not remove excess borylating reagent because of the amine-nitrogen to boron interaction. We would expect that a secondary amide nitrogen (compound **214**) would be much less likely to have the nitrogen to boron interaction and in the case of a tertiary amide (compound **259**), the interaction would likely be prevented altogether (due to much greater steric hindrance around the *N*-methylated amide nitrogen). So, one possibility for the ability to remove the excess reagent (in this case) could be due to the steric bulk of the amide nitrogen and its inability to coordinate to any excess borylating reagent. Or, it

could simply be a greater difference in retention factors of **259** to B₂Pin₂ during the purification on the silica column.

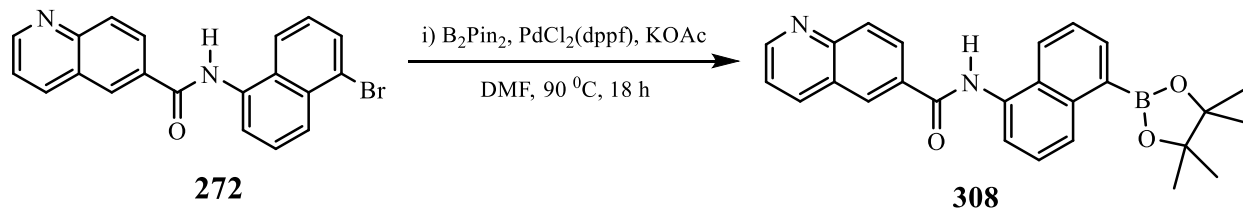
Interestingly, we saw the recurrence of the phenomenon of fractions eluting from the column to give *two* spots on TLC (as previously elaborated upon in Figure 2.2.2.4 “Preparative Scale TLC isolation attempt of **173**”). The ¹H NMR spectra of the isolated material showed a singlet at 1.37 ppm (12 H), which we attributed to the methyls of the pinacolborane. This was also confirmed by ¹³CNMR (methyl peak at 25.0 ppm and quaternary carbon at 84.1 ppm).

We now believe that this compound most likely exists as two rotamers as evidenced by an aromatic region of the ¹H NMR, which had similar peaks nearly overlapping but at slightly different ratios. One of the peaks to support this hypothesis is a singlet, which arises from the quinoline ring (β -carbonyl proton). If there *was* the presence of rotamers (due to the double bond character of the amide C-N bond as well as the steric bulk of the *N*-methylated nitrogen), then the β -carbonyl proton's singlet (on the quinoline ring) would show different signals in a ratio reflecting the rotamer equilibrium. In fact, this is what we saw. One of the future directions for this project would be a variable temperature NMR experiment during which the rotamers should coalesce at a certain temperature. This would potentially bolster our hypothesis.

2.5.5 *N*-(5-(4,4,5,5-Tetramethyl-1,3,2-dioxaborolan-2-yl)naphthalen-1-yl)quinoline-6-carboxamide, **308**

We synthesized **308** (Scheme 2.33) from **272** from a literature procedure.¹⁰⁵ It should be noted that **308** is different than **259** in that the amide nitrogen is not *N*-methylated and the respective boronate and amide positions on the naphthalene ring are also different. The key ¹H NMR spectral feature used to indicate formation of product **308** were the singlet at 1.43 ppm, (12

H), which we attributed to the pinacol boronate's methyls, and a doublet at 7.75 ppm (1H). The complete consumption of substrate **272** was confirmed by disappearance of a doublet at 7.85 ppm (1 H) and a triplet at 7.67 ppm (1 H).



Scheme 2.33: Miyaura Reaction of **272** to give **308**

Unsurprisingly, when normal phase chromatography was used for the attempted purification of the crude **308**, there was the usual elution of fractions which gave two spots on TLC. This had been a consistent occurrence in this project as has already been discussed in the previous sections. There were also around 0.1 equivalents of the B_2Pin_2 reagent remaining (determined by 1H NMR). Thus, the yield could be calculated by subtracting the mass of the remaining B_2Pin_2 reagent to give a crude yield near 100%, assuming the target consists of rotamers. As was previously stated, a variable temperature NMR experiment could have shed light on this recurring issue.

One important question we considered is why we should expect to see rotamers post-borylation (via Miyaura Reaction) when substrates **272**, **254**, **202**, and **171** (all amides) did not show *any* indication of the presence of rotamers. The compounds **272**, **254**, and **202** were synthesized at a low temperature range ($0^\circ C$ – rt) and the model compound **171** was synthesized at room temperature. If the free bond rotation is normally restricted at lower temperatures, then it seems possible that low-temperature reactions produced only the more stable rotamer, while reactions run at heat – and then cooled – could trap the molecule in its various rotameric forms.

A test of this possibility would be to take the aforementioned substrates, heat them using the same conditions (in DMF at 90°C for 18 hours), cool, then analyze by NMR. If there is a sort of trapping (of the rotamers) by heating followed by rapid cooling, then this should be evident by NMR. During the section of this dissertation dealing with the synthesis of the C and D-Fragments (Sections 2.6.2 – 2.6.3), we will return to this issue in more detail.

2.6 Syntheses of *N*-Alkyl Quinoliniums, C and D-Fragments

In this section, we will describe the syntheses of the C and D-Fragments. The C-Fragment was prepared by an *N*-alkylation of the A-intermediate quinoline nitrogen to give a cationic quinolinium. The D-Fragment synthesis was attempted by two different approaches. In one approach, the B-Fragment quinoline was *N*-alkylated give the D-Fragment. In the other approach, the C-Fragment aryl bromide was borylated to give the D-Fragment.

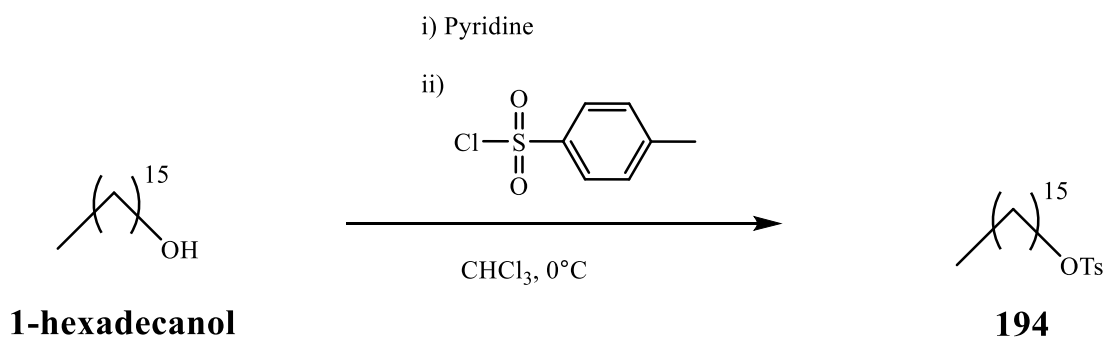
We prepared and fully characterized alkylating reagents using several methods. The alkylating reagents were either alkyl halides or alkyl pseudohalides and varied in the alkyl tail length. We found that some alkylating reagents resulted in products with more desirable physical characteristics. Furthermore, we will address alkyl halides that had poor reactivity with the substrates of the A and B-Fragment substrates.

2.6.1 Syntheses of Alkylhalides and Alkylpseudohalides

2.6.1.1 Hexadecyl 4-Methylbenzenesulfonate, **194**

We synthesized hexadecyl 4-methylbenzenesulfonate **194** (Scheme 2.34) from the commercially available 1-hexadecanol using an established literature procedure for this known compound.¹⁰⁶ We purified this material on normal phase chromatography. When there was some tosyl chloride which was not removed by chromatographing (it was in this case), we found it most expedient to add small amounts of ethylenediamine (EDA), then repeating a wash with

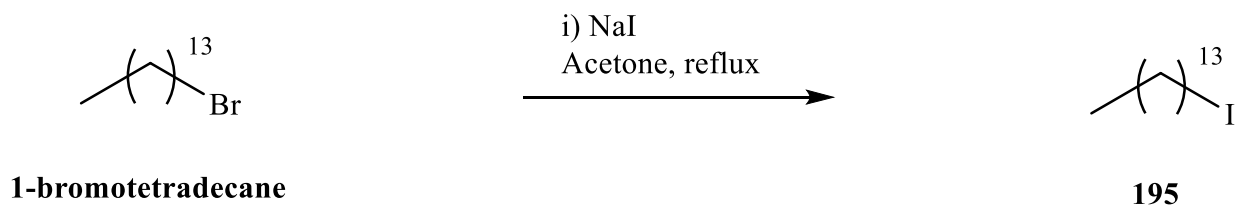
dilute HCl.¹⁰⁷ The EDA removal of TsCl works by the EDA amine-nitrogen attack on the tosyl chloride to form the tosyl amide that is also an amine salt. Addition of the dilute HCl protonates the remaining amine of the salt ensuring good aqueous solubility and rapid removal by the aqueous wash. We obtained a yield of 84%. Our spectral data matched that of the known literature compound.



Scheme 2.34: The synthesis of hexadecyl 4-methylbenzenesulfonate **194** from hexadecanol.

2.6.1.2 1-Iodotetradecane, **195**

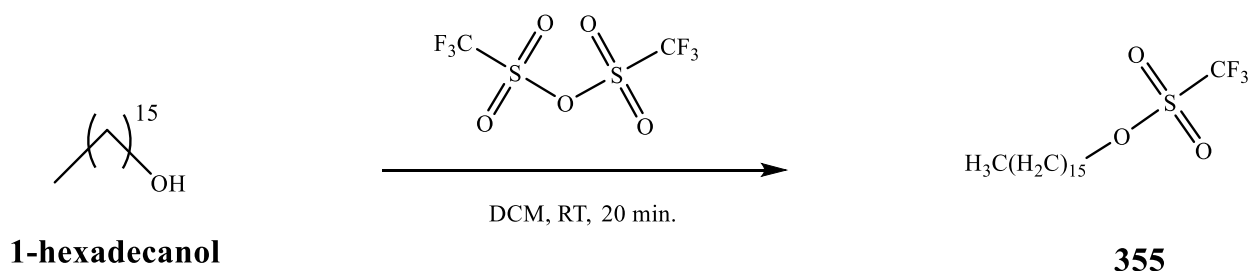
We synthesized 1-iodotetradecane **195** (Scheme 2.35) from the commercially available starting material 1-bromotetradecane using the Finkelstein Reaction and following an established literature procedure.¹⁰⁸ The nucleophilic attack of the iodide anion displaces bromide to form the acetone-insoluble salt NaBr. The insolubility of the by-product salt-formation drives the reaction to completion in high yields. The crude material was purified by distillation,¹⁰⁹ bp = 134-137°C at 3 mm Hg. A yield of 86% was obtained. This literature compound¹⁰⁸ was confirmed by ¹H NMR.



Scheme 2.35: Finkelstein Reaction synthesis of 1-iodotetradecane **195**

2.6.1.3 Hexadecyl Trifluoromethanesulfonate, **355**

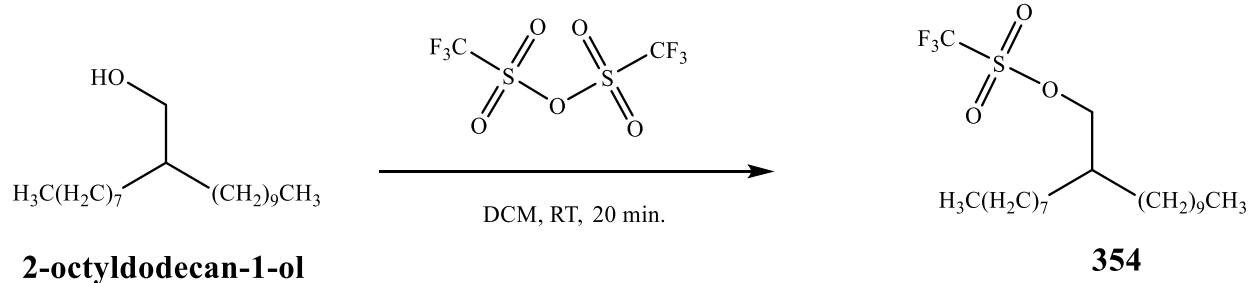
We synthesized hexadecyl trifluoromethanesulfonate, **355** (Scheme 2.36) from the commercially available 1-hexadecanol using an established literature procedure.¹¹⁰ When reacted with trifluoromethanesulfonic anhydride, the conversions of hexadecanol to the triflate were always quantitative. When the reaction was worked up with saturated NaHCO₃, no further purifications were required. Yield of the nearly pure liquid was 97%. This literature compound was confirmed by NMR spectroscopy.



Scheme 2.36: Synthesis of hexadecyl trifluoromethanesulfonate, **355**

2.6.1.4 2-Octyldodecyl trifluoromethanesulfonate, **354**

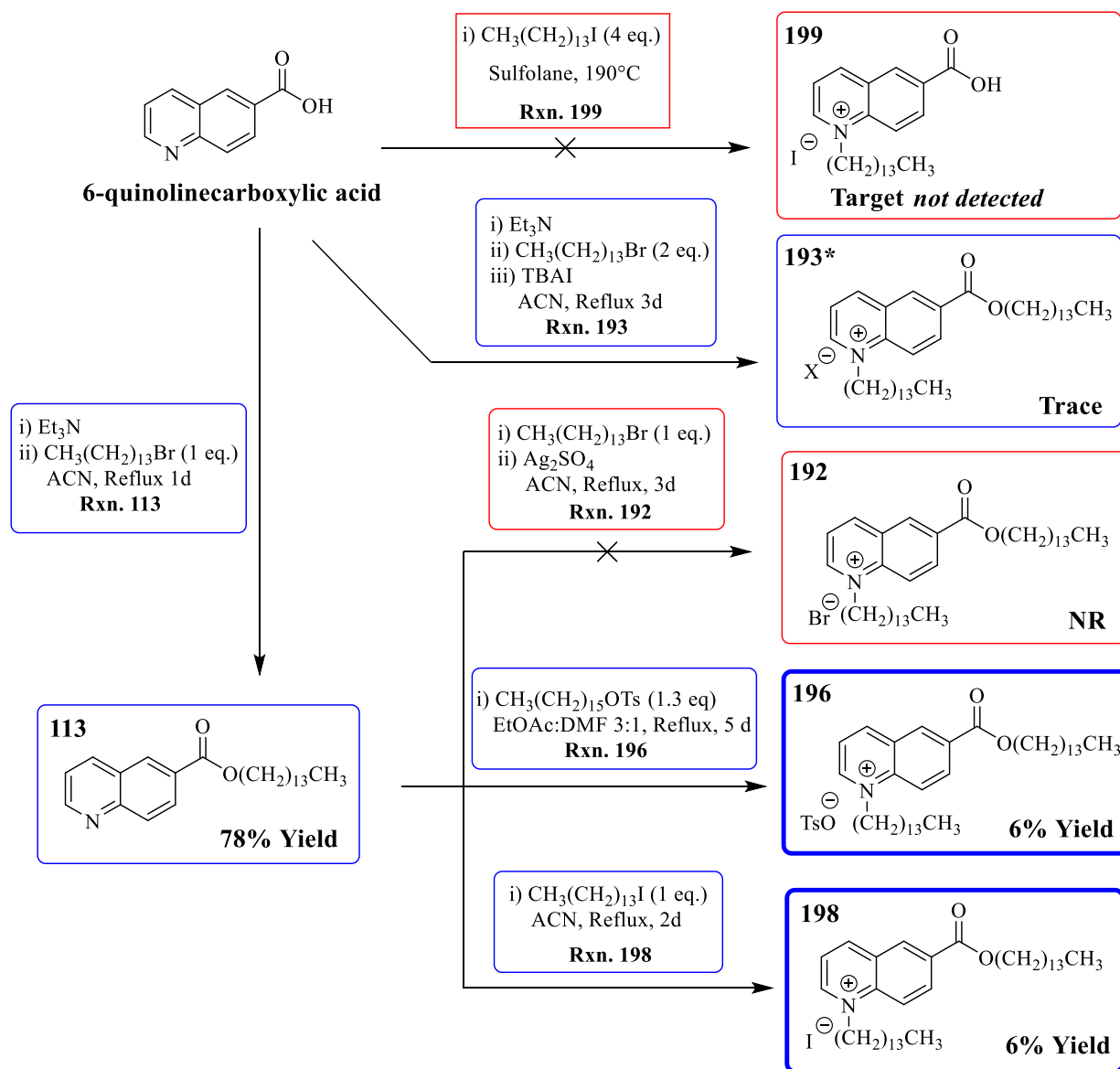
We synthesized 2-octyldodecyl trifluoromethanesulfonate, **354** (Scheme 2.37) by using the commercially available Guerbet alcohol 2-octyldodecan-1-ol by the same procedure as above.¹¹⁰ We obtained the triflate as a light-pink tinted liquid in 89% yield. We confirmed the product formation by appearance of a new doublet at 4.437 ppm (2H) using ¹H NMR.



Scheme 2.37: Synthesis of 2-octyldodecyl trifluoromethanesulfonate **354**

2.6.2 Syntheses of C-Fragments

In establishing the method to synthesize the C-fragment, we initially attempted to directly *N*-alkylate 6-quinolinecarboxylic acid to obtain the quinolinium salt **199** (Scheme 2.38). We had then planned to use the quinolinium-carboxylic acids for amidation with 1-amino-4-bromonaphthalene to give the C-Fragment. However, this proved to be impractical for reasons which we will explain.



Scheme 2.38: Direct attempts at the *N*-alkylation of 6-quinolinecarboxylic acid

In the attempted formation of **199** (Scheme 2.38), we attempted to directly *N*-alkylate 6-quinoline carboxylic acid following an analogous procedure.¹¹¹ Li and coworkers were able to directly *N*-methylate 2-methylquinoline-6-carboxylic acid (by use of autoclave at 110°C). Their reagent (iodomethane) was used in a 30-fold excess to their substrate. Because their substrate is more sterically hindered (methyl in the 2-position) than 6-quinolinecarboxylic acid (hydrogen in

the 2-position), it should be more difficult to *N*-alkylate than our substrate. However, their reagent (iodomethane) is much more reactive to *N*-alkylation than is iodotetradecane.

Jan Marek and coworkers *N*-alkylated quinolines using alkyl bromides of various lengths (C₈ – C₂₀) in dry ethanol.¹¹² They used their reagents (alkyl bromides) in a 14-fold excess to substrate quinoline in refluxing conditions for 48 hours. The various *N*-alkylated quinolinium salt-yields generally decreased with increasing alkyl length. The C₈ alkyl bromide represented the maximum yield of 41% while the C₂₀ alkyl bromide represented the minimum yield of 7%.

Pardal and coworkers *N*-alkylated 2-methylquinolines using alkyl iodides of various lengths (C₂, C₅, C₆, C₁₂) in acetonitrile.¹¹³ Their reagents (alkyl iodides) were used in 3 – 5-fold excess to substrate 2-methylquinoline in refluxing conditions for 24 hours. When the reagent was 1-iodododecane (C₁₂) the yield was 37%.

Our quinoline carboxylic acid substrates represented a greater synthetic challenge than quinolines *without* a carboxylic acid functional group for several reasons. If the compound exists in the zwitterionic form (protonated quinoline and deprotonated carboxylic acid), then one should expect *O*-alkylation of the carboxylate to give the ester. Under slightly basic conditions one should expect both *O*-alkylation *and* *N*-alkylation to occur to give a mixture of the ester *and* the alkyl quinolinium, respectively. Furthermore, if the ratio of alkyl halide to substrate is 2 equivalents or greater, there is also the possibility of forming the alkyl-quinolinium-ester (the result of *O*-alkylation *and* *N*-alkylation).

In the reaction where we attempted to synthesize **199** (Scheme 2.38), we were unable to purify the products sufficiently to determine if the target **199** had been achieved. Although we did not run this particular reaction again, we attempted other, gentler alkylations. We varied alkylating reagent (alkyl bromide, alkyl iodide, and alkyl tosylate), reagent-to-substrate ratios,

reaction time, reaction solvent, and various additives. When combined, we were ultimately able to optimize a set of reaction conditions which we would apply to the *N*-alkylation of the amide A-fragment.

In reaction 113 (Scheme 2.38), we used the mild organic base TEA and 1 equivalent of dodecyl bromide in refluxing acetonitrile. We had assumed that the substrate should exist in the zwitterionic form in the absence of TEA. In the zwitterionic form, the quinoline nitrogen is protonated (quinolinium) and should prevent *N*-alkylation. Thus, we believed the presence of a bulky base would help ensure *N*-alkylation of the quinoline by shifting the acid-base equilibrium to the deprotonated (quinoline) form, which we believed would react sufficiently under the conditions used. Instead of the desired quinolinium however, we obtained ester **113** in 78% yield. FTIR was used to confirm a sharp ester carbonyl stretching band at 1704 cm^{-1} and subsequent absence of carboxylic acid carbonyl stretching at 1688 cm^{-1} . The material was recrystallized from acetonitrile to give needles with a melting point of $58 - 60^{\circ}\text{C}$. Further characterization by $^1\text{H}/^{13}\text{C}$ NMR was also obtained. The ^1H NMR key spectral feature was the ester methylene triplet at 4.4 ppm (2H).

In the attempt to synthesize **192** (Scheme 2.38), we modified an existing procedure¹¹⁴ and attempted to *N*-alkylate the ester **113** with 1 equivalent of 1-bromotetradecane in refluxing acetonitrile. We monitored the reaction by TLC and after 24 hours there was little to no conversion of **113**. We added one equivalent of Ag_2SO_4 for the purpose of activating the alkyl bromide. We noticed the appearance of several new spots on the TLC (one fluoresced under long wave UV) and the mixture took on a metallic and reflective sheen. However, after another 48 hours a crude ^1H NMR was obtained, which indicated no reaction had occurred. It is possible

that the Ag_2SO_4 had formed a weak complex with the quinoline nitrogen, effectively locking it out from reaction with the alkyl halide. Thus, we abandoned this route.

In reaction **193** (Scheme 2.38) we reacted 6-quinolinecarboxylic acid with the mild organic base triethylamine and *two* equivalents of 1-bromotetradecane (we previously used one equivalent in reaction 113). Additionally, we added 1 equivalent of the phase transfer catalyst tetrabutylammonium iodide (TBAI) in refluxing acetonitrile. Based on our previous reaction 113, we knew that the first equivalent of alkylating reagent under mild basic conditions would give the ester. We wanted to see if by the addition of a second equivalent of alkylating reagent, in the presence of TBAI, we might be able to accelerate the *N*-alkylation of the quinoline to give the quinolinium salt. After three days, we could detect a small presence of quinolinium formation (~ 5%) as evidenced by a triplet at 5.4 ppm (2H), which we attribute to the quinolinium methylene. Unsatisfied with the lengthy reaction times we turned to other alkylating reagents.

In reaction **196** (Scheme 2.38) we obtained target quinolinium **193** (6% yield) by reaction of **113** with the alkylating reagent hexadecyl 4-methylbenzenesulfonate **194**.¹¹⁵ The material was purified by trituration with hexanes. Analysis of the product by ^1H NMR showed a triplet at 5.32 ppm (2H), which we attribute to the quinolinium methylene (α -nitrogen-methylene).

Lastly, in reaction **198** (Scheme 2.38), we obtained target quinolinium **198** (6% yield). In this case, the alkylating reagent was 1-iodotetradecane **195**. The purification was by trituration with hexanes. The ^1H NMR showed the triplet at 5.32 ppm (2H), which we attributed to the quinolinium methylene (α -nitrogen-methylene).

We decided to forgo any further efforts to optimize this route. Our initial goal had been direct *N*-alkylation of the 6-quinolinecarboxylic acid. However, when that had been unsuccessful (*O*-alkylated occurred instead), we thought to attempt *N*-alkylation of the quinoline ester and

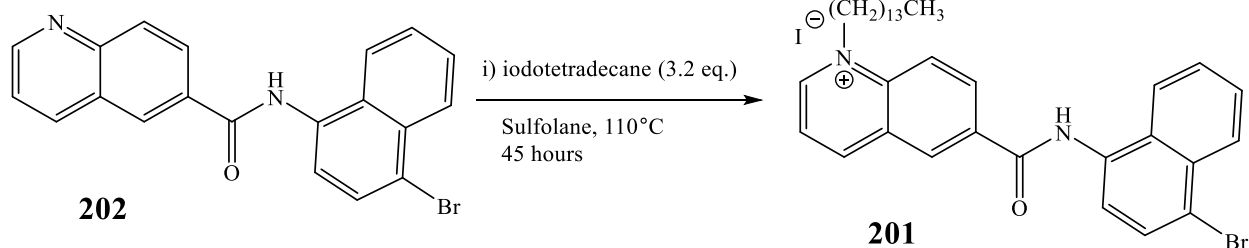
then hydrolyze the *N*-alkylated quinolinium-ester to give the target alkyl-quinolinium-carboxylic acid. This proved to be inefficient as it involved an extra step (deprotection of ester).

Furthermore, we were unsure how our substrate would fare under acidic or basic hydrolysis conditions. We realized there was a simpler way. If amidation *preceded* *N*-alkylation, then there could be no issue of ester formation. Thus, our synthetic route on this total synthesis uses amidation as the first step.

2.6.2.1 6-((4-Bromonaphthalen-1-yl)carbamoyl)-1-tetradecylquinolin-1-ium iodide, 201

We drew upon several literature procedures^{111-113, 116} for the synthesis of **201** (Scheme 2.39). After our previous efforts to *N*-alkylate the quinoline, we felt that acetonitrile was not the ideal solvent to perform the reaction in a timely manner due to the limitations of its boiling point (82°C). Since S_N2 reactions are accelerated by polar aprotic solvents, we decided to start with sulfolane as it has a higher dipole moment than either acetonitrile or DMSO.¹¹⁷ Furthermore, it allowed us to operate the reaction conditions at much higher temperatures than acetonitrile.

After 48 hours of reflux with iodotetradecane, we were able to crash out the yellow solid **201** by addition of EtOAc. We obtained the target in 67% yield. A ¹H NMR was used to confirm formation of quinolinium; the key spectral feature was a triplet at 4.94 ppm (2H), which we attribute to the quinolinium methylene (α -nitrogen-methylene). Although further purification was not required, we found the material to recrystallize from acetone to give beautiful golden-metallic flakes with a melting point of 209 - 211°C.



Scheme 2.39: The *N*-alkylation of **202** to form quinolinium **201**

2.6.2.2 6-((4-Bromonaphthalen-1-yl)carbamoyl)-1-tetradecylquinolin-1-ium 4-methylbenzenesulfonate, **207**

We were interested in synthesizing a quinolinium analogue where the presence of the counter-anion could be detected by ^1H NMR spectroscopy. The counter-anion of the previous example (Scheme 2.39, **201**) contained iodide. In the event future transformations effected an anion exchange, the absence of the tosylate anion would be verifiable (through ^1H NMR).

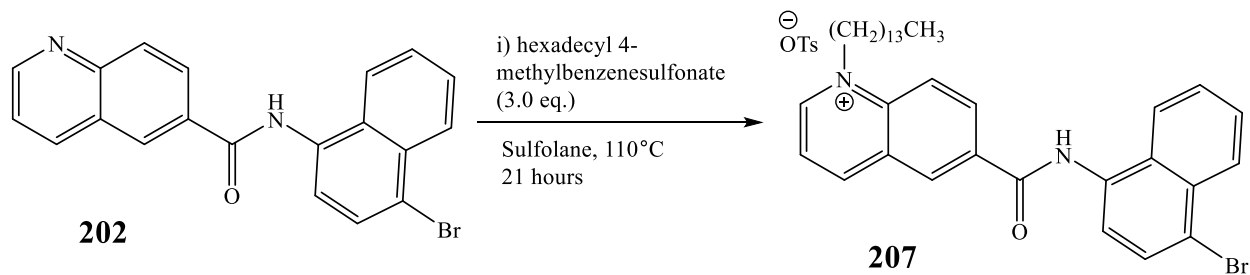
There are additional reasons why changing the counter-anion was considered. The judicious choice of counter-anion can play a huge role in the compound's solubility in organic solvents. Softer anions (iodide, tosylate, PF_6^-) tend to promote better solubility in organic solvents while hard anions (fluoride and chloride) are less soluble in organic solvents. This can aid in purification strategies where an organic-solvent-soluble quinolinium salt could be extracted in less polar solvents and then, through an anion exchange purification strategy, could be crashed-out as the hard-anion-salt.

In Scheme 2.40, we synthesized the quinolinium tosylate analogue **207**. We ran this reaction at approximately *half* the reaction time of that used for synthesis of the iodo-analogue. The tosylates *should* be better leaving groups than iodides and therefore proceed faster.

However, under the conditions used in scheme Scheme 2.40, the recrystallized yield (10%) was poor.

We increased the reaction temperature to 145°C in hopes of increasing the yield. Unlike the synthesis of **201** in Scheme 2.39, the spectra of crude **207** seemed to indicate the presence of multiple compounds (rotamers?). This is of interest as it is possibly related to our previous discussions (Section 2.54 and 2.55) regarding the formation of rotamers. Our working hypothesis was that at higher heats, a rotational barrier around the amide-nitrogen to carbon-carbonyl could be overcome, resulting in rotamers.

In Section 2.54 and 2.55, the reaction temperature had been 90°C and the solvent was DMF. In the synthesis of **201** in Scheme 2.39, the reaction temperature was higher (110°C) but the solvent was sulfolane. The synthesis of **201** did *not* appear to result in rotamers. However, during the synthesis of **207**, when we had increased the reaction temperature to 145°C, there seemed to be evidence of multiple compounds (rotamers?). Our working hypothesis with respect to amides of the type described in Sections 2.54, 2.55, 2.6.2.1, and 2.6.2.2 is that rotamer formation can occur in DMF at a lower temperature than in sulfolane. In DMF, rotamer formation *seems* to be evident at reactions run at 90°C while in sulfolane there is no indication of rotamer formation at 110°C. However, at 145°C rotamer formation seems to manifest.

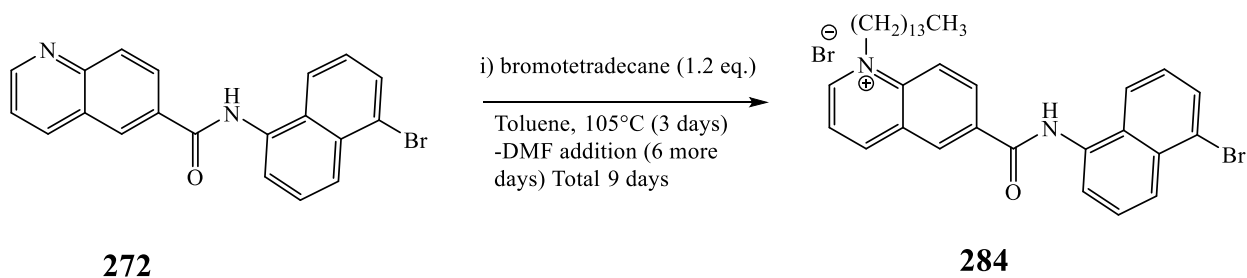


Scheme 2.40: The N-alkylation of **202** to form quinolinium **207**

We did not attempt further methods at optimization of the reaction conditions due to deterioration of the alkylating reagent hexadecyl 4-methylbenzenesulfonate. Finally, the recrystallized **207** was characterized by ^1H NMR. The key spectral feature was a triplet at 5.14 ppm (2H), which we attribute to quinolinium methylene (α -nitrogen-methylene). The counter-anion tosylate showed a doublet at 7.68 ppm (2H), a doublet at 7.20 ppm (2H), and a singlet at 2.35 ppm (3H).

2.6.2.3 6-((5-Bromonaphthalen-1-yl)carbamoyl)-1-tetradecylquinolin-1-ium bromide, **284**

The *N*-alkylation of **272** to form quinolinium **284** represents the first successful *N*-alkylation of this dissertation using an alkyl bromide as the alkylating reagent. We initially ran the reaction for three days in toluene at 105°C but saw little to no apparent conversion (by TLC) to target. This was not too surprising based on the results of our previously attempted *N*-alkylations using bromotetradecane (Scheme 2.38). Part of the problem seemed to be the poor solubility of **272** in toluene. Thus, after 3 days we decided to add in DMF as a cosolvent.



Scheme 2.41: The *N*-alkylation of **272** to form quinolinium **284**

The addition of DMF prompted a noticeable change as the substrate began to dissolve into solution. Within a day TLC analysis showed formation of a new, lower R_f spot (**284**). Most of the starting material had been consumed four days after first adding the DMF. At this point, further reaction time did not consume the remaining substrate **272** but instead seemed to begin forming two side products. We stopped the reaction and **284** was precipitated from the solution

by adding EtOAc. The material was collected by filtration to give a dry grainy-textured brown solid at a crude yield of 57%. We directly attempted recrystallization in various solvents.

We found the crude **284** was soluble in ethanol but only slightly soluble in toluene, acetone, and acetonitrile. We tried recrystallizing the material from each of these respective solvents (minus ethanol) but could not get crystals. Instead there seemed to be a fine suspension of solid which could not be made to grow large enough to collect by filtration. It is likely that some side contaminant was preventing formation of quality crystals. The purification in this method would likely have benefitted from a fractional recrystallization though this was not attempted at the time. Instead, the brown solid was chromatographed.

In this case, we obtained the target **284** in 25% yield. Confirmation of the target was made by $^1\text{H}/^{13}\text{C}$ NMR analysis. The ^1H NMR spectrum's triplet at 5.1 ppm (2H) is consistent with a quinolinium methylene (α -nitrogen-methylene). The ^{13}C NMR spectrum's peak at 59.7 ppm is consistent with quinolinium methylene.

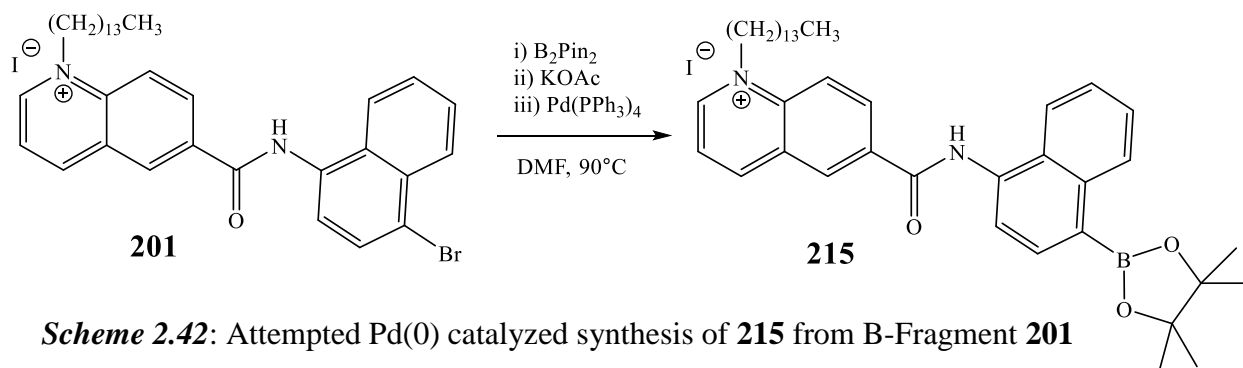
2.6.3 Synthesis of D-Fragments

The synthesis of the D-Fragment could be achieved when starting from either the C-Fragment or the B-Fragment (Scheme 2.15). If starting from the C-Fragment, the Miyaura reaction is likely the best choice. If starting from the B-Fragment, an *N*-alkylation will suffice. During this portion of the dissertation research, we attempted both methods concomitantly but first arrived at the D-Fragment when starting from the B-Fragment substrate.

2.6.3.1 Attempted Synthesis of **215** from C-Fragment **201**

We attempted the synthesis of **215** from **201** by a Miyaura Reaction.⁵ In Scheme 2.42, we used a Pd(0) catalyst. The reaction was monitored by TLC and showed a complete disappearance of **201**. We attempted purification by addition of EtOAc to the DMF, then filtration. From our

previous experience, we knew **201** to be insoluble in EtOAc. We had assumed (correctly as it turned out) that **215** should be soluble in EtOAc. We then further diluted the sample with EtOAc and washed it with aqueous wash several times.



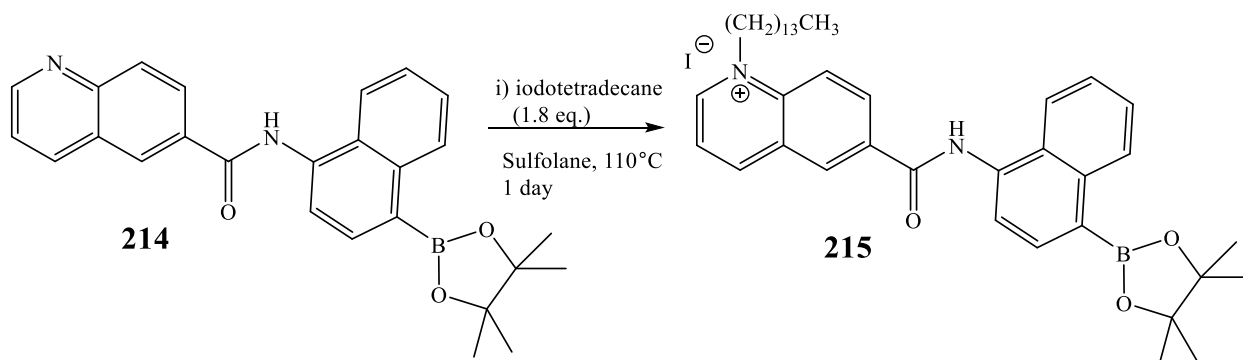
A crude ^1H NMR revealed a complex signal in the aromatic region. The complete absence of quinolinium methylenes (and low mass recovery) should have been signs that product had been lost. Based on information gleaned from a later synthesis of **215** (from a different route) it seems highly unlikely the material was lost in the aqueous layer. Before we could attempt this route a second time (to better account for the low mass recovery), we found success through an alternate route (starting from the B-Fragment instead of the C-Fragment). We reluctantly abandoned this route.

2.6.3.2 Synthesis of 1-tetradecyl-6-((4-(4,4,5,5-tetramethyl-1,3,2-dioxaborolan-2-yl)naphthalen-1-yl)carbamoyl)quinolin-1-ium iodide, **215**

We successfully synthesized **215** by the *N*-alkylation of B-Fragment **214** with iodotetradecane in sulfolane (Scheme 2.43). We ran this reaction twice and both times found the purification to be surprisingly complicated. After the first reaction, the crude **215** was diluted with ethyl acetate and washed with water (3X). However, during the third wash the mixture formed an inseparable emulsion. The addition of an excess of chloroform helped break the

emulsion and allowed the organic layer to be recovered. We then stripped the EtOAc/Chloroform under rotary evaporation and re-diluted the mixture with chloroform and washed with water three additional times. The problem of emulsion-formation was solved but the issue of removal of sulfolane was not. ^1H NMR indicated a 5-fold excess of sulfolane to **215**. We were forced to chromatograph the material.

Based on our previous experience with chromatographing boronate esters (i.e. **214**), when we had found that extended times on a column seemed to lead to low yields (boronate hydrolysis to boronic acid? Deborylation?), we were reluctant to chromatograph **215**. Nevertheless, after our first attempt at this reaction we chromatographed the material and removed almost all of the sulfolane. However, the yield was poor (27%).



Scheme 2.43: Synthesis of **215** from B-Fragment **214**

After we ran the reaction a second time, we dissolved our crude material in chloroform (instead of EtOAc) and this was washed with water (5X). Despite the multiple water-washes, the *bulk* of the sulfolane could *not* be removed! We did not continue with further washes. Instead, after we removed the excess chloroform via rotary evaporation, we attempted to crash out the

target by addition of various solvents. That was also unsuccessful. No precipitation could be made to occur by this method.

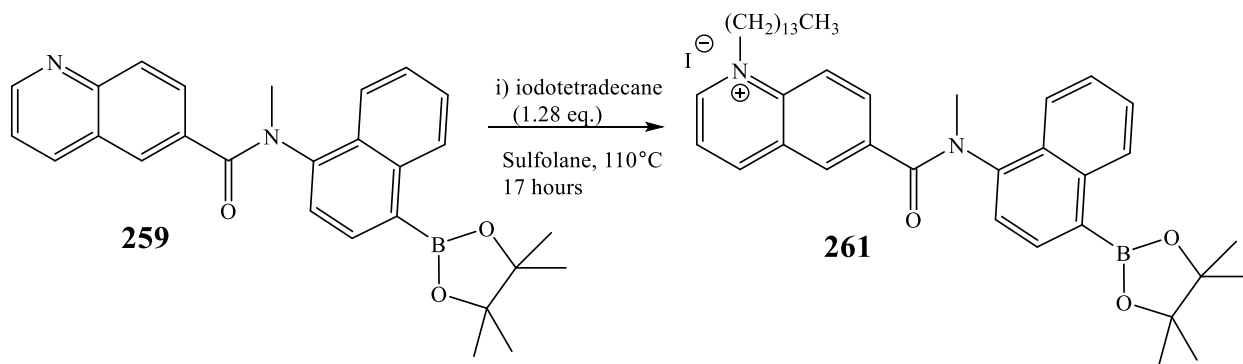
Purification was then attempted on normal phase chromatography. Although the first pass on the column failed to remove all sulfolane, it removed *most* of it. We weighed the option of attempting a second run on the column but were reluctant to do so based on our previous experiences with the low yields. The alkyl quinolinium **215** was confirmed by ¹H NMR analysis. The appearance of 4 new aromatic peaks in the 9-10 ppm region is consistent with a downfield (deshielded) quinolinium. Furthermore, a peak at 4.81 ppm (2H) is consistent with our previous *N*-alkylations and represents the quinolinium methylene (α -nitrogen-methylene).

As previously stated, we had to maintain a balance between obtaining either a low yield (but higher purity) or a higher yield (but with greater sulfolane contamination). In the first reaction, we chose the former. In the second reaction, we chose the latter. The first reaction gave a yield of less than 27% (0.1 eq of sulfolane remaining). The second reaction gave a yield of less than 71% (0.24 eq of sulfolane remaining). We decided to simply use each respective sample without further purification (and loss of yield).

2.6.3.3 6-(Methyl(4-(4,4,5,5-tetramethyl-1,3,2-dioxaborolan-2-yl)naphthalen-1-yl)carbamoyl)-1-tetradecylquinolin-1-ium iodide, 261

The *N*-alkylation of methylated B-Fragment* **259** to quinolinium **261** was successful but encountered the same purification difficulties as previously elaborated upon (Section 2.6.3.2) for the synthesis of **215**. The mixture was purified by normal phase chromatography but still contained residual sulfolane. Otherwise, the ¹H/¹³C NMRs both indicated successful *N*-alkylation. The key spectral features included a downfield shift of aromatic peaks by the

appearance of a doublet at 10.39 ppm (2H) and doublet at 8.64 ppm (2H). A peak at 5.1 ppm (2H) was consistent with a quinolinium methylene (α -nitrogen-methylene). For the ^{13}C NMR, a peak at 59.7 ppm was consistent with a quinolinium methylene.



Scheme 2.44: Synthesis of **261** from C-Fragment **259**

2.7 Synthesis of AQuANaB Compounds

To revisit one of the two goals of the work upon which this dissertation is based, this project portion of the dissertation has been directed towards the synthesis of zwitterionic **D- σ -A**'s. The initial goal was that the donor be an anionic triolborate. Although we were unable to successfully synthesize a triolborate type **D- σ -A**, we *were* able to synthesize a **D- σ -A** containing an anionic trifluoroborate type donor (compound **217**). To reiterate, this class of compounds is characterized by having a hydrophobic alkyl tail attached to a quinolinium acceptor tethered by an amide bridge to a naphthalene unit containing an anionic borate. These features have given rise to the *nom de chimique* “AQuANaB” shown in Figure 2.7.1.

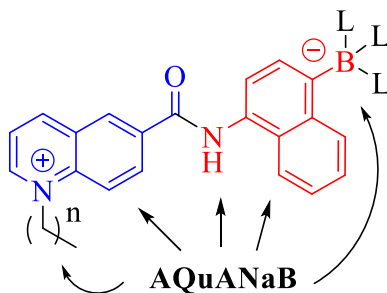
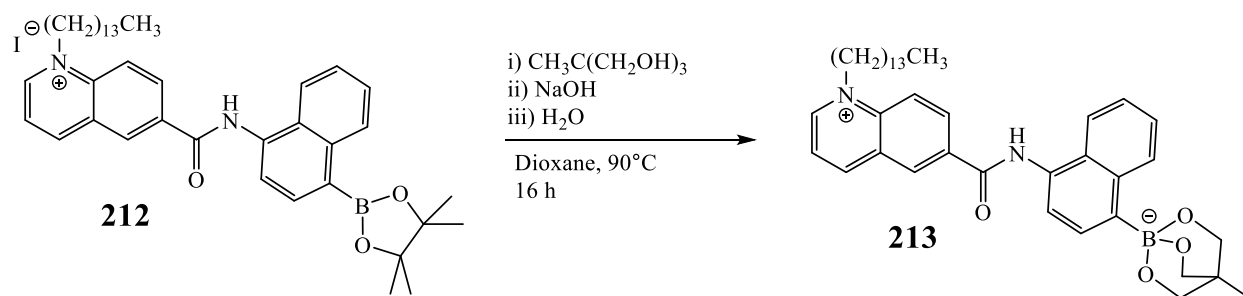


Figure 2.7.1: General form for AQuANaB type compounds

2.7.1 Attempted Synthesis of 4-Methyl-1-(4-(1-tetradecylquinolin-1-ium-6-carboxamido)naphthalen-1-yl)-2,6,7-trioxa-1-borabicyclo[2.2.2]octan-1-uide, **213**

The synthesis of borate **213** from boronate ester **212** by transesterification¹¹⁸ was attempted. The boronate ester **212** was treated with 1 equivalent of 2-(hydroxymethyl)-2-methylpropane-1,3-diol then 0.9 equivalents of NaOH and 3 equivalents of water. Spectral ¹H NMR evidence supports consumption of **212** by the complete disappearance of boronate methyl singlet at 1.37 ppm (12H). Although all mass was recovered, there was complete absence of the quinolinium methylene (α -nitrogen-methylene) triplet anywhere near 5 ppm. The aromatic region was a very broad indistinguishable hump with no discernible peaks.

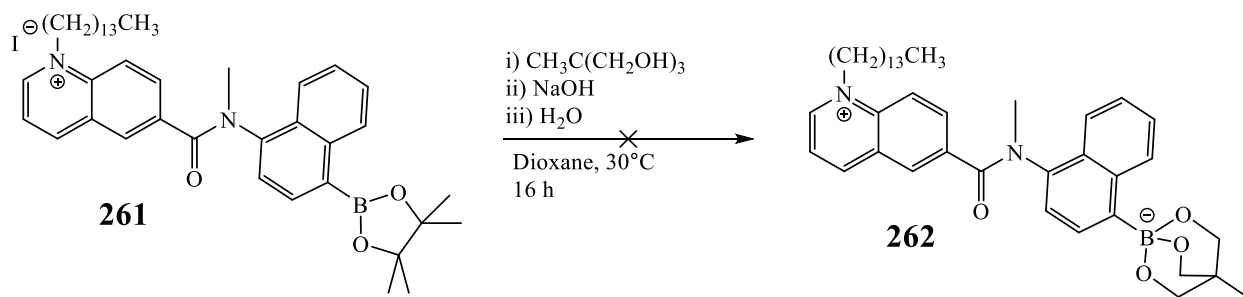
In order to better understand what had occurred, the mixture was purified on normal phase chromatography and ¹H NMR spectra were obtained. There were two singlets (ratio of 1:5) around 9.78 ppm, which could be the two rotamers corresponding to an amide N-H hydrogen. The only other peaks in the aromatic region were singlets of varying ratios around 8 ppm. All mass was accounted for but the spectrum most certainly did not contain the target **213**. An ESI-MS indicated mostly high molecular weight compounds (suggesting polymerization). Target **213** was not detected.



Scheme 2.45: Failed transesterification of **212** resulted in polymerization

2.7.2 Attempted Synthesis 4-Methyl-1-(4-(1-tetradecylquinolin-1-ium-6-carboxamido)naphthalen-1-yl)-2,6,7-trioxa-1-borabicyclo[2.2.2]octan-1-uide, **262**

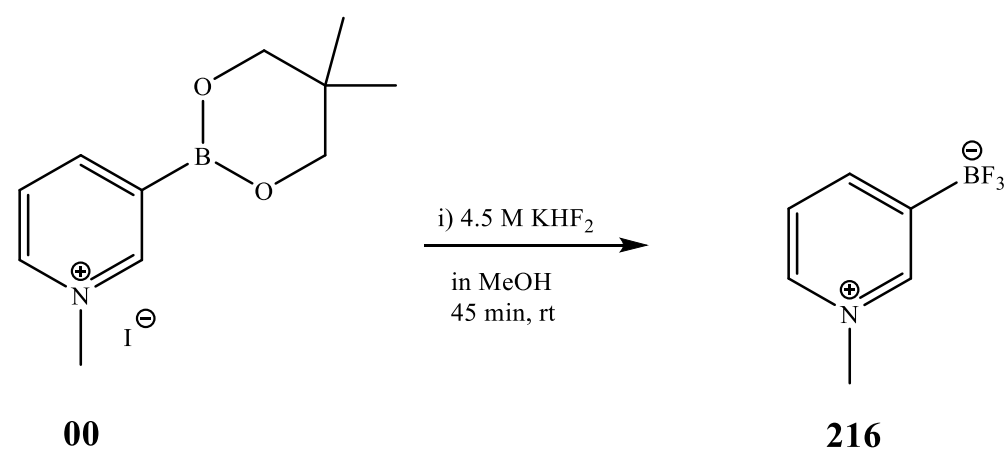
We believed the main problem with the transesterification attempt from Scheme 2.45 was that the reaction temperature had been too high. The presence of polymerization products suggested the temperature of subsequent reactions should be lower than 90°C. The reaction was run a second time at a lower temperature (30°C). In this reaction we used the *N*-methylated amide substrate **261**. This time, *both* the aromatic and quinolinium peaks were observed. No conclusion could be made from the complex NMR spectra as to whether the triolborate had been formed. Purification on normal phase chromatography was attempted. Approximately 24% of **261** was recovered. The remaining fractions gave spectra which could not be deciphered. This route was abandoned.



Scheme 2.46: Failed transesterification of **261**

2.7.3 Model, Trifluoro(1-methylpyridin-1-ium-3-yl)borate, 216

We thought that another way to access the triolborate could be through a multi-step procedure wherein a boronate ester was first converted to the trifluoroborate salt. The trifluoroborate salt could then be converted to the boronic acid. A triol could then be condensed onto the boronic acid to ultimately form the triolborate. We decided to test the concept by first converting a model boronate ester **00** to the trifluoroborate salt.¹¹⁸

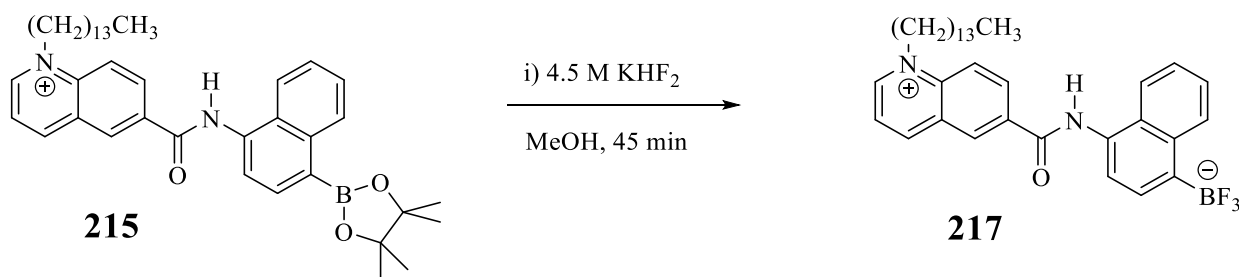


Scheme 2.47: Conversion of model substrate **00** to trifluoroborate zwitterion **216**

The conversion of the boronate ester **00** to trifluoroborate zwitterion **216** was confirmed by ¹H NMR. The key spectral features include disappearance of the boronate ester methylene singlet at 3.83 ppm (4H) and the boronate methyl singlet (6H), with subsequent upfield chemical shift of all aromatic peaks, which is consistent with expectations. The material was purified by precipitating the target by addition of ether to the acetone-filtrate of crude **216**. The crash-out gave a clear solid which had a yield of 71%.

2.7.4 Synthesis of Trifluoro(4-(1-tetradecylquinolin-1-ium-6-carboxamido)naphthalen-1-yl)borate, 217

Compound **217** was successfully synthesized from **215**.¹¹⁹ The material was purified by triturating the crude solid with hot diethyl ether, then hot acetone, and then hot methanol. We thought the hot methanol would remove the excess KHF_2 and side product KI , leaving a reasonable mass. However, we found our crude mass to be unexplainably large (135% yield!). We believed this to be due to some residual KI or KHF_2 . A ^1H NMR was used to confirm disappearance of the boronate ester **217**'s methyl singlet (12H) at 1.43 ppm and an ESI-MS confirmed target formation of **217**.



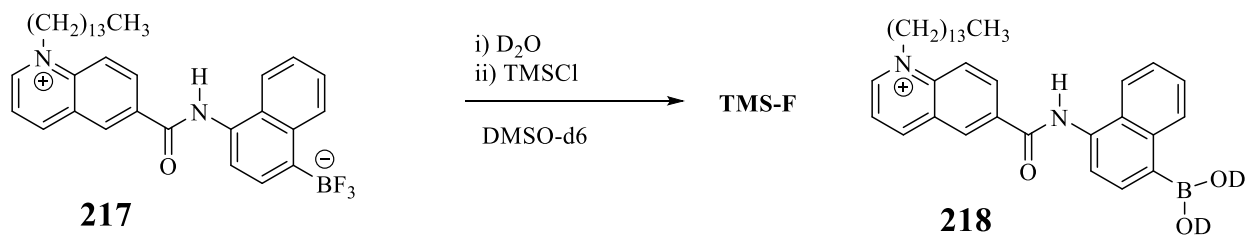
Scheme 2.48: Synthesis of trifluoroborate **217** via boronate ester **215**

Lastly, the ESI-MS in the negative mode showed presence of iodide anion, suggesting the continued presence of some KI . It is conceivable that – despite being a zwitterion – the fact that the donor is decoupled from the acceptor by the sigma-bridge, in addition to the naphthyl ring being out-of-plane with the acceptor quinoline, allows the acceptor's counteranion to be iodide and the donor's counter-cation to potassium. In this case, the percent yield would still be higher than theoretical (104%) suggesting something other than KI as being present such as KHF_2 .

Further purification was attempted by recrystallization from various solvents. The solvents attempted included THF, acetone, methanol, pyridine, acetonitrile, and DMF. As expected, the compound was insoluble in acetone and methanol. The compound was soluble in both pyridine and DMF. In THF and acetonitrile the compound was slightly soluble but failed to

give crystals. Instead, there was the formation of a very fine white sediment which could not be collected by filtration.

Aryl trifluoroborates can be converted to boronic acids in several ways. One way is a base promoted deprotection with alkali hydroxides.¹²⁰⁻¹²³ Another way is by first converting the trifluoroborate to the labile difluoroborane species with TMSCl¹²⁴ and then trapping the difluoroborane species under aqueous conditions in the presence of excess TMSCl.¹²⁵ Based on our previous failed transesterification reactions using base (which gave polymerized product), we wanted to avoid a base-promoted deprotection.



Scheme 2.49: ¹H NMR tube reaction to convert trifluoroborate **217** to boronic acid **218**.

We were interested in being able to convert trifluoroborate **217** to boronic acid **218** as outlined in Scheme 2.49. If we could convert **217** to the boronic acid, then it might be possible to condense a triol onto the boronic acid to achieve the elusive AQuANaB compound with the triolborate donor. We conducted a ¹H NMR experiment in DMSO-d₆ and monitored the ratio of TMSCl consumption (at 0.03 ppm) against formation of TMSF (at 0.19 ppm). The formation of TMSF is an indirect means of confirming that the starting substrate **217** is a trifluoroborate and to a lesser extent that the boronic acid **218** is being formed. We were interested in this method because we could also integrate the quinolinium methylene peak (2H) against the total amount of TMS-F which had been formed.

Three equivalents of TMSF should be formed at the completion of the reaction, thus giving a quinolinium methylene:TMSF ratio of 2:27 for the theoretical maximum. We found that within less than 5 minutes there was a quinolinium methylene to TMSF ratio of 2:60 and that after 100 minutes, the ratio of quinolinium methylene to TMSF was 2:90 (implying loss of the quinolinium alkyl tail or an extra fluoridation source as being present). Concomitantly, the TMSF:TMSCl ratio was 60:63 in less than 5 minutes, and after 100 minutes, the ratio was 90:55. It is difficult to account for why the TMSF ratio should be so much higher than the quinolinium methylene. We hypothesized that **217** contained some carryover KHF_2 .

We went back and tested the solubility of a small sample of pure KHF_2 and it was found to be insoluble in methanol. This means that our previous hypothesis about there being a possible carryover of excess KHF_2 reagent when we had synthesized **217** (which we had based on the 104% crude yield of **217**), was likely correct. The solubility behavior of KHF_2 agreed with *some* literature references.¹²⁶⁻¹²⁷ If there was excess KHF_2 remaining, then fluoridation of TMSCl would *also* result in TMSF. This finding helps make sense of the excessively high conversion of TMSF when TMSCl had been added.

Next, we tried a scaled-up version of the ^1H NMR reaction shown in Scheme 2.49. In this iteration of the hydrolysis of trifluoroborate **217** to boronic acid **218**, we used H_2O in place of D_2O . Furthermore, we used acetonitrile as our reaction solvent which more closely follows the literature procedure.¹²⁵ What followed was a very complicated effort to obtain some evidence of the target. This included extractions, filtrations, salting out, normal phase chromatography, and reverse phase chromatography. The ^1H NMR data was generally unhelpful. The aromatic regions (when we could see them) appeared to be wide unresolved peaks. As with virtually all other efforts to synthesize (but then purify) boronic acids during this project, the results seemed to give

more questions than answers. Ultimately, we decided to stop this portion of the project at having made at least *one* of the AQuANaB compounds. We successfully synthesized trifluoroborate **217**.

We attempted various methods of purification. We originally believed trituration to be enough, but it now seems possible that either some KI and KHF_2 potentially remained behind. This is due to the ESI-MS negative mode's presence of iodide. The presence of KHF_2 is indicated by the excess TMSF produced in the ^1H NMR experiment, which is indicative of an extra fluoridating source.

We had attempted method development for a purification using either normal phase or reversed phase chromatography. Normal phase silica resulted in the compound sticking to the plate. Reversed phase could not be run using methanol/water or ACN/water because the target was insoluble in these solvents. We considered dialysis but lengthy exposure to aqueous solutions would most certainly cause either hydrolysis or deborylation. We attempted to find a dialysis tubing, which would be compatible with the organic solvents needed to effect dissolution, but when we found such dialysis tubing, the molecular weight cut off was higher than the molecular weight of our target **217** or the tube membrane was not compatible with the organic solvents.

In summary, we have characterized **217** by $^1\text{H}/^{13}\text{C}$ NMR and ESI-MS. The NMR spectral data is consistent with target formation. The ESI-MS confirmed the target zwitterion in the positive mode as the cesium adduct $[\text{M} + \text{Cs}^+]^+$. However, there is also presence of the iodide anion in the negative mode which suggests KI is still present to some extent. The NMR tube

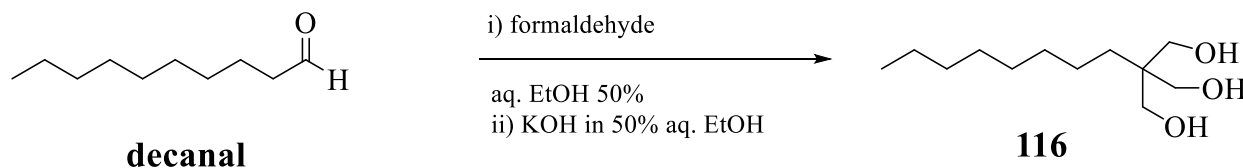
experiment in Scheme 2.49 indicated greater than three equivalents of TMSF having been produced as a by-product which indicates the presence of an extra fluoridating source (KHF_2).

2.8 Synthesis of Triol, E-Fragment

In the early model reactions, when we had found success in synthesizing the pyridinium triolborate **59** (Scheme 2.4), we went ahead and synthesized the E-Fragment. One of the commercially available triol E-Fragments, 2-(hydroxymethyl)-2-methylpropane-1,3-diol, was what we had used in the synthesis of **59**. However, we wanted to see what effect changing the alkyl length (of the pendant alkyl group on the triol) could have on controlling orientation on the Pockels-Langmuir trough. Thus, anticipating success, we synthesized a long-chain alkyl-triol E-Fragment, early in the project. This was very simple chemistry with straightforward purification.

2.8.1 Synthesis of 2-(Hydroxymethyl)-2-octylpropane-1,3-diol, **116**

Decanal was condensed onto formaldehyde to give triol **216** following an established literature procedure.¹²⁸ The crude product was purified by normal phase chromatography to give a white solid at a yield of 16%. The $^1\text{H}/^{13}\text{C}$ NMR matched the literature value. Material was further confirmed with FT-IR by disappearance of carbonyl stretch at 1730 cm^{-1} and appearance of alcohol-O-H stretch at 3361 cm^{-1} . The material was recrystallized from toluene and a melting point was obtained, mp = $73 - 74.5^\circ\text{C}$ (lit. $72 - 73^\circ\text{C}$).



Scheme 2.50: Tollens condensation of decanal onto formaldehyde to give triol **116**

2.9 Other Zwitterionic Donor- σ -Acceptors (D- σ -As)

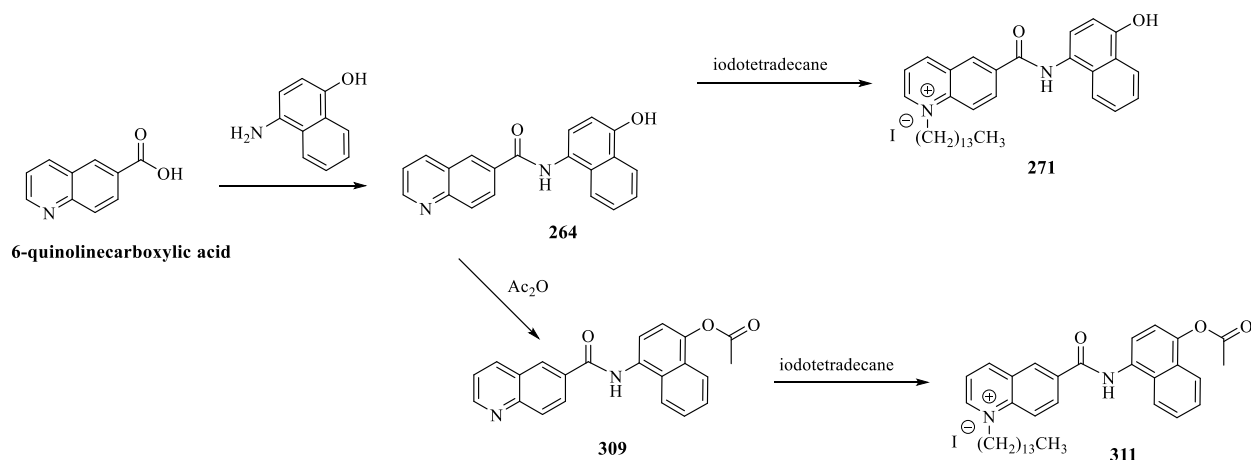
We wanted to continue to focus on zwitterionic D- σ -As by changing the donor type from the elusive boronate anions. The new D- σ -As we attempted to synthesize included aryl oxides, aryl carboxylate, aryl sulfonate and aryl thiolate as the donor anion. We also attempted several experiments in which we used 2-methylquinoline-6-carboxylic acid as an acceptor substrate in place of 6-quinoline carboxylic acid. We wanted to see if we could eliminate many of the side reactions which had consistently formed during these reactions. By using a 2-methyl substituted quinoline we believed that any unwanted reactivity, which previously might have occurred on the very electrophilic 2-position of the quinolinium, could be prevented. Furthermore, by using a 2-methyl substituted quinoline, we hoped to improve the poor solubility.

2.9.1 Aryl Oxide Donors

The aryl oxide donors proved to be one of the most difficult portions of this project. In Scheme 2.51, we attempted to obtain **264** by DCC coupling of 1-amino-4-naphthol to 6-quinoline carboxylic acid. The naphthol is commercially available as the hydrochloride salt in technical grade (90%). Prior to performing the reaction, we converted the amine salt to the free amine. However, there was always rapid decomposition of the free amine (as evidenced by TLC) over a short period of time (~20 min.).

We attempted to synthesize **264** by two DCC methods.^{97, 129} In the first method we converted the naphtholamine HCl to the free base and then directly used the organic extract for coupling to the carboxylic acid. In the second method we used the naphtholamine HCl salt directly, but added an excess of a bulky base (like DIPEA) to form the free naphtholamine in situ. In all cases, we obtained an extremely complex mixture of products which, despite multiple attempts, could never be purified by chromatography. Furthermore, in the method that started

with the pre-prepared free amine, we always detected the formation of aldehyde by the ^1H NMR chemical shift around 10 ppm.



Scheme 2.51: All routes using 1-amino-4-naphthol gave crude reaction mixtures which could not be purified.

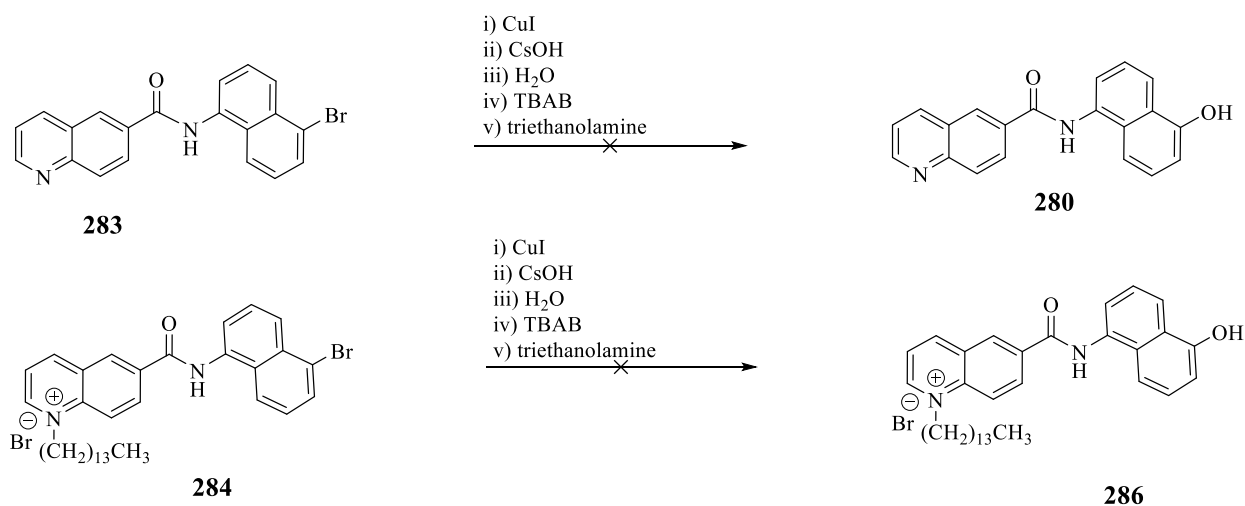
We attempted another route which involved first converting the carboxylic acid to the acid chloride, then introducing the naphtholamine. This method also failed to give a product which could be purified. We did not detect aldehyde formation when this route was used.

We thought that if **264** was present in the complex mixture, and we could protect the naphthol by *O*-acetylation, we would then be able to (hopefully) resolve *which* TLC spot had been the naphthol. Presumably, there should be a significant difference in R_f values for a naphthol compared to a naphthol acetate ester. The protection of a hydroxyl with an acetyl could also help purification on a column. We attempted this but could never obtain any pure **309**. At the very least, we were able to purify the complex mixture down to only two spots on TLC, but after a small amount of time, the chromatographed mixture would decompose into additional spots.

We attempted to *N*-alkylate the complex mixture of **264** directly to give **271**.^{112-113, 116, 130}

Although we could verify by ^1H NMR that *N*-alkylation had occurred, we simply could not find a way to purify the complex mixture. Similarly, we attempted *N*-alkylation of crude **309** but the mixture became impossibly complex when analyzed by TLC (10 or more spots!).

Next, we used two different substrates, **272** and **284**, and approached the synthesis from a different direction (Scheme 2.52). We attempted a copper-catalyzed hydroxylation¹³¹ of substrate **283** but the spectral data was inconclusive. We realized that there might be some chemistry going on between the quinoline nitrogen and the copper. As a result, we ran the hydroxylation reaction with a substrate **284** in which the quinoline had previously been *N*-alkylated, which would prevent a quinoline-copper complex. The reaction resulted in a significant mass of an insoluble black material which comprised the bulk of the mass.

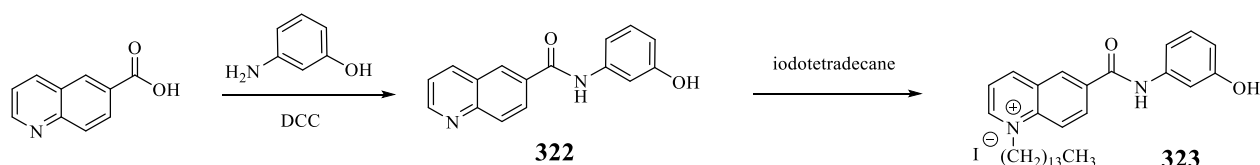


Scheme 2.52: Copper catalyzed hydroxylation failed to give targets.

At this point, we decided to go back to our original DCC coupling protocol,^{97, 129} but to begin with a simpler substrate, 1-amino-3-phenol, which was commercially available in high purity (unlike 1-amino-4-naphtholamine hydrochloride) and would have a much easier-to-interpret ^1H NMR spectrum including a singlet in the aromatic region. Furthermore, 1-amino-3-phenol is easier to work with (less labile) than 1-amino-4-naphtholamine hydrochloride. It is

believed the labile nature of the 1-amino-4-naphtholamine is due to an oxidative process wherein naphthoquinone is the end result. This is analogous to the well-studied oxidation behavior of p-aminophenols.¹³² When the amine and hydroxyl groups are para to each other, the rate of oxidation can be fast. When these two electron-donating groups are meta to each other, this rate can be slowed down.

In Scheme 2.53, substrate 1-amino-3-phenol was successfully coupled to 6-quinolinecarboxylic acid.^{97, 129} Although multiple spots were present on the crude TLC (indicating a complex mixture), there were fewer than had been visible when 1-amino-4-naphthol had been the substrate previously. This suggested that the 1,3-relationship of amino to hydroxyl resulted in a less labile product. We did a mild acid workup to remove any excess aminophenol and extracted the crude mixture. Purification was performed by recrystallization from EtOH and reluctantly gave powdery crystals (it took 2 days). Yield of the crystals was 12%. Material was characterized by melting point (mp = 238 - 240°C), FT-IR (amide N-H stretch at 3293 cm⁻¹), and ¹H/¹³C NMR.



Scheme 2.53: Successful amidation to obtain **322** and attempted *N*-alkylation to give **323**

Next, multiple attempts at *N*-alkylation with iodotetradecane were made.^{112-113, 116, 130} These were unsuccessful. There appeared to be some side reaction occurring, which we could not account for, but that predominated. We observed a large peak (likely a triplet) at 7.35 ppm and a

large singlet at 4.7 ppm in both reactions. Furthermore, these reactions seemed to be somehow producing an aldehyde by-product, indicated by a ^1H NMR signal at ~ 10 ppm.

The aldehyde by-product is very curious. Much time has been devoted to trying to extrapolate a reasonable mechanism on how such a reaction could occur. My hypothesis is that, first, the quinolinium is involved (either protonated quinoline or *N*-alkylated quinoline); second, that the 2-position (carbon α to the nitrogen) of the quinolinium is one of the reactive sites; and third, that presence of a hydroxyl (in this case aryl hydroxyl) is required.

There are several reactions which are *possibly* related to what is occurring here. One such named reaction is called the Minisci-Porta reaction which is a reaction used to alkylate or acylate an *N*-heterocycle at the 2-position.¹³³ An excellent review by Tauber and colleagues goes into detail on the nature of radical addition to cationic *N*-heterocycles.¹³⁴ A recent publication by Sen and Ghosh reports C2-alkylation of quinoline *N*-oxides with secondary and tertiary alcohols as the alkyl source.¹³⁵ The result of the C2-alkylation of quinoline *N*-oxide with a tertiary alcohol (*t*-BuOH in this case) gives, as a by-product, ketone, whereas, when a secondary alcohol is used, the by-product is an *aldehyde*!

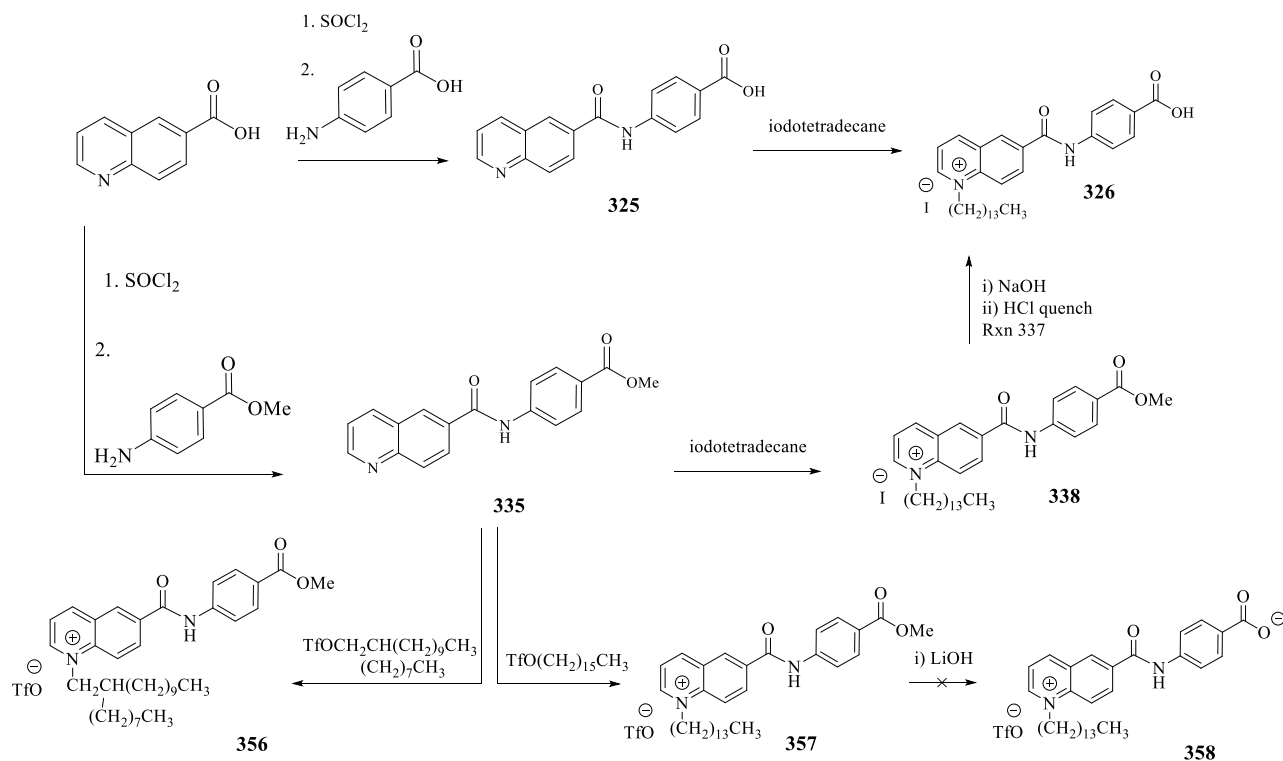
2.9.2 Aryl Carboxylate Donors

We next turned our focus to the syntheses of **D- σ -As** with aryl carboxylate donors. We began by coupling substrate *p*-aminobenzoic acid (PABA) or methyl-4-aminobenzoate to 6-quinoline carboxylic acid by the DCC route^{97, 129} or by a pre-conversion of 6-quinoline carboxylic acid to the acid chloride.¹⁰¹ Amide formation was followed by *N*-alkylation with either iodotetradecane or hexadecyl trifluoromethanesulfonate.^{109-110, 113, 127} If the initial substrate had been methyl-4-aminobenzoate, then various methods of deprotection to either carboxylic acid or carboxylate were attempted. These methods included base hydrolysis of the ester to the

carboxylic acid/carboxylate.¹³⁶⁻¹³⁷ Although we were able to obtain some of the intermediate targets outlined in Scheme 2.54 (vide infra), the final deprotection step (zwitterion formation) did not result in detectable formation of carboxylate product.

Our first synthesis used p-aminobenzoic acid (PABA) as the substrate. When the synthesis was attempted from the quinoline-6-carbonyl chloride (via SOCl_2 of 6-quinolinecarboxylic acid), we were able to obtain the target **325** in very low yields (6-9%). Purification was *extremely* problematic.

Normal phase chromatography served as a sort of pre-purification. It could remove some of the side products, but not all. At best, there would always elute two spots concomitantly. This behavior is similar to what was seen with the amphoteric quinoline-amide-naphthyl-boronate esters (see compound **173** in Figure 2.2.2.4).



Scheme 2.54: Multistep, multi-route synthetic attempts to obtain D- σ -As with a carboxylate donor.

Ultimately we were able to obtain **325** by recrystallization from acetone. If the material was directly recrystallized from acetone (no pre-purification), then the yield of crystals was 4%. If, instead, the crude material was passed through a silica column beforehand and *then* recrystallized from acetone, a yield of 9% could be obtained. However, in both instances there always remained a small percentage of triethylamine HCl as a contaminant, thus purity was not great (~90% purity). A melting point of the twice-recrystallized material was obtained and found to be 261 - 265°C. A TLC gave a single spot with no indication of 6-quinoline carboxylic acid nor PABA. ¹H NMR was used to confirm the complete disappearance of starting material PABA (d, 6.5 ppm).

Next, **325** was *N*-alkylated with iodotetradecane to give **326**.^{109-110, 113, 127} The crude sample was purified by fractional recrystallization from EtOH to give a white solid at 3% yield. Successful *N*-alkylation was confirmed by ¹H NMR in the form of a triplet at 5.14 ppm (2H), which we attribute to quinolinium methylene (α -nitrogen-methylene). An FT-IR was used to confirm the carboxylic acid's carbonyl and -O-H stretches at 1691 cm⁻¹ and 3167 cm⁻¹, respectively.

There are many reasons to explain the poor yield encountered on both steps (amidation and *N*-alkylation). We believed a better yield could be obtained if the substrate had been methyl 4-aminobenzoate (instead of PABA). The problem with the substrate PABA (and subsequent products obtained from amidation and *N*-alkylation, respectively) was likely due to the presence of the free carboxyl group.

The substrate methyl 4-aminobenzoate, when used to make an amide (from coupling to 6-quinoline carboxylic acid or the acid chloride) should have better solubility. Furthermore, the

amide obtained from substrate methyl 4-aminobenzoate **335** *wouldn't be amphoteric*, whereas the amide obtained from PABA, **325**, *is*. This would give us a better ability to clean up the crude mixture by employing mild acidic/basic washes.

In Scheme 2.54 (*vide supra*), we synthesized amide **337** by coupling methyl 4-aminobenzoate to quinoline-6-carbonyl chloride (via SOCl_2 of 6-quinolinecarboxylic acid).¹⁰¹ The crude residue was purified by recrystallization from EtOH to give a yield of 22% (mp = 213 - 215°C). The material was fully characterized by a battery of $^1\text{H}/^{13}\text{C}$ NMR, COSY, HSQC, and HMBC. All protons and carbons were assigned.

^1H NMR was used to confirm disappearance of substrate methyl 4-aminobenzoate's methyl singlet at 3.84 ppm (3H) and aromatic doublet at 6.6 ppm (2H). Furthermore, the appearance of two new aromatic peaks at 7.8 ppm (2H) and 8.1 ppm (2H) were consistent with a coupling event to form amide. An FT-IR was used to confirm the amide -N-H stretch, amide carbonyl stretch, and an ester carbonyl stretch at 3336 cm^{-1} , 1663 cm^{-1} and 1710 cm^{-1} respectively. Lastly, when methyl 4-aminobenzoate (instead of PABA) is used as the substrate, the yield – while still poor – was four-fold higher for this step.

Next, we *N*-alkylated **335** to obtain quinolinium **338**.^{109-110, 113, 127} The crude material was purified by column chromatography to give a yield of 11%. Successful *N*-alkylation was confirmed by ^1H NMR observation of a triplet at 5.0 ppm (2H). Furthermore, there was an overall downfield shift of all aromatic peaks, which is consistent with the formation of the electron deficient quinolinium. For this step, as compared to the PABA derived analogue, the percent yield was *also* four-fold higher.

We next attempted a base hydrolysis of ester **338** to carboxylic acid **326** with NaOH. The ^1H NMR only showed faint traces of aromatic peaks while the singlet from the methyl ester was

still visible at 3.86 ppm. There was a large peak (doublet or triplet) at 8.0 ppm which is similar to formic acid. A similar peak at 7.97 ppm was seen when quinoline **325** was *N*-alkylated to quinolinium **326**. We could not account for these results.

Next, in Scheme 2.54, we used hexadecyl trifluoromethanesulfonate to *N*-alkylate **335** to **357**.¹¹⁰ Although the substrate **335** is only *slightly* soluble in DCM – and initially the reaction appears as a suspension – as the reaction progressed, the mixture turned to a pale-yellow tinted solution. In short, the target quinolinium triflate **335** shows *much* greater solubility characteristics than the analogue quinolinium iodide **338**. Furthermore, purification was simple. We simply triturated the mixture with hexanes to remove any remaining alkylating reagent. The yield of the tan solid was 75% (~ 90 % purity). Product was characterized by ¹H/¹³C NMR and showed a triplet at 5.14 ppm (2H) consistent with formation of quinolinium formation. FT-IR was used to confirm the amide N-H stretch, amide carbonyl stretch, and ester carbonyl stretch at 3380 cm⁻¹, 1731 cm⁻¹, and 1678 cm⁻¹. Furthermore, ESI-MS was used to confirm both the quinolinium cation and triflate anion in the positive and negative modes, respectively.

Next, hydrolysis (with LiOH) of ester **357** to carboxylate **358** was attempted.¹³⁷⁻¹³⁸ This was unsuccessful. An ESI-MS spectrum was obtained. The target's molecular ion peak was not present. We decided to probe the problem by a ¹H NMR experiment. We monitored the disappearance of the methyl singlet over time. A negative control was included using the same reaction conditions but absent the LiOH.

By using ¹H NMR, we were able to verify the disappearance of the methyl singlet at 4 ppm with subsequent appearance of two new doublets in the aromatic region at 8.0 ppm and 7.7 ppm. The other aromatic peaks were minor. We believe a bond-breaking event occurred at either the amide-nitrogen to carbonyl-carbon bond or the carbonyl-carbon to 6-carbon on the

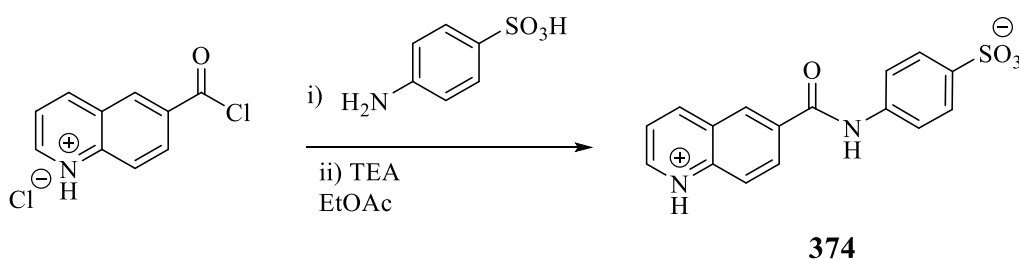
quinolinium. In either scenario, this would give a 1,4-disubstituted aromatic ring which would give rise to two doublets such as those we have observed in the aromatic region. It leads us to conclude that while deprotection of the methyl ester occurred, so did the scission of the two ring fragments. While the former is good, the latter is not. We abandoned this deprotection route.

Since we had found improved solubility characteristics when using alkyl triflates to form quinolinium triflate salts (as opposed to alkyl iodides to form quinolinium iodide salts), we wanted to see the effect of using a branched chain alkyl triflate. As a result, in Scheme 2.54 we *N*-alkylated quinoline **335** with 2-octadodecyl trifluoromethanesulfonate to form quinolinium triflate **356**. Unlike quinolinium triflate **357**, which could be triturated with hexanes to purify, the branched-chain alkyl quinolinium triflate **356** was too soluble to be able to separate excess alkylating reagent with hexanes. Trituration with hexanes resulted in an unfilterable gummy emulsion.

Ultimately, **356** could be purified by normal phase chromatography but a poor yield of 5% was obtained. Confirmation of target formation was made by ¹H NMR. The key spectral features, which indicate quinolinium formation, were a doublet at 4.79 ppm (2H), a multiplet at 2.07 ppm (1H), and an overall downfield shift of the aromatic protons. A COSY was obtained to correlate the aforementioned doublet and multiplet to each other. A ¹³C NMR showed a peak at 63.3 ppm, which was attributed to the quinolinium methylene (α -nitrogen-carbon). Although we did not pursue further studies with **356** (low yield and 2-octadodecyl trifluoromethanesulfonate was too labile to be of practical use), we were able to show that the solubility was much improved over that of the *n*-alkyl analogue.

2.9.3 Aryl Sulfonate Donor

We synthesized the zwitterionic **374** bearing an aryl sulfonate donor by coupling 4-aminobenzenesulfonic acid to the *in situ* prepared acid chloride of 6-quinoline carboxylic acid (via SOCl_2).¹³⁹ We found purification by normal phase chromatography to be insufficient. Instead, the water soluble **374** was washed with DCM at pH = 8 and then at pH = 3.5. We tried to salt-out **374** by addition of NaCl, but surprisingly the aqueous solubility of **374** is greater than that of NaCl and the target **374** simply would not crash out of solution.



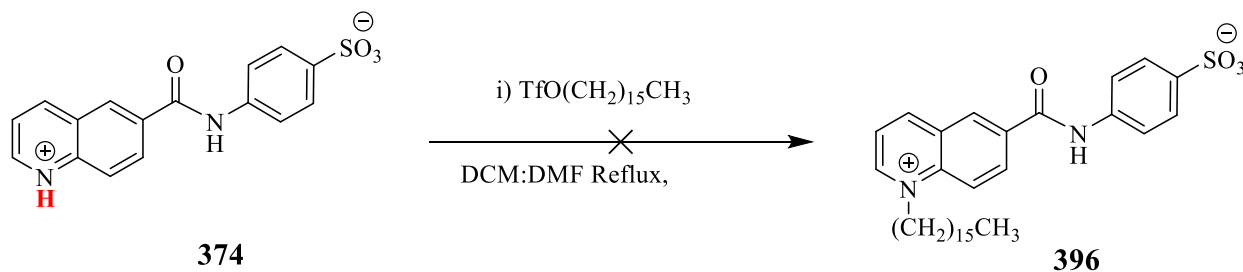
Scheme 2.55: Synthesis of sulfonate-donor containing **374**

We believed we could take advantage of this characteristic by performing a Soxhlet extraction. The aqueous solution was concentrated to dryness. We pulverized all of the salt mixtures with a mortar-and-pestle and then added this to a Soxhlet cup. We first attempted the Soxhlet extraction with DCM for four days but obtained only a trace amount of mass. Next, we attempted to use ACN as the extraction solvent but after 2 days, we again obtained only a trace amount of mass. Lastly, we tried EtOH and found it to be an excellent solvent for the Soxhlet extraction of **374**.

Next, a ^1H NMR of the extracted product was obtained in D_2O and another was obtained in DMSO-d_6 . In both cases the ^1H NMR spectral data was difficult to explain. The integration values in the aromatic region suggested the possible presence of rotamers. For characterization,

we turned to ESI-MS and were able to confirm presence of the molecular ion peak in the negative mode.

Next, in Scheme 2.56 we attempted to *N*-alkylate **374** to quinolinium triflate **396**. However, at the time of the attempted *N*-alkylation, we had mistakenly overlooked our pre-Soxhlet work-up procedure, which was acidification of the aqueous layer. Therefore, when we set up the reaction (*N*-alkylation of **374** to **396**), we did not account for the fact that what we had believed to be a “quinoline” was in fact a *quinolinium*. As a result, when we attempted to *N*-alkylate **374**, the reaction didn't proceed (due to protonated nitrogen). At the time we did not realize *why* the reaction had failed. With this new evidence, we now believe this reaction could be successful with the addition of some bulky, non-nucleophilic base. By deprotonating the quinolinium to the quinoline, the reaction should proceed.



Scheme 2.56: Attempted *N*-alkylation of zwitterionic **374** to zwitterion **396**

2.9.4 Aryl Thiolate Donor

Prior to attempting the synthesis of **D- σ -As** containing an aryl thiolate donor we wanted to explore the possibility of using an analogue of the 6-quinoline carboxylic acid substrate. We have previously mentioned that one of the most electrophilic positions of *N*-heterocycles is the carbon alpha to the nitrogen (the other is the 4-position). When an *N*-heterocycle (quinoline) is either protonated or *N*-alkylated (to form quinolinium), the electrophilicity of the 2-position carbon is dramatically increased. This increase in electrophilicity can potentially result in side

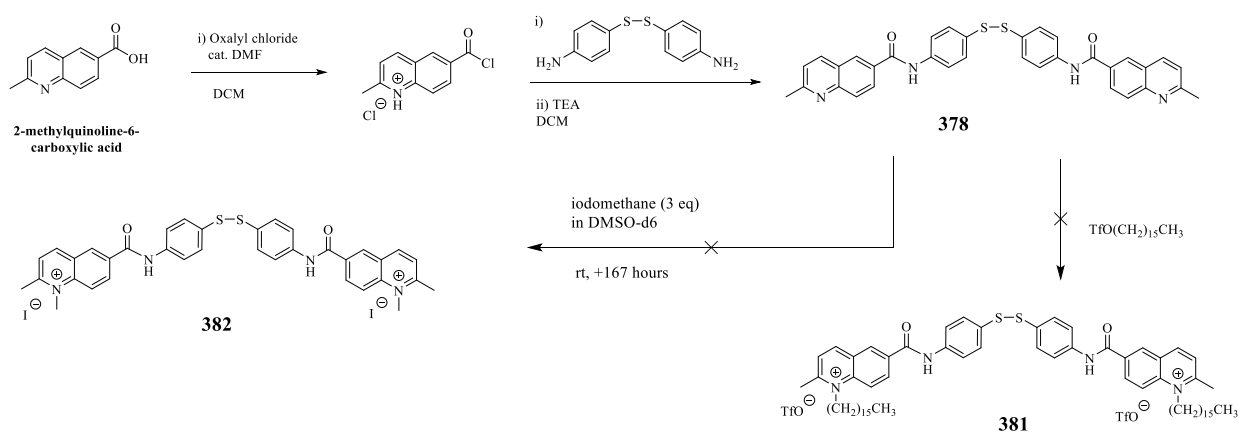
reactions (see Section 2.9.1, Aryl Oxides). If the side reactions are due to the 2-position carbon on the quinoline (or quinolinium), then perhaps blocking that position by using a quinoline carboxylic acid substrate with an alkyl group in the 2-position (we used 2-methylquinoline-6-carboxylic acid) will prevent some side reactions.

Previously, when we had attempted synthesis of **D- σ -As** containing aryl oxide donors (Section 2.9.1), we found 1-amino-4-naphtholamine to be highly labile. We attributed this problem to the 1,4-position of the two EDG groups amine and hydroxyl, respectively, which are likely to oxidize to the naphthoquinone, in the same way p-aminophenol is known to oxidize to benzoquinone.¹³² We found that m-aminophenols were much less labile (and amenable to amide formation) but that the *N*-alkylation step of quinoline **322** to quinolinium **323** (Scheme 2.53) resulted in *many* side reactions occurring (we detected formation of aldehyde as one of the side products). Since aryl thiolates are analogous to aryl oxides, it is reasonable to expect that a similar behavior could potentially occur. We hoped to preempt such a situation by using the substrate 4-aminophenyl disulfide. As a disulfide (as opposed to thiol), there is no reactive free-hydrogen available, which effectively results in the sulfur-functionality being protected until, we hoped, the final step.

In Scheme 2.57, we converted 2-methylquinoline-6-carboxylic acid to the acid chloride with the reagent oxalyl chloride¹⁴⁰ (previously we use the SOCl₂ route). This labile intermediate was always used directly without characterization. The dimer amide **378** was obtained by coupling two equivalents of 4-aminophenyl disulfide to the acid chloride.¹⁴¹ We confirmed the complete disappearance of the 4-aminophenyl disulfide by TLC. We found that at pH = 8, the target **378** would remain behind in the aqueous layer and would not go into the organic DCM layer. We spent a significant amount of time in purification method development. By using a

mixture of IPA:water, we could recrystallize the material *but* there was always triethylamine HCl at about 1-2 equivalents present. The crude 218 - 228°C melting point reflected the impurity.

We found we could get a 69% yield if purified by normal phase chromatography but would see a few small broad peaks in the ^1H NMR aromatic region which represented about 10% by integration. If purified on an alumina column, the recovery was poor (despite using highly polar solvent to force out the remaining adsorbate) and purity was worse (more triethylamine HCl was present) than when the material had been purified by silica.



Scheme 2.57: Amidation of 4-aminophenyl disulfide to give **378** with *N*-alkylation attempts.

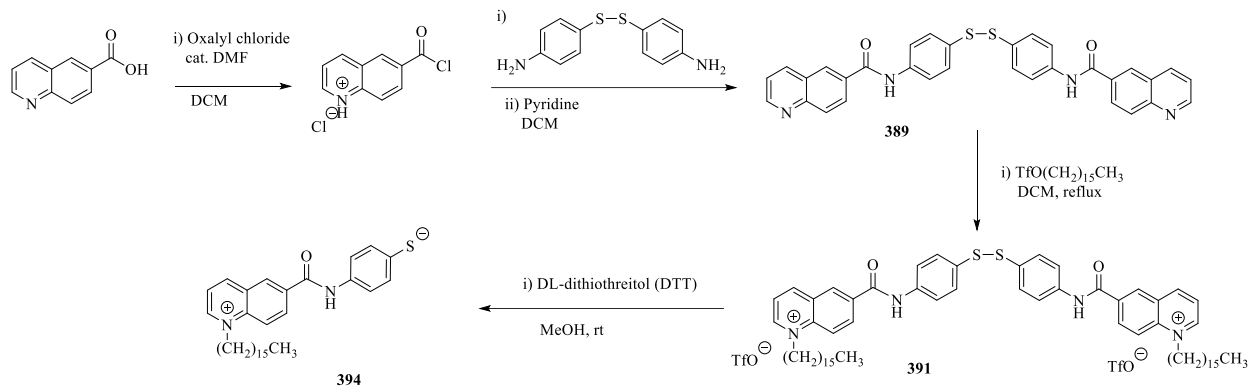
We characterized the target **378** by the ^1H NMR peak at 10.62 ppm, which we attribute to the amide -N-H proton. We also obtained a ^{13}C NMR and then an HMBC. From the combined NMR spectra, culminating in the HMBC, we were able to correlate the proton doublet at 7.55 ppm (2H) (from the donor phenyl) to the acceptor quinoline carbonyl-carbon at 165.3 ppm. This indicates that the two fragments (acid chloride + amine) were coupled to form the amide. Lastly, the molecular ion peak was confirmed by ESI-MS. We were satisfied we had obtained target **378**.

We next attempted to *N*-alkylate **378** to form quinolinium triflate **381** and then quinolinium iodide **382**.¹¹⁰ We found that *N*-alkylation of the 2-methyl substituted quinoline **378**

could not be achieved under the reaction conditions we used. We changed the conditions by increasing the alkylating reagent hexadecyl trifluoromethanesulfonate by four-fold, but we could not detect *any* evidence, through either ^1H NMR or ESI-MS, that *N*-alkylation had occurred.

We performed a ^1H NMR experiment where we used one equivalent of **378** and three equivalents of iodomethane in DMSO-d_6 and ran the reaction at room temperature for 7 days. This type of reaction is easily monitored by NMR as the iodomethane-methyl singlet at 2.18 ppm (3H) can be monitored against the disappearance of the quinoline 2-methyl substituent at 2.72 ppm (3H) and – we had hoped – a singlet near the 4.3 ppm (3H) region. However, this never occurred. The iodomethane was consumed over time while an unknown singlet at 3.84 ppm was formed. Interestingly, the small amount of water present in the NMR solvent was *also* consumed over time. Nevertheless, we never saw any evidence of *N*-alkylation having occurred. It is likely that the steric bulk of the 2-methyl substituent is blocking *N*-alkylation.

In Scheme 2.58 (vide infra), we returned to using 6-quinolinecarboxylic acid for our substrate (in lieu of 2-methyl-6-quinolinecarboxylic acid). We converted the carboxylic acid to the acid chloride by the oxalyl chloride route.¹⁴⁰ The acid chloride was coupled to 4-amino disulfide to give the dimer amide **389**.¹⁴¹ Due to the fact that the previous dimer amide **378** (Scheme 2.57) synthesis would always be contaminated with triethylamine HCl, this time we wanted to prevent that possibility and so we used pyridine (instead of triethylamine) as our organic base.



Scheme 2.58: Amidation of 4-aminophenyl disulfide to give **389** followed by *N*-alkylation to give **391** and then attempted disulfide cleavage.

The purification of **389** was successful. Initially, the crude **389** had a very undesirable gummy texture. We attempted filtration with washings using hexanes and toluene, but the stickiness would not lessen. The gummy mess seemed hygroscopic in that the longer it was exposed to the air, the wetter and gummier it seemed to become. We transferred the sticky mess to a separatory funnel and diluted with DCM and then added half-saturated NaHCO₃ until the pH = 8. We noted that there was a large amount of undissolved solid in the DCM layer. We expected it might be the target yet we were careful not to disturb it as we performed extractions with DCM (5X). The solid, however, could not be extracted with DCM. If it was the target **389** it would mean that at pH = 8, it is both water insoluble and DCM insoluble.

As a result, we were left with the pH = 8 aqueous layer *plus* a large amount of undissolved solid. Perplexed, we acidified the mixture with HCl until pH ~1.5. Fortunately, the mixture dissolved to give a yellow-tinted solution. This told us we were likely on the right track, that the dimer amide **389** should be – when protonated to the diacid HCl salt – soluble in the aqueous layer. We then washed the aqueous layer with DCM (5X) to further clean up the mixture.

Previously, during the synthesis of an amide with an aryl sulfonate donor **374** (Scheme 2.55), we had begun to experiment with the technique of salting out. In *that* example, we believe salting out the zwitterionic **374** was unsuccessful due to the higher aqueous solubility of sulfonates over sodium chloride. Our working hypothesis is informed by application of the Hofmeister series.

Recently, the solubility trends of salts in aqueous solutions has received renewed interest in the form of several highly informative publications. Hyde and coworkers at the Department of Process Chemistry at Merck & Co. Inc. propose some general principles and strategies for salting out based on the Hofmeister series.¹⁴²

The Hofmeister series, as originally defined, is the ordering of ions by their ability to affect the solubility of proteins in water. This has been extended to organic molecules which possess water solubility. In the Hofmeister series' approach to effect precipitation of the target from the aqueous solution, a salt of greater aqueous solubility is added to the aqueous solution, which then results in the precipitation of the target.

Hill and Sweeney of AstraZeneca PLC and the University of Huddersfield, respectively, have laid out an impressive 20-step systematic approach to the work-up of hydrophilic targets.¹⁴³ We have drawn upon both of these publications, successfully applying them to the purification of target **389**.

As a result (of the aforementioned publications) we decided to raise the pH *by using solid sodium bicarbonate*. We wanted to avoid the addition of any further water. At a pH = 6.5 – 7, the solution began to lose its color and solid began to crash out. The pK_a of quinolinium HCl is approximately 4.5 – 5. Thus, it makes sense that we would see solid precipitated (almost

completely) at a pH 2-units higher than the pK_a value. However, we believe there must have been some slight solubility of the now-deprotonated **389**. As a result, we began the addition of solid NaCl (followed by stirring until complete dissolution of NaCl) to salt out any remaining **389**.

After multiple additions of solid NaCl (followed by complete dissolution), we could detect no further pale-yellow color to the solution. Furthermore, we observed that we had obtained additional solid **389**, which we would not have otherwise obtained by simple control of pH alone (**389** is likely slightly hydrophilic). Finally, we filtered the mixture over a Büchner funnel and collected the solid.

The solid was repeatedly dried using a rotary evaporation apparatus in the presence of toluene (to effect azeotropic removal of water). A tan powdery solid was obtained which was of high purity and required no chromatography. The material was characterized by ¹H NMR. The key spectral features were the amide -N-H at 10.78 ppm and the two phenyl doublets (from the disulfide donor) at 7.92 ppm and 7.56 ppm. The amide -N-H singlet to phenyl doublets should be at a ratio of 2:8, respectively. This was indeed the case.

The integration of all peaks was *surprisingly* straightforward (no rotamers or contaminants). In particular, the splitting pattern of all peaks was easily attributed to the target **389**. The ¹³C NMR was perfectly clean and showed 14 distinct peaks in the aromatic region (which represent 28 carbons because this is a dimer). No further characterization was made.

Next, we *N*-alkylated **389** with hexadecyl trifluoromethanesulfonate to give the dimer quinolinium triflate salt by updating a previously used procedure.¹¹⁰ When we had previously *N*-alkylated quinoline-containing amides, they were all monomers. They could be obtained by

reacting for 2 days at room temperature (using hexadecyl trifluoromethanesulfonate) in DCM. However, the dimer **389** would only give poor conversion (8% to monoalkylated dimer) when reacted at room temperature for one day. Thus, we held the reaction mixture at reflux for 5 days and the conversion had only reached 69%. We added more alkylating reagent and allowed the mixture to react further. However, after 10 *additional* days, no further reaction seemed to be occurring.

We attempted purification by triturating off the excess alkylating reagent with hexanes (as we had done for other examples), but the mixture took an extremely long time to separate. We thought we might acidify the mixture with dilute HCl (to remove unreacted **389**) and extract with DCM. This resulted in an inseparable emulsion. It is possible that monoalkylated dimers, which have one free quinoline nitrogen, become protonated and begin to act as a sort of detergent. The protonated quinolinium (of the monoalkylated dimer) likely has strong interactions with the water whereas the *N*-alkylated portion of the molecule's alkyl tail is interacting with the organic solvent, resulting in an emulsion.

We found that making the mixture strongly basic with NaOH would rapidly break the emulsion and a clean separation was rapid. After multiple DCM extractions, the organic extracts were chromatographed on neutral alumina to give a mixture of mono and di-alkylated products. We used ¹H NMR to confirm a triplet at 5.09 ppm (which for the dialkylated dimer represents 4H), which we attribute to the quinolinium methylene (α -nitrogen-methylene). We obtained an ESI-MS and confirmed the presence of the target molecular ion of the dialkylated quinolinium triflate **391**.

Next, in Scheme 2.58 we attempted to reduce the disulfide bond of dimer **391** to thiolate **394** by using DL-dithiothreitol following an established literature procedure wherein a similar substrate was used.¹⁴¹ We worked up the mixture but the ¹H NMR was simply too complicated to draw a conclusion. We obtained an ESI-MS and believe it to be evidence of the zwitterionic target **394**. The isotopic distribution is as expected but the accuracy of the m/z is not 0.003 accurate.

As a result, we ran the reaction a second time. If there had been successful reduction of the disulfide, then there should be an upfield shift in the aromatic region of the ¹H NMR spectrum. Most notably we would expect the greatest upfield movement of the doublet on the donor phenyl-ring bearing the sulfide. However, the spectrum was simply too complex to draw a conclusion. A large part of the problem here is the lack of purity of the disulfide substrate **391**. Thus, in light of the ESI-MS spectrum – which shows (we believe) the successful formation of zwitterionic target **394** – some additional time spent at purification method-development seems warranted.

2.10 Conclusion

In concluding the syntheses of zwitterionic Donor-σ-Acceptors (D-σ-As) portion of this project, we have successfully synthesized the trifluoroborate-containing zwitterionic D-σ-A **217**, which contains the trifluoroborate donor (so called AQuANaB compound). We attempted the syntheses of zwitterionic D-σ-As, which contain the following donors: naphthoxide, phenoxide, aryl carboxylate, aryl sulfonate, and aryl thiolate. Of these donors, we believe that the aryl sulfonate and the aryl thiolate still warrant further efforts.

We found we were able to purify sulfonate **374** by Soxhlet extraction. Although our *N*-alkylation failed, we have laid out the reason why in Section 2.9.3. If *N*-alkylation can be successfully achieved (we believe it can be), that would be the final synthetic step to obtain the target **396**.

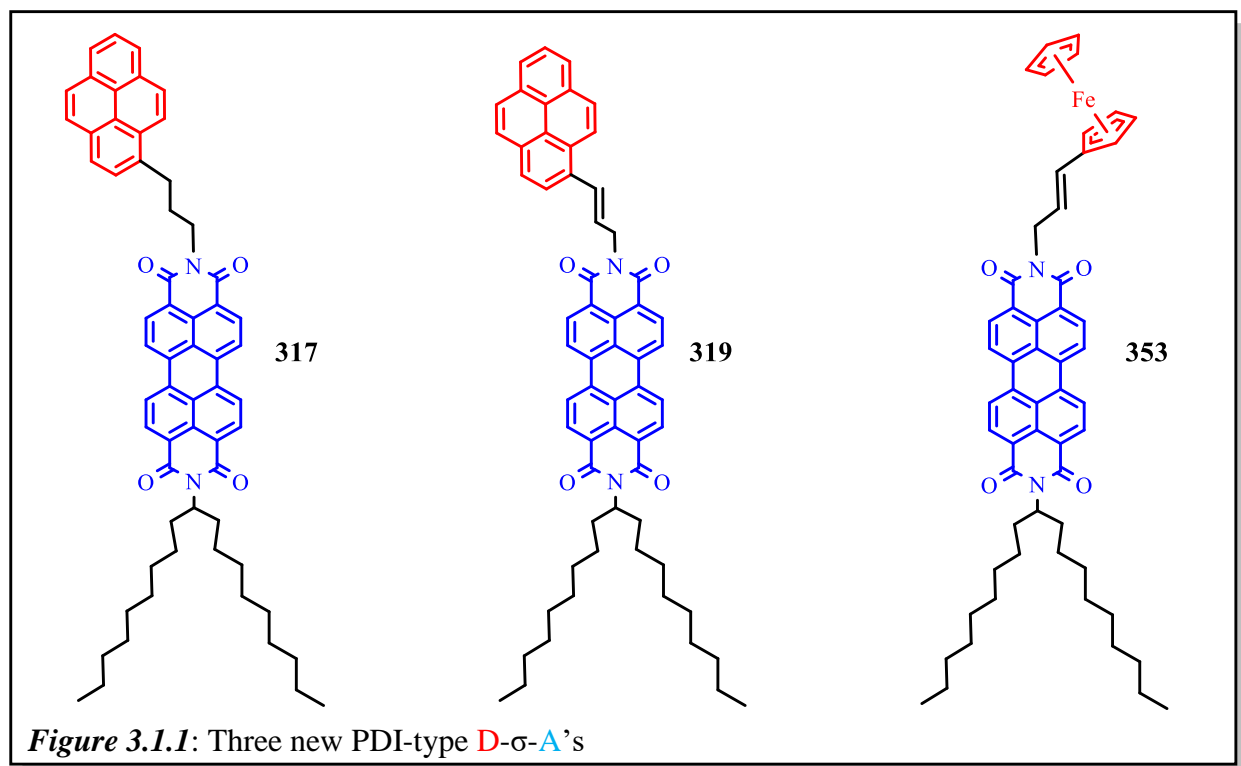
The synthesis of the aryl thiolate – which begins with 4-aminophenyl disulfide as the substrate to form dimer amide disulfide **389** – is especially interesting. It was the first amide we were able to purify through a very simple salting-out procedure based on the Hofmeister series. The ability to produce pure intermediates has been very difficult on this project but in this example, once we figured out how to employ this technique, it turned out to be simpler than recrystallization or even chromatography.

Although we were able to di-alkylate the amide dimer **389** to the quinolinium triflate dimer **391**, there remains some further work to develop a good purification method. We have shown – through ESI-MS – what we believe to be evidence of the successful DTT reduction of **391** to obtain the zwitterionic target **394**. However, that will also likely require some purification method development before a neat sample can be procured for testing as a potential D-σ-A.

CHAPTER 3: NEW PERYLENE DIIMIDE DONOR- σ -ACCEPTOR COMPOUNDS

3.1 The Synthesis of Perylene Diimide Donor- σ -Acceptors (D- σ -A's)

This project portion of the dissertation encompasses the syntheses of various perylene diimide donor- σ -A's. Three new perylene diimides (PDIs) were synthesized which differed in either donor type and/or sigma bridge type. The three PDIs synthesized are shown below in Figure 3.1.1. The first donor used was pyrene with a three-carbon aliphatic bridge. The second donor was also pyrene, but with an α,β -unsaturated three-carbon bridge. The third donor was ferrocene with an α,β -unsaturated three carbon bridge.

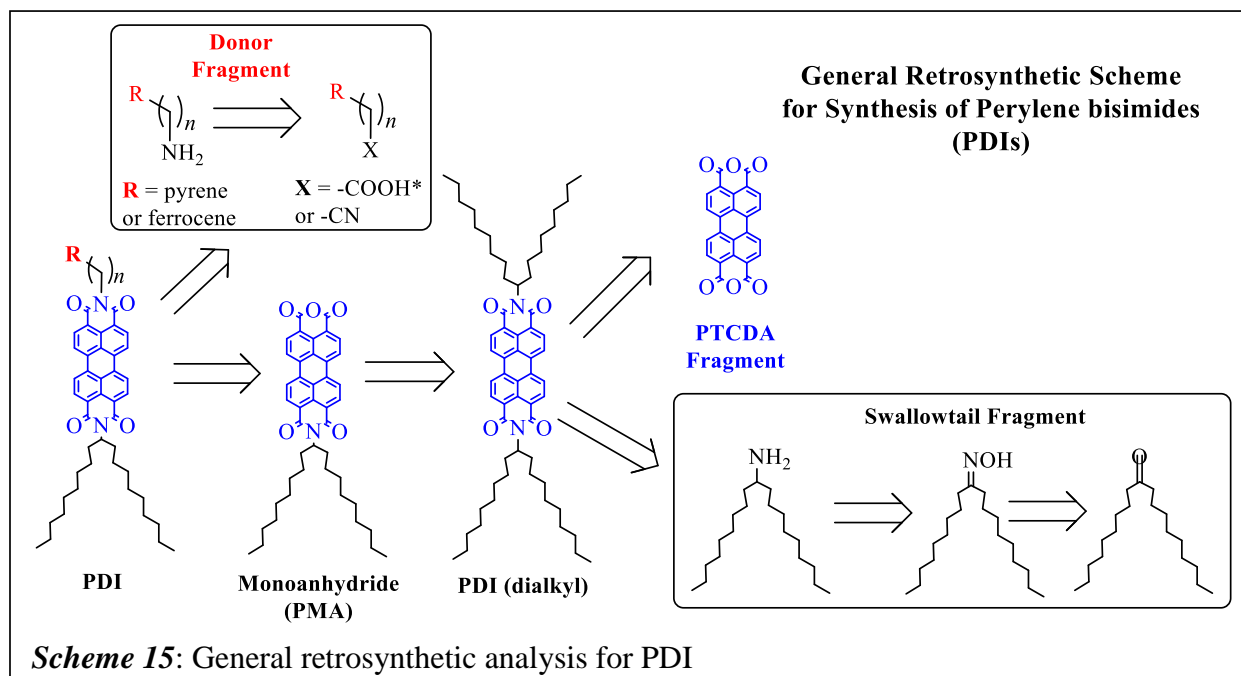


The rationale for selection of these targets was based on previously studied analogues in this laboratory. In those previous studies the donors are pyrene or ferrocene and the acceptor is perylene diimide (Figure 1.7.2).^{31, 47} Those analogues varied the length of the alkyl sigma-bridge (two carbons and four carbons). Our targets have three-carbon sigma-bridges. Whereas the previous studies focus solely on aliphatic sigma bridges, our work included allyl bridges, which should be less flexible and should form better monolayers. It may also be the case that the allyl bridges result in faster tunneling of donor to acceptor than does the aliphatic sigma bridges.

3.2 General Retrosynthetic Scheme for Synthesis of Perylene Diimides (PDIs)

The general retrosynthetic approach (Scheme 15) applied in the syntheses of our PDIs is based on a convergent synthesis comprised of three fragments. The swallowtail fragment synthesis begins from the commercially available aliphatic ketone 10-nonadecanone. The 10-nonadecanone is converted to the oxime via hydroxylamine condensation. The oxime is reduced to the amine via Red-Al. The swallowtail amine fragment is then condensed onto the commercially available perylene tetracarboxylic dianhydride (PTCDA) to form the bis-alkylated intermediate PDI. The bis-alkylated PDI is hydrolyzed via basic conditions to give the mono-alkylated imide anhydride.

The donor fragment can begin from a variety of starting materials which will be covered fully in further sections. In Scheme 15, **R** = either pyrene or ferrocene and **X** = either a carboxylic acid or a cyano group. These substrates can be reacted in various ways to give the donor fragment amine. In the final step, the donor amine is condensed onto the monoanhydride to give the target PDI **D-σ-A**.

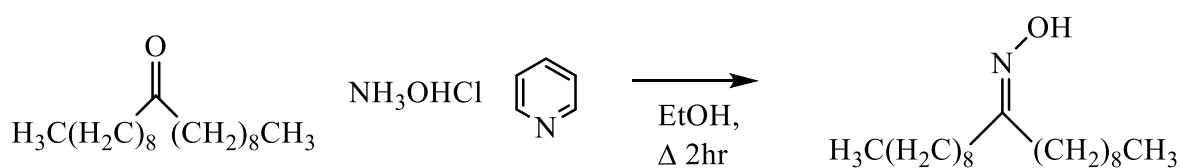


3.3 Synthesis of the Swallowtail Fragment

The synthesis of the swallowtail fragment was easily achieved in two steps. 10-Nonadecanone was converted to the oxime. The oxime was then reduced to the amine. Minimal purification on either step was required.

3.3.1 Synthesis of 10-Nonadecanone Oxime via 10-Nonadecanone

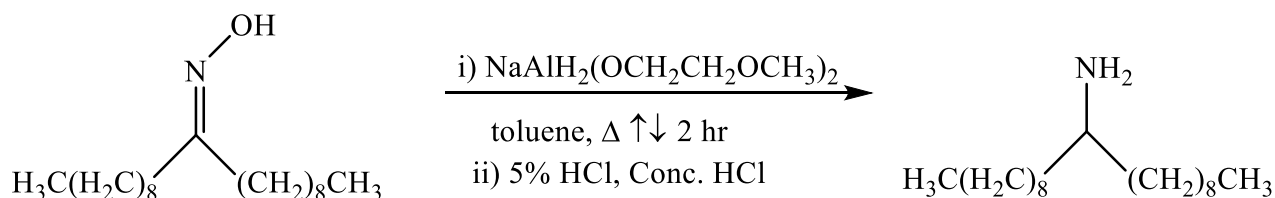
10-Nonadecanone was converted to the oxime by condensation of hydroxylamine HCl under basic conditions following an established procedure.^{13, 57} Conversion from ketone to oxime was easily followed via TLC using Hanessian's Stain (CAM). NMR and FTIR were consistent with literature values. Crude yield = 99%.



Scheme 16: Synthesis of 10-nonadecanone oxime

3.3.2 Synthesis of 10-Nonadecanamine via 10-Nonadecanone Oxime

10-Nonadecanone oxime was reduced to the amine via excess Red-Al (Scheme 17) following the aforementioned established procedure.^{13, 57} It was sufficient to monitor reaction conversion via TLC using CAM. ¹H NMR was also used to confirm the presence of the methine hydrogen (~ 2.97 ppm, multiplet), which is on the α -carbon to the amine nitrogen, and disappearance of oxime starting material (2.33 ppm, triplet). The target amine was initially a golden liquid, which formed light yellow golden crystals if left under hi-vac overnight.



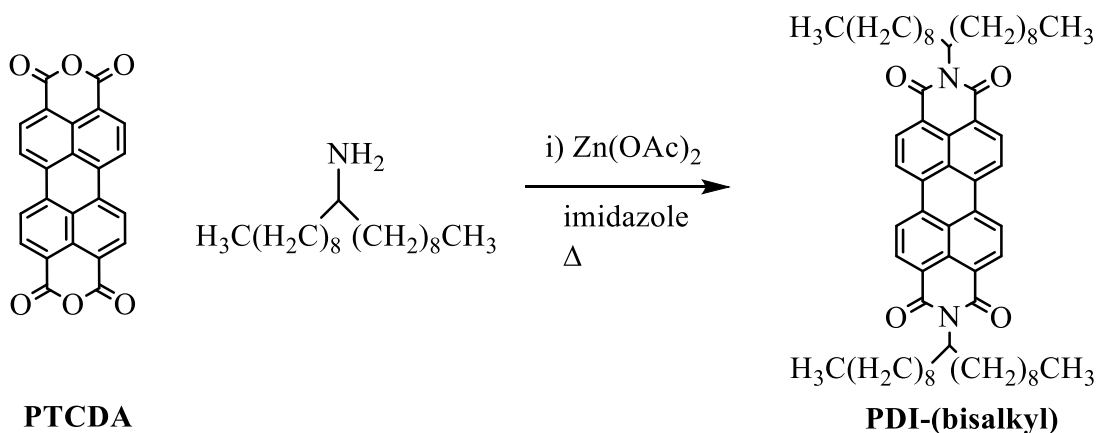
Scheme 17: Oxime reduction to amine via Red-Al.

3.4 Synthesis of the Perylene Monoanhydride (PMA) Fragment

The synthesis of the PMA fragment was through a two-step procedure, which used the cheap PTCDA starting material. The PTCDA was first coupled with the crude swallowtail amine fragment and was purified via column to give the bis-alkylated PDI fragment. This was hydrolyzed under basic conditions to give the monoanhydride (PMA).

3.4.1 Synthesis of PDI-(bisalkyl)

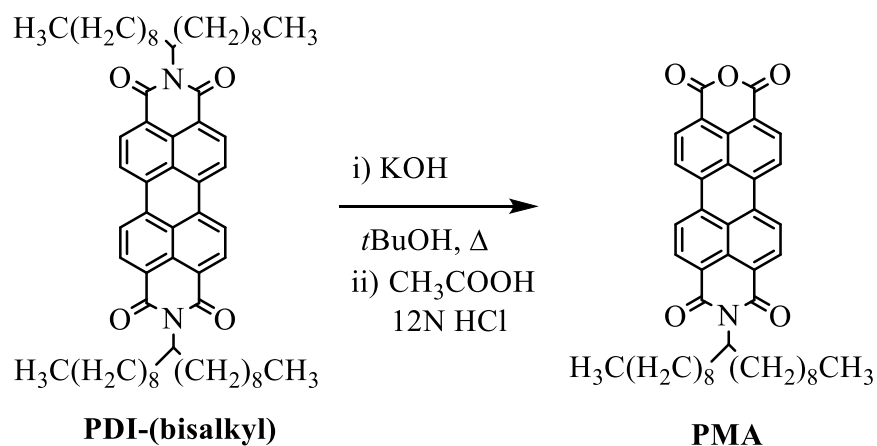
The crude amine (see Scheme 17) was condensed onto PTCDA following established literature procedure (Scheme 10).¹³ The crude product was directly purified (no workup required!) via column chromatography. Yield was 77%.



Scheme 18: Synthesis of PDI-(bisalkyl).

3.4.2 Synthesis of PMA

PDI-(bisalkyl) was hydrolyzed under basic conditions to form the perylene mono-imide dicarboxylate salt with the expected subsequent loss of a single alkyl swallowtail (Scheme 19). This was treated with acid to convert the perylene mono-imide dicarboxylate salt to the target PMA, which is a compound with a deep red color. The general procedure followed established literature precedent.^{13, 144} Yield = 95%



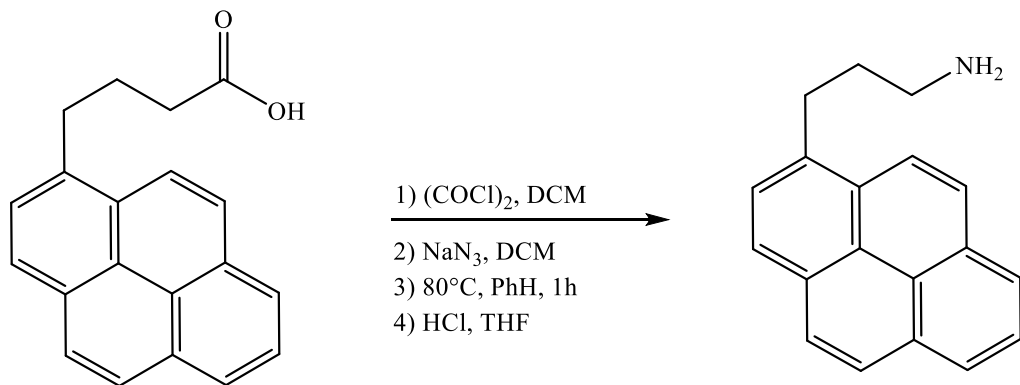
Scheme 19: Formation of PMA via base-hydrolysis.

3.5 Synthesis of the Donor Fragments

Three separate donor fragments were synthesized. The first and second donors were both pyrene but varied in their respective carbon-amine tethers. The former was a 3-carbon aliphatic tether while the latter was an α,β -unsaturated 3-carbon tether. The third donor was ferrocene with an α,β -unsaturated 3-carbon tether. Their respective syntheses will be covered in the following sections.

3.5.1 Synthesis of 1-Pyrenepropylamine 313

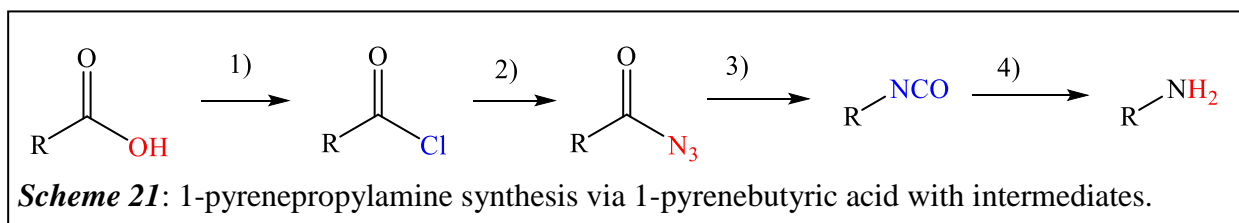
The synthesis of the 1-pyrenepropylamine (Scheme 20) began from commercially available 1-pyrenebutyric acid. First, the carboxylic acid was converted to the acyl chloride. The acyl chloride was then converted to the acyl azide. Subsequent decomposition of the acyl azide to the isocyanate (via Curtius Rearrangement) was followed by hydrolysis to give the target amine donor fragment **313**.¹⁴⁵



313

Scheme 20: 1-Pyrenepropylamine **313** synthesis from 1-pyrenebutyric acid.

The stepwise intermediates in the 1-pyrenepropylamine synthesis are shown in Scheme 21. In step 4, when the isocyanate is decomposed to the amine via acidic hydrolysis, the amine hydrochloride is then basified and extracted and is reported in the literature to give 74% yield of pure material. In our hands, the procedure/purification gave a 95% yield but with slight impurities. It is possible that some of the isocyanate had not yet hydrolyzed to the amine and got carried into the basified extracts. A separate literature procedure for recrystallization as the HBr salt¹⁴⁶ was attempted. It helped in purifying the material sufficiently for condensation onto the perylene monoanhydride (PMA).

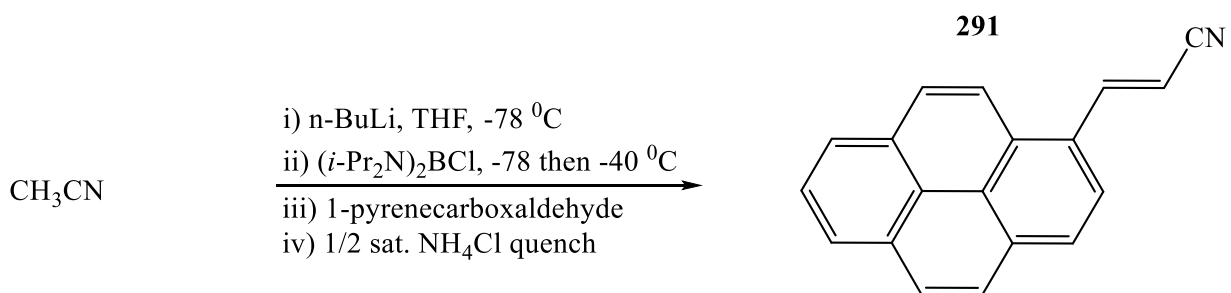


3.5.2 Synthesis of 3-(Pyren-1-yl)prop-2-en-1-amine

The synthesis of **295** begins from the commercially available 1-pyrenecarboxaldehyde. In the first reaction (Section 3.5.2.1), 1-pyrenecarboxaldehyde is converted to an acrylonitrile (Scheme 22). In the second reaction (Section 3.5.2.2), reduction of the acrylonitrile gives the allyl amine (Scheme 23). The details of each reaction are given below.

3.5.2.1 Conversion of 1-Pyrenecarboxaldehyde to (*E*)-3-(Pyren-1-yl)acrylonitrile (**291**)

In a method developed in this author's (and coworkers') undergraduate research, under the guidance of Dr. Takashi Tomioka, an α -boryl carbanion species converts aldehydes into the resultant (*E,Z*)-acrylonitriles in near quantitative conversion with high (*Z*)-stereoselectivity.¹⁴⁷⁻¹⁴⁸ Although the (*E*)-isomer **291** was the goal, and the prior publications had shown (*Z*)-stereoselectivity to predominate, an example using a large polycyclic system (such as 1-pyrenecarboxaldehyde) as the substrate had not previously been performed. It was therefore of great interest to perform this reaction to see what the stereoselectivities would be (and of course to achieve the target **291**).



Scheme 22: Synthesis of (*E*)-3-(pyren-1-yl)acrylonitrile **291**

In a one-pot reaction, an α -boryl carbanion species was generated via lithiated acetonitrile *in situ*. This was treated with 1-pyrenecarboxaldehyde. The post-work-up NMR of the crude

reaction mixture indicated 99% conversion of 1-pyrenecarboxaldehyde to the expected acrylonitrile isomers. The (*E/Z*)-isomer ratio was 48:52, respectively.

The tricky part of this reaction was in the unexpected lability of the product. During isolation on a column it could be seen (by TLC analysis of column fractions) that some decomposition was occurring because *new* spots were appearing on the TLC plates *during* isolation. ¹H NMR confirmed appearance of new peaks not previously present in the crude NMR sample, mostly in the upfield region between ~0.9 – 1.9 ppm for the latter fractions. Furthermore, there was a *significant* decrease in the presence of the (*Z*)-isomer (despite all mass having been accounted for post-column). This is evidence which suggests that the (*Z*)-isomer is polymerizing (possibly to the poly acrylonitrile) to some extent upon isolation on silica.

There are two spectroscopic advantages to a reaction which involves aldehyde conversion to β -unsubstituted acrylonitriles. The first advantage is the ability to easily quantify the percent conversion via ¹H NMR of the crude product. The disappearance of a distinct aldehyde signal at ~10 ppm with concomitant appearance of vinylic peak doublets at ~6 ppm is quite easily determined. The second advantage is the ability to quantify the (*E/Z*)-isomer ratio. The former can tell us what our maximum yield should be. But more importantly, if there is a large deviation of the isolated yield from that suggested by the percent conversion (as determined by ¹H NMR), then it becomes easier to identify problems inherent in a particular isolation strategy (i.e. normal phase chromatography vs. recrystallization). And in the latter spectroscopic advantage – that of being able to easily quantify the (*E/Z*)-isomer ratio – we have an idea as to what our expected isolated yield for respective isomers *should* be.

As an alternative to chromatography, recrystallization of the crude product was attempted. Initially, all suitable recrystallization solvents which were attempted failed to give crystal formation. Upon boiling any of the solvents in the presence of the bright-yellow crude-crystalline solid, the color and composition of the crude material would rapidly change to a gummy neutral colored sticky mess. TLC analysis indicated formation of new, undesirable side-products. Thus, direct recrystallization of the crude product was unsuccessful.

In the first case, where purification via column chromatography was attempted as the purification strategy, it had been obvious that the (*Z*)-isomer suffered the most from purification on the column (it polymerized). It was reasoned that in the second case, where recrystallization of the crude product was attempted as the purification strategy, the gummy mess was also likely the result of the (*Z*)-isomer polymerizing and then interfering with the ability of the solution to form crystals. Thus, fractions saved from the first reaction's chromatographic isolation were all subjected to recrystallization in EtOH. To our delight we were able to finally generate crystals.

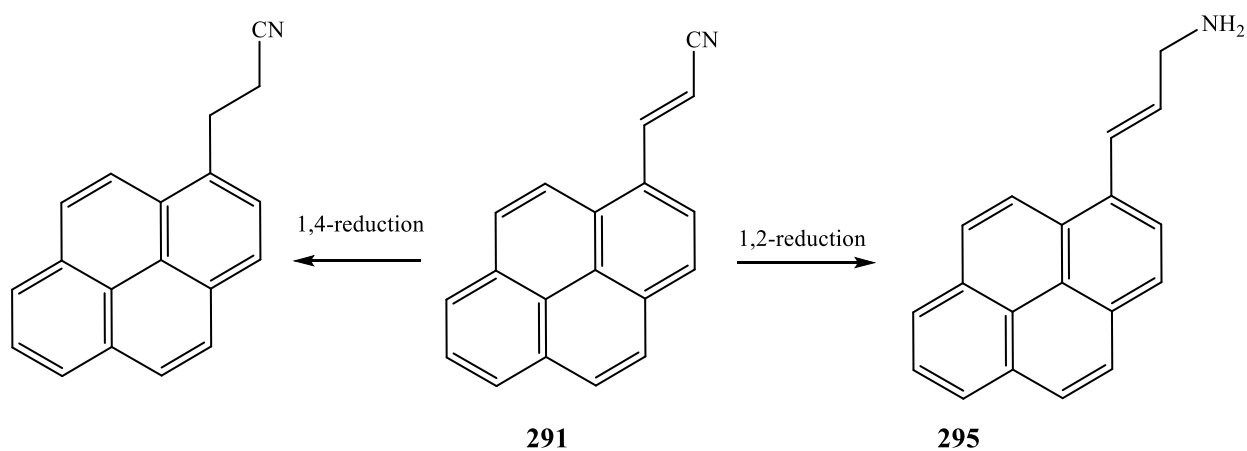
A correlation between the column fraction compositions which *successfully* gave crystals was compared against ¹H NMR of those same fractions. It was found that the early (1st) fractions contained *mostly* (*Z*)-isomer with some unidentified contaminant. The mid fractions (2nd and 3rd) contained both (*E,Z*)-isomers with a different unidentified contaminant than the first fraction. The latter fractions (4th and 5th) contained no detectable vinylic peaks at all. Only the mid fractions gave crystals. It was concluded that presence of either (*E*)-isomer or (*Z*)-isomer had no direct negative effect on the ability to produce crystals. It was likely a high R_f (early fraction) contaminant that was the cause of the previous inability of directly recrystallizing the crude material.

As a result, we finally approached the purification by using a sort of hybrid purification

technique. The crude material was subjected to a quick pre-isolation on silica ((*Z*)-isomer was of course damaged in this process but fortunately this is not the isomer needed), followed by a fractional recrystallization (five separate fractions). This method worked well. Each fraction from the fractional recrystallization gave crystals of increasing quality with respect to prior fractions. Thus, **291** was successfully purified and characterized. The mp = 164 – 165.5°C.

3.5.2.2 Conversion of (*E*)-3-(Pyren-1-yl)acrylonitrile to (*E*)-3-(Pyren-1-yl)prop-2-en-1-amine **295**

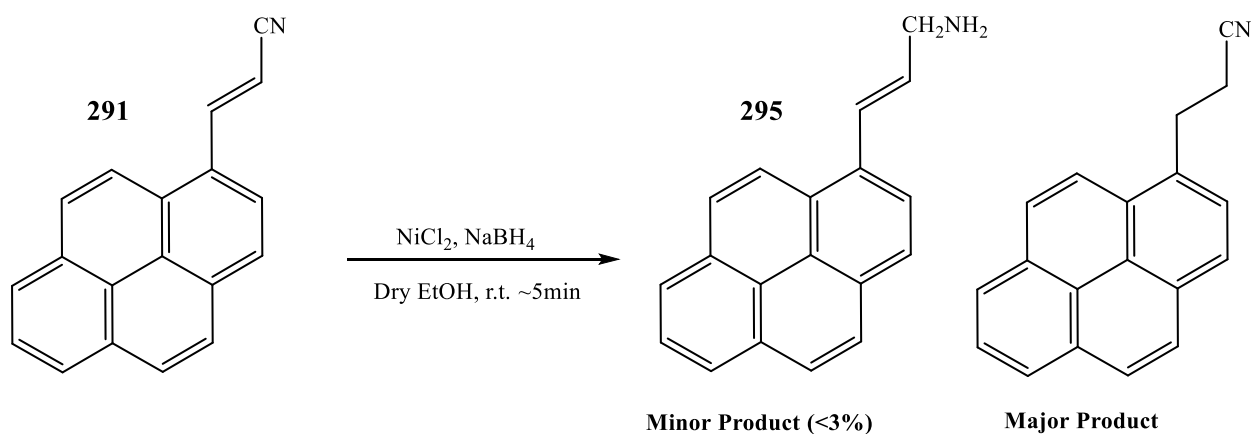
The reduction of an acrylonitrile type functional group generally occurs as two competing reactions which are shown in Scheme 23. The reduction of pyrene acrylonitrile as a 1,4-reduction results in reduction of the olefin. Conversely, a 1,2-reduction results in the conversion of the cyano group to the amine. We ultimately tried two separate reaction conditions to obtain the target (*E*)-3-(pyren-1-yl)prop-2-en-1-amine.



Scheme 23: Competing reductions of acrylonitriles.

We initially attempted a nickel boride reduction of the acrylonitrile **291** using a procedure¹⁴⁹ outlined in Scheme 24 wherein nickel boride is generated *in situ* by the combination of NiCl₂ and NaBH₄. This was unsuccessful. In our hands, although there *was* complete conversion of substrate **291**, unfortunately it had been converted to the 1,4-product with only trace evidence of the target amine **295**.

Since the initial reaction was run on such a small scale (0.1 mmol) and the difficulty of measuring out such a small amount of NaBH₄ might have caused a problem, we ran it again on a larger (0.2 mmol) scale. On the second run, ~60% of the starting material remained. There was again evidence of 1,4-product but no evidence of the target amine. This led us to the conclusion that in our hands, the undesired 1,4-product was being primarily formed.

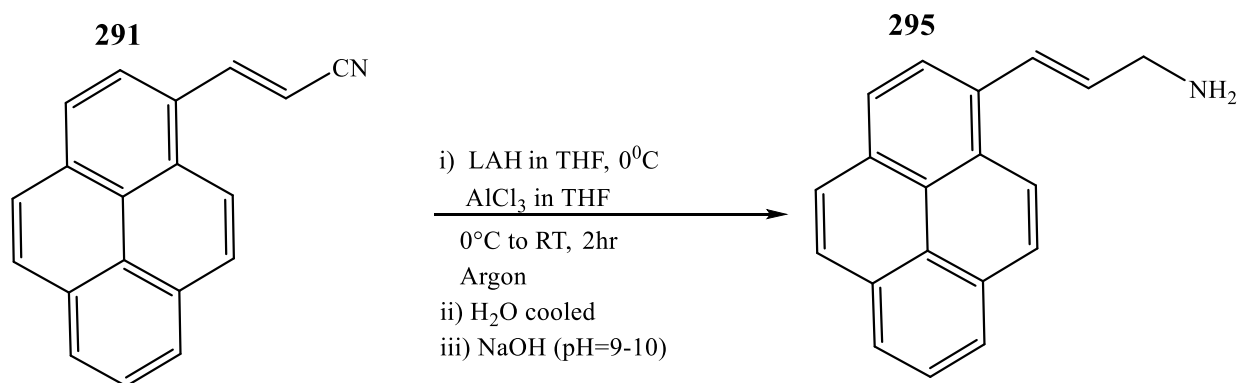


Scheme 24: Attempted 1,2-reduction of **291** was *unsuccessful*.

We decided not to continue to trouble-shoot the nickel boride route and instead examined alternate ways to perform the necessary 1,2-reduction of **291**. Normally, LAH will reduce both the vinylic bond (1,4-reduction) and the cyano group to amine (1,2-reduction). However,

addition of the Lewis acidic AlCl_3 is known to activate the cyano nitrogen, which in turn directs the LAH reduction to become more chemoselective towards the cyano carbon.

In Scheme 25, based on established literature procedures,^{92, 150-151} LAH was combined with AlCl_3 . This was then added to a cold solution of (*E*)-acrylonitrile **291**. Presumably, the cyano nitrogen lone pair donates into the AlCl_3 's empty p-orbital to form the nitrile-aluminum complex, which makes the cyano carbon more electrophilic. After workup, ^1H NMR of the crude material indicated complete disappearance of the starting material's vinylic peak (doublet, ~ 6 ppm) with subsequent appearance of what seems to be a new vinylic peak (dt, ~ 6.5 ppm) as well as an allylic peak (m, ~3.4 ppm). Crude yield was 87%.



Scheme 25: Successful 1,2-reduction of **291**.

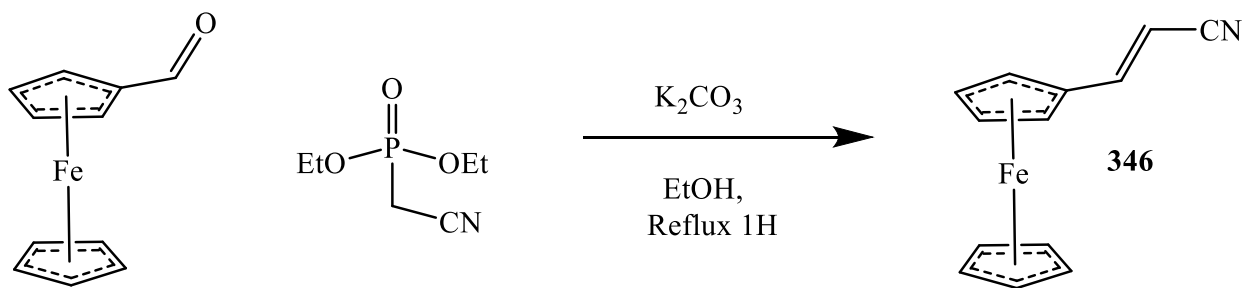
Purification was first attempted by generating the HCl salt in an anhydrous ethereal solution. This did not yield solid as was hoped. The mixture was basified, back extracted, and isolation via normal phase silica column was attempted. The column isolation seemed to cause a little decomposition along with loss of mass. It was decided to use the material without further attempts at purification for the final (condensation onto perylene monoahydrate) step.

3.5.3 Synthesis of (*E*)-3-Ferrocenylprop-2-en-1-amine **352**

The synthesis of (*E*)-3-ferrocenylprop-2-en-1-amine **352** was performed in a two-step procedure from the commercially available ferrocenecarboxaldehyde. In the first step (Section 3.5.3.1, Scheme 26), a Wittig-Horner type reaction, a stabilized phosphonium ylide was generated *in situ*. Nucleophilic attack on the aldehyde was followed by an oxaphosphetane intermediate and subsequent elimination to form the target nitrile with the potassium diethyl phosphate salt by-product.¹⁵² In the second step (Section 3.5.3.2, Scheme 27), the (*E*)-nitrile was reduced via LAH to form the corresponding (*E*)-allyl amine.¹⁵³

3.5.3.1 Conversion of Ferrocenecarboxaldehyde to (*E*)-3-Ferrocenylacrylonitrile **346**

Unlike in the synthesis of **291** (Scheme 23), where the pyrenecarboxaldehyde was converted to the respective acrylonitriles using an α -boryl carbanion,¹⁴⁷⁻¹⁴⁸ this synthesis utilized a phosphonium ylide generated *in situ* which we believed would be more (*E*)-selective towards acrylonitrile formation. In a very simple procedure (Scheme 26), ferrocenecarboxaldehyde was combined with diethyl cyanomethylphosphonate and potassium carbonate in ethanol. After reflux, the mixture was simply extracted.¹⁵² The crude product was analyzed by ¹H NMR. Disappearance of the aldehyde peak (s, ~10 ppm) with subsequent appearance of vinylic peaks (d, ~7.3 ppm and d, ~5.4 ppm) indicated quantitative conversion of the ferrocenecarboxaldehyde to the (*E,Z*)-3-ferrocenylacrylonitrile mixture (*E:Z* = 9:1).



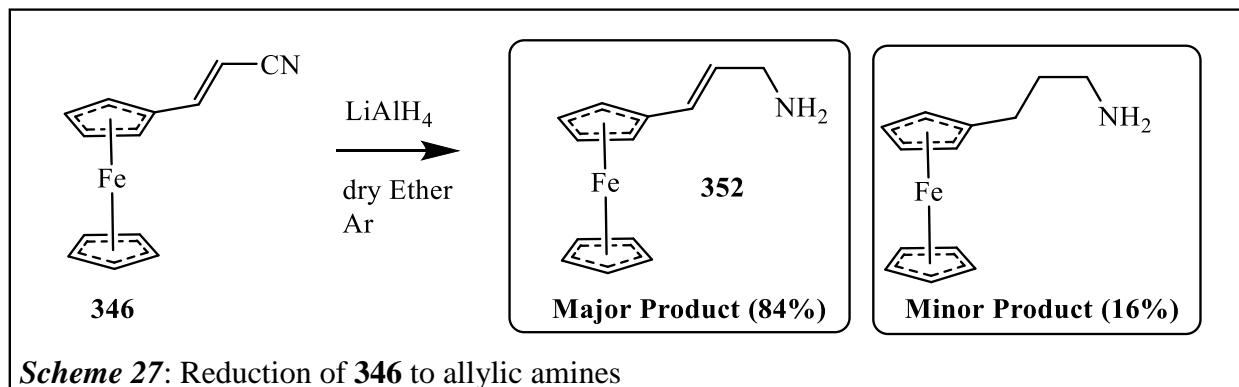
Scheme 26: Wittig-Horner conversion of ferrocenecarboxaldehyde to (*E*)-3-ferrocenylacrylonitrile.

The material was isolated as the (*E,Z*)-mixture (*E:Z* = 75:25), yield = 82%. It was found the (*E*)-isomer **346** could be successfully recrystallized from *n*-pentane to give deep, ruby red colored crystals (mp = 95 - 97°C). Literature values report melting point range for the isolated (*E,Z*)-mixture (mp = 89 - 90°C).¹⁵²

3.5.3.2 Conversion of (*E*)-3-Ferrocenylacrylonitrile to (*E*)-3-Ferrocenylprop-2-en-1-amine

352

The conversion of (*E*)-3-ferrocenylacrylonitrile **346** to (*E*)-3-ferrocenylprop-2-en-1-amine **352** followed a general literature procedure for LAH reduction.¹⁵³ In Scheme 27, the reduction of **346** was followed by Fieser's workup method. Presence of target was confirmed by disappearance of the vinylic peaks (d, ~7.3 ppm and d, ~5.4 ppm) with subsequent formation of new vinylic peaks (d, ~6.2 ppm, and dt, ~5.9 ppm) and an allylic peak (d, ~ 3.3). The material was isolated to give a mixture of the target unsaturated amine **352** with a smaller amount of accompanying saturated amine (84:16) at a yield of 74%. Further purification was not required as it is *much* easier and more efficient to purify the final PDI target once the amine has been condensed onto the PMA.

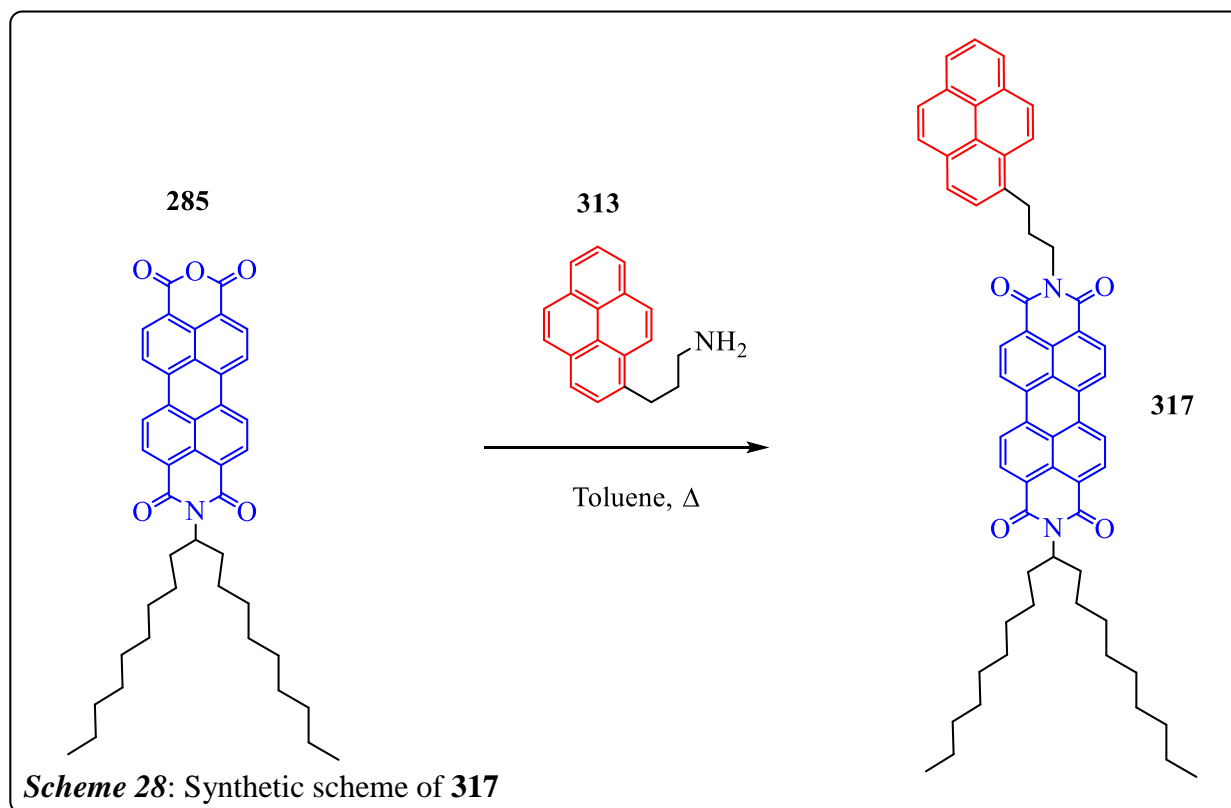


3.6 Syntheses of PDIs 317, 319, 353

As was previously shown in the retrosynthetic analysis (Section 3.2, Scheme 15), the final step in the syntheses of the PDI targets **317**, **319**, **353** was via amine condensation onto PMA. The general procedure was the same in all three cases and follows well established literature precedent.^{13, 144} An excess of the donor amine was combined with the PMA in toluene and aged at reflux. In all cases, the crude material was easily purified via chromatography. Compounds **317** and **319** were found to recrystallize from either benzene or hexanes. Compound **353** was too soluble in the normal recrystallization solvents for PDIs (i.e. hexane, benzene, and toluene) and was therefore purified solely by column chromatography.

3.6.1 The Synthesis of PDI 317

The amine 1-pyrenepropylamine **313** was easily condensed onto PMA **285** in a solution of heated toluene (Scheme 28). Since the general synthetic protocol^{13, 144} calls for an excess of amine, following the reaction progress with TLC involves looking for disappearance of the PMA. In this case, the R_f values of **285** and **317** were nearly identical and the reaction was (initially) believed not to have been progressing. At that point, the only evidence for any change in the reaction was that the TLC spot fluoresced differently under long-wave UV than did the starting PMA. However, after increasing the reaction time from 1.5 hours to ~ 20 hours, and with no change with respect to TLC analysis (other than the long wave fluorescence), a different TLC solvent was sought where the PMA would have lower R_f . By using a solvent system of chloroform for the TLC analysis and running the same TLC plate three times (because the retention fraction was small), it was obvious that all starting material PMA was gone and that a new product had formed.

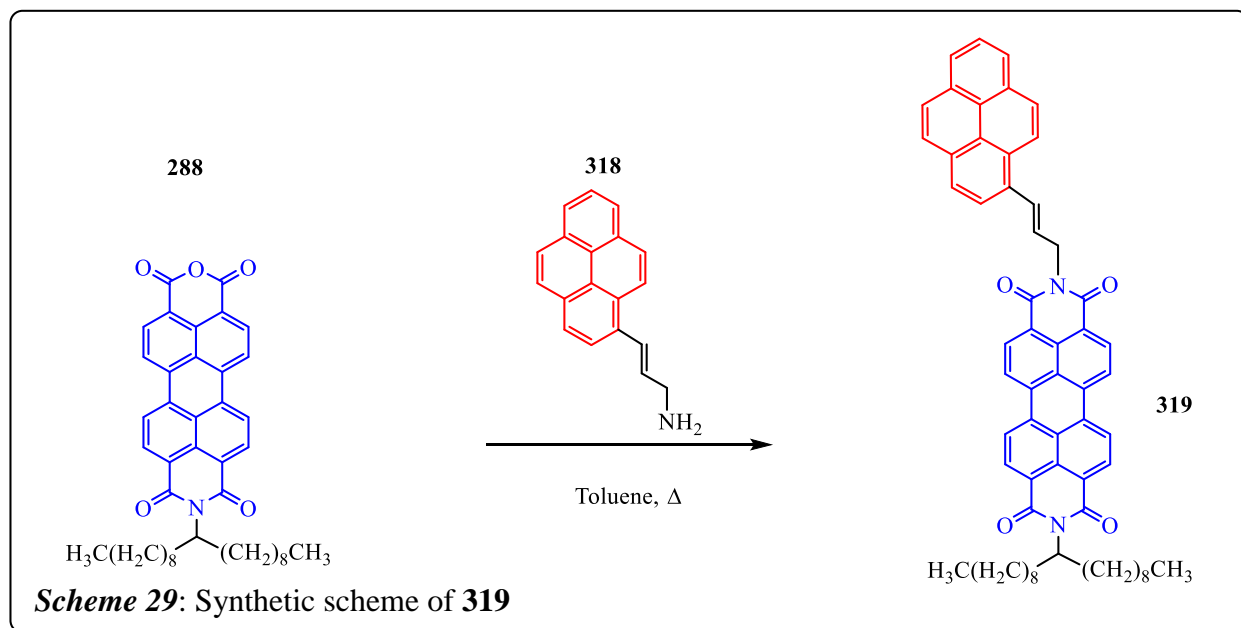


The key spectral feature for initially deciding that a successful reaction had occurred was the formation of a triplet around 4.4 ppm for the new -CH₂-N group. The mixture was then purified several times via column chromatography until the purity of the material was suitable for our study. NMR and FTIR spectra were compared against the literature value of a synthesis of the 1-pyrenebutylamine analogue.¹³ They were found to be in good agreement. The yield from chromatographic isolation was 43%. The purified mixture was recrystallized from benzene (mp = 245 - 247°C).

3.6.2 The Synthesis of PDI 319

The synthetic procedure for synthesis of **319** (Scheme 29) mirrored that of **317** and followed the established literature.^{13, 144} The key ¹H NMR spectral features necessary in confirming formation of the target were the appearance of a new peak at ~ 5 ppm (d, 2H) with

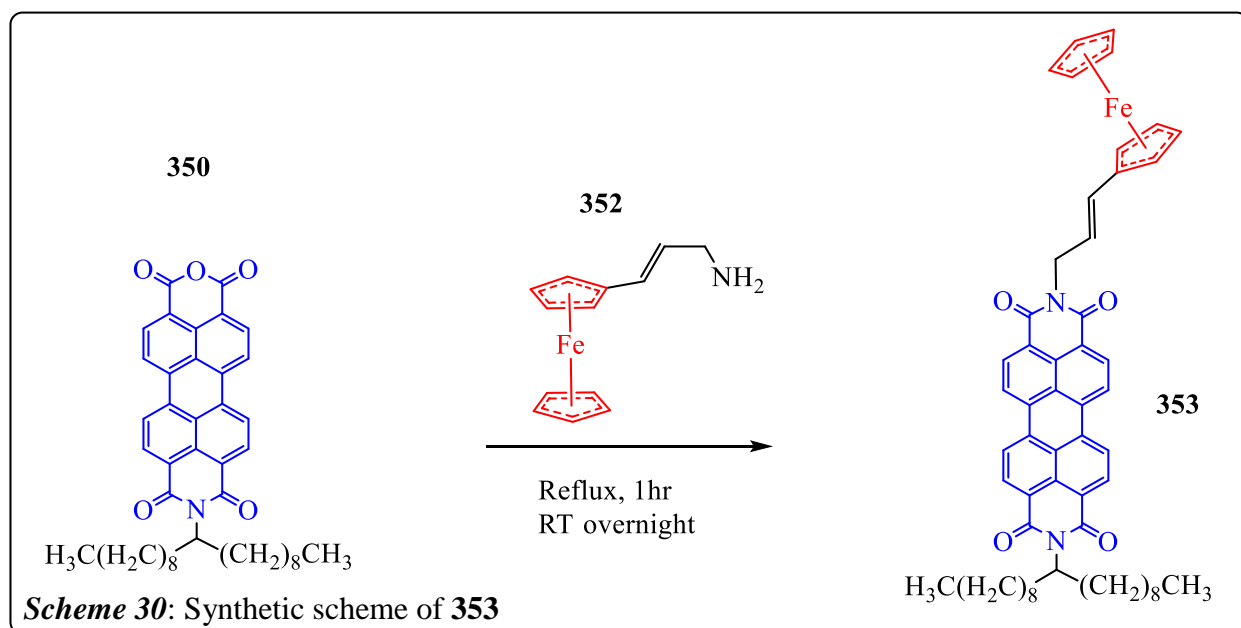
subsequent disappearance of an allylic peak ~3.4 ppm (m, 2H). The new peak is consistent with formation of the allyl methylene, which is α to the imide nitrogen.



The purification of **319** required multiple runs on a column to reach a high purity. It seems common that the ^1H NMR integrated aliphatic peaks are always at a higher ratio than the aromatics. However, with each purification on a silica column, the ratio of aliphatic to aromatic peaks improves. In this case, we isolated the compound four times on silica with no apparent decomposition of compound. The inherent stability of most of the PDIs synthesized in this project were at a stark contrast to the lability of the amine donors and – to a lesser extent – the acrylonitrile precursors. Thus, the best synthetic strategy (for these examples) seems to have been forgoing purification of the donor until it's been condensed onto the PMA. In this case the yield was pretty decent at 64%. Recrystallization was achieved from benzene (mp = 309 - 312°C).

3.6.3 The synthesis of PDI 353

The synthetic procedure for synthesis of **353** (Scheme 30) mirrored that of the previous two examples (**317** and **319**) and followed the established literature for condensation of donor amines onto PMA.^{13, 144} The key spectroscopic feature used to determine formation of target **353** was the ¹H NMR appearance of a new doublet (2H, *J* = 6, ~ 4.8 ppm) with simultaneous disappearance of **352**'s doublet (2H, *J* = 5, ~ 3.3 ppm). The former is attributed to an allyl methylene, which is α to the imide nitrogen. The latter is attributed to **352**'s allyl peak (methylene unit α to the amine nitrogen). The downfield shift that the methylene peak undergoes after **352** is coupled to PMA **350** to make PDI **353** is significant and shows how strong of a deshielding effect the acceptor has on the methylene. It is a useful (though not the only) spectroscopic indicator of a successful coupling of amine donor to PMA acceptor.



This compound purified quite easily to give a yield of 79%. Unlike the previous two PDI examples, this compound only required a single run on a silica column to give publication quality spectra. However, while the previous two examples were recrystallizable, we were never

able to find an adequate recrystallization solvent for this example. On the other hand, this compound differed from PDIs **317** and **319** in that an ESI-MS was obtainable, while **317** and **319** were not amenable to ESI-MS.

3.7 Conclusion

In concluding the PDI project portion of this dissertation – which is the synthesis and spectroscopic characterization of novel PDIs for use as potential D- σ -A's – three new PDIs were successfully made. The biggest hurdle faced during this portion of the project was in the difficulty of purification of the three amine donors **313**, **318**, **352**. This purification difficulty was made easier by simply condensing the impure amine mixture directly onto the PMA and *then* purifying of the final product PDI. Furthermore, this strategy seems to be the most efficient.

CHAPTER 4: EXPERIMENTAL

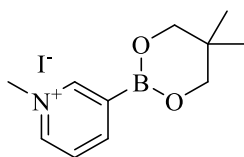
General Methods:

All reagents were procured from Sigma-Aldrich unless otherwise noted. Sodium iodide and KOtBu were from Alfa-Aesar. Acetonitrile, B₂Pin₂, bromine, DMF, DMSO, 1-hexadecanol, 1*H*-benzotriazole, imidazole, KHF₂, KOAc, 3,4,9,10-perylenetetracarboxylic dianhydride, Pd(PPh₃)₄, THF, tosyl chloride, and zinc (II) iodide were from Acros. Ferrocenecarboxaldehyde was from Bean Town Chemical. The reagents NaN₃ and *p*-aminobenzoic acid were from Eastman. Triethylamine and diethyl ether were from Fisher-Scientific. Hydroxybenzotriazole was from Lancaster. The starting materials and/or reagents 4-bromonaphthalen-1-amine, 6-quinolinecarboxylic acid, 1,2-bis[(dimethylamino)-dimethylsilyl]ethane, diethyl cyanomethylphosphonate, 4,4'-disulfaneyldianiline, NaBH₄, SOCl₂, TBSCl, were from TCI. Iron was from Matheson, Coleman, and Bell.

Moisture and oxygen sensitive reactions were carried out in flame-dried glassware fitted with rubber septa under an inert gas (e.g., argon) atmosphere. Anhydrous tetrahydrofuran (THF) was distilled over sodium metal in the presence of benzophenone indicator. Anhydrous dichloromethane, toluene, and any types of liquid amine reagents were distilled over calcium hydride (CaH₂) upon necessity. Dried solvents were stored over activated molecular sieves. All commercially available reagents and starting materials were used without further purification unless otherwise noted. ¹H Nuclear Magnetic Resonance (NMR) spectra were recorded on Bruker Avance DRX 300 (300 MHz) or DRX 500 (500 MHz) spectrometers.

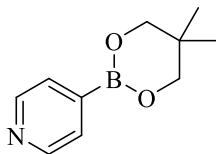
Data are presented as follows: chemical shift (in ppm on the δ scale relative to δ H 7.26 for the residual protons in CDCl_3), multiplicity (s = singlet, d = doublet, t = triplet, q = quartet, p = pentet, dd = doublet of doublets, dt = doublet of triplets, m = multiplet, br = broad, brs = broad singlet), coupling constant (J/Hz), and integration. Coupling constants were taken directly from the spectra and are uncorrected. ^{13}C NMR spectra were recorded at 75 or 125 MHz using the spectrometers above. All the chemical shift values are reported in ppm on the δ scale, with an internal reference of δ C 77.16 for CDCl_3 . Infrared (IR) spectra were recorded on either a Bruker TENSOR 27 or an ALPHA-P FT-IR spectrometer and are reported in units of cm^{-1} . High-resolution mass spectra (HR-MS) were recorded using a Waters SYNAPT HDMS quadrupole time of flight (Q-TOF) mass spectrometer. All the HR-MS experiments were performed by the Dass research group at the University of Mississippi.

3-(5,5-Dimethyl-1,3,2-dioxaborinan-2-yl)-1-methylpyridin-1-ium iodide (00)



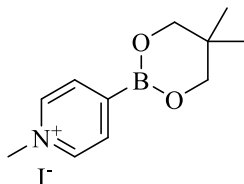
Pyridine-3-boronic acid neopentyl glycol ester (0.191 g, 1.00 mmol) was suspended in acetonitrile (5 mL) and iodomethane (0.310 mL, 5.00 mmol). The mixture was brought to heat at reflux overnight. The mixture was then concentrated via rotary evaporation to afford the target in quantitative yield. ^1H NMR (300 MHz, CDCl_3) δ 9.64(d, J = 6 Hz, 1H), 8.82 (s, 1H), 8.66 (d, J = 7.5 Hz, 1H), 8.12 (t, J = 6.6 Hz, 1H), 4.47 (s, 3H), 3.82 (s, 4H), 1.03 ppm(s, 6H).

4-(5,5-Dimethyl-1,3,2-dioxaborinan-2-yl)pyridine (24)



4-Pyridinylboronic acid (1.25 g, 9.00 mmol) and neopentyl glycol (1.04 g, 10.0 mmol) were added to toluene (150 mL) in a round-bottom flask. The flask was fitted with a Dean-Stark apparatus and then fitted with a condenser. The suspension was brought to heat at reflux and aged for three hours. The mixture was then allowed to cool to room temperature then washed with water (3 x 50 mL). The aqueous layers were combined and concentrated via rotary evaporation to give a white solid (1.74 g, 91 %). ^1H NMR (300 MHz, CDCl_3) δ 8.61 (d, $J = 3.9$ Hz, 2H), 7.63 (d, $J = 3.9$ Hz, 2H), 3.78 (s, 4H), 1.03 ppm (s, 6H).

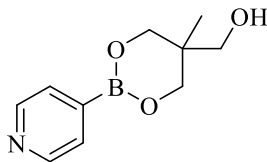
4-(5,5-Dimethyl-1,3,2-dioxaborinan-2-yl)-1-methylpyridin-1-ium iodide (27)



4-(5,5-Dimethyl-1,3,2-dioxaborinan-2-yl)pyridine **24** (1.35 g, 7.07 mmol) was suspended in acetonitrile (35 mL) and methyl iodide (2.20 mL, 35.35 mmol) was added. The mixture was brought to heat at reflux and aged for 6 h. The solvent was stripped via rotary evaporation to afford a bright yellow solid (2.166 g, 92% yield). ^1H NMR (300 MHz, DMSO) δ 8.91 (d, $J = 6.3$ Hz, 2H), 8.17 (d, $J = 6.3$ Hz, 2H), 4.35 (s, 3H), 3.78 (s, 4H), 0.96 (s, 6H). ^{13}C NMR (75 MHz, DMSO) δ 144.13, 130.89, 71.60, 31.48, 21.32 (C-B is not observed). ^1H NMR (300 MHz,

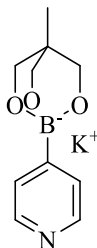
CDCl_3) δ 9.23 (d, $J = 6.3$ Hz, 2H), 8.28 (d, $J = 6$ Hz, 2H), 4.72 (s, 3H), 3.83 (s, 4H), 1.04 ppm (s, 6H).

(5-Methyl-2-(pyridin-4-yl)-1,3,2-dioxaborinan-5-yl)methanol (69)



4-Pyridinylboronic acid (2.03 g, 15.0 mmol), 2-(hydroxymethyl)-2-methylpropane-1,3-diol (1.80 g, 15.0 mmol), and dry toluene (30 mL) were added to a round-bottom flask. The flask was fitted with a Dean-Stark apparatus and then fitted with a condenser. The mixture was brought to heat at reflux for 4.5 hours. The solvent was stripped via rotary evaporation to give a white solid at quantitative yield. ^1H NMR (500 MHz, DMSO) δ 8.57 (d, $J = 7.5$ Hz, 2H), 7.55 (d, $J = 7.5$ Hz, 2H), 4.86 (s, 1H), 3.71 (brs, 6H), 0.87 ppm (s, 3H).

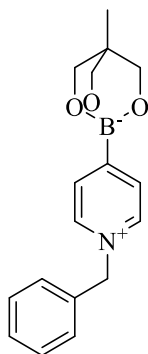
Potassium 4-Methyl-1-(pyridin-4-yl)-2,6,7-trioxa-1-borabicyclo[2.2.2]octan-1-uide (37)



(5-Methyl-2-(pyridin-4-yl)-1,3,2-dioxaborinan-5-yl)methanol **69** (0.208 g, 1.00 mmol) was suspended in toluene (2 mL). KOH (0.050 g, 0.90 mmol) was added to the suspension and the mixture was fitted with a Dean-Stark apparatus. A reflux column was fitted and the mixture was brought to heat at reflux for 4 hours. The solvent was then stripped via rotary evaporation. Conversion was near quantitative. ^1H NMR (500 MHz, DMSO) δ 8.20 (d, $J = 5$ Hz, 2H), 7.31

(d, $J = 4.5$ Hz, 2H), 3.55 (s, 6H), 0.53 (s, 3H). ^{13}C NMR (75 MHz, DMSO) δ 146.17, 127.82, 71.69, 35.07, 16.45 ppm (C-B is not observed).

1-(1-Benzylpyridin-1-ium-4-yl)-4-methyl-2,6,7-trioxa-1-borabicyclo[2.2.2]octan-1-uide (59)



Part 1 (N-benylation)

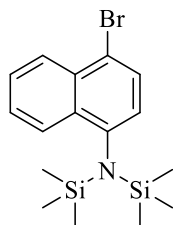
In a dry round-bottom flask was suspended (5-methyl-2-(pyridin-4-yl)-1,3,2-dioxaborinan-5-yl)methanol **69** (0.068 g, 0.33 mmol) in acetonitrile (1.67mL). Benzyl bromide (0.040 mL, 0.33 mmol) was added dropwise. The mixture was fitted with a reflux condenser and brought to heat at reflux. The solvent was stripped and a ^1H NMR was obtained to confirm complete *N*-alkylation. ^1H NMR (500 MHz, DMSO) δ 9.15 (d, $J = 6.3$ Hz, 2H), 8.20 (d, $J = 6.0$ Hz, 2H), 7.54-7.51 (m, 2H), 7.44 – 7.42 (m, 3H), 5.90 (s, 2H), 3.70 (s, 6H), 0.86 (s, 3H). ^{13}C NMR (75 MHz, DMSO) δ 143.37, 134.38, 131.52, 129.30, 129.18, 128.77, 62.92, 36.53, 35.43, 17.17 ppm (C-B is not observed).

Part 2 (Ring closure to form the triolborate)

To the alkylated sample was added dry K_2CO_3 (0.046 g, 0.30 mmol) and then acetonitrile (1.67 mL). The mixture was stirred at room temperature overnight. The acetonitrile was then stripped in vacuo. ^1H NMR (500 MHz, DMSO) δ 8.76 (d, $J = 4.5$, 2H), 7.91 (d, $J = 5.4$, 2H),

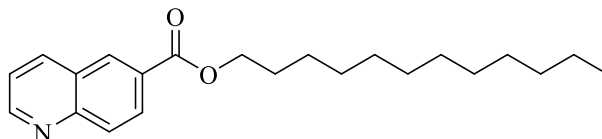
7.40 (s, 5H), 5.73 (s, 2H), 3.61 (s, 6H), 0.50 (s, 3H). ^{13}C NMR (75 MHz, DMSO) 140.77, 135.06, 130.80, 129.09, 129.00, 128.30, 61.91, 34.84, 15.75 (C-B is not observed).

***N*-(4-Bromonaphthalen-1-yl)-1,1,1-trimethyl-*N*-(trimethylsilyl)silanamine (80)**



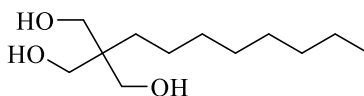
In a flame-dried round-bottom flask with a stir bar was dissolved 4-bromonaphthalen-1-amine (0.211 g, 1.00 mmol) in dry THF (2.21 mL) under nitrogen atmosphere. Next, 2.5 M *n*-butyllithium in hexanes (0.220 mL, 2.20 mmol) was added dropwise over 2.5 hours while keeping the temperature at 0°C. TMSCl (0.278 mL, 2.20 mmol) was added dropwise over 2.5 hours to give a brown colored solution. The ice bath was removed, and the mixture was aged overnight. The mixture was then concentrated via rotary evaporation to give 0.512 g of a dark brown liquid which was quenched with satd. NH_4Cl (4 mL), then extracted with chloroform (3X). The pooled organic extracts were washed once with brine (4 mL), dried over MgSO_4 then filtered over Celite to give an orange-tinted brown liquid, which was concentrated via rotary evaporation. The crude residue was purified on normal-phase silica using a hexanes:EtOAc 9:1 solvent system. Yield 61%. ^1H NMR (300 MHz, CDCl_3) δ 8.22-8.17 (m, $J = 7.05$ Hz, 2H), 7.66 (d, $J = 7.8$ Hz, 1H), 7.60-7.49 (m, 2H), 6.93 (d, $J = 8.1$ Hz, 1H), 0.06 (s, 18H). (75 MHz, CDCl_3) 145.24, 135.69, 132.90, 129.68, 127.54, 127.21, 127.01, 126.14, 125.81, 118.23, 2.05.

Dodecyl quinoline-6-carboxylate (113)



To a flame-dried round-bottom flask and stir bar was added 6-quinolinecarboxylic acid (1.74 g, 10.0 mmol) dissolved in acetonitrile. Triethylamine (2.09 mL, 15.0 mmol) was added dropwise followed by addition of dodecyl bromide (2.40 mL, 10.0 mmol). The mixture was fitted with a reflux condenser and brought to heat at reflux for 24 h. The solvent was stripped via rotary evaporation. The purple colored solid was purified on normal-phase silica (acetone:DCM 1:9). Yield 78% (2.66 g) tan colored solid. Needle-like crystals from acetonitrile, mp = 58 - 60°C. ^1H NMR (300 MHz, CDCl_3) δ 9.01 (d, $J = 3.6$, 1H), 8.59 (s, 2H), 8.30 (t, $J = 9.6$, 1H), 8.15 (d, $J = 8.7$, 2H), 7.49 (dd, $J = 8.3, 4.2$ Hz, 1H), 4.40 (t, $J = 6.7$ Hz, 2H), 1.83 (p, $J = 6.7$ Hz, 2H), 1.56 – 1.16 (m, 18H), 0.88 (t, $J = 6.6$ Hz, 3H). ^{13}C NMR (75 MHz, CDCl_3) 166.30, 152.57, 150.23, 137.43, 131.00, 129.17, 129.12, 128.67, 127.56, 121.92, 65.71, 32.04, 29.77, 29.73, 29.67, 29.47, 29.44, 28.89, 26.20, 22.81, 14.24. (one aliphatic carbon signal is not seen and is likely buried between 29.77 - 29.67). IR (neat): 1704.2 cm^{-1} .

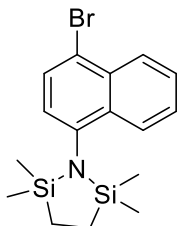
2-(Hydroxymethyl)-2-octylpropane-1,3-diol (116)



To a round-bottom flask and stir bar was added decanal (3.77 mL, 20.0 mmol). A solution of formaldehyde (3.13 mL, 42.0 mmol) in 50% aqueous ethanol (59 mL) was prepared and added to the decanal-containing flask. The mixture was cooled to 0°C. Next, a solution of KOH (2.36 g, 42.0 mmol) in 50% aqueous ethanol solution was prepared. A dropping funnel was fitted to the decanal-containing flask. The KOH solution was added from the dropping funnel

over 1 hour. The mixture was removed from the ice bath and heated at 50°C for 2 hours. Next, the heat was removed and the ethanol was stripped via rotary evaporation. The remaining aqueous solution was extracted with diethyl ether (4X), dried over MgSO₄, filtered, and then concentrated via rotary evaporation to give semi-transparent liquid. The residue was isolated via normal phase silica (Hexanes:EtOAc:MeOH 4:6:1). Yield 16%. Crystals from toluene, mp = 73 – 74.5 °C. ¹H NMR (300 MHz, CDCl₃) δ 3.75 (s, 6H), 2.49 (s, 3H), 1.25 – 1.28 (m, 14H), 0.88 (t, *J* = 6.75, 3H). ¹³C NMR (75 MHz, CDCl₃) 67.74, 42.92, 32.01, 31.17, 30.75, 29.62, 29.43, 23.18, 22.80, 14.236. IR (neat): 3360.6 (m), 3302.0 (m), 3260.0 (m), 2915.7 (s), 2848.2 (s), 1003.8 (s) cm⁻¹.

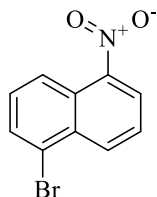
2,2,5,5-Tetramethyl-1-octyl-1,2,5-azadisilolidine (132)



To a dry round-bottom flask and stir bar was added 4-bromonaphthalen-1-amine (2.221 g, 10.00 mmol), zinc (II) iodide (0.798 g, 2.50 mmol), methylamine HCl (0.0473 g, 0.700 mmol), and 1,2-bis[(dimethylamino)-dimethylsilyl]ethane (3.50 g, 14.0 mmol). The mixture was brought to 105 °C for one hour and then elevated to 170°C over the next two hours. The crude material was triturated with hexanes and then filtered over a bed of Celite. The filtrate was dried over MgSO₄ and then concentrated via rotary evaporation to give a yellowish-brown product that solidified upon standing. The crude product was isolated by normal phase silica to obtain a clear viscous liquid with a slight yellow tint, which solidified to a white crystalline material upon standing. Yield = 95% (3.450 g). ¹H NMR (300 MHz, CDCl₃) δ 8.21 (d, *J* = 8.4 Hz, 1H), 8.13 (d,

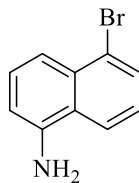
$J = 8.3$ Hz, 1H), 7.68 (d, $J = 7.8$ Hz, 1H), 7.56 (t, $J = 7.4$ Hz, 1H), 7.48 (t, $J = 7.6$ Hz, 1H), 6.86 (d, $J = 7.8$ Hz, 1H), 1.02 (s, 4H), 0.01 (s, 12H).

1-Bromo-5-nitronaphthalene (144)



To a round-bottom flask and stir bar was added 1-nitronaphthalene (10.0 g, 58.0 mmol) combined with FeCl_3 (Fisher-Scientific, 0.066 g, 0.41 mmol) and the mixture was heated to 90 °C. Bromine (3.00 mL, 58.0 mmol) was added dropwise over ~5 minutes. This was aged for 2 hours, then cooled to rt. The mixture was recrystallized from hot ethanol. Yield 37% (5.40 g). mp = 120 – 121 °C (lit. 118 - 121 °C). ^1H NMR (300 MHz, CDCl_3) δ 8.60 (d, $J = 8.4$ Hz, 1H), 8.46 (d, $J = 8.7$ Hz, 1H), 8.22 (d, $J = 7.5$ Hz, 1H), 7.93 (d, $J = 7.2$ Hz, 1H), 7.66 (t, 1H), 7.54 (t, 1H). ^{13}C NMR (75 MHz, CDCl_3) 147.28, 133.63, 132.85, 131.81, 129.54, 126.53, 125.65, 124.47, 123.66, 123.02. This literature compound⁸⁷ was used without further characterization.

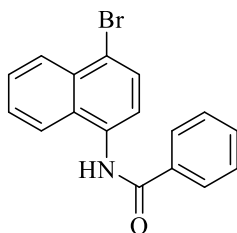
1-Amino-5-bromonaphthalene (149)



To a round-bottom flask and stir bar were added water (20 mL) and iron powder (0.800 g, 14.4 mmol). The mixture was brought to heat at reflux and then glacial acetic acid (50 mL) was added. 5-Nitro-1-bromonaphthalene **144** (1.00 g, 4.00 mmol) was added in small portions to the

suspension. Additional iron powder (0.400 g, 7.20 mmol) was added and the mixture aged at reflux for 1 hour. The reaction was then cooled to room temperature, diluted with water (30 mL) and DCM and filtered through Celite to remove the residual iron powder. The aq. filtrate was placed in a separatory funnel and basified with 1M NaOH until pH = 9 whereupon a solid precipitated. The solid was then dissolved in the previous DCM layer. The solution was passed over a bed of Celite to remove a black solid. The filtrate was concentrated via rotary evaporation to give a crude brown liquid, which solidified upon standing. The solid was purified via normal phase silica (hexanes:DCM 4:6). Yield (195 mg, 22 %) mp = 62 – 66°C (lit. 63 – 66°C). ¹H NMR (300 MHz, CDCl₃) δ 7.79 (d, *J* = 7.8 Hz, 1H), 7.76 (d, *J* = 6.9 Hz, 1H), 7.71 (d, *J* = 8.7 Hz, 1H), 7.39 (t, *J* = 7.5 Hz, 1H), 7.26 (t, *J* = 8 Hz, 1H), 6.82 (d, *J* = 7.4 Hz, 1H), 4.16 (s, 2H). This literature compound^{89, 154} was used without further characterization.

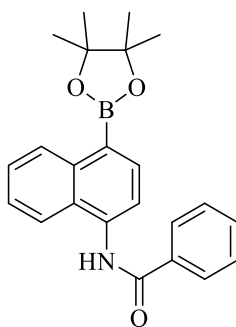
***N*-(4-Bromonaphthalen-1-yl)benzamide (171)**



To an oven dried round-bottom flask and stir bar was added 4-bromonaphthalen-1-amine (4.442 g, 20.00 mmol) dissolved in THF (45 mL). Next pyridine (4.04 mL, 50.0 mmol) then benzoyl chloride (2.79 mL, 24.0 mmol) were added and the mixture was aged overnight. Next, the THF was stripped via rotary evaporation. The mixture was diluted with toluene and was then filtered over Celite. The filtrate was concentrated via rotary evaporation. The solid was separated on a Büchner funnel, washed with water (50 mL), then air dried, then washed with hexane (30 mL). The solid cake was purified via recrystallization from EtOH. Yield (3.652 g, 56%). mp = 235 - 237°C. ¹H NMR (500 MHz, CDCl₃) δ 8.32 (d, *J* = 8.1 Hz, 1H), 8.17 (s, 1H), 7.99 (d, *J* =

7.3 Hz, 2H), 7.93 (d, $J = 8.3$ Hz, 2H), 7.84 (d, $J = 8.1$ Hz, 1H), 7.63 (dq, $J = 14.2, 6.8$ Hz, 3H), 7.56 (t, $J = 7.4$ Hz, 2H). ^{13}C NMR (126 MHz, CDCl_3) δ 166.31, 134.70, 132.57, 132.44, 132.36, 129.97, 129.14, 128.77, 128.44, 127.66, 127.41, 127.34, 121.85, 121.22, 120.22. IR (neat): 3263 (m, br), 3085 (w), 1645 (s), 1593 (s), 1522 (s), 1486 (s), 1454 (s), 1416 (s), 1376 (s), 1318 (s), 1281 (s), 1198 (m), 1024 (m), 896 (m), 753 (s), 707 (s), 682 (s), 501 (m), 415 (m). HRMS (ESI-MS+) calcd = 324.00240 $[\text{M} - \text{H}]^-$, obsd = 324.0005.

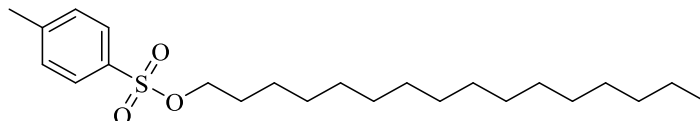
***N*-(4-(4,4,5,5-Tetramethyl-1,3,2-dioxaborolan-2-yl)naphthalen-1-yl)benzamide (178)**



To a flame dried round-bottom flask and stir bar were added *N*-(4-bromonaphthalen-1-yl)benzamide **171** (1.21 g, 3.31 mmol), B_2Pin_2 (1.26 g, 4.96 mmol), KOAc (1.95 g, 19.8 mmol), and $\text{Pd}(\text{PPh}_3)_4$ (382 mg, 0.100 mmol). This was purged/backfilled with argon three times. Dry degassed DMF (40 mL) was added and the mixture was aged at 90°C for 45 hours. The mixture was cooled, diluted with EtOAc and then filtered over a bed of Celite. The mixture was washed with H_2O followed by satd. NaCl. The organic extract was dried over MgSO_4 , filtered over glass floss, then concentrated via rotary evaporation. The residue was purified via normal phase silica (hexanes:EtOAc:acetic acid 70:25:5). Yield 51 %, 624 mg. Crystals from ACN/ H_2O . mp = $180 - 182.5^\circ\text{C}$. ^1H NMR (300 MHz, CDCl_3) δ 8.87 (d, $J = 8$ Hz, 1H), 8.32 (s, 1H), 8.21 (d, $J = 7.5$ Hz, 1H), 8.14 (d, $J = 7.5$ Hz, 1H), 7.99 (d, $J = 7.5$ Hz, 2H), 7.92 (d, $J = 8$ Hz, 1H), 7.60 – 7.53 (m,

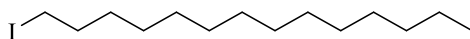
5H), 1.43 (s, 12H). ^{13}C NMR (126 MHz, CDCl_3) δ 137.99, 136.26, 135.44, 135.17, 132.18, 129.80, 129.10, 127.34, 126.60, 126.42, 126.16, 120.16, 119.19, 83.92, 25.12. IR (neat): 3315.4 (m), 3065.8 (m), 2984.8 (m), 2954.9 (m), 2926.0 (m), 1651.3 (s), 1587.9 (m), 1575.9 (m), 1503.7 (s), 1483.3 (s), 1374.3 (s), 1271.3 (s), 1096.6 (s), 1076.8 (s), 765.5 (s), 712.1 (s).

Hexadecyl 4-Methylbenzenesulfonate (194)



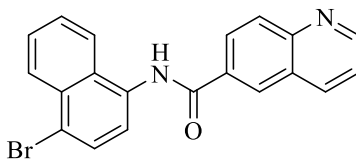
To an oven dried round-bottom flask and stir bar was added 1-hexadecanol (5.04 g, 20 mmol) dissolved in chloroform (20 mL). The mixture was cooled to 0°C and then pyridine (3.24 mL, 40.0 mmol) was added. Next, tosyl chloride (5.72 g, 30.0 mmol) was added in small portions with constant stirring. The reaction was monitored via TLC until no further conversion occurred. The mixture was diluted with ether and then washed with 5% HCl, then 5% NaHCO_3 , and then H_2O . The organic layer was dried over MgSO_4 , filtered, then concentrated via rotary evaporation. The material was isolated via normal phase silica (hexanes:DCM 9:1) but still contained some tosyl chloride. The remaining tosyl chloride contaminant was removed by addition of small amounts of ethylenediamine and then washing with 2M HCl. Yield 84%, 6.65 g. ^1H NMR (300 MHz, CDCl_3) δ 7.78 (d, $J = 8.3$ Hz, 2H), 7.33 (d, $J = 8.1$ Hz, 2H), 4.01 (t, $J = 6.5$ Hz, 2H), 2.65 (s, 3H), 1.63 (m, 2H), 1.27 – 1.21 (m, 26H), 1.00 – 0.76 (m, 3H). ^{13}C NMR (75 MHz, CDCl_3) δ 144.67, 133.46, 129.88, 127.97, 70.77 (CH_2O), 32.03, 29.80, 29.77, 29.71, 29.61, 29.50, 29.47, 29.03, 28.93, 25.44, 25.38, 22.79, 22.75, 21.68, 14.20. (one aliphatic peak is apparently buried in the 29.8 – 29.4 region).

1-Iodotetradecane (195)



To a round-bottom flask and stir bar was added 1-bromotetradecane (6.23 mL, 20.6 mmol) dissolved in acetone (12.0 mL). To this was added NaI (7.64 g, 51.0 mmol) and the flask was fitted with a reflux condenser. The mixture was aged for 27 hours at reflux. Next, the mixture was diluted with ether and then filtered to remove the insoluble salts. The filtrate was washed with half saturated Na₂S₂O₃, then H₂O (2X), and then once with satd. NaCl. The organic layer was dried over MgSO₄, filtered and then concentrated via rotary evaporation. The residue was distilled under hi-vac. Yield 5.755 g, 86%, bp = 134-137°C at 3 mm Hg. ¹H NMR (300 MHz, CDCl₃) δ 3.18 (t, *J* = 7.0 Hz, 2H), 1.87 – 1.77 (m, 2H), 1.40 – 1.26 (m, 22H), 0.88 (t, *J* = 6.6 Hz, 3H). This literature compound¹⁰⁸⁻¹⁰⁹ was used without further characterization.

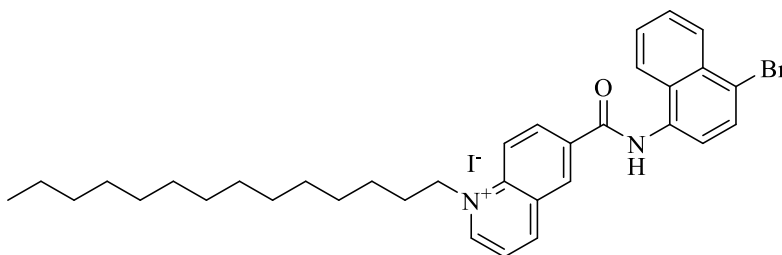
***N*-(4-Bromonaphthalen-1-yl)quinoline-6-carboxamide (202)**



To round-bottom flask and stir bar was added 4-bromonaphthalen-1-amine (170 mg, 0.75 mmol) dissolved in DCM (15 mL) and the mixture was cooled to 0°C. Quinoline-6-carboxylic acid (132.5 mg, 0.75 mmol), DCC (185.7 mg, 0.90 mmol), and HOBt (124.1 mg, 0.90 mmol) were combined in a separate flask. To this mixture was added DCM and the mixture was transferred into the first solution with several washings. Remaining undissolved carboxylic acid required acetonitrile (0.5 mL) and then DMF (1 mL) to effect dissolution and subsequent transfer. The mixture was cooled to 0°C and then allowed to come to room temperature overnight. After 18 hrs. the mixture was concentrated, diluted with toluene, filtered, and rinsed with toluene. The filtrate was washed with half satd. NaCl followed by satd. NaCl. The organic extract was dried over MgSO₄ and filtered once again to remove residual dicyclohexyl urea by-product. The filtrate was concentrated via rotary evaporation. The resulting crude product was

purified via normal phase silica (acetone:DCM 1:15). Yield 241.3 mg, 85%. Crystals from EtOH with white pinkish tint, mp = 217 - 220°C. ¹H NMR (500 MHz, CDCl₃) δ 9.05 (dd, *J* = 4.2, 1.7 Hz, 1H), 8.52 (s, 1H), 8.39 – 8.29 (m, 3H), 8.26 (s, 2H), 7.97 (d, *J* = 8.6 Hz, 1H), 7.92 (d, *J* = 8.0 Hz, 1H), 7.84 (d, *J* = 8.1 Hz, 1H), 7.64 (dddd, *J* = 19.5, 8.2, 6.8, 1.3 Hz, 2H), 7.53 (dd, *J* = 8.3, 4.2 Hz, 1H). ¹³C NMR (126 MHz, CDCl₃) δ 165.74, 152.60, 149.74, 137.26, 132.61, 132.50, 132.27, 130.70, 129.95, 128.89, 128.48, 128.34, 127.86, 127.76, 127.52, 127.14, 122.40, 122.18, 121.30, 120.62 (one aromatic peak presumably buried in the aromatic region). IR (neat): 3212 (m), 1645 (s) 1488 (m), 1379 (m), 892 (m), 851 (m), 823 (s), 799 (s), 758 (s), 665 (m), 479 (m).

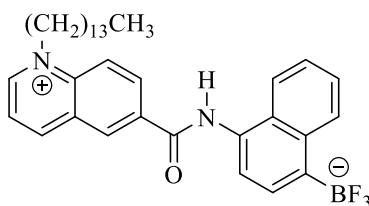
6-((4-Bromonaphthalen-1-yl)carbamoyl)-1-tetradecylquinolin-1-ium iodide (201)



To an oven dried flask and stir bar was added *N*-(4-bromonaphthalen-1-yl)quinoline-6-carboxamide **202** (76.6 mg, 0.200 mmol), in sulfolane (400 μL). To this suspension was added iodotetradecane **195** (206.1 mg, 0.636 mmol). The suspension was aged at 110°C for 45 hours. Next, the mixture was cooled to room temperature then was diluted with EtOAc to give a yellow precipitate. The precipitate was collected by filtration. Yield 91.2 mg, 65%. Bright yellow metallic crystals from acetone, mp = 209 - 211°C. ¹H NMR (500 MHz, MeOD-d₄) δ 9.56 (d, *J* = 4.9 Hz, 1H), 9.38 (d, *J* = 7.9 Hz, 1H), 9.14 (s, 1H), 8.84 (d, *J* = 8.1 Hz, 1H), 8.75 (d, *J* = 8.2 Hz, 1H), 8.31 (d, *J* = 7.9 Hz, 1H), 8.25 – 8.20 (m, 1H), 8.16 (d, *J* = 7.2 Hz, 1H), 7.93 (d, *J* = 7.6 Hz, 1H), 7.69 (dq, *J* = 20.5, 6.8 Hz, 3H), 5.19 – 5.13 (m, 2H), 2.19 – 2.11 (m, 2H), 1.58 – 1.51 (m, 2H), 1.47 – 1.40 (m, 2H), 1.29 (s, 18H), 0.89 (t, *J* = 6.3 Hz, 3H) (-NH hydrogen not seen). ¹³C

NMR (126 MHz, MeOD- d^4) δ 166.93, 151.81, 150.06, 140.74, 136.97, 135.62, 134.29, 133.79, 131.93, 131.83, 131.49, 130.79, 128.98, 128.57, 128.51, 125.62, 124.49, 124.04, 122.27, 120.65, 59.76, 33.08, 31.23, 30.80, 30.77, 30.74, 30.64, 30.56, 30.48, 30.24, 27.55, 23.74, 14.44. (one peak apparently buried under aliphatic signals). IR (neat): 3250 (w), 2920 (m), 2850 (m), 1663 (m), 1519 (s), 1500 (m), 1376 (m), 1329 (m), 1260 (m), 1159 (m), 920 (m), 839 (m), 820 (m), 764 (s), 585 (m), 415 (m) cm^{-1} . HRMS (ESI-MS) calcd = 705.1478 $[\text{M}+\text{Cs}]^+[-\text{H}]$, obsd = 705.1456. It was found as the cesium adduct.

Trifluoro(4-(1-tetradecylquinolin-1-ium-6-carboxamido)naphthalen-1-yl)borate (217)

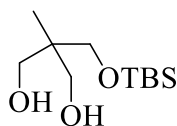


In a round-bottom flask with a stir bar, 4.5 M KHF_2 (2.03 mL, 9.12 mmol) was added dropwise to a solution of 1-tetradecyl-6-((4-(4,4,5,5-tetramethyl-1,3,2-dioxaborolan-2-yl)naphthalen-1-yl)carbamoyl)quinolin-1-ium **201** (72 mg, 0.95 mmol) in MeOH (10 mL). After 45 minutes the mixture was concentrated via rotary evaporation. The brownish-green solid was triturated with boiling acetone (4X), then boiling MeOH (3X). The remaining solid was stripped of excess solvent via rotary evaporation to give a dark green olive-colored solid. Yield 81% ^1H NMR (300 MHz, DMSO- d_6) δ 10.77 (s, 1H), 9.61 (d, $J = 5.8$ Hz, 1H), 9.41 (d, $J = 8.4$ Hz, 1H), 9.19 (s, 1H), 8.87 – 8.66 (m, 2H), 8.53 – 8.40 (m, 1H), 8.25 (t, $J = 7.1$ Hz, 1H), 7.91 (t, $J = 4.7$ Hz, 1H), 7.61 (d, $J = 7.3$ Hz, 1H), 7.41 (d, $J = 7.0$ Hz, 1H), 7.39 – 7.32 (m, 2H), 5.09 (t, $J = 7.6$ Hz, 2H), 1.99 (t, $J = 7.7$ Hz, 2H), 1.46 – 1.36 (m, 2H), 1.23 (s, 20H), 0.84 (t, $J = 6.8$ Hz, 3H). ^{13}C NMR (126 MHz, DMSO) δ 164.08, 150.70, 148.33, 138.50, 137.24, 135.41, 133.81, 130.67,

130.64, 130.58, 129.45, 128.98, 128.05, 128.02, 124.19, 123.68, 123.17, 122.87, 122.42, 119.41, 57.60, 31.27, 29.57, 29.03, 29.03 29.01, 28.99, 28.90, 28.81, 28.68, 28.50, 25.73, 22.07, 13.93.

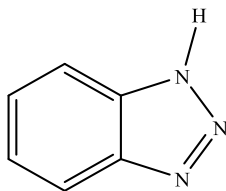
HRMS (ESI-MS) calcd = 695.2403 [M + Cs]⁺ obsd = 695.2403. It was found as the cesium adduct.

2-(((tert-Butyldimethylsilyl)oxy)methyl)-2-methylpropane-1,3-diol (222)



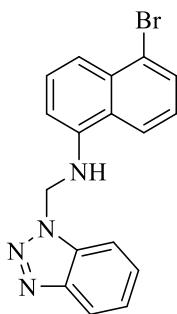
The 2-(hydroxymethyl)-2-methylpropane-1,3-diol (29.98 mmol, 3.6025 g) was dissolved in dry THF (20 mL). Next, 60% NaH (10.85 mmol, 0.4340 g) was added. The flask was fitted with a reflux column and then was stirred at 80°C under nitrogen for 24 hours. Next, the flask was removed from heat and then allowed to cool to room temperature. TBSCl was added (1.5 g, 10 mmol) and the white suspension was stirred overnight. Next, the mixture was filtered through glass floss. The filtrate was concentrated via rotary evaporation to give a white syrupy suspension. The suspension was diluted with hexanes and filtered through glass floss and celite. The filtrate was concentrated via rotary evaporation to give a clear, thick liquid. The mixture was purified by normal phase silica normal phase silica (hexanes to EtOAc gradient). Mass = 1.040 g, 44.4%. ¹H NMR (500 MHz, CDCl₃) δ 3.71 (d, *J* = 11 Hz, 2H), 3.60 (s, 2H), 3.57 (d, *J* = 11 Hz, 2H), 0.90 (s, 9H), 0.79 (s, 3H), 0.07 (s, 6H). ¹³C NMR (CDCl₃): 69.15, 68.00, 41.13, 26.00, 25.90, 18.26, -5.56. This literature compound¹⁰² was used without further characterization.

1*H*-Benzo[*d*][1,2,3]triazole (238)



In a round-bottom flask was dissolved 1*H*-benzo[*d*][1,2,3]triazol-1-ol (1.80 g, 13.31 mmol) in CHCl₃ (3.6 mL), and then PCl₃ (1.99 mL) was added dropwise with cooling over 1h. Next, the mixture was brought to heat at reflux and aged for 3 hours. The heat was removed and the mixture was concentrated via rotary evaporation to afford a crude white solid. To the white solid were added several mL of 2M HCl. Charcoal was added and the mixture was boiled for approximately 5 min. Upon cooling, the charcoal was removed via Büchner funnel filtration. The filtrate was basified with 20% KOH until pH=8, then extracted with EtOAc (4X), washed once with H₂O (5 mL), dried over MgSO₄, filtered, and concentrated to give an off-white solid. Yield 798.9 mg, 52%. Crystals from benzene, mp = 91-95°C. ¹H NMR (500 MHz, CDCl₃) δ 7.96 – 7.95 (m, 2H), 7.42 – 7.40 (m, 2H) (one proton was unobserved and presumably further downfield according to literature) ¹³C NMR (126 MHz, CDCl₃) δ 139.07, 126.23, 115.05. IR (neat): 3244 (w), 2704 (m), 1382 (m), 1004 (m), 777 (m), 738 (s), 607 (m), 423 (m), 407 (m). This literature compound was used without further purification.

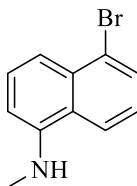
***N*-((1*H*-Benzo[*d*][1,2,3]triazol-1-yl)methyl)-5-bromonaphthalen-1-amine (250)**



To a round-bottom flask and stir bar were added 5-bromonaphthalen-1-amine **149**

(1.7768 g, 8.000 mmol), 1*H*-benzotriazole (953.0 mg, 8.000 mmol), 95% EtOH (36 mL) and then 37% formaldehyde (601 microliters, 8.00 mmol). The reaction was stirred under N₂ overnight at room temp. Next, the mixture was concentrated via rotary evaporation. The crude material was purified via recrystallization from EtOH. Yield 1.950 g, 69%, mp = 191-193°C. ¹H NMR (300 MHz, CDCl₃) δ 8.05 (d, *J* = 8.6 Hz, 1H), 7.85 (d, *J* = 8.3 Hz, 1H), 7.81 – 7.68 (m, 2H), 7.59 (d, *J* = 8.9 Hz, 1H), 7.49 – 7.28 (m, 4H), 7.11 (d, *J* = 8.1 Hz, 1H), 6.28 (d, *J* = 6.4 Hz, 2H), 5.49 (s, 1H). ¹³C NMR (75 MHz, CDCl₃) δ 140.34, 133.02, 132.65, 130.50, 127.89, 127.79, 125.71, 125.23, 124.32, 124.14, 120.41, 119.77, 119.72, 109.60, 108.82, 58.56. (two aromatic carbons apparently overlap. IR (neat): 3377 (w), 1591 (w), 1536 (m), 1277 (m), 1150 (m), 1208 (w), 1028 (w), 989 (w), 768 (s), 752 (s), 554 (w), 431 (w) cm.⁻¹

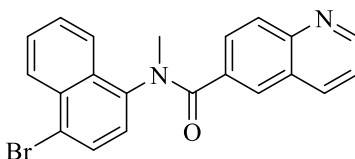
5-Bromo-*N*-methylnaphthalen-1-amine (240)



In a dry round-bottom flask and stir bar, *N*-((1*H*-benzo[*d*][1,2,3]triazol-1-yl)methyl)-5-bromonaphthalen-1-amine **250** (220 mg, 0.623 mmol) was dissolved in dry THF (3.1mL) and NaBH₄ (117.8 mg, 3.114 mmol) was quickly added with vigorous stirring. The solution was aged at 50°C overnight. Next, the mixture was concentrated via rotary evaporation. The crude product was dissolved in DCM, washed with 5% NaHCO₃ (3x3mL), dried over MgSO₄, filtered, and concentrated via rotary evaporation, giving a thick golden liquid. Yield 112 mg (76%). ¹H NMR (300 MHz, CDCl₃) δ 7.73 (d, *J* = 6.9 Hz, 2H), 7.63 (d, *J* = 8.5 Hz, 1H), 7.46 (t, *J* = 8.1 Hz, 1H),

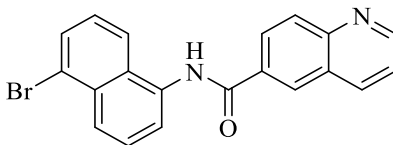
7.20 (d, $J = 7.6$ Hz, 1H), 6.63 (d, $J = 7.6$ Hz, 1H), 4.41 (s, 1H), 2.99 (s, 3H). ^{13}C NMR (75 MHz, CDCl_3) δ 144.91, 132.94, 130.14, 128.29, 124.79, 124.76, 123.93, 119.86, 116.40, 104.82, 31.23.

***N*-(4-Bromonaphthalen-1-yl)-*N*-methylquinoline-6-carboxamide (254)**



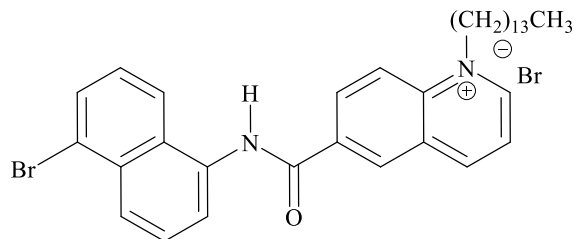
To a dry round-bottom flask containing a precooled mixture of 60% NaH (200. mg, 5.00 mmol) in dry THF (16 mL) and a stir bar, *N*-(4-bromonaphthalen-1-yl)quinoline-6-carboxamide **202** (770. mg, 2.00 mmol) in dry THF (18 mL) was quantitatively transferred. After 15 minutes at 0°C , MeI (312 microliters, 5.00 mmol) was added dropwise and then the ice bath was removed. The mixture was aged for 3 hrs. Next, the mixture was quenched with water (~25 mL) and then it was extracted with DCM (3x25 mL). The pooled organic extracts were washed twice with satd. NaCl, dried over MgSO_4 , filtered, and then concentrated via rotary evaporation to give a crude solid. The material was purified by recrystallization from benzene. Yield 521 mg, 66%, mp = $172 - 174^\circ\text{C}$. ^1H NMR (500 MHz, CDCl_3) δ 8.83 (d, $J = 2.6$ Hz, 1H), 8.26 (d, $J = 8.4$ Hz, 1H), 8.12 (d, $J = 8.3$ Hz, 1H), 7.90 (d, $J = 8.2$ Hz, 1H), 7.85 (s, 1H), 7.74 (t, $J = 7.3$ Hz, 1H), 7.71 – 7.64 (m, 2H), 7.53 (d, $J = 7.8$ Hz, 1H), 7.44 (d, $J = 8.8$ Hz, 1H), 7.31 (dd, $J = 8.3, 4.2$ Hz, 1H), 6.99 (d, $J = 7.8$ Hz, 1H), 3.58 (s, 3H). ^{13}C NMR (126 MHz, CDCl_3) δ 171.17, 151.71, 148.45, 140.92, 136.76, 133.96, 133.08, 131.12, 129.73, 129.11, 128.56, 128.51, 128.28, 128.27, 128.16, 127.33, 127.05, 123.24, 122.95, 121.73, 38.87. IR (neat): 3322 (w), 3069 (w), 2927 (w), 2849 (w), 1641 (s), 1462 (m), 1415 (m), 1384 (m), 1349 (s), 1317 (m), 1283 (m), 1719 (m), 921 (m), 843 (m), 783 (s), 756 (s), 594 (m), 462 (m), 426 (m) cm^{-1} .

***N*-(5-Bromonaphthalen-1-yl)quinoline-6-carboxamide (272)**



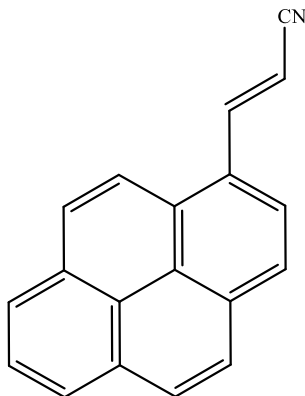
An ice-cold solution of 1,5-bromonaphthylamine **149** (2.221 g, 10 mmol) in DCM (200 mL) was quantitatively transferred to an ice-cold solution containing quinoline-6-carboxylic acid (1.732 g, 10.00 mmol), DCC (2.476 g, 12.00 mmol), and HOBT (1.6216 g, 12.00 mmol) dissolved in DCM (70 mL), ACN (7 mL) and dry DMF (14 mL). The ice bath was removed and the mixture aged at room temperature overnight. Next, the mixture was filtered through a Büchner funnel to remove DCU. The filtrate was concentrated via rotary evaporation and then filtered again. The filtrate was washed with half satd. NaCl (3x20 mL), then satd. NaCl (2x20 mL). The organic layer was concentrated via rotary evaporation. The light orange-colored solid residue was recrystallized from 95% EtOH to give a bone-colored solid. Yield 1.076 g, 29%, mp = 216 - 218°C ¹H NMR (500 MHz, DMSO-*d*₆) δ 10.83 (s, 1H), 9.03 (d, *J* = 2.7 Hz, 1H), 8.80 (s, 1H), 8.57 (d, *J* = 8.1 Hz, 1H), 8.39 (d, *J* = 8.7 Hz, 1H), 8.17 (d, *J* = 8.9 Hz, 2H), 8.11 (d, *J* = 8.4 Hz, 1H), 7.95 (d, *J* = 7.3 Hz, 1H), 7.80 (d, *J* = 7.2 Hz, 1H), 7.75 (t, *J* = 7.9 Hz, 1H), 7.66 (dd, *J* = 8.3, 4.2 Hz, 1H), 7.48 (t, *J* = 8.0 Hz, 1H). ¹³C NMR (126 MHz, DMSO) δ 165.96, 152.29, 148.89, 137.29, 135.11, 132.48, 131.89, 130.68, 130.40, 129.13, 128.79, 128.28, 127.53, 127.21, 126.58, 124.76, 124.50, 124.01, 122.31, 122.04. IR (neat): 3276 (m), 1642 (s), 1527 (s), 1393 (m), 1282 (m), 902 (m), 847 (s), 779 (s), 695 (m) cm.⁻¹

6-((5-Bromonaphthalen-1-yl)carbamoyl)-1-tetradecylquinolin-1-ium bromide (284)



To an oven dried round-bottom flask and stir bar, *N*-(5-bromonaphthalen-1-yl)quinoline-6-carboxamide **272** (1.00 mmol, 314 mg) was suspended in dry toluene (5 mL). To the suspension was added bromotetradecane (1.20 mmol, 389 mg). The mixture was brought to heat at reflux allowed to age with stirring for 72 hours. No conversion was detected by TLC. As a result, dry DMF (3 mL) was added and the temperature was maintained at 105°C. The reaction progress was monitored by TLC for an *additional* 7 days. The reaction was removed from heat, diluted with EtOAc (~25 mL) and a brown solid was precipitated from the solution and filtered to give a dry grainy brown solid (mass = 375 mg, 57%). The material was purified on silica with a gradient of toluene:methanol 95:5 to toluene:MeOH 80:20 and finally MeOH 100%. The fractions were combined and then concentrated via rotary evaporation to give a brown residue. mass=164 mg, 25%). ¹H NMR (300 MHz, MeOD-*d*₄) δ 9.54 (d, *J* = 5.2 Hz, 1H), 9.29 (t, *J* = 7.0 Hz, 1H), 9.09 (s, 1H), 8.79 (d, *J* = 7.0 Hz, 1H), 8.69 (d, *J* = 5.8 Hz, 1H), 8.26 – 8.05 (m, 3H), 7.90 – 7.74 (m, 2H), 7.74 – 7.60 (m, 1H), 7.42 (t, *J* = 7.5 Hz, 1H), 7.33 (d, *J* = 5.5 Hz, 1H), 5.12 (t, *J* = 7.3 Hz, 2H), 2.22 – 2.02 (m, 2H), 1.53 – 1.28 (m, 22H), 0.89 (t, *J* = 6.5 Hz, 3H). NMR (75 MHz, MeOD-*d*₄) δ 166.79, 151.72, 149.96, 140.54, 136.76, 135.57, 133.24, 131.90, 131.71, 131.30, 129.32, 128.09, 127.97, 127.90, 127.37, 126.16, 124.12, 123.98, 123.88, 120.54, 59.71, 49.84, 33.04, 31.21, 30.76, 30.74, 30.61, 30.53, 30.45, 30.21, 27.52, 23.71, 14.43. (one aliphatic peak is presumably buried between 31.21 and 30.21 ppm).

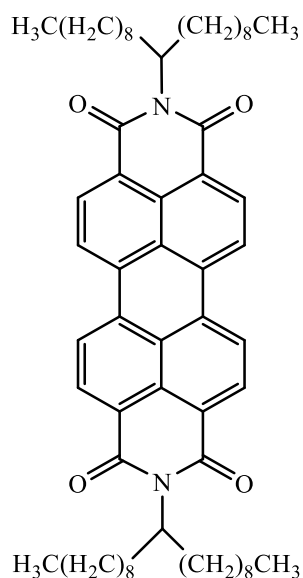
(E)-3-(Pyren-1-yl)acrylonitrile (291)



A flame-dried round-bottom flask containing a stir bar and Na-benzophenone THF (90 mL) was cooled in a dry-ice acetone bath to -78°C . *n*BuLi in hexane (14.35 mL, 33.00 mmol) and dry ACN (2.601 mL, 49.5 mmol) were added dropwise sequentially. This was allowed to stir for 20 min. at -78°C . Next, $(i\text{Pr}_2\text{N})_2\text{BCl}^{155}$ (4.52 mL, 16.50 mmol) was added and the flask was placed in a dry-ice/ACN bath at -40°C and allowed to stir for 1h. Next, the mixture was returned to the dry-ice/acetone -78°C bath and cooled. 1-Pyrenecarboxaldehyde (3.4541 g, 15.00 mmol), was dissolved in minimal THF and quantitatively transferred in three portions to the parent flask. This was stirred for an hour at -78°C . The mixture was then quenched with half-satd. NH_4Cl (150 mL) for 30 min. and allowed to come to room temp. The biphasic mixture was extracted with EtOAc (4X). The pooled organic extracts were combined and dried over MgSO_4 , filtered through a Büchner funnel, and concentrated on rotary evaporation to give a yellow-orange solid which was purified via normal phase silica (toluene:EtOAc 99:1) to yield the mixed E/Z isomers (1.723 g, 45.4%, E:Z 87:13) as a yellow-orange solid. In order to isolate the (*E*)-isomer from the E:Z mixture, fractional recrystallization with ethanol gave the pure (*E*)-isomer in the latter fractions. (*E*)-isomer yield 808 mg, 21%, mp = $164 - 165.5^{\circ}\text{C}$. $^1\text{H NMR}$ (500 MHz, CDCl_3) δ

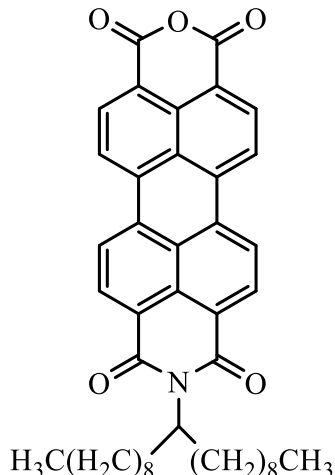
8.49 (d, $J = 16.4$ Hz, 1H), 8.30 – 8.22 (m, 3H), 8.20 – 8.10 (m, 4H), 8.09 – 8.02 (m, 2H), 6.10 (d, $J = 16.4$ Hz, 1H). ^{13}C NMR (126 MHz, CDCl_3) δ 147.58, 133.50, 131.43, 130.73, 129.43, 129.30, 127.41, 127.24, 126.70, 126.63, 126.36, 125.26, 124.99, 124.65, 123.44, 121.87, 118.81, 98.03. (one aromatic peak presumably buried in aromatic region). This literature compound¹⁵⁶ was used without further characterization.

***N,N'*-Di(10-Nonadecyl)perylene-3,4,9,10-bis(dicarboximide) (288) “PDI”**



A mixture of 3,4,9,10-perylenetetracarboxylic dianhydride (1.417 g, 3.610 mmol), 10-nonadecanamine (8.850 mmol, 2.509 g), imidazole (7.011 g, 103.0 mmol), and zinc acetate (595 mg, 2.71 mmol) was heated, with stirring, at 160 °C for 2 h. The mixture was then removed from heat and allowed to cool to room temperature. Product was purified via normal phase silica (chloroform 100%). Yield 2.579 g, 77%.

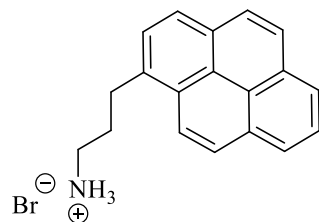
***N*-(10-Nonadecyl)-3,4,9,10-perylenetetracarboxylic acid 3,4-anhydride-9,10-imide (350)
“PMA”**



In a round-bottom flask with a stir bar, *t*-BuOH (225 mL) was added to a mixture of *N,N'*-di(10-nonadecyl)perylene-3,4,9,10-bis(dicarboximide) **288** (20.75 g, 22.47 mmol) and 85% KOH pellets (5.13 g, 77.7 mmol). The flask was fitted with a reflux condenser and brought to heat at reflux. After 30 minutes, approximately 15 additional pellets of KOH were added and the reflux was resumed for 1 hour. The mixture was removed from heat and then poured with stirring into a mixture of acetic acid (225 mL) and 2M HCl (225 mL). The red precipitate was filtered over a bed of Celite on a glass-fritted 600 mL C-40-60 filter. The red filter cake was washed with H₂O (3 x 400 mL), air dried, then placed into an oven to dry at 100°C for several days. The Celite/red precipitate mixture was jointly removed from the funnel, dissolved in CHCl₃/acetic acid and filtered. Due to filter clogging, this had to be repeated 4 times. The organic filtrates were pooled and filtered once more through the C-40-60 filter. The filtrate was concentrated via rotary evaporation. Purification was via normal phase silica on a gradient (chloroform:acetic acid 96:4 with increasing acetic acid). Yield 14.035 g, 95% ¹H NMR (500 MHz, CDCl₃) δ 8.76 – 8.55 (m, 8H), 5.18 (tt, *J* = 9.4, 5.8 Hz, 1H), 2.24 (qd, *J* = 9.7, 5.3 Hz, 2H), 1.87 (tt, *J* = 13.4, 10.6, 4.8 Hz, 2H), 1.39 – 1.15 (m, 28H), 0.82 (t, *J* = 6.9 Hz, 6H). IR (neat): 2920 (s), 2851 (s), 1769 (s), 1698 (s), 1657 (s), 1592 (s), 1505 (w), 1456 (m), 1404 (m), 1313 (s),

1247 (w), 1123 (m), 1012 (m), 862 (m), 808 (s), 734 (s), 433 (m). This literature compound^{13, 144} was used without further characterization.

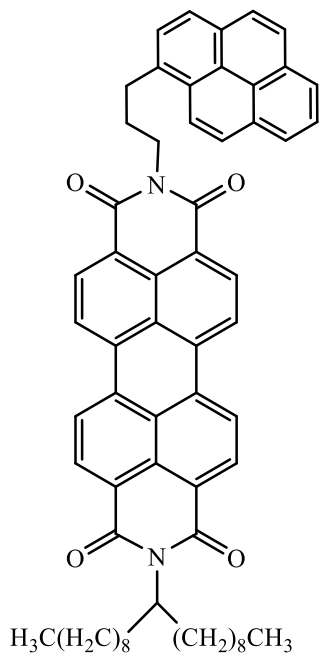
3-(Pyren-1-yl)propan-1-aminium bromide (313)



To a stirring yellow suspension of 1-pyrenebutyric acid (2.20 g, 7.6 mmol) in 70 mL of DCM and a small amount of DMF (< 0.1 mL), oxalyl chloride (0.75 mL, 8.6 mmol) was added dropwise under an argon atmosphere. The solution was stirred for 35 min. at room temperature and then the solvent was removed via rotary evaporation. The solid residue was dissolved in 10 mL of dry acetone and added dropwise to a stirring solution of NaN₃ (0.6 g, 9.3 mmol) in 2 mL of water at 0°C. The reaction was warmed to room temperature and stirred for 1h before pouring it over 30 mL of water to precipitate the acyl azide intermediate. The mixture was filtered and the solid material was washed with water before being dried under vacuum. The dried solid was suspended in 10 mL of dry benzene and heated to boiling for ~ 90 min. until no more gas was evolved. The solution was then cooled to room temperature and the solvent was removed via rotary evaporation leaving a brown oil. The oil was dissolved in 10 mL of dry THF and heated to 60°C and concentrated HCl was added dropwise until no further gas evolution was observed. The mixture was stirred for 30 min. and then made alkaline using a 10% NaOH aqueous solution. The solution was extracted with 50 mL of CHCl₃ 5 times and then the pooled organic fractions were collected and then washed once with sat. NaCl, dried with MgSO₄, and filtered before removing the solvent via rotary evaporation. The residue was placed under high vac. overnight. A ¹H NMR was obtained of this literature compound¹⁴⁵, which confirmed the

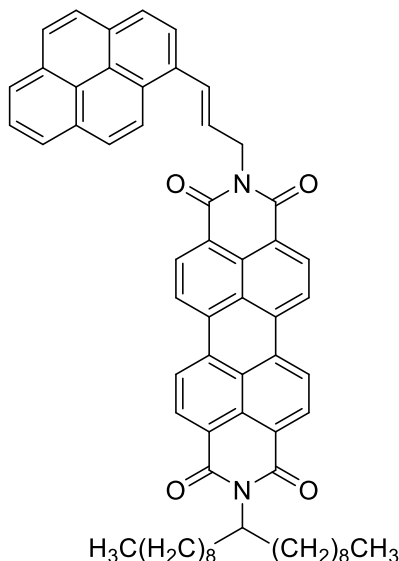
presence of the target along with impurities. The crude yield was 1.879 g, 94.9%. Next, to the flask was added THF (17 mL) and 25% HBr in AcOH (12.4 mL). The mixture was stirred for several hours (~3 hrs). Ether was added to precipitate a tan colored solid which was collected on a Büchner funnel and then air dried (mass was not obtained). The purity of the HBr salt was analyzed by converting the HBr salt to the free base and obtaining a TLC. A small portion of the solid was recrystallized from H₂O but did not give a sharp melting point. This too was converted to the free base and a TLC was obtained against the material which had *not* been recrystallized. The TLCs were identical, both showed a major and a minor spot. A qualitative assay for amine was performed on TLC with ninhydrin (both spots were positive for amine). No further purification was attempted of **313**.

2-(Nonadecan-10-yl)-9-(3-(pyren-1-yl)propyl)anthra[2,1,9-def:6,5,10-d'e'f']diisoquinoline-1,3,8,10(2H,9H)-tetraone (317)



In a stirred solution of 3-(pyren-1-yl)propan-1-aminium bromide **313** (126 mg, 0.37 mmol) in 10 mL of MeOH were dissolved 3 pellets of 85% KOH. An equal volume of water was added and the cloudy mixture was extracted with DCM (3x) and the pooled organic extracts were dried over MgSO₄, filtered and concentrated in vacuo. The free amine was then dissolved in 10 mL of toluene containing the perylene imide anhydride **350** (85 mg, 0.13 mmol). The mixture was brought to heat at reflux. After 85 min., the heat was lowered to 55°C and the mixture was aged overnight. The heat was removed and the mixture was concentrated in vacuo. The residue was isolated via gradient on normal phase silica (toluene:CHCl₃ 1:9 to DCM:acetic acid 95:5). Yield 49 mg, 42%. A sample was recrystallized from hexanes, mp = 245 - 247°C. ¹H NMR (500 MHz, CDCl₃) δ 8.58 (d, *J* = 13.6 Hz, 2H), 8.39 – 8.24 (m, 4H), 8.24 – 8.07 (m, 3H), 8.00 (d, *J* = 6.6 Hz, 1H), 7.95 (d, *J* = 9.2 Hz, 1H), 7.83 (s, 2H), 7.79 (d, *J* = 6.7 Hz, 2H), 7.64 (d, *J* = 8.8 Hz, 1H), 7.57 (d, *J* = 8.8 Hz, 1H), 5.20 (ddd, *J* = 15.0, 9.2, 5.9 Hz, 1H), 4.39 (t, *J* = 6.9 Hz, 2H), 3.44 (t, *J* = 7.3 Hz, 2H), 2.41 (q, *J* = 7.8, 7.4 Hz, 2H), 2.33 – 2.20 (m, 2H), 1.90 (ddt, *J* = 14.6, 10.7, 5.3 Hz, 2H), 1.43 – 1.13 (m, 28H), 0.83 (t, *J* = 6.9 Hz, 6H). ¹³C NMR (126 MHz, CDCl₃) δ 164.76, 163.72, 163.28, 135.71, 134.21, 131.77, 131.23, 130.94, 130.80, 129.54, 129.44, 128.80, 128.53, 127.35, 127.29, 126.83, 126.23, 126.13, 125.88, 125.69, 125.02, 124.80, 124.72, 124.68, 124.66, 123.39, 123.18, 122.92, 122.78, 122.51, 54.96, 40.59, 32.55, 32.02, 30.82, 29.74, 29.72, 29.44, 28.72, 27.20, 22.80, 14.24. IR (neat): 2920 (m), 2851 (m), 1693 (s), 1652 (s), 1593 (s), 1436 (m), 1403 (m), 1336 (s), 1249 (m), 1249 (m), 840 (s), 808 (s), 743 (s), 618 (w), 431 (w) cm.⁻¹

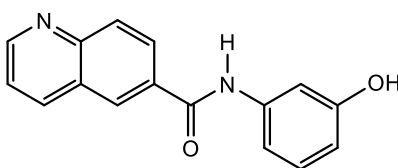
(E)-2-(Nonadecan-10-yl)-9-(3-(pyren-1-yl)allyl)anthra[2,1,9-def:6,5,10-d'e'f']diisoquinoline-1,3,8,10(2H,9H)-tetraone (319)



(E)-3-(Pyren-1-yl)prop-2-en-1-amine **295** (57 mg, 0.22 mmol,) was dissolved in 7 mL of toluene containing the perylene imide anhydride **350** (46 mg, 0.13 mmol). The mixture was brought to heat at reflux. After 120 min., the mixture was cooled to 30°C and aged overnight. The mixture was then concentrated via rotary evaporation. The residue was isolated via gradient on normal phase silica (DCM to DCM:acetic acid). Yield (40.2 mg, 64%). Recrystallization from benzene, mp = 309 - 312°C. ¹H NMR (500 MHz, CDCl₃) δ 8.42 (t, *J* = 9.1 Hz, 4H), 8.24 – 8.11 (m, 4H), 8.04 (d, *J* = 7.6 Hz, 1H), 7.89 (d, *J* = 7.8 Hz, 2H), 7.83 (d, *J* = 6.8 Hz, 1H), 7.81 – 7.71 (m, 3H), 7.65 (q, *J* = 8.4 Hz, 2H), 7.51 (d, *J* = 15.7 Hz, 1H), 6.48 (dt, *J* = 14.9, 6.4 Hz, 1H), 5.23 – 5.12 (m, 1H), 5.02 (d, *J* = 6.4 Hz, 2H), 2.32 – 2.18 (m, 2H), 1.91 (dd, *J* = 11.9, 6.4 Hz, 2H), 1.45 – 1.09 (m, 28H), 0.82 (t, *J* = 6.7 Hz, 6H). ¹³C NMR (126 MHz, CDCl₃) δ 164.64, 163.65, 163.22, 134.38, 133.98, 133.97, 131.51, 131.40, 131.16, 130.99, 130.77, 130.63, 130.58, 129.17,

129.07, 127.84, 127.45, 127.26, 127.00, 126.40, 126.01, 125.85, 125.14, 124.95, 124.89, 124.47, 124.44, 123.70, 122.90, 122.89, 122.77, 122.67, 54.89, 42.69, 32.56, 32.02, 29.75, 29.73, 29.44, 27.24, 22.80, 14.24, 0.15. IR (neat): 3041 (w), 2920 (m), 2851 (s), 1683 (s), 1651 (s), 1591 (s), 1554 (s), 1434 (m), 1402 (m), 1328 (s), 1245 (s), 1168 (m), 963 (m), 840 (m), 807 (s), 746 (s), 712 (m), 492 (m).

***N*-(3-Hydroxyphenyl)quinoline-6-carboxamide (322)**

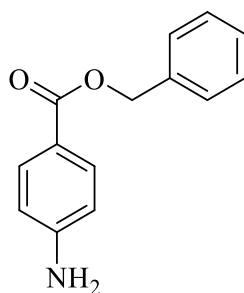


To a 250 mL round-bottom flask with a stir bar was added THF (54 mL) distilled from Na-benzophenone. This mixture was then sparged with dry argon for 30 min. and then cooled to 0°C. Next, 6-quinolinecarboxylic acid (1.7317 g, 10.00 mmol), DCC (2.6823 g, 13.00 mmol), HOBt (1.7567 g, 13.00 mmol), and 3-aminophenol (1.0913 g, 10.00 mmol) were added. The ice bath was removed and the mixture was allowed to age overnight at room temperature. Next, the mixture was concentrated via rotary evaporation to remove THF. The mixture was then diluted with EtOAc (30 mL) and was acidified with 5% HCl to pH = 1-2 and was stirred at room temperature for 45 min. The mixture was filtered through a Büchner funnel and the solid was rinsed with EtOAc.

The filtrate was diluted with water and 5% HCl then washed with EtOAc (3x40 mL) and the pooled organic extracts were discarded. The filter-cake was returned to the aqueous layer and the pH was adjusted to pH = 7.5 with satd. NaHCO₃. The mixture was extracted with EtOAc

(3x20 mL). The pooled organic extracts were filtered via Büchner funnel to remove the DCU by-product and then were concentrated via rotary evaporation. The semi-pure solid was recrystallized from EtOH. Yield 314.1 mg, 12%. mp = 238 - 240°C. ¹H NMR (500 MHz, DMSO-d₆) δ 10.37 (s, 1H), 9.44 (s, 1H), 9.01 (d, *J* = 4.1 Hz, 1H), 8.61 (s, 1H), 8.54 (d, *J* = 8.4 Hz, 1H), 8.24 (d, *J* = 8.9 Hz, 1H), 8.13 (d, *J* = 8.7 Hz, 1H), 7.64 (dd, *J* = 8.3, 4.1 Hz, 1H), 7.40 (s, 1H), 7.21 (d, *J* = 8.2 Hz, 1H), 7.14 (t, *J* = 8.0 Hz, 1H), 6.53 (d, *J* = 7.8 Hz, 1H). ¹³C NMR (75 MHz, DMSO-d₆) δ 165.57, 158.07, 152.70, 149.20, 140.65, 137.67, 133.43, 129.82, 129.55, 128.89, 128.63, 127.55, 122.75, 111.59, 111.45, 107.94. IR (neat): 3293 (m), 3131 (m), 3078 (m), 3030 (m), 2982 (m), 2931 (m), 2851 (m), 2732 (m), 2655 (m), 2732 (m), 2655 (m), 2605 (m), 1635 (m), 1614 (s), 1550 (s), 1443 (s), 1376 (m), 1274 (s), 1237 (s), 1200 (s), 1158 (m), 979 (m), 899 (m), 871 (s), 836 (s), 766 (s), 687 (s), 583 (m), 502 (m), 477 (m), 456 (m) cm⁻¹. HRMS (ESI-MS+) calcd = 396.9953 [M - Cs]⁺[-H], obsd = 396.9945. It was found as the cesium adduct.

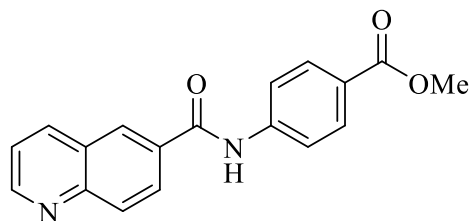
Benzyl 4-Aminobenzoate (332)



To an oven-dried round-bottom flask and stir bar was added p-aminobenzoic acid (137 mg, 1.00 mmol), diluted with dry DMF (10 mL) and cooled under argon to 0°C. KOtBu (123 mg, 1.10 mmol) was then added. After 15 min, freshly opened benzyl bromide (131 μL, 1.10 mmol) was added dropwise and the reaction was aged overnight at room temperature. Next, the

mixture was quenched with H₂O (5 mL) and after 1 hr the mixture was diluted with additional water (25 mL) and extracted with EtOAc (3 x 20 mL). The pooled organic extracts were washed alternatively with brine and then water until DMF was gone. Unreacted p-aminobenzoic acid, as detected by TLC, was removed by washing with 5% NaHCO₃. The organic layer was then dried over MgSO₄, filtered through cotton, and then concentrated via rotary evaporation. The residue was isolated via normal phase silica (hexanes:EtOAc 3:1). Yield = 65.4 mg, 29 %. ¹H NMR (500 MHz, CDCl₃) δ 7.90 (d, *J* = 8.6 Hz, 2H), 7.44 (d, *J* = 6.9 Hz, 2H), 7.38 (t, *J* = 7.2 Hz, 2H), 7.35 – 7.29 (m, 1H), 6.64 (d, *J* = 8.6 Hz, 2H), 5.32 (s, 2H), 4.05 (s, 2H). This literature compound¹⁵⁷ was used without further characterization.

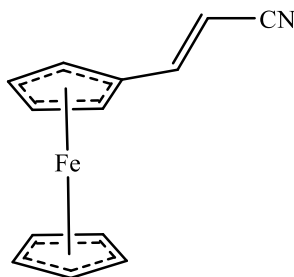
Methyl 4-(Quinoline-6-carboxamido)benzoate (335)



To a flame-dried round-bottom flask and stir bar were added 6-quinolinecarboxylic acid (3.536 g, 20.00 mmol) and SOCl₂ (11.6 mL). The flask was fitted with a septum and a nitrogen balloon. The mixture was brought to heat at reflux for ~30 minutes; additional SOCl₂ (11.6 mL) was added. After 3.5 hrs the mixture was removed from heat. Excess SOCl₂ was stripped via rotary evaporation. Next, the mixture was diluted with DCM (50 mL), then transferred dropwise via cannula to a pre-made solution of p-aminobenzoate (3.023 g, 20.00 mmol) and dry distilled triethylamine (11.5 mL) in DCM (80 mL) in an oven-dried round-bottom flask with a stir bar. The mixture was brought to heat at reflux for 45 min., then the heat was turned down and the

mixture was aged overnight at 30°C. Next, the mixture was quenched with DI H₂O (50 mL). After stirring for 30 min. the mixture was transferred to a 1L sep. funnel and additional DCM was added until the total organic volume was ~250 mL. The organic layer was washed with 5 % NaHCO₃ (5 x 125 mL) and then once with satd. NaCl (50 mL), dried over MgSO₄, filtered through cotton, and then concentrated via rotary evaporation to give a crude sticky orange residue (mass=2.2147 g). The residue was purified by recrystallization from EtOH. Yield = 1.348 g, 22%. mp = 213 - 215°C. ¹H NMR (500 MHz, DMSO-d₆) δ 10.82 (s, 1H), 9.02 (s, 1H), 8.66 (s, 1H), 8.54 (d, *J* = 8.1 Hz, 1H), 8.26 (d, *J* = 8.6 Hz, 1H), 8.15 (d, *J* = 8.6 Hz, 1H), 8.00 (s, 4H), 7.66 (s, 1H), 3.85 (s, 3H). ¹³C NMR (126 MHz, DMSO-d₆) δ 165.84, 165.58, 152.42, 148.86, 143.60, 137.22, 132.38, 130.18, 129.20, 128.74, 128.06, 127.04, 124.45, 122.36, 119.62. IR: 3336 (m), 3061 (w), 2989 (w), 2944 (m), 2845 (w), 1710 (s), 1663 (s), 1592 (m), 1520 (m), 1493 (m), 1436 (m), 1318 (m), 1276 (s), 1181 (m), 1108 (m), 1020 (w), 972 (w), 918 (m), 845 (m), 799 (m), 782 (m), 769 (s), 666 (m), 594 (m), 480 (m), 382 (m) cm⁻¹

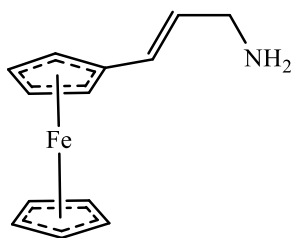
(*E*)-3-Ferrocenylacrylonitrile (346)



To a round-bottom flask and stir bar were added ferrocenecarboxaldehyde (2.650 g, 12.00 mmol), diethyl cyanomethylphosphonate (2.37 mL, 14.40 mmol), solid K₂CO₃ (5.08 g, 36.00 mmol), and EtOH (33 mL). The mixture was brought to heat at reflux and was stirred

under an argon atmosphere for 1h, then cooled to room temperature. The solvent was stripped via rotary evaporation. Next, the residue was transferred to a separatory funnel with diethyl ether and water (40 mL:40 mL). The aqueous layer was extracted with diethyl ether (3 x 30 mL). The pooled organic extracts were then washed with water, 0.5 M HCl, water, and brine, and then dried over MgSO₄, filtered to remove MgSO₄, and the filtrate was concentrated via rotary evaporation to give a reddish-amber colored solid. The residue was isolated via normal phase silica (cyclohexane:diethyl ether 9:1). Yield 2.337 g, 82% as a 9:1 mixture of (*E*:*Z*)-isomers. (*E*)-isomer only (2.1 g, 74%) was obtained following recrystallization from *n*-pentane. (mp = 95 - 97°C). ¹H NMR (300 MHz, CDCl₃) δ 7.27 (d, *J* = 16.3 Hz, 1H), 5.42 (d, *J* = 16.3 Hz, 1H), 4.44 (d, *J* = 7.9 Hz, 4H), 4.17 (d, *J* = 7.9 Hz, 5H). ¹³C NMR (75 MHz, CDCl₃) δ 151.65, 119.12, 91.71, 77.97, 71.40, 69.82, 68.10. IR (neat): 3086 (w), 3046 (w), 2917 (w), 2850 (w), 2205 (m), 1607 (m), 1446 (w), 1408 (w), 1374 (w), 1247 (m), 1104 (m), 1044 (m), 1030 (m), 997 (s), 928 (w), 867 (w), 816 (s), 740 (m), 666 (w), 635 (w), 494 (s), 470 (s), 418 (s). HRMS (ESI-MS+) calcd = 369.9295[M - Cs]⁺[-H], obsd = 369.9084. It was found as the cesium adduct.

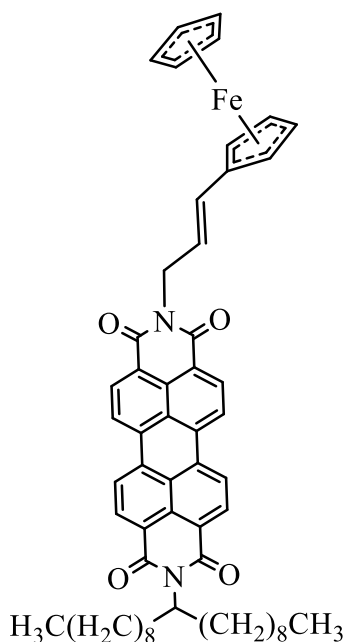
(*E*)-3-Ferrocenylprop-2-en-1-amine (352)



To a flame-dried pear-shaped 10 mL flask was added **346** (474 mg, 2.00 mmol) dissolved in dry diethyl ether (4.5 mL). This solution was added dropwise to a suspension of LAH (190. mg, 5.00 mmol) in dry diethyl ether (1.4 mL). The mixture was aged overnight at room

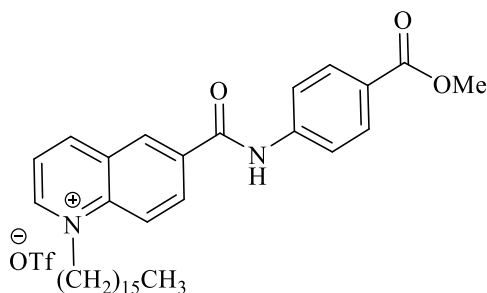
temperature. Next, the mixture was cooled to 0°C. Fieser's workup method was employed: slow addition of H₂O (190 μL) then 15% NaOH (190 μL) then H₂O (570 μL). The ice bath was removed and the mixture was warmed to room temperature and then stirred for 30 min. MgSO₄ was added with continued stirring for 15 min. Next, the mixture was filtered over a bed of ether-washed Celite on an ASTM 10-15 fritted filter. The filtrate was concentrated via rotary evaporation to give a dark golden viscous liquid which was purified via normal phase silica column to give an 84:16 mixture of unsaturated:saturated products, **346**:3-Ferrocenylpropylamine, respectively. Yield 358 mg 74%. The NMR spectra were *only* used to confirm the presence of the target's 2 vinylic peaks and 1 allylic peak. ¹H NMR (300 MHz, CDCl₃) δ 6.21 (d, *J* = 15.4 Hz, 1H), 5.90 (d, *J* = 15.6 Hz, 1H), 3.32 (s, 2H). ¹³C NMR (75 MHz, CDCl₃) 128.65, 127.06, 44.46. IR (neat): 3360 (m), 3089 (m), 1578 cm.⁻¹ This literature compound¹⁵³ was used without further purification.

***N*-(10-Nonadecyl)-*N*'-(3-ferrocenylallyl)perylene-3,4,9,10-bis(dicarboximide) (353)**



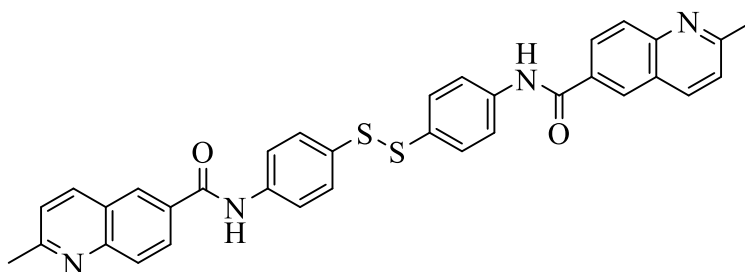
To a round-bottom flask with a stir bar was added ferroceneallylamine **352** (152 mg, 0.231 mmol) dissolved in toluene (20 mL). A reflux condenser was fitted to the flask and the mixture was brought to heat at reflux. After 100 minutes the heat was removed. The mixture was aged overnight at room temperature. The mixture was stripped of solvent via rotary evaporation. The solid was purified on normal phase silica (chloroform:acetic acid 97:3). Yield 162 mg, 79%. ^1H NMR (500 MHz, CHCl_3) δ 8.74 – 8.29 (m, 8H), 6.54 (d, $J = 14.9$ Hz, 1H), 5.92 (s, 1H), 5.19 (td, $J = 10.2, 9.2, 4.6$ Hz, 1H), 4.82 (d, $J = 5.9$ Hz, 2H), 4.61 – 4.04 (m, 9H), 2.36 – 2.17 (m, 2H), 1.91 – 1.87 (m, 2H), 1.42 – 1.15 (m, 28H), 0.83 (t, $J = 6.8$ Hz, 6H). ^{13}C NMR (126 MHz, CDCl_3) δ 164.65, 164.63, 163.07, 134.65, 134.24, 132.78, 131.89, 131.82, 131.37, 131.12, 129.57, 129.37, 126.41, 126.29, 124.20, 123.24, 123.14, 123.01, 120.23, 70.14, 70.05, 69.60, 67.54, 54.98, 42.56, 32.52, 32.01, 29.71, 29.42, 27.15, 22.79, 14.23. HRMS (ESI-MS) calcd = 1013.2958 $[\text{M}+\text{Cs}^+]^+$, observed = 1013.2359. Found as the cesium adduct. IR (neat): 3089 (w), 2929 (m), 2851 (m), 2349 (w), 2330 (w), 2324 (w), 1695 (s), 1654 (s), 1592 (m), 1458 (w), 1433 (m), 1402 (m), 1330 (s), 1245 (m), 1167 (m), 1124 (m), 1104 (m), 961 (m), 851 (m), 808 (s), 744 (s), 670 (m), 666 (m), 494 (m), 482 (m), 429 (m).

1-Hexadecyl-6-((4-(methoxycarbonyl)phenyl)carbamoyl)quinolin-1-ium trifluoromethanesulfonate, 357



To a flame-dried flask containing a stir bar under an argon atmosphere was added methyl 4-(quinoline-6-carboxamido)benzoate **335** (0.100 mmol, 30.6 mg) suspended in dry DCM (2.5 mL). Next, hexadecyl trifluoromethanesulfonate **355** (0.350 mmol, 131 mg) was added dropwise at room temperature and was then aged for two days. The suspension had become a clear yellow-tinted solution. The solution was concentrated via rotary evaporation and was then triturated with hexanes (2X) to remove the excess alkylating reagent. The remaining tan-colored solid was transferred into a Büchner funnel with the addition of several mLs of cold hexanes and was air dried to give a tan solid mass = 52 mg, 75% yield. ¹H NMR (500 MHz, Methanol-d₄) δ 9.52 (d, *J* = 5.8 Hz, 1H), 9.34 (d, *J* = 8.2 Hz, 1H), 9.01 (d, *J* = 1.8 Hz, 1H), 8.76 (d, *J* = 9.3 Hz, 1H), 8.71 (d, *J* = 9.3 Hz, 1H), 8.20 (dd, *J* = 8.3, 5.8 Hz, 1H), 8.07 (d, *J* = 8.8 Hz, 2H), 7.94 (d, *J* = 8.8 Hz, 2H), 5.19 – 5.07 (m, 2H), 3.92 (s, 3H), 2.14 (m, *J* = 2H), 1.52 (dt, *J* = 15.2, 7.2 Hz, 2H), 1.43 (dt, *J* = 14.1, 6.4 Hz, 2H), 1.28 (s, 22H), 0.89 (t, *J* = 7.0 Hz, 3H). FT-IR (neat): N-H at 3380, ester carbonyl at 1731, amide carbonyl at 1678 cm⁻¹. HRMS (ESI-MS⁺) calcd = 532.3665 [M + H]⁺, obsd = 532.3105

***N,N'*-(Disulfanediylbis(4,1-phenylene))bis(2-methylquinoline-6-carboxamide) (378)**

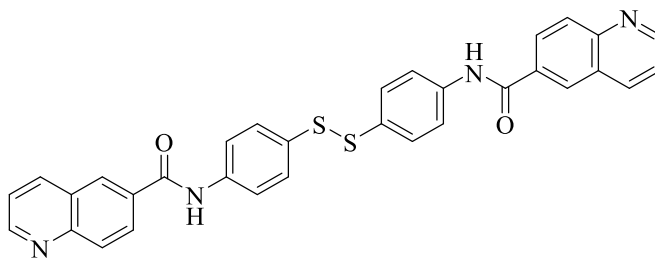


4,4'-Disulfanediyl dianiline (2.35 mmol, 596 mg) was dissolved in DCM (20 mL) and anhydrous triethylamine (21.5 mmol, 2.18 g, 3.00 mL). A suspension of 6-(chlorocarbonyl)-2-

methylquinolin-1-ium chloride **377** (4.93 mmol, 1.19 g) in dry DCM (20 mL) was quantitatively transferred in three portions over 15 minutes at 0°C to the amine-containing flask. The mixture was stirred at room temperature overnight. Next, the mixture was concentrated via rotary evaporation to give a green-tinted brown solid (3.42 g, 248% crude yield). The solid was diluted with water (100 mL), washed with diethyl ether (3x75 mL), and then DCM (4x50 mL). The aqueous layer was found to have a pH~8 and was then concentrated to give a mustard/turmeric-colored crude powder (2.972 g, 215%). Next, a small portion of the solid was triturated with minimal boiling H₂O (to remove the TEA HCl) followed by boiling IPA trituration/hot filtration. The IPA filtrate was boiled with activated charcoal, hot filtered, and then hot filtered again (to remove a trace amount of charcoal still present). This mixture was cooled to room temperature and then a small amount of H₂O was added (as an antisolvent) and then left uncovered to give an off-white solid growing in the mother liquor. Material was diluted with additional water, 8.5 then filtered and rinsed with water to give a crude semi-pure green solid (mp=218-228°C).

Separately, a small portion of the *pre-H₂O-triturated* semi-pure mustard-colored solid (503.9 mg) was purified via a normal phase silica using ethyl acetate:MeOH 8:2 as the eluent. The collected fractions gave a single spot on TLC and were concentrated via rotary evaporation to give a yellow solid. Normalized yield = 102 mg, 69%. ¹H NMR (500 MHz, DMSO-d₆) δ 10.62 (s, 2H), 8.57 (s, 2H), 8.40 (d, *J* = 8.4 Hz, 2H), 8.20 (d, *J* = 8.7 Hz, 2H), 8.02 (d, *J* = 8.8 Hz, 2H), 7.87 (d, *J* = 8.5 Hz, 4H), 7.66 – 7.37 (m, 6H), 2.70 (s, 6H). ¹³C NMR (126 MHz, DMSO-d₆) δ 165.33, 160.90, 148.46, 139.39, 137.20, 131.64, 130.20, 129.78, 128.33, 128.02, 125.31, 123.05, 121.08, 25.03. (one carbon peak in the aromatic region is presumably buried)

***N,N'*-(Disulfanediylbis(4,1-phenylene))bis(quinoline-6-carboxamide) (389)**



4,4'-Disulfanediyldianiline (4.76 mmol, 1.21 g) was dissolved in a solution of anhydrous DCM (30 mL) and pyridine (20 mL). Next, 6-(chlorocarbonyl)quinolin-1-ium chloride **388** (10.0 mmol, 2.28 g) was dissolved in dry DCM (40 mL) and was then quantitatively transferred to the amine-containing solution in three portions over 15 min at 0°C. The clear brown solution was stirred at room temperature overnight. Next, the brown suspension was concentrated via rotary evaporation to give a sticky brown solid. To the brown solid was added cold toluene and the suspension was transferred into a Büchner funnel, rinsed with 50 mL of cold toluene, and then 15 mL of hexanes. The crude material was air dried to give a brown sticky/gummy hygroscopic solid (mass= 6.35 g, 239% yield). Next, the gummy brown solid was diluted with half saturated sodium bicarbonate and the aqueous phase was washed at a pH = 8 with DCM (5X), taking care not to disturb the undissolved solid. The remaining solid and DCM-washed aqueous layer were acidified to pH ~ 1-2, at which point the solid dissolved into the aqueous layer. The aqueous solution was then washed with DCM (5X). Next, the aqueous solution was basified with solid sodium bicarbonate to pH = 6.5-7.0, at which point the yellow-brown aqueous layer lost its color and solid precipitated. To the separatory funnel was repeatedly added solid NaCl followed by stirring until no further solid precipitated. The stirring was continued overnight.

The aqueous suspension was filtered in a Büchner funnel and was then rinsed with sat. NaCl and air dried until only slightly damp (~1h). The damp tan solid was then transferred to a

large vial and was dried consecutively by addition of small portions of toluene on a rotary evaporation apparatus to give a tan powdery solid. Yield = 2.34 g (88%). ^1H NMR (500 MHz, DMSO- d_6) δ 10.78 (s, 2H), 9.01 (s, 2H), 8.70 (s, 2H), 8.53 (d, $J = 7.5$ Hz, 2H), 8.28 (d, $J = 8.2$ Hz, 2H), 8.13 (d, $J = 8.5$ Hz, 2H), 7.92 (d, $J = 7.3$ Hz, 4H), 7.70 – 7.60 (m, 2H), 7.56 (d, $J = 7.7$ Hz, 4H). ^{13}C NMR (126 MHz, DMSO- d_6) δ 165.22, 152.31, 148.79, 139.35, 137.20, 132.44, 130.27, 129.75, 129.09, 128.68, 128.09, 127.04, 122.28, 121.13.

BIBLIOGRAPHY

1. Ryan, M. F.; Eyler, J. R.; Richardson, D. E., Adiabatic ionization energies, bond disruption enthalpies, and solvation free energies for gas-phase metallocenes and metallocenium ions. *Journal of the American Chemical Society* **1992**, *114* (22), 8611-8619.
2. Metzger, R. M., Unimolecular electronics. *Chem Rev* **2015**, *115* (11), 5056-115.
3. Clikeman, T. T.; Bukovsky, E. V.; Wang, X. B.; Chen, Y. S.; Rumbles, G.; Strauss, S. H.; Boltalina, O. V., Core Perylene Diimide Designs via Direct Bay- and ortho-(Poly)trifluoromethylation: Synthesis, Isolation, X-ray Structures, Optical and Electronic Properties. *European Journal of Organic Chemistry* **2015**, *2015* (30), 6641-6654.
4. Langmuir, I., THE CONSTITUTION AND FUNDAMENTAL PROPERTIES OF SOLIDS AND LIQUIDS. II. LIQUIDS.1. *Journal of the American Chemical Society* **1917**, *39* (9), 1848-1906.
5. Miyashita, K.; Sakai, T.; Imanishi, T., Total Synthesis of (\pm)-Spiroxin C. *Organic Letters* **2003**, *5* (15), 2683-2686.
6. Van Dyck, C.; Ratner, M. A., Molecular Rectifiers: A New Design Based on Asymmetric Anchoring Moieties. *Nano Letters* **2015**, *15* (3), 1577-1584.
7. H., L.; St., D.; Th., P., The Relation between Packing Effects and Solid State Fluorescence of Dyes. *Journal für Praktische Chemie* **1991**, *333* (5), 733-748.
8. Ashwell, G. J.; Urasinska, B.; Tyrrell, W. D., Molecules that mimic Schottky diodes. *Physical Chemistry Chemical Physics* **2006**, *8* (28), 3314-3319.
9. Molander, G. A.; Cavalcanti, L. N.; García-García, C., Nickel-Catalyzed Borylation of Halides and Pseudohalides with Tetrahydroxydiboron [B₂(OH)₄]. *The Journal of Organic Chemistry* **2013**, *78* (13), 6427-6439.
10. Chen, X.; Roemer, M.; Yuan, L.; Du, W.; Thompson, D.; del Barco, E.; Nijhuis, C. A., Molecular diodes with rectification ratios exceeding 10⁵ driven by electrostatic interactions. *Nature Nanotechnology* **2017**, *12*, 797.
11. Rayleigh, Surface tension [3]. *Nature* **1891**, *43* (1115), 437-439.
12. Aviram, A.; Ratner, M. A., Molecular rectifiers. *Chemical Physics Letters* **1974**, *29* (2), 277-283.
13. Wescott, L. D.; Mattern, D. L., Donor- σ -Acceptor Molecules Incorporating a Nonadecyl-Swallowtailed Perylenediimide Acceptor. *The Journal of Organic Chemistry* **2003**, *68* (26), 10058-10066.
14. Mallouk, T. E.; Lee, H., Designer solids and surfaces. *Journal of Chemical Education* **1990**, *67* (10), 829.
15. Alberto, G.; Cristina, S.; Francesca, T.; Anna, P.; Anna, C.; J., A. G., In Situ Spectroscopic Characterization of Rectifying Molecular Monolayers Self-Assembled on Gold. *ChemPhysChem* **2007**, *8* (15), 2195-2201.
16. Ashwell, G. J.; Chwialkowska, A., Controlled alignment of molecular diodes via ionic assembly of cationic donor-([small pi]-bridge)-acceptor molecules on anionic surfaces. *Chemical Communications* **2006**, (13), 1404-1406.
17. Ashwell, G. J.; Ewington, J.; Robinson, B. J., Organic rectifying junctions fabricated by ionic coupling. *Chemical Communications* **2006**, (6), 618-620.
18. Ashwell, G. J.; Tyrrell, W. D.; Whittam, A. J., Molecular Rectification: Self-Assembled Monolayers in Which Donor-(π -Bridge)-Acceptor Moieties Are Centrally Located and Symmetrically Coupled to Both Gold Electrodes. *Journal of the American Chemical Society* **2004**, *126* (22), 7102-7110.

19. Ashwell, G. J.; Hamilton, R.; High, L. R. H., Molecular rectification: asymmetric current-voltage curves from self-assembled monolayers of a donor-([small pi]-bridge)-acceptor dye. *Journal of Materials Chemistry* **2003**, *13* (7), 1501-1503.
20. Ashwell, G. J.; Tyrrell, W. D.; Whittam, A. J., Molecular rectification: self-assembled monolayers of a donor-([small pi]-bridge)-acceptor chromophore connected via a truncated Au-S-(CH₂)₃ bridge. *Journal of Materials Chemistry* **2003**, *13* (12), 2855-2857.
21. Beverina, L.; Pagani, G. A., π -Conjugated Zwitterions as Paradigm of Donor–Acceptor Building Blocks in Organic-Based Materials. *Accounts of Chemical Research* **2014**, *47* (2), 319-329.
22. Franklin, B.; Brownrigg, W.; Farish, XLIV. Of the stilling of waves by means of oil. Extracted from sundry letters between Benjamin Franklin, LL. D. F. R. S. William Brownrigg, M. D. F. R. S. and the Reverend Mr. Farish. *Philosophical Transactions* **1774**, *64*, 445-460.
23. Pockels, A., On the relative contamination of the water-surface by equal quantities of different substances. *Nature* **1892**, *46* (1192), 418-419.
24. Pockels, A., Relations between the surface-tension and relative contamination of water surfaces. *Nature* **1893**, *48* (1233), 152-154.
25. Pockels, A., On the spreading of oil upon water [2]. *Nature* **1894**, *50* (1288), 223-224.
26. Langmuir, I., The mechanism of the surface phenomena of flotation. *Transactions of the Faraday Society* **1920**, *15* (June), 62-74.
27. Kaganer, V. M.; Möhwald, H.; Dutta, P., Structure and phase transitions in Langmuir monolayers. *Reviews of Modern Physics* **1999**, *71* (3), 779-819.
28. Roberts, G. G., *Langmuir-Blodgett films*. Plenum Press: New York, 1990.
29. Metzger, R. M., Unimolecular rectifiers: Present status. *Chemical Physics* **2006**, *326* (1), 176-187.
30. Langmuir, I.; Schaefer, V. J., Activities of Urease and Pepsin Monolayers. *Journal of the American Chemical Society* **1938**, *60* (6), 1351-1360.
31. Jaiswal, A.; Rajagopal, D.; Lakshmikantham, M. V.; Cava, M. P.; Metzger, R. M., Unimolecular rectification of monolayers of CH₃C(O)S-C₁₄H₂₈Q⁺-3CNQ⁻ and CH₃C(O)S-C₁₆H₃₂Q⁺-3CNQ⁻ organized by self-assembly, Langmuir-Blodgett, and Langmuir-Schaefer techniques. *Physical Chemistry Chemical Physics* **2007**, *9* (30), 4007-4017.
32. Johnson, M. S.; Kota, R.; Mattern, D. L.; Hill, C. M.; Vasiliu, M.; Dixon, D. A.; Metzger, R. M., A two-faced "Janus-like" unimolecular rectifier exhibits rectification reversal. *Journal of Materials Chemistry C* **2014**, *2* (46), 9892-9902.
33. Nijhuis, C. A.; Reus, W. F.; Whitesides, G. M., Molecular Rectification in Metal–SAM–Metal Oxide–Metal Junctions. *Journal of the American Chemical Society* **2009**, *131* (49), 17814-17827.
34. Nijhuis, C. A.; Reus, W. F.; Barber, J. R.; Dickey, M. D.; Whitesides, G. M., Charge Transport and Rectification in Arrays of SAM-Based Tunneling Junctions. *Nano Letters* **2010**, *10* (9), 3611-3619.
35. Nijhuis, C. A.; Reus, W. F.; Siegel, A. C.; Whitesides, G. M., A Molecular Half-Wave Rectifier. *Journal of the American Chemical Society* **2011**, *133* (39), 15397-15411.

36. Heath, J. R., Molecular Electronics. *Annual Review of Materials Research* **2009**, *39* (1), 1-23.
37. Reichert, J.; Ochs, R.; Beckmann, D.; Weber, H. B.; Mayor, M.; Löhneysen, H. v., Driving Current through Single Organic Molecules. *Physical Review Letters* **2002**, *88* (17), 176804.
38. Diez-Perez, I.; Hihath, J.; Lee, Y.; Yu, L.; Adamska, L.; Kozhushner, M. A.; Oleynik, II; Tao, N., Rectification and stability of a single molecular diode with controlled orientation. *Nat Chem* **2009**, *1* (8), 635-41.
39. Batra, A.; Darancet, P.; Chen, Q.; Meisner, J. S.; Widawsky, J. R.; Neaton, J. B.; Nuckolls, C.; Venkataraman, L., Tuning Rectification in Single-Molecular Diodes. *Nano Letters* **2013**, *13* (12), 6233-6237.
40. Lee, Y.; Carsten, B.; Yu, L., Understanding the Anchoring Group Effect of Molecular Diodes on Rectification. *Langmuir* **2009**, *25* (3), 1495-1499.
41. Johnson, M. S.; Kota, R.; Mattern, D. L.; Metzger, R. M., Janus Reversal and Coulomb Blockade in Ferrocene-Perylenebisimide and N,N,N',N'-Tetramethyl-para-phenylenediamine-Perylenebisimide D- σ -A Rectifiers. *Langmuir* **2016**, *32* (27), 6851-6859.
42. Zhang, Z.; Pan, J.; Guo, C.; Deng, X.; Qiu, M., The transport properties of D- σ -A molecules: A strikingly opposite directional rectification. *Applied Physics Letters* **2011**, *98* (1), 013503-013503-3.
43. Sutin, N.; Brunschwig, B. S.; Creutz, C., Using the Marcus Inverted Region for Rectification in Donor–Bridge–Acceptor “Wire” Assemblies. *The Journal of Physical Chemistry B* **2003**, *107* (39), 10687-10690.
44. Nijhuis, C. A.; Reus, W. F.; Whitesides, G. M., Mechanism of Rectification in Tunneling Junctions Based on Molecules with Asymmetric Potential Drops. *Journal of the American Chemical Society* **2010**, *132* (51), 18386-18401.
45. Garrigues, A. R.; Yuan, L.; Wang, L.; Mucciolo, E. R.; Thompon, D.; Del Barco, E.; Nijhuis, C. A., A Single-Level Tunnel Model to Account for Electrical Transport through Single Molecule- and Self-Assembled Monolayer-based Junctions. *Sci Rep* **2016**, *6*, 26517.
46. Honciuc, A.; Metzger, R. M.; Gong, A.; Spangler, C. W., Elastic and Inelastic Electron Tunneling Spectroscopy of a New Rectifying Monolayer. *Journal of the American Chemical Society* **2007**, *129* (26), 8310-8319.
47. Metzger, R. M.; Mattern, D. L., Unimolecular Electronic Devices. In *Unimolecular and Supramolecular Electronics II: Chemistry and Physics Meet at Metal-Molecule Interfaces*, Metzger, R. M., Ed. Springer Berlin Heidelberg: Berlin, Heidelberg, 2012; pp 39-84.
48. Shumate, W. J.; Mattern, D. L.; Jaiswal, A.; Dixon, D. A.; White, T. R.; Burgess, J.; Honciuc, A.; Metzger, R. M., Spectroscopy and Rectification of Three Donor–Sigma–Acceptor Compounds, Consisting of a One-Electron Donor (Pyrene or Ferrocene), a One-Electron Acceptor (Perylenebisimide), and a C19 Swallowtail. *The Journal of Physical Chemistry B* **2006**, *110* (23), 11146-11159.

49. Ruoff, R. S.; Kadish, K. M.; Boulas, P.; Chen, E. C. M., Relationship between the Electron Affinities and Half-Wave Reduction Potentials of Fullerenes, Aromatic Hydrocarbons, and Metal Complexes. *The Journal of Physical Chemistry* **1995**, *99* (21), 8843-8850.
50. Kota, R.; Samudrala, R.; Mattern, D. L., Synthesis of Donor- σ -Perylenebisimide-Acceptor Molecules Having PEG Swallowtails and Sulfur Anchors. *The Journal of Organic Chemistry* **2012**, *77* (21), 9641-9651.
51. Chen, E. C. M.; Wentworth, W. E., Experimental Determination of Electron Affinities of Organic Molecules. *Molecular Crystals and Liquid Crystals Incorporating Nonlinear Optics* **1989**, *171* (1), 271-285.
52. Kebarle, P.; Chowdhury, S., Electron affinities and electron-transfer reactions. *Chemical Reviews* **1987**, *87* (3), 513-534.
53. O'Neil, M. P.; Niemczyk, M. P.; Svec, W. A.; Gosztola, D.; Gaines, G. L.; Wasielewski, M. R., Picosecond Optical Switching Based on Biphotonic Excitation of an Electron Donor-Acceptor-Donor Molecule. *Science* **1992**, *257* (5066), 63-65.
54. Andreas, R.; Suse, M.; Heinz, L., Lösliche Perylen-Fluoreszenzfarbstoffe mit hoher Photostabilität. *Chemische Berichte* **1982**, *115* (8), 2927-2934.
55. Langhals, H., Synthese von hochreinen Perylen-Fluoreszenzfarbstoffen in großen Mengen – gezielte Darstellung von Atrop-Isomeren. *Chemische Berichte* **1985**, *118* (11), 4641-4645.
56. Langhals, H., Increasing the solubility of aromatic compounds. *Chem. Abstr.* **1982**, *96*, P70417x.
57. Demmig, S.; Langhals, H., Leichtlösliche, lichtechte Perylen-Fluoreszenzfarbstoffe. *Chemische Berichte* **1988**, *121* (2), 225-230.
58. Langhals, H., Cyclic carboxylic imide structures as structure elements of high stability. Novel developments in perylene dye chemistry. *Heterocycles* **1995**, *40* (1), 477-500.
59. Huang, C.; Barlow, S.; Marder, S. R., Perylene-3,4,9,10-tetracarboxylic Acid Diimides: Synthesis, Physical Properties, and Use in Organic Electronics. *The Journal of Organic Chemistry* **2011**, *76* (8), 2386-2407.
60. Sadrai, M.; Bird, G. R., A new laser dye with potential for high stability and a broad band of lasing action: Perylene-3,4,9,10-tetracarboxylic acid-bis-N,N'(2',6' xylidyl)diimide. *Optics Communications* **1984**, *51* (1), 62-64.
61. Li, G.; Zhao, Y.; Li, J.; Cao, J.; Zhu, J.; Sun, X. W.; Zhang, Q., Synthesis, Characterization, Physical Properties, and OLED Application of Single BN-Fused Perylene Diimide. *The Journal of Organic Chemistry* **2015**, *80* (1), 196-203.
62. Liu, Z.; Zhang, G.; Cai, Z.; Chen, X.; Luo, H.; Li, Y.; Wang, J.; Zhang, D., New organic semiconductors with imide/amide-containing molecular systems. *Advanced Materials* **2014**, *26* (40), 6965-6977.
63. Würthner, F.; Stolte, M., Naphthalene and perylene diimides for organic transistors. *Chemical Communications* **2011**, *47* (18), 5109-5115.

64. Zhan, X.; Facchetti, A.; Barlow, S.; Marks, T. J.; Ratner, M. A.; Wasielewski, M. R.; Marder, S. R., Rylene and related diimides for organic electronics. *Advanced Materials* **2011**, *23* (2), 268-284.
65. Rogovik, V. G., L. , *Zh. Org. Khim.* **1988**, *24*, 635-639
66. Seybold, G.; Wagenblast, G., New perylene and violanthrone dyestuffs for fluorescent collectors. *Dyes and Pigments* **1989**, *11* (4), 303-317.
67. Fennel, F.; Gershberg, J.; Stolte, M.; Wurthner, F., Fluorescence quantum yields of dye aggregates: a showcase example based on self-assembled perylene bisimide dimers. *Physical Chemistry Chemical Physics* **2018**, *20* (11), 7612-7620.
68. Ozser, M. E.; Sarkodie, S. A.; Mohiuddin, O.; Ozesme, G., Novel derivatives of regioisomerically pure 1,7-disubstituted perylene diimide dyes bearing phenoxy and pyrrolidinyl substituents: Synthesis, photophysical, thermal, and structural properties. *Journal of Luminescence* **2017**, *192*, 414-423.
69. Nakazono, S.; Easwaramoorthi, S.; Kim, D.; Shinokubo, H.; Osuka, A., Synthesis of Arylated Perylene Bisimides through C–H Bond Cleavage under Ruthenium Catalysis. *Organic Letters* **2009**, *11* (23), 5426-5429.
70. Nakazono, S.; Imazaki, Y.; Yoo, H.; Yang, J.; Sasamori, T.; Tokitoh, N.; Cédric, T.; Kageyama, H.; Kim, D.; Shinokubo, H.; Osuka, A., Regioselective Ru-catalyzed direct 2,5,8,11-alkylation of perylene bisimides. *Chemistry - A European Journal* **2009**, *15* (31), 7530-7533.
71. Battagliarin, G.; Li, C.; Enkelmann, V.; Müllen, K., 2,5,8,11-Tetraboronic Ester Perylenediimides: A Next Generation Building Block for Dye-Stuff Synthesis. *Organic Letters* **2011**, *13* (12), 3012-3015.
72. Battagliarin, G.; Zhao, Y.; Li, C.; Müllen, K., Efficient Tuning of LUMO Levels of 2,5,8,11-Substituted Perylenediimides via Copper Catalyzed Reactions. *Organic Letters* **2011**, *13* (13), 3399-3401.
73. Li, C.; Wonneberger, H., Perylene imides for organic photovoltaics: Yesterday, today, and tomorrow. *Advanced Materials* **2012**, *24* (5), 613-636.
74. Maki, T.; Ishihara, K.; Yamamoto, H., N-Alkyl-4-boronopyridinium Salts as Thermally Stable and Reusable Amide Condensation Catalysts. *Organic Letters* **2005**, *7* (22), 5043-5046.
75. Yasunori, Y.; Miho, T.; Xiao-Qiang, Y.; Norio, M., Cyclic Triolborates: Air- and Water-Stable Ate Complexes of Organoboronic Acids. *Angewandte Chemie International Edition* **2008**, *47* (5), 928-931.
76. Masato, N.; Makoto, K.; Hiroyoshi, K., Photochromism of Viologen Hexacyanoferrate(II) Complexes via Intramolecular Electron Transfer. *Bulletin of the Chemical Society of Japan* **1993**, *66* (6), 1764-1767.
77. Bard, A. J.; Ledwith, A.; Shine, H. J., Formation, Properties and Reactions of Cation Radicals in Solution. In *Advances in Physical Organic Chemistry*, Gold, V.; Bethell, D., Eds. Academic Press: 1976; Vol. 13, pp 155-278.
78. Das, S.; Alexeev, V. L.; Sharma, A. C.; Geib, S. J.; Asher, S. A., Synthesis and crystal structure of 4-amino-3-fluorophenylboronic acid. *Tetrahedron Letters* **2003**, *44* (42), 7719-7722.

79. Ahn, S.-J.; Lee, C.-Y.; Kim, N.-K.; Cheon, C.-H., Metal-Free Protodeboronation of Electron-Rich Arene Boronic Acids and Its Application to ortho-Functionalization of Electron-Rich Arenes Using a Boronic Acid as a Blocking Group. *The Journal of Organic Chemistry* **2014**, *79* (16), 7277-7285.
80. Lee, C.-Y.; Ahn, S.-J.; Cheon, C.-H., Protodeboronation of ortho- and para-Phenol Boronic Acids and Application to ortho and meta Functionalization of Phenols Using Boronic Acids as Blocking and Directing Groups. *The Journal of Organic Chemistry* **2013**, *78* (23), 12154-12160.
81. Kallepalli, V. A.; Gore, K. A.; Shi, F.; Sanchez, L.; Chotana, G. A.; Miller, S. L.; Maleczka, R. E.; Smith, M. R., Harnessing C–H Borylation/Deborylation for Selective Deuteration, Synthesis of Boronate Esters, and Late Stage Functionalization. *The Journal of Organic Chemistry* **2015**, *80* (16), 8341-8353.
82. Kuivila, H. G.; Reuwer Jr, J. F.; Mangravite, J. A., ELECTROPHILIC DISPLACEMENT REACTIONS: XV. KINETICS AND MECHANISM OF THE BASE-CATALYZED PROTOBORONATION OF ARENEBORONIC ACIDS. *Canadian Journal of Chemistry* **1963**, *41* (12), 3081-3090.
83. Kuivila, H. G.; Nahabedian, K. V., Electrophilic Displacement Reactions. X. General Acid Catalysis in the Protodeboronation of Areneboronic Acids1-3. *Journal of the American Chemical Society* **1961**, *83* (9), 2159-2163.
84. Lozada, J.; Liu, Z.; Perrin, D. M., Base-Promoted Protodeboronation of 2,6-Disubstituted Arylboronic Acids. *The Journal of Organic Chemistry* **2014**, *79* (11), 5365-5368.
85. Zhichkin, P. E.; Krasutsky, S. G.; Beer, C. M.; Rennells, W. M.; Lee, S. H.; Xiong, J.-M., Preparation of 2-Fluoro-3-aminophenylboronates via Directed ortho-Metalation. *Synthesis* **2011**, *2011* (10), 1604-1608.
86. Djuric, S.; Venit, J.; Magnus, P., Silicon in synthesis: stabase adducts - a new primary amine protecting group: alkylation of ethyl glycinate. *Tetrahedron Letters* **1981**, *22* (19), 1787-1790.
87. Gao, X.; Zhang, Y.; Wang, B., Naphthalene-based water-soluble fluorescent boronic acid isomers suitable for ratiometric and off-on sensing of saccharides at physiological pH. *New Journal of Chemistry* **2005**, *29* (4), 579-586.
88. Yanling, Z.; Xingming, G.; Kenneth, H.; Binghe, W., Water-Soluble Fluorescent Boronic Acid Compounds for Saccharide Sensing: Substituent Effects on Their Fluorescence Properties. *Chemistry – A European Journal* **2006**, *12* (5), 1377-1384.
89. M., B. S.; M., Y. R.; N., R. K., Design and Formation of a Large Tetrahedral Cluster Using 1,1'-Binaphthyl Ligands. *Angewandte Chemie International Edition* **2008**, *47* (32), 6062-6064.
90. Klemm, L. H.; Sprague, J. W.; Mak, E. Y. K., Syntheses and Ultraviolet Spectra of 1-(5- and 8-Methyl-1-naphthyl)-1-cyclopentenes and 1-Cyclohexenes1-3. *The Journal of Organic Chemistry* **1957**, *22* (2), 161-166.
91. Martin, B.; Possémé, F.; Le Barbier, C.; Carreaux, F.; Carboni, B.; Seiler, N.; Moulinoux, J.-P.; Delcros, J.-G., N-Benzylpolyamines as Vectors of Boron and Fluorine for Cancer Therapy

- and Imaging: Synthesis and Biological Evaluation. *Journal of Medicinal Chemistry* **2001**, *44* (22), 3653-3664.
92. Zhang, Q.; Zhang, L.; Tang, C.; Luo, H.; Cai, X.; Chai, Y., Cascade reaction of propargylic alcohols with hydroxylamine hydrochloride: facile synthesis of α,β -unsaturated oximes and nitriles. *Tetrahedron* **2016**, *72* (44), 6935-6942.
93. Brown, D. G.; Boström, J., Analysis of Past and Present Synthetic Methodologies on Medicinal Chemistry: Where Have All the New Reactions Gone? *Journal of Medicinal Chemistry* **2016**, *59* (10), 4443-4458.
94. Valeur, E.; Bradley, M., Amide bond formation: beyond the myth of coupling reagents. *Chemical Society Reviews* **2009**, *38* (2), 606-631.
95. Moffat, D. F. C. D., Stephen John; Charlton, Michael Hugh; Hirst, Simon Christopher; Onions, Stuart Thomas; Williams, Jonathon Gareth, *PCT Int. Appl.* **2008**, (WO 2008053185 A1).
96. Jenkins, T. J.; Guan, B.; Dai, M.; Li, G.; Lightburn, T. E.; Huang, S.; Freeze, B. S.; Burdi, D. F.; Jacutin-Porte, S.; Bennett, R.; Chen, W.; Minor, C.; Ghosh, S.; Blackburn, C.; Gigstad, K. M.; Jones, M.; Kolbeck, R.; Yin, W.; Smith, S.; Cardillo, D.; Ocain, T. D.; Harriman, G. C., Design, Synthesis, and Evaluation of Naphthalene-Sulfonamide Antagonists of Human CCR8. *Journal of Medicinal Chemistry* **2007**, *50* (3), 566-584.
97. Chen, J.; Fu, X.-G.; Zhou, L.; Zhang, J.-T.; Qi, X.-L.; Cao, X.-P., A Convergent Route for the Total Synthesis of Malyngamides O, P, Q, and R. *The Journal of Organic Chemistry* **2009**, *74* (11), 4149-4157.
98. Lebedyeva, I. O.; Ostrov, D. A.; Neubert, J.; Steel, P. J.; Patel, K.; Sileno, S. M.; Goncalves, K.; Ibrahim, M. A.; Alamry, K. A.; Katritzky, A. R., Gabapentin hybrid peptides and bioconjugates. *Bioorganic and Medicinal Chemistry* **2014**, *22* (4), 1479-1486.
99. Randell, D. R. H., James Roger, Preparation of Benzotriazoles. *US Patent* **1971**, (1242955).
100. Chabaud, L.; Clayden, J.; Helliwell, M.; Page, A.; Raftery, J.; Vallverdú, L., Conformational studies of tertiary oligo-m-benzanilides and oligo-p-benzanilides in solution. *Tetrahedron* **2010**, *66* (34), 6936-6957.
101. Font, M.; Lizarraga, E.; Ibáñez, E.; Plano, D.; Sanmartín, C.; Palop, J. A., Structural variations on antitumour agents derived from bisacylimidoselenocarbamate. A proposal for structure–activity relationships based on the analysis of conformational behaviour. *European Journal of Medicinal Chemistry* **2013**, *66*, 489-498.
102. Sogabe, Y.; Namikoshi, T.; Watanabe, S.; Murata, M., Synthesis of Aryl Triolborates via Nickel-Catalyzed Borylation of Aryl Halides with 5-(tert-Butyldimethylsilyloxymethyl)-5-methyl-1,3,2-dioxaborinane. *Synthesis* **2012**, *44* (08), 1233-1236.
103. Rosen, B. M.; Wilson, D. A.; Wilson, C. J.; Peterca, M.; Won, B. C.; Huang, C.; Lipski, L. R.; Zeng, X.; Ungar, G.; Heiney, P. A.; Percec, V., Predicting the Structure of Supramolecular Dendrimers via the Analysis of Libraries of AB₃ and Constitutional Isomeric AB₂ Biphenylpropyl Ether Self-Assembling Dendrons. *Journal of the American Chemical Society* **2009**, *131* (47), 17500-17521.

104. Wilson, D. A.; Wilson, C. J.; Moldoveanu, C.; Resmerita, A.-M.; Corcoran, P.; Hoang, L. M.; Rosen, B. M.; Percec, V., Neopentylglycolborylation of Aryl Mesylates and Tosylates Catalyzed by Ni-Based Mixed-Ligand Systems Activated with Zn. *Journal of the American Chemical Society* **2010**, *132* (6), 1800-1801.
105. Mortezaei, S.; Catarineu, N. R.; Canary, J. W., A Redox-Reconfigurable, Ambidextrous Asymmetric Catalyst. *Journal of the American Chemical Society* **2012**, *134* (19), 8054-8057.
106. Moussa, I. A.; Banister, S. D.; Beinat, C.; Giboureau, N.; Reynolds, A. J.; Kassiou, M., Design, synthesis, and structure-affinity relationships of regioisomeric N-benzyl alkyl ether piperazine derivatives as σ -1 receptor ligands. *Journal of Medicinal Chemistry* **2010**, *53* (16), 6228-6239.
107. Kabalka, G. W.; Varma, M.; Varma, R. S.; Srivastava, P. C.; Knapp Jr, F. F., Tosylation of alcohols. *Journal of Organic Chemistry* **1986**, *51* (12), 2386-2388.
108. Miyata, O.; Takahashi, S.; Tamura, A.; Ueda, M.; Naito, T., Novel synthesis of substituted pyrrolidines and piperidines via radical addition–ionic cyclization reaction of oxime ethers. *Tetrahedron* **2008**, *64* (7), 1270-1284.
109. Mori, K., Synthesis of all the six components of the female-produced contact sex pheromone of the German cockroach, *Blattella germanica* (L.). *Tetrahedron* **2008**, *64* (18), 4060-4071.
110. Shi, Y.; Frattarelli, D.; Watanabe, N.; Facchetti, A.; Cariati, E.; Righetto, S.; Tordin, E.; Zuccaccia, C.; Macchioni, A.; Wegener, S. L.; Stern, C. L.; Ratner, M. A.; Marks, T. J., Ultra-High-Response, Multiply Twisted Electro-optic Chromophores: Influence of π -System Elongation and Interplanar Torsion on Hyperpolarizability. *Journal of the American Chemical Society* **2015**, *137* (39), 12521-12538.
111. Li, J.-Y.; Chen, C.-Y.; Ho, W.-C.; Chen, S.-H.; Wu, C.-G., Unsymmetrical Squaraines Incorporating Quinoline for Near Infrared Responsive Dye-Sensitized Solar Cells. *Organic Letters* **2012**, *14* (21), 5420-5423.
112. Marek, J.; Buchta, V.; Soukup, O.; Stodulka, P.; Cabal, J.; Ghosh, K. K.; Musilek, K.; Kuca, K., Preparation of quinolinium salts differing in the length of the alkyl side chain. *Molecules (Basel, Switzerland)* **2012**, *17* (6), 6386-6394.
113. Pardal, A. C.; Ramos, S. S.; Santos, P. F.; Reis, L. V.; Almeida, P., Synthesis and spectroscopic characterisation of N-alkyl quaternary ammonium salts typical precursors of cyanines. *Molecules* **2002**, *7* (3), 320-330.
114. Wang, Y.; Jiang, X.; Zhou, L.; Wang, C.; Liao, Y.; Duan, M.; Jiang, X., A Comparison of New Gemini Surfactant Modified Clay with its Monomer Modified One: Characterization and Application in Methyl Orange Removal. *Journal of Chemical & Engineering Data* **2013**, *58* (6), 1760-1771.
115. Youngman, M.; McNally, J. J.; McDonnell, M.; Jetter, M.; Dax, S. L.; Codd, E. QUINOLINE-DERIVED AMIDE MODULATORS OF VANILLOID VR1 RECEPTOR. 2004.
116. Ashraf, M.; Teshome, A.; Kay, A. J.; Gainsford, G. J.; Bhuiyan, M. D. H.; Asselberghs, I.; Clays, K., NLO chromophores containing dihydrobenzothiazolydene and

- dihydroquinolinylidene donors with an azo linker: Synthesis and optical properties. *Dyes and Pigments* **2013**, *98* (1), 82-92.
117. Tilstam, U., Sulfolane: A versatile dipolar aprotic solvent. *Organic Process Research and Development* **2012**, *16* (7), 1273-1278.
118. Gao-Qiang, L.; Shunsuke, K.; Yasunori, Y.; Norio, M., Direct Conversion of Pinacol Arylboronic Esters to Aryl Triolborates. *Chemistry Letters* **2011**, *40* (7), 702-704.
119. Inglis, S. R.; Woon, E. C. Y.; Thompson, A. L.; Schofield, C. J., Observations on the deprotection of pinanediol and pinacol boronate esters via fluorinated intermediates. *Journal of Organic Chemistry* **2010**, *75* (2), 468-471.
120. Molander, G. A.; Ito, T., Cross-Coupling Reactions of Potassium Alkyltrifluoroborates with Aryl and 1-Alkenyl Trifluoromethanesulfonates. *Organic Letters* **2001**, *3* (3), 393-396.
121. Molander, G. A.; Biolatto, B., Efficient Ligandless Palladium-Catalyzed Suzuki Reactions of Potassium Aryltrifluoroborates. *Organic Letters* **2002**, *4* (11), 1867-1870.
122. Thadani, A. N.; Batey, R. A., A Mild Protocol for Allylation and Highly Diastereoselective Syn or Anti Crotylation of Aldehydes in Biphasic and Aqueous Media Utilizing Potassium Allyl- and Crotyltrifluoroborates. *Organic Letters* **2002**, *4* (22), 3827-3830.
123. Batey, R. A.; Quach, T. D., Synthesis and cross-coupling reactions of tetraalkylammonium organotrifluoroborate salts. *Tetrahedron Letters* **2001**, *42* (52), 9099-9103.
124. Vedejs, E.; Chapman, R. W.; Fields, S. C.; Lin, S.; Schrimpf, M. R., Conversion of Arylboronic Acids into Potassium Aryltrifluoroborates: Convenient Precursors of Arylboron Difluoride Lewis Acids. *The Journal of Organic Chemistry* **1995**, *60* (10), 3020-3027.
125. Yuen, A. K. L.; Hutton, C. A., Deprotection of pinacolyl boronate esters via hydrolysis of intermediate potassium trifluoroborates. *Tetrahedron Letters* **2005**, *46* (46), 7899-7903.
126. Comey, A. M., *A dictionary of chemical solubilities: inorganic*. Macmillan and co: London; New York, 1896.
127. O'Neil, M. J., *The Merck index: an encyclopedia of chemicals, drugs, and biologicals*. 14th ed.; Merck: Whitehouse Station, NJ, 2006.
128. Halder, J.; Kondaiyah, P.; Bhattacharya, S., Synthesis and Antibacterial Properties of Novel Hydrolyzable Cationic Amphiphiles. Incorporation of Multiple Head Groups Leads to Impressive Antibacterial Activity. *Journal of Medicinal Chemistry* **2005**, *48* (11), 3823-3831.
129. Johnson, T. W.; Corey, E. J., Enantiospecific Synthesis of the Proposed Structure of the Antitubercular Marine Diterpenoid Pseudopteroxazole: Revision of Stereochemistry. *Journal of the American Chemical Society* **2001**, *123* (19), 4475-4479.
130. Jia, Z.; Zhu, Q., 'Click' assembly of selective inhibitors for MAO-A. *Bioorganic & Medicinal Chemistry Letters* **2010**, *20* (21), 6222-6225.
131. Deping, W.; Daizhi, K.; Fuxing, Z.; Siping, T.; Wujiu, J., Triethanolamine as an Inexpensive and Efficient Ligand for Copper-Catalyzed Hydroxylation of Aryl Halides in Water. *European Journal of Organic Chemistry* **2014**, *2014* (2), 315-318.
132. Lerner, L., Identity of a Purple Dye Formed by Peroxidic Oxidation of p-Aminophenol at Low pH. *The Journal of Physical Chemistry A* **2011**, *115* (35), 9901-9910.

133. Fontana, F.; Minisci, F.; Nogueira Barbosa, M. C.; Vismara, E., Homolytic acylation of protonated pyridines and pyrazines with .alpha.-keto acids: the problem of monoacylation. *The Journal of Organic Chemistry* **1991**, *56* (8), 2866-2869.
134. Tauber, J.; Imbri, D.; Opatz, T., Radical Addition to Iminium Ions and Cationic Heterocycles. *Molecules* **2014**, *19* (10), 16190.
135. Chiranjit, S.; C., G. S., Transition-Metal-Free Regioselective Alkylation of Quinoline N-Oxides via Oxidative Alkyl Migration and C–C Bond Cleavage of tert-/sec-Alcohols. *Advanced Synthesis & Catalysis* **2018**, *360* (5), 905-910.
136. Kasai, S.; Kamata, M.; Masada, S.; Kunitomo, J.; Kamaura, M.; Okawa, T.; Takami, K.; Ogino, H.; Nakano, Y.; Ashina, S.; Watanabe, K.; Kaisho, T.; Imai, Y. N.; Ryu, S.; Nakayama, M.; Nagisa, Y.; Takekawa, S.; Kato, K.; Murata, T.; Suzuki, N.; Ishihara, Y., Synthesis, Structure–Activity Relationship, and Pharmacological Studies of Novel Melanin-Concentrating Hormone Receptor 1 Antagonists 3-Aminomethylquinolines: Reducing Human Ether-a-go-go-Related Gene (hERG) Associated Liabilities. *Journal of Medicinal Chemistry* **2012**, *55* (9), 4336-4351.
137. Wiley, M. R.; Weir, L. C.; Briggs, S.; Bryan, N. A.; Buben, J.; Campbell, C.; Chirgadze, N. Y.; Conrad, R. C.; Craft, T. J.; Ficorilli, J. V.; Franciskovich, J. B.; Froelich, L. L.; Gifford-Moore, D. S.; Goodson, T.; Herron, D. K.; Klimkowski, V. J.; Kurz, K. D.; Kyle, J. A.; Masters, J. J.; Ratz, A. M.; Milot, G.; Shuman, R. T.; Smith, T.; Smith, G. F.; Tebbe, A. L.; Tinsley, J. M.; Towner, R. D.; Wilson, A.; Yee, Y. K., Structure-Based Design of Potent, Amidine-Derived Inhibitors of Factor Xa: Evaluation of Selectivity, Anticoagulant Activity, and Antithrombotic Activity. *Journal of Medicinal Chemistry* **2000**, *43* (5), 883-899.
138. Bagley, M. C.; Bashford, K. E.; Hesketh, C. L.; Moody, C. J., Total Synthesis of the Thiopeptide Promothiocin A. *Journal of the American Chemical Society* **2000**, *122* (14), 3301-3313.
139. Idzik, K.; Nödler, K.; Maier, F.; Licha, T., Efficient Synthesis and Reaction Kinetics of Readily Water Soluble Esters Containing Sulfonic Groups. *Molecules* **2014**, *19* (12), 21022.
140. Cheeseman, M. D.; Chessum, N. E. A.; Rye, C. S.; Pasqua, A. E.; Tucker, M. J.; Wilding, B.; Evans, L. E.; Lepri, S.; Richards, M.; Sharp, S. Y.; Ali, S.; Rowlands, M.; O'Fee, L.; Miah, A.; Hayes, A.; Henley, A. T.; Powers, M.; te Poele, R.; De Billy, E.; Pellegrino, L.; Raynaud, F.; Burke, R.; van Montfort, R. L. M.; Eccles, S. A.; Workman, P.; Jones, K., Discovery of a Chemical Probe Bisamide (CCT251236): An Orally Bioavailable Efficacious Pirin Ligand from a Heat Shock Transcription Factor 1 (HSF1) Phenotypic Screen. *Journal of Medicinal Chemistry* **2017**, *60* (1), 180-201.
141. Bracchi, M. E.; Fulton, D. A., Orthogonal breaking and forming of dynamic covalent imine and disulfide bonds in aqueous solution. *Chemical Communications* **2015**, *51* (55), 11052-11055.
142. Hyde, A. M.; Zultanski, S. L.; Waldman, J. H.; Zhong, Y.-L.; Shevlin, M.; Peng, F., General Principles and Strategies for Salting-Out Informed by the Hofmeister Series. *Organic Process Research & Development* **2017**, *21* (9), 1355-1370.

143. Hill, G. B.; Sweeney, J. B., Reaction Workup Planning: A Structured Flowchart Approach, Exemplified in Difficult Aqueous Workup of Hydrophilic Products. *Journal of Chemical Education* **2015**, 92 (3), 488-496.
144. Langhals, H.; Sprenger, S.; Brandherm, M. T., Perylenamidine-imide dyes. *Liebigs Annalen* **1995**, 1995 (3), 481-486.
145. Dale, T. J.; Rebek Jr, J., Fluorescent sensors for organophosphorus nerve agent mimics. *Journal of the American Chemical Society* **2006**, 128 (14), 4500-4501.
146. Fujii, A.; Sekiguchi, Y.; Matsumura, H.; Inoue, T.; Chung, W.-S.; Hirota, S.; Matsuo, T., Excimer Emission Properties on Pyrene-Labeled Protein Surface: Correlation between Emission Spectra, Ring Stacking Modes, and Flexibilities of Pyrene Probes. *Bioconjugate Chemistry* **2015**, 26 (3), 537-548.
147. Tomioka, T.; Takahashi, Y.; Vaughan, T. G.; Yanase, T., A Facile, One-Pot Synthesis of β -Substituted (Z)-Acrylonitriles Utilizing an α -Diaminoboryl Carbanion. *Organic Letters* **2010**, 12 (10), 2171-2173.
148. Tomioka, T.; Sankranti, R.; Vaughan, T. G.; Maejima, T.; Yanase, T., An α -Diaminoboryl Carbanion Assisted Stereoselective Single-Pot Preparation of α,β -Disubstituted Acrylonitriles. *The Journal of Organic Chemistry* **2011**, 76 (19), 8053-8058.
149. Khurana, J. M.; Kukreja, G., RAPID REDUCTION OF NITRILES TO PRIMARY AMINES WITH NICKEL BORIDE AT AMBIENT TEMPERATURE. *Synthetic Communications* **2002**, 32 (8), 1265-1269.
150. Huang, X.; Jiao, N., Bronsted acid mediated nitrogenation of propargylic alcohols: an efficient approach to alkenyl nitriles. *Organic & Biomolecular Chemistry* **2014**, 12 (25), 4324-4328.
151. Man-Bo, L.; Yong, W.; Shi-Kai, T., Regioselective and Stereospecific Cross-Coupling of Primary Allylic Amines with Boronic Acids and Boronates through Palladium-Catalyzed C-N Bond Cleavage. *Angewandte Chemie International Edition* **2012**, 51 (12), 2968-2971.
152. Granzhan, A.; Teulade-Fichou, M.-P., Synthesis of mono- and bibrachial naphthalene-based macrocycles with pyrene or ferrocene units for anion detection. *Tetrahedron* **2009**, 65 (7), 1349-1360.
153. Khand, I. U.; Lanez, T.; Pauson, P. L., Ferrocene derivatives. Part 24. Synthesis of dihydro-2-pyridines and dihydro-3H-2-cyclopent[c]azepines by photolysis of their cyclopentadienyliron derivatives. *Journal of the Chemical Society, Perkin Transactions 1* **1989**, (11), 2075-2078.
154. Newman, M. S.; MacDowell, D.; Swaminathan, S., The Synthesis of Some Monofluoro-1,2-benzanthracenes. *The Journal of Organic Chemistry* **1959**, 24 (4), 509-512.
155. Haberecht, J.; Krummland, A.; Breher, F.; Gebhardt, B.; Rügger, H.; Nesper, R.; Grützmacher, H., Functionalized borazines as precursors for new silica gels. *Dalton Transactions* **2003**, (11), 2126-2132.
156. Sinisterra, J. V.; Mouloungui, Z.; Delmas, M.; Gaset, A., Barium Hydroxide as Catalyst in Organic Reactions; V. Application in the Horner Reaction under Solid-Liquid Phase-Transfer Conditions. *Synthesis* **1985**, 1985 (12), 1097-1100.

157. Haftchenary, S.; Luchman, H. A.; Jouk, A. O.; Veloso, A. J.; Page, B. D. G.; Cheng, X. R.; Dawson, S. S.; Grinshtein, N.; Shahani, V. M.; Kerman, K.; Kaplan, D. R.; Griffin, C.; Aman, A. M.; Al-awar, R.; Weiss, S.; Gunning, P. T., Potent Targeting of the STAT3 Protein in Brain Cancer Stem Cells: A Promising Route for Treating Glioblastoma. *ACS Medicinal Chemistry Letters* **2013**, *4* (11), 1102-1107.

VITA

Trey Gautier Vaughan was born in Gautier, Mississippi, United States on December 19th, 1978. After a decade of involvement in the family business of mechanical contracting catering to large industries like Northrop Grumman, he decided to attend the University of Mississippi to study chemistry. He joined the research group of Dr. Takashi Tomioka and was published twice in peer reviewed journals. In 2011 he obtained his B.S. in Chemistry.

He entered the Ph.D. program at the University of Mississippi and studied synthetic chemistry applied to molecular electronics. During his time at the University of Mississippi he became active in student government and served for three years as the graduate student senator (and as vice president pro tempore during the final year) representing the Department of Chemistry & Biochemistry. He was also a passionate advocate of integrating business and technology to address social challenges and even led an interdisciplinary interdepartmental team to win second place in the Gillespie Social Business Challenge in 2015.

Trey Vaughan

230 James Circle · Oxford MS 38655 · (662) 607 4833 · tvaughanmsu@gmail.com

EDUCATION

B.S., Chemistry, University of Mississippi, Spring, 2011

TEACHING EXPERIENCE

Qualitative Organic Analysis Lab (2012 – 2018)

Integrated Science (2017)

Head Teaching Assistant for General Chemistry (2016)

General Chemistry Lab (2014 - 2015)

Organic Chemistry Lab (2012 – 2013)

HONORS AND FELLOWSHIPS

Blueprint Mississippi Social Business Challenge, 2nd place, 2015

Chancellor's Honor roll, Spring 2011

Chancellor's Honor roll, Fall 2008

PUBLICATIONS AND PRESENTATIONS

Research Poster Presentation. Synthesis of Two Candidate Donor-Sigma-Acceptor (D- σ -A)

Molecular Rectifiers with Anionic Donors and a Quinolinium Acceptor. 67th SERMACS in

Memphis, TN, Nov. 4 – 7, **2015**.

Research Poster Presentation. Borate Zwitterions as Donor-Sigma-Acceptor (D- σ -A) Molecules.

Model Compound Synthesis. 245th American Chemical Society national meeting, New Orleans,

LA, April 7 – 11, **2013**.

Takashi Tomioka, Rambabu Sankranti, Trey Vaughan, Toshihide Maejima, and Takayoshi Yanase. An α -Diaminoboryl Carbanion Assisted Stereoselective Single-Pot Preparation of α,β -Disubstituted Acrylonitriles. *The Journal of Organic Chemistry*. **2011**, 76 (19), pp 8053-8058

Vaughan, Trey G. A one-pot stereoselective preparation of a series of acrylonitriles employing an α -diaminoboryl carbanion. The 32nd Annual Undergraduate Research Conference in Memphis, TN. **2011**

Takashi Tomioka, Yusuke Takahashi, Trey Vaughan, Takayoshi Yanase. A Facile, One-Pot Synthesis of β -Substituted (Z)-Acrylonitriles Utilizing an α -Diaminoboryl Carbanion. *Organic Letters*. **2010**, 12 (10), pp 2171–2173